# Direct Geothermal Energy: Reducing the Poultry Industries' Carbon footprint

Yu Zhou

*Submitted in total fulfilment of the requirements of the degree of Doctor of Philosophy*

*May 2020*

Department of Infrastructure Engineering

The University of Melbourne

# Abstract

A Ground Source Heat Pump (GSHP) system is a type of highly efficient renewable energy system which utilizes the ground as the heat source when heating and as the heat sink when cooling. Since the initial installation cost of GSHP systems can be relatively high, hybrid GSHP systems can be designed to reduce the initial cost by coupling with other energy technologies, including solar technology. One promising area where hybrid GSHP systems can be applied to is in the rural industries which has high requirement for heating and lack of reticulated gas infrastructure and land availability. This research aims to contribute to the development of hybrid GSHP system with horizontal ground heat exchangers (GHEs) suitable for the rural industry, with poultry sheds in Australia investigated as cases studies.

A full-scale instrumented hybrid geothermal system for the poultry shed in Peats Ridge was then designed and built to verify, demonstrate the performance. Providing 80 kW heating, the ground heat exchanger field consists of 12 horizontal trenches at the depth of 1.5 m totalling 4,800 m of ground loop and 400 m of pond loop in a nearby pond submerged at a depth of 4 to 6 m.

This work then investigated energy efficient solutions for poultry sheds in Australia. The space heating and cooling demand cycles of a typical poultry sheds in Peats Ridge, NSW, Australia have been simulated in detail, using TRNSYS 18. It is found that heating systems, operational schedule (raising batches of chicks) and ventilation strategies have a great impact on energy consumption. An optimum scheduling strategy was developed, and energy demands were minimised.

Furthermore, this work contributed to the improvement of the design of hybrid geothermal system with horizontal GHEs. As hourly simulation of GSHP with horizontal GHEs is not yet available in major commercial software packages, Artificial Neural Network (ANN) models were proposed, which can potentially be generally applied to similar sheds at different locations and under different climate conditions, with readily available and limited types of input data, hourly heating loads, accumulated heating loads and ambient air temperature. Trained with simulated data from a verified TRNSYS model, the ANNs can predict the performance of GSHPs systems with identical

GHEs even under climatic conditions (and locations) that has not been specifically trained for. This represents a major advance in this area. With only limited input data and showing a high accuracy (no more than 5% error in most cases tested), the presented ANN is 100 times computationally faster than TRNSYS model and 10,000 times faster than comparable Finite Element models.

Finally, to reduce the lifecycle cost and greenhouse gas (GHG) emissions of heating the shed, multi-objective optimisation regarding hybrid geothermal-solar-gas heating systems are investigated. In these systems, the baseload heating demand is satisfied by GSHPs, with solar photovoltaic panels providing the electricity needed to drive the pumps and LPG gas boilers toping up the balance of the heating. This study investigated and optimised lifecycle cost along with GHG emissions arising from the three components of these hybrid systems, considering three different electricity offsetting scenarios. The results indicated that a considerable reduction in the lifecycle heating costs (up to 55%) and GHG emissions (up to 50%) can be achieved when optimised hybrid systems are used for heating. The Pareto front solutions for this hybrid geothermal-solar-gas heating system were also determined. By comparing the Pareto front solutions in different scenarios, it has been identified that the shave factor, a measure of the proportion of GSHP to the overall heating system, has the highest impact when to comes to reducing the lifecycle cost, while the size and utilisation of solar PV panels contributes more to the lifecycle GHG emissions.

The findings obtained from this study can contribute to the design and optimisation of hybrid geothermal systems to reduce its lifecycle cost and carbon footprint as well as assist in wide spreading the application of GSHPs for the rural industry.

# Declaration

This is to certify that:

- the thesis comprises only my original work towards the degree of Doctor of Philosophy,
- due acknowledgement has been made in the text to all other material used,
- the thesis is fewer than 100,000 words in length, exclusive of tables, maps, bibliographies and appendices.

周钰

_____

Yu Zhou

May 2020

# Publications Relating to this Work

As part of the research undertaken to produce this doctoral thesis, several independent research works were produced and are described here as they related directly to the chapters of this thesis. Three journal papers have been submitted:

1. Zhou Y, Aye L, Narsilio G, Improving energy efficiency of a typical poultry shed in Australia (Submitted to Renewable and Sustainable Energy Reviews)
2. Zhou Y, Narsilio G, Makasis N, Soga K, Aye L, Ground-source heat pump systems: Artificial neural networks for the performance of horizontal ground heat exchangers under rural industries' loading conditions (Submitted to Applied Energy)
3. Zhou Y, Narsilio G, Bidarmaghz A, Aye L, Soga K, Minimising lifecycle cost and greenhouse gas emissions of hybrid geothermal-solar (PV)-gas heating systems (Submitted to Energy Conversion and Management)

Publication 1, 2 and 3 are the basis for Chapter 4, 5 and 6 of the thesis and are inserted in the body of the text as the original submitted work. Modifications have only been made to the numbering of page numbers, sections, references, tables and figures to keep the consistency of the thesis. Additionally, four published conference papers that contain preliminary results have been attached as Appendices.

4. Zhou Y, Narsilio G, Makasis N, Aye L (2019), A machine learning approach for the performance of GSHPs with horizontal ground heat exchangers, XVI Panamerican Conference on Soil Mechanics and Geotechnical Engineering, 17-20 November 2019, Cancún, Mexico
5. Zhou Y, Narsilio G, Aye L, Mikhaylova O, Bidarmaghz A, Soga K (2018), Optimisation of a hybrid geothermal-solar-gas system: A case study for a typical poultry shed in New South Wales, Australia, Proceedings of Building Simulation and Optimisation 2018; pp. 358-365, 11-12 September 2018, Cambridge, UK
6. Zhou Y, Mikhaylova O, Bidarmaghz A, Donovan B, Narsilio G, Aye L (2018), Hybrid geothermal-gas and geothermal-solar-gas heating systems for poultry sheds. Proceedings of Zero Energy Mass Custom Home 2018, ISBN: 978-0-7340-5486-9; pp. 545-554, 29 Jan – 01 Feb 2018, Melbourne, Australia
7. Zhou Y, Bidarmaghz A, Narsilio G, Aye L (2017), Heating and Cooling Loads of a Poultry House in Central Coast, NSW, Australia, Proceedings of World Sustainable Built Environment Conference 2017, ISBN 978-988-77943-0-1; pp. 2127-2133, 5-7 June 2017, Hong Kong, China.

In all the cases the candidate contributed more than 50% of the work, including gathering of experimental data in the field and laboratory, analysis of research data, numerical modelling, creation of figures and tables presenting research findings, and first drafts of manuscripts. The co-authors contributed with their ideas and valuable insights, as well as with reviewing the written material, editing and providing comments, feedback and advice towards the improvement and clarity of manuscripts, figures and content. The required co-author authorisation forms related to each future or current publication described above have been provided with submission of this thesis.

# Acknowledgments

I warmly thank and appreciate my principle supervisor Associate Prof. Guillermo Narsilio, for his kind and continuous guidance, caring and patience. Over many high-pressure meetings and discussions, overseas trips and conferences, stressful management of industry partners and suppliers, I believe we are now one small step closer to the renewable and sustainable future.

I would like to thank my co supervisors, Prof. Lu Aye and Dr Asal Bidarmaghz, for their helpful advice, suggestions and support for my PhD. I especially appreciate the patience and expertise that Prof. Aye shown to me when helping me with the EnergyPlus and TRNSYS models. I would also like to thank Prof. Kenichi Soga, Prof. John McCartney for hosting and advising me during my short visit to the University of California, Berkeley and the University of California, San Diego. The support from Prof. Andrew Western, the chair of my supervisory committee is also much appreciated.

I would like to thank Dr Nikolas Makasis, Dr Olga Mikhaylova, Dr Qi Lu, Dr Linden Jenson-Page, Dr Stuart Colls and Brad Donovan who have directly helped me with the project and my thesis. My colleague Gregorius Riyan Aditya deserves special thanks, for being my companion for one month during the construction of the project as well as providing other the valuable discussions and advice.

Finally, I would like to thank all my family and friends. I would definitely now pursuit this far without your love and friendship.

# Contents


1. Introduction ..... 1
1.1. Background ..... 1
1.2. Research Objectives ..... 3
1.3. Thesis Outline ..... 3
2. Hybrid Geothermal Systems and Research Methods ..... 5
2.1. Introduction ..... 5
2.2. Hybrid Geothermal Systems ..... 5
2.3. Research Questions ..... 6
2.4. Methods and Approaches ..... 6
2.4.1. Research Methodology ..... 6
2.4.2. Stage One: Understanding the demand of hybrid geothermal systems ..... 7
2.4.3. Stage Two: Instrumentation and numerical simulation of hybrid geothermal systems ..... 8
2.4.4. Stage Three: Optimisation of the hybrid system ..... 11
3. Experimental set-ups of the hybrid geothermal system in NSW, Australia ..... 13
3.1. Introduction ..... 13
3.2. Previous Experiments on Horizontal GHEs ..... 13
3.3. Experimental Set-up ..... 15
3.3.1. Site location and building description ..... 15
3.3.2. Climatic and geological conditions ..... 16
3.3.3. Configuration of hybrid geothermal system ..... 21
3.3.4. Ground Heat Exchangers ..... 22
3.3.5. Monitoring instrumentation ..... 26
3.3.6. Construction and Installation ..... 31
3.4. Preliminary Experimental Results and Discussion ..... 31
3.4.1. Monitoring Results of the Poultry Shed Building ..... 31
3.4.2. Instrumentation Results from the Horizontal GHEs ..... 33
3.4.3. Laboratory ground thermal cond. measurements ..... 39
3.5. Summary ..... 39
3.6. Acknowledgement ..... 39
4. Improving energy efficiency of a typical poultry shed in Australia ..... 40
4.1. Abstract ..... 40
4.2. Introduction ..... 41
4.3. Energy Efficiency Improvement Options ..... 42

4.3.1. Building envelope ..... 42
4.3.2. Operational schedule and ventilation ..... 43
4.3.3. Energy efficient HVAC systems ..... 44
4.3.4. Summary of findings ..... 46
4.4. Methods ..... 46
4.4.1. Simulation parameters: location, construction, operation and climate ..... 46
4.4.2. Building envelope ..... 48
4.4.3. Energy efficient HVAC systems ..... 48
4.4.4. Farm operations schedule and shed ventilation ..... 49
4.5. Results ..... 49
4.5.1. Heating and cooling loads for different farm operational schedules ..... 50
4.5.2. Effect of the thickness of the building envelope ..... 50
4.5.3. Effect of ventilation/purging ..... 51
4.5.4. Cost estimation for different HVAC systems ..... 52
4.5.5. Operational optimisation under different climate conditions ..... 53
4.6. Discussion ..... 57
4.7. Summary and conclusions ..... 57
5. Artificial neural networks for the performance of horizontal ground heat exchangers under rural industries' loading conditions ..... 59
5.1. Abstract ..... 59
5.2. Introduction ..... 60
5.3. Rural Industries' Heating Loads Patterns and Locations ..... 64
5.4. TRNSYS Simulation ..... 67
5.4.1. TRNSYS Simulation Model ..... 67
5.4.2. Simulation Results from TRNSYS ..... 69
5.5. ANN Models of the GSHPs and GHEs ..... 72
5.5.1. Modelling of the GSHPs with FFNN ..... 72
5.5.2. Modelling of the horizontal GHEs with NARX ..... 74
5.5.3. Learning algorithm, training and testing samples ..... 75
5.5.4. Prediction Results from ANNs ..... 75
5.5.5. COP prediction from FFNN ..... 75
5.5.6. Temperature predictions from NARX ..... 78
5.6. Discussions ..... 79
5.7. Conclusions ..... 80
6. Minimising lifecycle cost and greenhouse gas emissions of hybrid geothermal-solar (PV)-gas heating systems ..... 82

6.1. Abstract ..... 82
6.2. Introduction ..... 83
6.3. Data and Methodology ..... 84
6.3.1. Poultry Shed: Location, Construction, Operation and Climate ..... 84
6.3.2. Hybrid System: Shave Factor ..... 86
6.3.3. Hybrid System: Configuration ..... 87
6.3.4. Hybrid System Components: Efficiency, Pricing and Embodied Emissions ... 87
6.3.5. Lifecycle Analysis and Objective Functions ..... 88
6.3.6. Different Scenarios for Multi-Objective Optimisation ..... 89
6.4. Results and Discussions ..... 90
6.4.1. Heating Cycles of Poultry Sheds in different locations ..... 90
6.4.2. Hourly Coefficient of Performance of the GSHPs ..... 92
6.4.3. Hourly Solar PV Panel Electricity Generation ..... 95
6.4.4. Lifecycle Analysis: Cost and GHG Emission ..... 97
6.4.5. Multi-objective Optimisation: Pareto Front Solutions ..... 99
6.4.6. Pareto Front Solutions for other location and pricing scenarios ..... 101
6.4.7. Applicability of results to other worldwide locations within similar climate zones ..... 103
6.5. Conclusions ..... 104
7. Conclusions and Recommendations ..... 105
7.1. Conclusions ..... 105
7.1.1. Experimental Set-ups for hybrid geothermal heating systems ..... 105
7.1.2. Unique heating and cooling loads for poultry sheds ..... 105
7.1.3. Energy efficient solutions for poultry sheds ..... 106
7.1.4. Numerical simulation of GSHP systems with horizontal GHEs in TRNSYS . 106
7.1.5. Machine learning predictions of the GHEs and GSHPs ..... 106
7.1.6. Lifecycle analyses and multi-objective optimisation of hybrid geothermal-solar-gas systems ..... 107
7.2. Recommendations for future works ..... 107
7.2.1. Further investigation of indoor environment of rural industry ..... 107
7.2.2. Further validation of horizontal GHE models against future observations ... 107
7.2.3. Verification for various climate and ground conditions ..... 108
7.2.4. Application in different industries ..... 108
8. References ..... 109
Appendix A Original publications ..... 117
Appendix B Golder Associate Pty Ltd Reports ..... 151

Appendix C System design and instrumentation drawings .....195
Appendix D Parameters for FEM model .....211

# List of Figures

Figure 1-1 Schematic view of (vertical) geothermal direct\ heating and cooling system [13]. 2

Figure 2-1 Research methods in three stages. 7

Figure 2-2 Schematic hybrid system full scale experimental design. 9

Figure 3-1 Horizontal GHE configurations from the literature: a) Horizontal Slinky [45], b) meandering GHE field [44]. 14

Figure 3-2 Experimental site: a) location, b) top view of the GHE field, c) side view of the shed and existing evaporative cooler fans, and d) inside view of the shed. 16

Figure 3-3 Weather data: (a) Hourly outdoor and ground temperature,(b) Hourly direct normal solar radiation, (c) Hourly global horizontal solar radiation. 17

Figure 3-4 Rainfall by hour. 18

Figure 3-5 Soil report pit 1. 19

Figure 3-6 Soil report pit 2. 20

Figure 3-7 Soil report lab test 21

Figure 3-8 Schematic design drawing (for site pictures, see Figures 3-11, 3-16). 23

Figure 3-9 Hydraulic schematic drawing. 24

Figure 3-10 Construction drawing. 25

Figure 3-11 Ground Heat Exchangers (GHEs) configurations: a) Horizontal straight pipe in trench, b) horizontal straight pipe, c) slinky pipe, and d) “dense” slinky pipe. 26

Figure 3-12 Instrumentation in between trenches (Dimensions in mm). 28

Figure 3-13 Instrumentation for horizontal loops. Pit No. 1 is used to connect all cables and channel them into the central datalogger. 29

Figure 3-14 Instrumentation for far field borehole. 30

Figure 3-15 Instrumentation for pond loops. 30

Figure 3-16 Aerial views of the field while under construction as part of the research project (construction by industry partner Ground Source Systems and others). 31

Figure 3-17 Monitored shed indoor temperature 32

Figure 3-18 Monitored shed indoor and outdoor temperatures on 2nd April 2019 (HVAC system not in operation). 32

Figure 3-19 Monitored far-field temperatures: a) Far-field temperatures with depth, b) Far-field temperatures in comparison with TMY monthly mean and TRNSYS simulated temperatures. 34

Figure 3-20 Monitored ground temperature at different depths (see legend) between Trench 10 & 11. 35

Figure 3-21 Temperatures recorded at the GHEs of GHE Trench No. 8 (Slinky): a) Inlet, outlet and mean fluid temperatures b) Temperature recorded by sensors attached to the pipe c) Location of sensors. ..... 36

Figure 3-22 Temperatures recorded at the GHEs of Trench No. 12 (Dense slinky): a) Inlet, outlet and mean fluid temperatures b) Temperature recorded by sensors attached to the pipe c) Location of sensors. ..... 37

Figure 3-23 Temperatures recorded for Trench No. 10 (Dense slinky) and between Trench No. 10 & 11: a) Temperature measured at 2019-10-08 00:00:00, b) Temperature measured at 2019-10-08 00:00:00, c) Temperature measured at 2019-10-08 00:00:00. ..... 38

Figure 3-24 Thermal Conductivity Test Results from Golder Report (Appendix B). 39

Figure 4-1 TRNSYS simulation model for heating and cooling loads. ..... 48

Figure 4-2 Seven-week summer batch for a typical poultry shed in Central Coast, NSW: (a) Hourly indoor and outdoor air temperatures, (b) Hourly heating and cooling loads. ..... 50

Figure 4-3 Effect of thickness of the building envelope for a typical poultry shed in Central Coast, NSW on (a) annual heating demand , and (b) annual cooling demand. ..... 50

Figure 4-4 One-week cooling loads under discontinuing purging for a typical poultry shed in Central Coast, NSW starting 1st of April (week 14 of the year)..... 51

Figure 4-5 Operational heating and cooling cost with different heating options and locations. ..... 55

Figure 4-6 Annual operational heating and cooling cost distribution with different heating options and locations. ..... 56

Figure 5-1 Diagram of hybrid geothermal systems for poultry shed. Each trench is 75 m long and contains ~300 m of HDPE pipe (highlighted in red). ..... 64

Figure 5-2 Hourly heating demand of the chicken shed: a) yearly loading pattern showing the six batches b) detail of these six heating cycles over one year. ..... 65

Figure 5-3 Chicken industry profile in Australia [108]. ..... 66

Figure 5-4 Schematic drawing of TRNSYS model. ..... 69

Figure 5-5 One hourly heating loads pattern example for a 20-kW capacity ground source heat pump (GSHP): (a) overall yearly load, and (b) detail of the lowest (Batch 1, Jan) and highest (Batch 4, July) GSHP run fraction batch loads. ..... 70

Figure 5-6 Typical TRNSYS simulation results: (a) hourly COP of an individual heat pump, (b) GHE inlet and outlet temperatures, (c) temperatures for the starting of the third batch. ..... 71

Figure 5-7 Correlations between a 2nd year and 10th year. ..... 72

Figure 5-8 Structure of the FFNN model to calculate the COP of a 20 kW GSHP.... 73

Figure 5-9 Structure of the NARX model for GHE. ..... 74

Figure 5-10 Hourly COP from TRNSYS simulation vs ANN prediction (100% shave factor test case in VIC). ..... 76

Figure 5-11 Error distribution for all the testing cases: (a) $COPGSHPhr$, (b) GHE inlet temperature, (c) GHE outlet temperature. ..... 77

Figure 5-12 RMSE for different number of neurons in the hidden layer. ..... 78

Figure 5-13 Hourly GHE temperatures from TRNSYS simulation and ANN: a) GHE inlet b) GHE outlet. ..... 78

Figure 6-1 Chicken industry profile in Australia [108]. ..... 86

Figure 6-2 Schematic representation of a hybrid geothermal-solar (PV)-gas system. 87

Figure 6-3 Hourly heating demand of the poultry shed at Central Coast, NSW: a) Annual heating demand b) Heating demand for the first cycle c) Heating demand for the fourth cycle. ..... 91

Figure 6-4 Images of a full-scale hybrid system being installed in Central Coast, NSW: a) A pipe and trench configuration b) A view of the GHE field c) A top view of the farm. ..... 93

Figure 6-5 Hourly system COP for 50% shave factor in Central Coast, NSW: a) Hourly system COP for the whole year b) Hourly system COP for the first cycle in a year c) Hourly system COP for the fourth cycle in a year. ..... 94

Figure 6-6 Annual system COP under the full range of shave factors for the NSW shed case study. ..... 95

Figure 6-7 Hourly radiation and electricity generation from solar PV panels in Central Coast, NSW ..... 97

Figure 6-8 Lifecycle cost and GHG emission for three scenarios in Central Coast, NSW. 98

Figure 6-9 Pareto optimum solutions for Scenario 1 (no electricity storage, no grid sells) in Central Coast, NSW. ..... 99

Figure 6-10 Pareto optimum solutions for Scenario 2 (farm offset) in Central Coast, NSW. 100

Figure 6-11 Pareto optimum solutions for Scenario 3 (grid sells) in Central Coast, NSW. 100

Figure 6-12 Pareto optimum solutions for three scenarios in Central Coast, NSW.. 101

Figure 6-13 Pareto optimum solutions for average pricing cases in: a) Central Coast, NSW b) Sunshine Coast, QLD c) Mornington Peninsula, VIC. Please note different axis scales for each case. ..... 103

Figure 6-14 World climate map for humid subtropical and temperate oceanic regions [178, 192]. ..... 104

# List of Tables

Table 2-1 Total numbers of different types of sensors. ..... 10
Table 2-2 Types and numbers of control points required. ..... 10
Table 3-1 Pipe and trench lengths for three pipe configurations. ..... 22
Table 4-1 Poultry shed simulation parameters. ..... 46
Table 4-2 Chicken growth and metabolic heat generation. ..... 47
Table 4-3 Selected locations in Australia and their annual average outdoor air temperatures (℃) [109]. ..... 47
Table 4-4 Energy prices for SME in Australia [111, 112]. ..... 49
Table 4-5 Annual cooling and ventilation electricity consumption for a typical poultry shed in Central Coast, NSW. ..... 52
Table 4-6 Heating and cooling cost summary for optimum schedules for GSHP and LPG (gas) heating options in different locations. ..... 53
Table 4-7 Comparison for the average cost saving by switching LPG (gas) to GSHP in different locations. ..... 54
Table 5-1 Summary of published research regarding ANN for GSHP systems. ..... 62
Table 5-2 Typical broiler house dimensions and temperate climate case study location. ..... 64
Table 5-3 Simulation locations and key climate data [166]. ..... 67
Table 5-4 RMSE and MAE for test cases. ..... 76
Table 5-5 Computational time comparison for ANN, TRNSYS and FEM simulation. 80
Table 6-1 Poultry shed parameters. ..... 84
Table 6-2 Chicken growth and metabolic heat generation. ..... 85
Table 6-3 Simulation locations and key climate data for Australia [103, 109]. ..... 86
Table 6-4 Energy prices of gas and electricity for investigated systems. ..... 87
Table 6-5 Initial GHG emission and lifetime for different components. ..... 88
Table 6-6 Parameters for solar PV panel used in this investigation. ..... 96
Table 6-7 Optimum lifecycle cost and GHG emissions under different scenarios and locations. ..... 102

# 1. Introduction

## 1.1. Background

The annual global energy consumption is about 13,000 Millions of tonnes of oil equivalent (Mtoe) (~544 EJ) [1], resulting in nearly 50 Gigatons carbon dioxide-equivalent (CO2-e) greenhouse gas (GHG) emissions. It is widely accepted that our long-term future energy could no longer primarily rely on fossil resources (coal, oil and gas) since these resources are finite, and more importantly the majority of GHG emissions come from burning of these fossil fuels (65%) [2]. The situation is even worse for Australia, with nearly 90% of the energy supplied by fossil fuels. To provide our next generation with a sustainable energy future, alternative approaches must be pursued as soon as possible.

Space heating and cooling comprise a significant part (40%-50%) of the overall final energy usage [3], resulting in 20 Gt CO2-e GHG emissions. By using advanced technologies (e.g. energy efficient HVAC systems, well-insulated construction materials) for space heating and cooling, up to 1,509 Mtoe of global energy annual consumption could be reduced by 2050 [4]. To develop sustainable buildings and improve energy efficiency in existing buildings, several approaches are being considered, including increasing the energy efficiency of Heating, Ventilating, and Air Conditioning (HVAC) systems and determining suitable operational schedules.

In Australia, the agriculture and its add-on processing industry constitutes a significant part of its economy, comprising 12% of Australian total Gross Domestic Product (GDP) [5] [6]. Within this industry, nearly 600 million birds are raised annually for producing chicken meats [7]. One typical poultry shed provides about 200,000 chickens a year. Therefore, it is estimated that there are currently about 3,000 poultry sheds for chicken meat in Australia. The overall heating and cooling costs for poultry farms are estimated to be $ 80 million per year.

To raise chicken/broiler efficiently, poultry sheds are designed to meet specific requirement for chickens during different stages. The indoor temperature is a vital factor for the chicken to grow properly in an efficient timeframe. Within each growing cycle, typically lasting less than 60 days, the indoor air temperature requirement changes from 33°C at the beginning of the cycle to 21°C in the end, which results in a unique heating/cooling loads cycle depending on the start date. These heating/cooling loads cycles can have unique characteristics that are highly different from other residential and commercial buildings, including highly imbalance of heating and cooling, sharp peak demands, as well as shortly (~weeks) alternating heating and cooling cycles [8, 9]. Meanwhile, since outdoor temperature changes, a considerable amount of energy is sometimes needed to maintain the required indoor air temperature (i.e., to reach 33°C in winter). Researchers have conducted building energy simulations for poultry sheds for the heating/cooling load cycles in recent years [10, 11]. However, different agricultural practices among countries (i.e., construction materials, operational schedules) and the various climate conditions of the poultry sheds results in highly varying heating/cooling demands.

Ground source heat pump (GSHP) is a widely used renewable energy technology and has been employed in many parts of the world for space heating and cooling [12-14]. As shown in Figure 1-1, the principles for ultilising direct geothermal energy via GSHP is as follows: The ground temperature deeper than the seasonal fluctuation depth is more stable than the ambient air temperature year-round. At around 10 m below the surface, the ground temperature is nearly constant throughout the year. Therefore, during winter, the ground temperature is higher than the outdoor air temperature, which means the ground could be employed as a heat source (the heat can be extracted via GSHPs and ground heat exchangers - GHEs). In summer, the ground is cooler than the atmosphere and can work as a heat sink, accessible via GSHPs and GHEs. In China, US, and Europe, large capacities of GSHPs have been installed [15, 16]. In Australia, this geothermal energy technology only comprises a small portion of the overall market [13, 17]. One factor that drawbacks wide application of GSHP systems is the high initial installation costs and its associated GHG emission. However, these costs and GHG emission can be reduced by coupling GSHPs with other energy technology to form a hybrid system [18-21]. Previous studies indicated that a hybrid geothermal system could not only be financially attractive, but also help to balance the energy extracted and injected in the ground [22-24]. In this investigation, gas heaters (boilers and burners) can be integrated with GSHP systems due to their relatively low installation costs. To further reduce the operating costs of GSHP systems, renewable solar PV systems can be utilised to offset the electricity consumed by the GSHP systems, which can also help reduce GHG emissions.

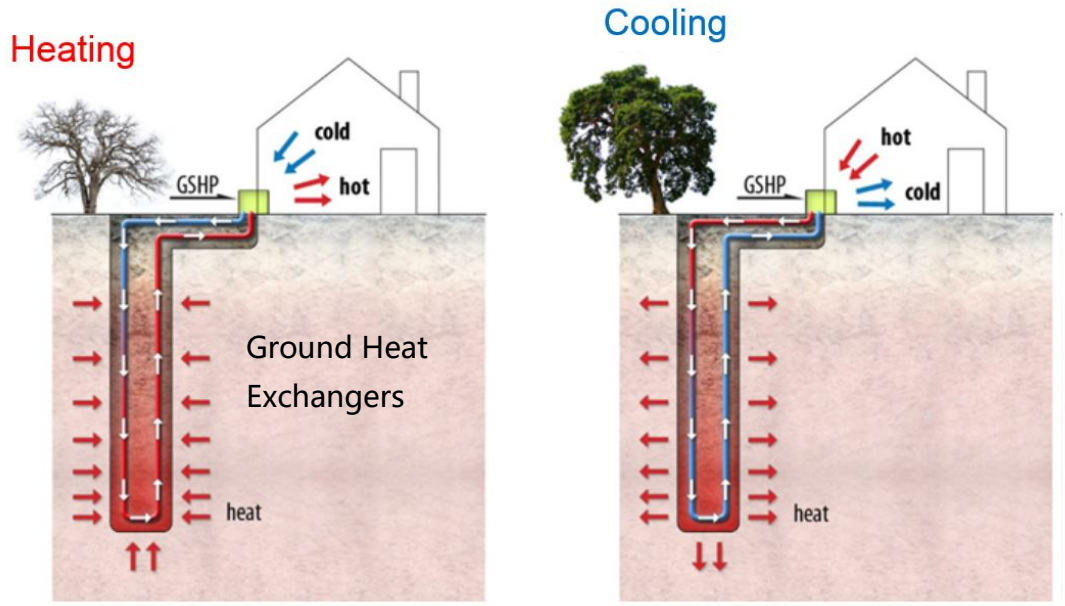


Figure 1-1 Schematic view of (vertical) geothermal direct\ heating and cooling system [13].

For the GSHPs, the GHEs are vital component that impacts the performance of GSHPs. There are different forms of GHEs, including vertical boreholes, horizontal trenches, energy piles, energy retaining walls and energy tunnels [25]. Among them, vertical boreholes and horizontal trenches are the two most commonly utilised GHEs. For horizontal ground heat exchangers, those where geo-loops are embedded in shallow (1-1.5 m deep) trenches, there is only very limited applications in Australia (only a few

dozens of systems have been installed) [15]. Most of the applications in Australia are based on vertical boreholes (e.g., vertical ground heat exchangers – as schematically shown in Figure 1-1), as it requires less land area to be installed. However, for the rural industry, in particular for agriculture, there is usually sufficient land to use. Hence, the more economical horizontal geothermal system would be the more desirable option as its construction cost can be much less than vertical boreholes [25]. As the heating and cooling loading pattern demand has a significant influence on the induced long-term ground temperature, hence the thermal performance of the ground heat exchangers, it is important to investigate the performance of horizontal GHEs when used for poultry sheds.

This PhD research investigates a hybrid geothermal system with horizontal ground heat exchangers for typical poultry sheds in Australia. A full-scale installation at the Central Coast, NSW is available for verifying and showcasing the findings. Only very limited studies have been undertaken for the utilisation of geothermal energy in agricultural settings and no horizontal geothermal system for the poultry sheds has been investigated in detail [10, 11]. With some experimental data arising from a fully instrumentation site, this research will provide valuable information regarding the performance of the hybrid geothermal system under rural industries' unique loading condition to both the rural industry and the geothermal and solar industries. Furthermore, numerical models for both the building side and ground component were developed and validated with this dataset, which are also valuable for the industries. The knowledge boundary in this area can be further pushed upon the optimisation of this hybrid geothermal-solar-gas system. Various influential factors for the system will be evaluated to identify the importance of these factors on the system and the optimum design based on financial and environmental considerations will be suggested.

## 1.2. Research Objectives

This PhD aims to contribute to knowledge about hybrid geothermal systems for the poultry industry. To achieve the research aim, four research objectives have been identified as follows:

a. To investigate the heating and cooling load patterns for a typical poultry sheds in Australia in order to size, design and install a full-scale hybrid geothermal heating system.
b. To instrument its horizontal ground heat exchangers and the hybrid geothermal systems itself for a above typical poultry shed to understand the performance of these systems and provide a dataset for model validation.
c. To develop a detailed numerical model for horizontal ground heat exchangers and to derive computational efficient simplified models to further study and understand the performance hybrid geothermal heating system.
d. To conduct multi-objective optimisation for hybrid geothermal systems for the poultry industry in Australia, and thus provide guidelines for reduction of cost and carbon emission for both geothermal and poultry industries.

## 1.3. Thesis Outline

There are seven chapters and four appendixes in this thesis, including this introduction chapter. In this study, detailed literature reviews are included in each chapter.

Chapter 2 provides an overview of current states of hybrid GSHP systems and the potential application of horizontal GHE systems in rural industries, especially for the poultry industry. The research methods are also introduced in this chapter, while more specific methods are included in each self-contained core chapter.

Chapter 3 discusses the experimental set-up of the hybrid GSHPs with horizontal GHEs in Peats Ridge, NSW, Australia. The explanation and discussion are also made while presenting dataset that are currently available.

Chapter 4 evaluates heating and cooling loads as well as the energy efficient solutions for the rural, especially the poultry industry. Different HVAC systems, building envelopes, ventilation strategies and farming operational schedules (in this thesis, refers to raising batches of chicks) are analysed. The optimum ventilation strategies and operational schedules are also proposed for this study.

Chapter 5 focuses on the numerical simulation of the GSHPs and horizontal GHEs. Firstly, a simulation model in TRNSYS is developed. Then, different Artificial Neural Networks (ANNs) are developed and trained with the simulated datasets from the TRNSYS model. The performance and computational speed of the ANNs are then evaluated against the TRNSYS model and a FEM model.

Chapter 6 presents a multi-objective optimisation of the hybrid geothermal-solar-gas systems. Two objective functions, i.e. the 40-y lifecycle cost and 40-y lifecycle GHG emissions, are considered. The Pareto optimum solutions for these systems are then presented while considering three different scenarios for the usage of electricity generated by Solar PV panels.

Chapter 7 concludes this study and presents the recommendations for the future works.

# 2. Hybrid Geothermal Systems and Research Methods

## 2.1. Introduction

Direct geothermal energy is a type of the thermal energy in the ground accessible within shallow depths. There are many advantages and benefits for direct geothermal energy, including its applicable flexibility, renewability and high energy efficiency. One common form of its utilisation is through ground source heat pumps. Recent years have witnessed a growing public interest in this energy resource, which intrigues its potential application in the rural industry. However, some challenges also arise when considering its optimum design under complex and unique conditions. Therefore, detailed attention must be paid when deciding the research methods and approaches for this study.

This chapter firstly introduces hybrid geothermal systems as an attractive option to deal with the challenges in utilising the direct geothermal energy for rural industry. Attentions are later drawn to three research questions that the study aims to answer. Then, the research methodology used in this study is illustrated. Lastly, detailed methods and approaches are discussed in three stages.

## 2.2. Hybrid Geothermal Systems

As explained in the introduction chapter, a ground source heat pump (GSHP) system provides low-carbon outcomes for space heating and cooling, extracting thermal energy from the ground when operating in heating mode, and dissipating heat into the ground when in cooling mode [13]. The GSHP systems have been used for a number of applications worldwide, including for both residential and commercial buildings and have also been introduced for the heating of poultry sheds in recent years [10, 15, 16, 26, 27]. Drawbacks of GSHP systems include high upfront construction costs, typically the GHE installation costs, as well as the embodied energy and associated GHG emissions. These may sometimes lead to even higher lifecycle GHG emissions when compared to traditional oil and gas systems, especially in unmatured markets [28, 29]. However, it can be improved by coupling GSHPs with other energy sources to form a hybrid system [18, 19, 22-24, 30-33]. Previous studies indicated that a hybrid geothermal system could not only be financially attractive, but also help to balance the energy extracted from and injected into the ground [22-24]. In this study, for example, gas boilers and gas burners have relatively low installation costs and can be integrated with GSHP systems. To further reduce the operating costs of GSHP systems, renewable solar PV systems can be utilised to offset the electricity consumed by the GSHP systems, which will also help reduce GHG emissions.

There are typical two types of solar collectors, the solar PV panels which convert the solar energy directly to electricity and the solar thermal collectors which convert the solar energy to thermal energy [34]. From previous studies, even though the solar thermal collectors are commonly used to boost the performance of the GSHP by up to 10% [33, 35-38], the benefits are significantly less than for the solar PV (up to 100% operating cost savings) [39]. Therefore, in this study, only the solar PV will be employed and analysed. By combining these three sources of energy - hybrid geothermal-solar-gas system - reduced costs and GHG emissions can be achieved [40, 41].

## 2.3. Research Questions

The hybrid geothermal-solar-gas system could be promising to be utilised in the poultry sheds in Australia. However, since a very limited number of previous studies have been conducted to investigate GSHP systems with horizontal GHEs under rural industries' loading conditions, three research questions have been proposed for the optimum design of the hybrid geothermal-solar-gas systems with horizontal GHEs.

**One:** The energy demand cycle for the poultry shed is entirely different from the residential or the commercial properties. Even though the geothermal energy is a highly flexible renewable energy resource and could be utilised under most circumstances, it is essential to determine the heating and cooling loads for optimum design of such hybrid geothermal systems. In this study, the first research question is "***What is the unique energy demand cycle for poultry brooder houses in NSW, part of the Australian rural industry?***" The building simulation software package TRNSYS would be utilised to investigate this issue in detail.

**Two:** In order to optimise this hybrid geothermal system, computational models with reasonable accuracy must be developed. The models will also help to achieve a better understanding of the ground component and the associated equipment. Hence, the second research question will focus on "***How can the simulation model for the hybrid horizontal geothermal system be developed and validated?***" The proposed approach to answering this question includes a detailed simulation of the ground component with COMSOL Multiphysics and TRNSYS as well as Artificial Neural Networks for fast prediction. Details of these models will be illustrated in next section.

**Three:** When utilising the hybrid geothermal systems, the financial factor is normally the priority while reasonable attention should also be drawn to the environmental aspects. Therefore, it is important to undertake the multi-objective optimisation considering both the economic and the environmental factors. The last research question here is "***To what extent can a hybrid horizontal geothermal system be optimised for poultry sheds based on financial and environmental considerations?***" Lifecycle analysis regarding the cost and GHG emissions will be conducted to answer this question. Multi-objective optimisation considering these two factors will be conducted with different variables and constraints being considered.

## 2.4. Methods and Approaches

### 2.4.1. Research Methodology

This research was conducted in three stages as shown in Figure 2-1, covering various aspects including investigation of energy efficiency solutions for the rural industry, numerical simulation and experimental instrumentation as well as multi-objective optimisation. The research methodology is briefly explained as follows.

As depicted Fig. 2-1, a building energy models were developed to estimate the heating and cooling loads of a typical poultry shed in Peats Ridge, NSW, Australia. Later, by considering the heating and cooling loads together with field data (soil properties) obtained, the design and instrumentation for this hybrid system were undertaken. After the design was finalised with industry partners and clients, the installation for this system together with the instrumentation and control system were materialised.

Further computational works including Artificial Neuron Networks (ANNs), detailed numerical modelling of horizontal GHEs and updated building energy model were then developed. Later, after field data being collected, the models will be verified. It is worth noting that while ANNs can predict the results almost instantly, it usually lacks the high accuracy as the detailed ground component simulation model. However, detailed simulation can be computationally expensive and may not be used directly for the optimisation. Therefore, Artificial Neuron Networks were proposed to accelerate this process with marginal sacrifice of accuracy. Moreover, a verified model for horizontal GHEs can provide a valuable dataset for the long-term performance of the hybrid horizontal geothermal system under this condition, which perfectly amends the disadvantage for the building energy model. At last, the multi-objective optimisations were pursued, considering both financial and environmental aspects.

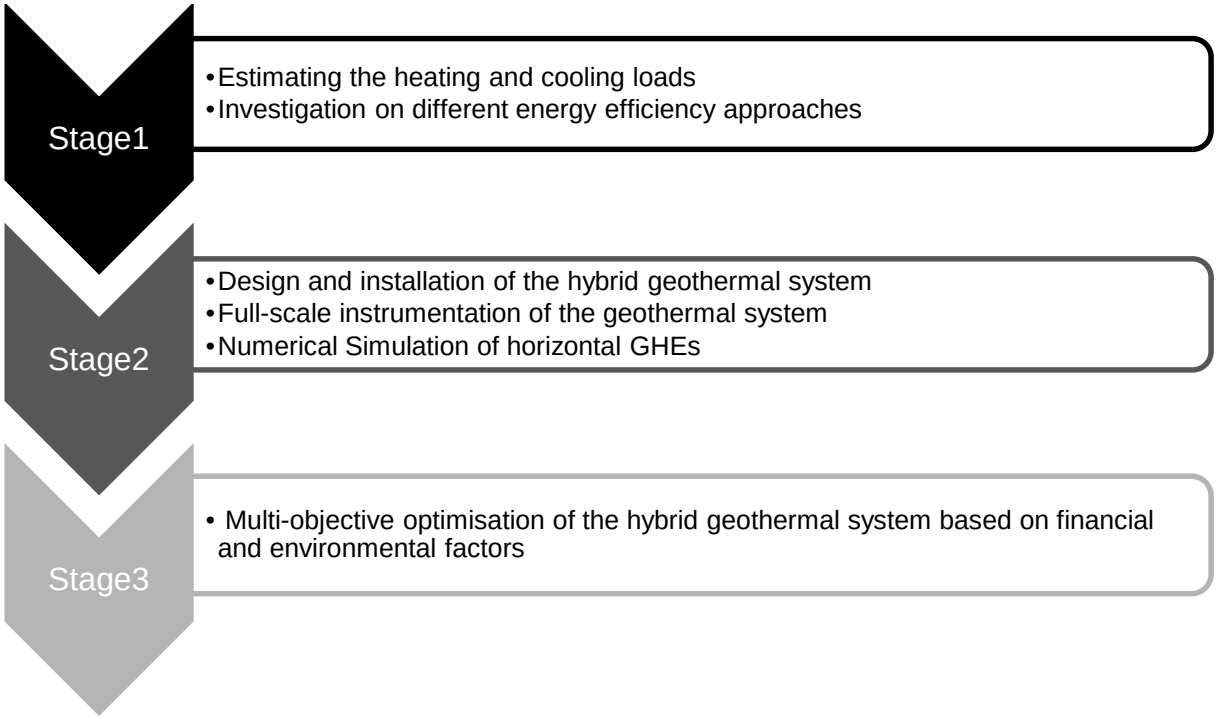


Figure 2-1 Research methods in three stages.

### 2.4.2. Stage One: Understanding the demand of hybrid geothermal systems

The work for stage one is to understand the demand of the hybrid geothermal systems. There are two primary objectives for this stage:

The first one is to estimate the heating and cooling loads for the poultry sheds (chicken broiler house). A detailed energy model regarding an exemplary property located in NSW in TRNSYS (Transient System Simulation Tool), a widely-used and well-recognized building energy simulation software package, has been developed for this purpose. There are several parameters that have been considered for the simulation, including the location of the poultry shed, climate conditions, heat generated by the chickens of different age, construction materials of the poultry shed, the varying set point temperatures and the ventilation rates of the shed. The model is verified by the comparison between the actual energy bill of the poultry shed from the farmer and the heating and cooling cost estimated from TRNSYS simulation results and shows a reasonable accuracy.

Based on the heating and cooling loads, the second task is the investigation of different energy efficiency solutions for the rural industry. Four different potential approaches have been investigated, including different HVAC systems, operational schedules, ventilation strategy as well as building envelopes. The annual operational costs for heating and cooling were calculated to evaluate these approaches.

#### 2.4.3. Stage Two: Instrumentation and numerical simulation of hybrid geothermal systems

The second stage of this work includes design, installation, full-scale instrumentation of such a system in a poultry brooder house (in collaboration with the industry partners) and the numerical simulation of the geothermal system. There are three objectives for this stage:

The first objective is the design and installation of the hybrid horizontal geothermal system. The sizes of different components (i.e. GSHPs, gas boilers and burners) within this hybrid geothermal system were decided based on the preliminary financial analysis and available field data [9]. Once the capacity of the Ground Heat Exchangers (GHEs) based on modelling and preliminary field data has been decided, a detailed design of the geothermal system was conducted, which includes determining the type, length, and configuration of the ground loop, connections and distribution of the heat pumps and the operational control for the hybrid system. Upon the detailed design plan being negotiated with the client and the industry partners, the hybrid solar-geothermal-gas system was installed to the designated poultry house, which is one shed out of eight at Peats Ridge (NSW).

As shown in Figure 2-2, the proposed design includes a solar PV panel system for providing electricity. A buffer water tank of 1,500 Litres total capacity was also installed, connecting the building side and the GSHPs, in order to prevent frequent turning on and off of the GSHP. Four identical GSHPs were installed, each of them will be connected to different ground loop configurations, which includes horizontal systems of different pipe density, a slinky system and a surface water system (in a pond). Hence, by applying the same thermal load distribution to the heat pumps, the performance of different configurations of the GSHP systems can be studied.

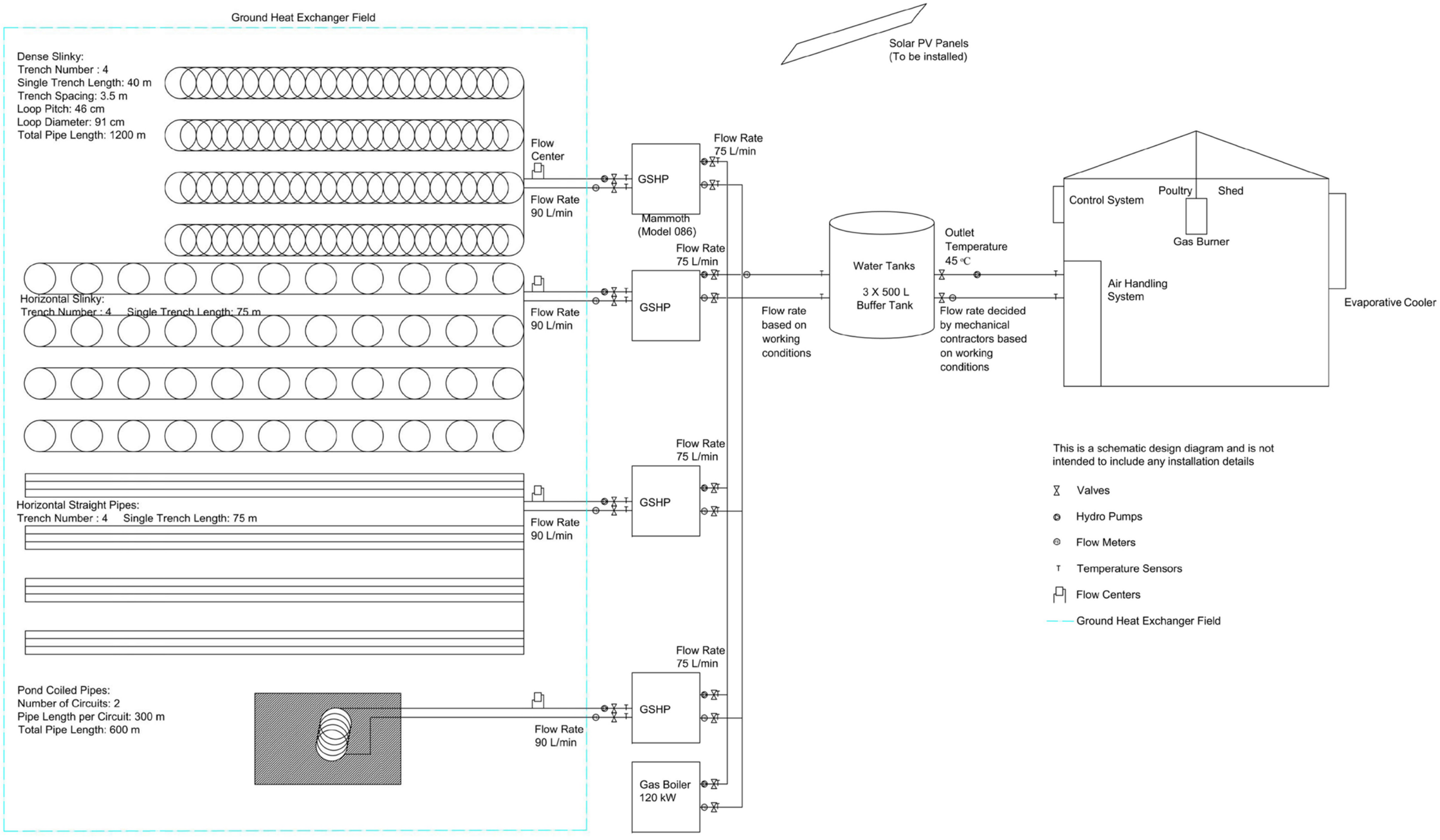


Figure 2-2 Schematic hybrid system full scale experimental design.

The second objective of this stage is to complete full-scale instrumentation of the hybrid geothermal system, for which the data to be monitored includes far-field ground temperature, temperatures along the GHEs, ground temperature in between the GHEs (to assess thermal interference between the GHEs in a GHE fields). Various instrumentation points have been shown in figure 2-2 and further instrumentation details are available in chapter 4. Table 2-1 shows the number and types of sensors required for the instrumentation.

Table 2-1 Total numbers of different types of sensors.

| **Type of Sensors** | **Number** |
|---|---|
| Temperature Sensor | 170 |
| Flow Meter | 11 |
| Gas Meter | 2 |
| Power Meter | 4 |
| TDR Water Content Transducer | 8 |
| Weather Station | 1 |
| Data Logger | 1 |

Meanwhile, control systems, as shown in Table 2-2, will also be installed to allow individual GHEs and/or pipe loops within the GHEs to be shut off with remotely operated actuator valves (to also assess the actual radius of influence, partly by also using the closed off GHEs as ground temperature monitoring points), and different circulation pumps and header valves will be used to vary flow rates. The weather data and geothermal characteristics, including the temperature profile, will also be assessed. This data set will provide important experimental information with respect to the overall physical performance of horizontal geothermal systems. This data will be contrasted with numerical modelling results towards building confidence on modelling validation and calibration.

Table 2-2 Types and numbers of control points required.

| **Equipment Requiring Control** | **Number** |
|---|---|
| Water to Water Heat Pump | 4 |
| Hydro Water Pump | 11 |
| Valves | 11 |

The third objective is to develop and verify the numerical models for the hybrid geothermal systems. There are two different models for the GHEs in this study.

The first model is a GSHP system model in TRNSYS. This model aims to provide comprehensive analyses of the whole GSHP systems by coupling the governing equations for heat and mass transfer and the prevalent physics in GSHP systems. A yearly Typical Meteorological Year (TMY) dataset was used as the boundary condition of the soil surface. The soil is then meshed three-dimensionally, and a fully implicit finite difference method is used in the model.

A machine learning approach could also be adopted to save the computational expenses of the TRNSYS models. An artificial neural network (ANN) is a mathematical approach that simulates a network of artificial neurons to mimic the human brain. With a well-trained ANN, the computer can be taught to solve problems, including generalisation, classification, forecasting and even decision making [42]. In this study, two ANNs are developed and implemented within MATLAB: i) a feedforward artificial neural network is used to predict the performance of the GSHPs and ii) a NARX (nonlinear autoregressive network with exogenous inputs) network is used to predict the inlet and outlet temperatures of the horizontal GHEs. The ANN models are used to provide instant and robust results with high accuracy.

#### 2.4.4. Stage Three: Optimisation of the hybrid system

The overall goal for utilising the geothermal system is to minimise the lifecycle cost together with the GHG emission. To achieve this goal, different optimisation parameters, constraints as well as the objective functions are presented as followed:

**Optimisation parameters**

Two different types of parameters for optimisation are considered here:

1. Size of the GSHP components

   As this system is a hybrid system, factors for energy resources are the key parameters for the optimisation:

   $$\alpha_{Geo} + \alpha_{LPG} = 100\% \qquad \text{(Eq. 2-1)}$$

   where, $\alpha_{Geo}$ is the fraction of geothermal energy, $\alpha_{LPG}$ is the fraction of energy provided by LPG/gas.

2. Size of the Solar PV components

   The solar PV panels are installed to provide electricity for the GSHP systems. Different scenarios including offsetting the electricity by other type of equipment in the farm as well as selling it to the grid are also considered in this study.

**Constraints for the optimisation**

1. Heating loads

   The heating loads pattern for the poultry shed is the primary constraint since the optimisation considers heating only, which is subject to the temperature requirement within the building. The reason that cooling is not considered is that the current evaporative coolers are very cost effective to run, leaving almost no potential to reduce the cooling operational cost by switching to other systems. This will be explained in detailed in Chapter 4 and a batch schedule operational strategy to reduce to heating and cooling cost will be proposed.

2. Climate condition

   The climate condition affects the performance of the solar PV as well as the ground temperature, which influences the performance of the GHE. Here, the climate data is a TMY (Typical Meteorological Year) data for one year. Despite the fact that the climate condition is not technically a parameter for optimisation,

several different climate data will be used to check the validity of the optimisation representing different cases/locations as to generalise or highlight applicability of this technology under different climatic conditions (e.g., would geothermal system become a better option on a cooler climate?).

3. Ground Properties

   The soil properties limit the performance of GHEs as well. At the same time, the land and space availability impact the trench length as well as the distribution of the pipes.

4. Investment Cost

   As the funding is limited, the initial capital cost should be considered as budgeted. Meanwhile, the ongoing cost for the hybrid system should at least be less than the previous ones.

**Objective functions for optimisation**

The last stage of this work will focus on the optimisations of the hybrid horizontal geothermal system based on economic and environmental factors. To achieve this goal, firstly, lifecycle analysis (for GHG) and lifecycle cost analysis for the hybrid geothermal system will be conducted. Accordingly, two different objective functions will be employed for the optimisation. The first one will focus on the financial part, i.e. minimising the lifecycle cost, while the second one will aim the environmental part to minimise the lifecycle greenhouse gas emission. The result of this optimisation will answer the last research question "How can a hybrid horizontal geothermal system be optimised for the rural industry based on economic and environmental factors?" as well as to provide a better understanding of the geothermal system. The detailed objective functions for the Lifecycle Cost and GHG Emissions are shown below:

1. Lifecycle Cost in Net Present Value [43]:

$$LCC = C + \sum_{n=1}^{t} C_r \left( \frac{1}{1+d} \right)^n \qquad \text{(Eq. 2-2)}$$

where, C is the initial capital cost, $C_r$ is the recurring cost in a time period, d is the real discount rate, and t is the project lifetime in years.

2. Lifecycle GHG Emission [43]:

$$LGE = ME + \sum_{n=1}^{t} OE_n \qquad \text{(Eq. 2-3)}$$

where, LGE is the lifecycle GHG emission, $ME$ is the manufacture GHG emissions, $OE_n$ is operational GHG emission in year n, t is analysis period.

# 3. Experimental set-ups of the hybrid geothermal system in NSW, Australia

## 3.1. Introduction

In order to achieve the research aims, a full-scale experimental study of a hybrid geothermal system with horizontal GHEs has been proposed (see Chapter 2). The 200-kW hybrid system (80 kW from Geothermal Energy and 120 kW from LPG) for an existing poultry shed building located at Peats Ridge, NSW, Australia was designed and selected as an experiment for this study. A total length of 4.8 km of HDPE pipes were buried as heat exchangers in 12 horizontal trenches, each at 1.5 m depth below the ground surface and 4 groups of loops in a pond nearby, at the depth of about 4 to 6 m below the water surface (actual depth varying by season due to the change of water level). This system was designed in 2017 and the construction of this system happened from March 2018 to May 2019. The monitoring of this system starts from early 2019. However, due to an unfortunate outbreak of Salmonella, the farm has been strictly regulated and the system is not in full operation since Q2 2019 until the end of 2019. Hence, only limited monitoring data for the field and the short test run is presented. The system, however, will continue to serve as an experimental bed for future works.

This chapter describes the design, instrumentation and construction of the hybrid geothermal system, including the set-up of the monitoring system installed to record the performance of this hybrid system and thermal interaction with the ground and pond. The analysis and discussions in this chapter help to explain the assumptions made in Chapter 4, in which we focus on operational costs of heating and cooling poultry sheds. In this chapter, the main observations made during the two-month monitoring are presented and discussed. Some of these results are subsequently used further in the thesis.

## 3.2. Previous Experiments on Horizontal GHEs

Field experiments are vital for determining the thermal performance of the horizontal GHEs and their associated GSHP systems. There are limited amount experimental works regarding horizontal GHEs, which are discussed next.

The thermal performance evaluation of two GSHPS systems with horizontal GHEs in Fırat University, Turkey (38.41° N, 39.14° E) were conducted [44]. As described in the paper, the two systems each have 50 meters of pipes with 0.3 m of pipe separation and 0.016 m nominal diameter, and 15 $m^2$ spacing, buried at 1 m and 2 m deep [44]. The average COP (coefficient of performance) of the tested horizontal system has been measured and reported. For a trench of 1 m depth, the COP for heating is reported to be 2.66, and for 2 m depth, it increased to 2.81. However, this COP is relatively low for a geothermal system (usually more than 3), the authors attributed this to a poor design of the system. Despite that, the horizontal GSHP system still has a better thermal performance than typical Air Source Heat Pump (ASHP) system. They stressed that pre-design analysis is necessary for optimal design. One shortcoming is that soil properties have not been reported in this work. Since soil properties include thermal conductivity,

which influences the thermal performance of the system, the understanding of soil property in the site is vital for any further numerical simulation used for back-analysis.

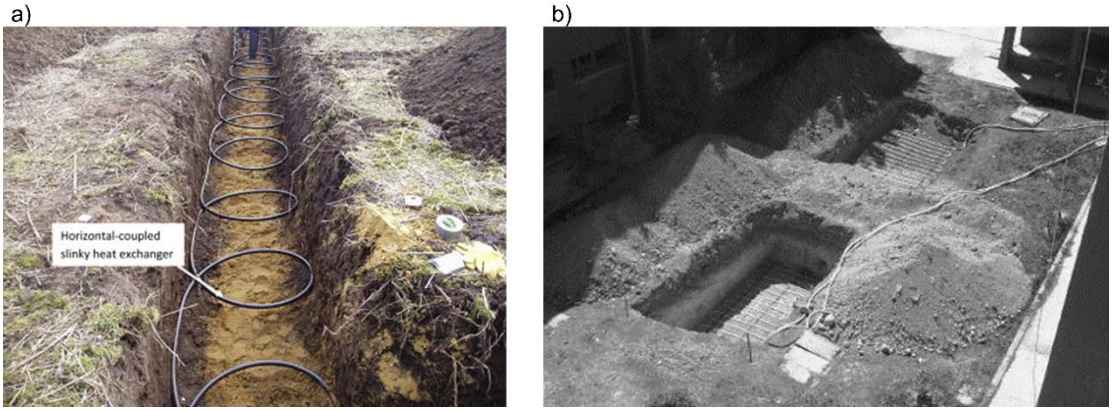


Figure 3-1 Horizontal GHE configurations from the literature: a) Horizontal Slinky [45], b) meandering GHE field [44].

Wu et al. (2010) [45] have conducted experimental and numerical work regarding the thermal performance of a slinky-configured horizontal GSHP system in the UK at a purposed-constructed experimental site. In the experimental part, four horizontals slinky GHEs were installed in an 80 by 20 m area at the depth of 1.2 m. They have measured the system performance and ground temperature distribution for a two-month period. Their results showed that the system COP was slightly decrease from 2.7 to 2.5 after two-month continuous heating operation and the ground temperature ceased to fluctuate with ambient air temperature at the depth of 0.5 m. The site soil properties have also been measured. With a low average thermal conductivity of 1.24 W/m K, it can explain the low performance of the horizontal GHEs. Comparing to Inalli and Esen (2004), Wu et al. can provide more useful information for understanding the performance of horizontal GHEs.

Based on the work in Wu et al. (2010), Wu et al. (2011) developed a transient 2D model to predict the thermal performance of a horizontal-coupled heat exchanger and surrounding soil under different ambient air temperature, soil thermal properties and wind speed [46]. It is noted that the soil temperature at a certain distance from the centre of the heat exchanger vertically has a lower temperature in the horizontal direction due to the influence of the cold ambient air. The author also suggested that soil had higher thermal conductivity had higher specific heat transfer. It is then reported that there was no significant impact of different wind speed. The significant impact of the soil conductivity on the performance of horizontal GHEs was further verified through another numerical study [47]. It was found that the soil conductivity is significant on the performance of GHEs. The study showed that increased soil thermal conductivity could increase the heat exchanger rate regardless of the configuration of horizontal GHEs. Additionally, the impact of the difference between the inlet and outlet fluid temperature on the performance of the horizontal GHE has been studied via another numerical study with experimental verification [48]. Meanwhile, Xuedan et al. (2012) [49] studied the parameters that influence the performance of horizontal GHE under cold climate. It is suggested that the optimal highest inlet temperature should be kept lower than 30 °C. However, the study mainly focused on the cold region and the results may not be applicable under other climate conditions.

More recently, an experiment of horizontal GHEs was carried out at Northern Tunisia to test its performance [50]. The experiments focused on the space cooling efficiency by comparing the outlet fluid temperature with a variety of inlet fluid temperature from 30°C and 50°C. The horizontal GHE had 25-meter of length and was buried at 1-meter depth. The results indicated that the horizontal GHE was able to meet 38.5% of the total cooling requirement with 12m$^2$ area. The coefficient of performance of the heat pump was further estimated in another publication by the same research team, and a high average value of 4.25 was reported [51]. It revealed that the horizontal GHE worked appropriately under the current geothermal condition at Northern Tunisia for space cooling.

In Australia, Kivi (2015) [52] has instrumented two properties with a geothermal system. One horizontal system for a residential building located at Main Ridge, Victoria and one vertical system for the Walter Boas Building at the University of Melbourne. For the horizontal GHE, there are 4.9 km of pipe buried in two GHE filed, providing both 70 kW for heating and cooling. The configuration is (dense) slinky, with about 1 m diameter, 0.5 m loop pitch and 2 m of spacing between adjacent loops. There are 4 loops with about 1.4 m loop pitch as a comparison. Various datasets including the ground temperature at different depths, flow rates and power consumption have been collected for further use.

To summarise, there is only limited experimental data available for horizontal geothermal systems, and even less to none for the rural and poultry industries' farm operational conditions. Furthermore, previous experiments primarily focused on small scale experimental sites, which typically operates under well-defined experimental conditions not always mimicking real life conditions. A rare exception is the instrumentations and monitoring on Kivi (2015)'s work, which focus on one residential and educational properties. The unique rural poultry sheds loading characteristics are highly different from other residential and commercial buildings, including highly imbalance of heating and cooling, sharp peak demands, as well as shortly (~weeks) alternating heating and cooling cycles. In order to conduct optimum design for the poultry sheds, well-planned instrumentation is needed and important, as the dataset acquired from the field is essential for the model verification and adjustment.

## 3.3. Experimental Set-up

### 3.3.1. Site location and building description

The experimental hybrid geothermal-solar-gas system was installed in an existing poultry shed building. The poultry shed building investigated in this study locates in Peats Ridge, NSW 2250, Australia, a ridge suburb at about 100 km north of Sydney (Figure 3-2 a). The longitude and latitude coordinates of this building are about 33°21'18.4"S 151°14'11.9"E.

This building was constructed in 2015 and is one of the eight poultry shed buildings within a large farm. The width and depth of this building is about 18 m and 137 m, which makes a total floor area of about 2500 $m^2$. The roof of the shed is a side gable type roof, with a maximum height of 4.6 m in the middle and the minimum of 2.3 m at the edges. The construction material of this shed is 'Coolroom' Wall (thickness: 75 mm, thermal

conductivity: 0.039 W $m^{-1} \cdot K^{-1}$, density: 16 kg $m^{-3}$, specific heat: 340 J $kg^{-1} \cdot K^{-1}$). There are no windows in the building, but multiple fans and funnels are available for controlled ventilation (as shown in Fig 4-2 b, c, d). Inside this building, this is only one whole area for the chicken to live and grow. The current HVAC system for this building is gas burners for heating (6 burners with about 400 kW total heating capacity) and evaporative coolers for cooling. Three thermistors have been installed inside the shed to monitor the indoor temperatures.

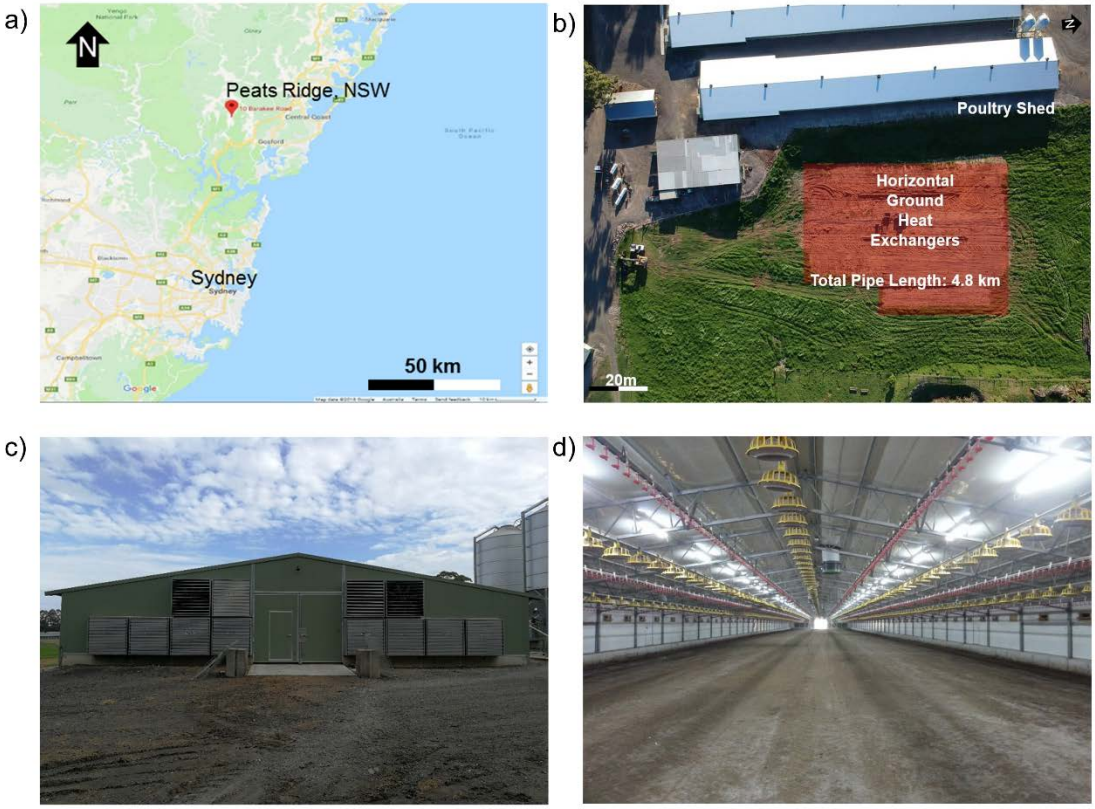


Figure 3-2 Experimental site: a) location, b) top view of the GHE field, c) side view of the shed and existing evaporative cooler fans, and d) inside view of the shed.

### 3.3.2. Climatic and geological conditions

As Australia has a vast land crossing a variation of longitudes and latitudes, the climate variation in the country is high. In Peats Ridge, NSW, it is oceanic climate, which is very changeable and often overcast throughout the year [53]. With Meteonorm, a widely used climate software, a typical meteorological data was generated from 20 years of recorded data in the software database [54]. Based on this TMY data, an analysis were made and shown in  and .

Form these results, the maximum temperature happens in mid-January, which is 35.8 °C, and the minimum temperature happens in mid-July, which is 2.3 °C. The variation of the monthly mean dry bulb temperature is form 10 °C in July to 21 °C in January. The ground temperature (at one m depth) showed a same but more stable trend, with the maximum of 17 °C in January and the minimum of 13 °C in August, September and October. This temperature difference illustrates the advantage of the GSHPs as the

ground temperature is relatively stable throughout the year and is lower than the atmosphere in summer and higher than the atmosphere in winter.

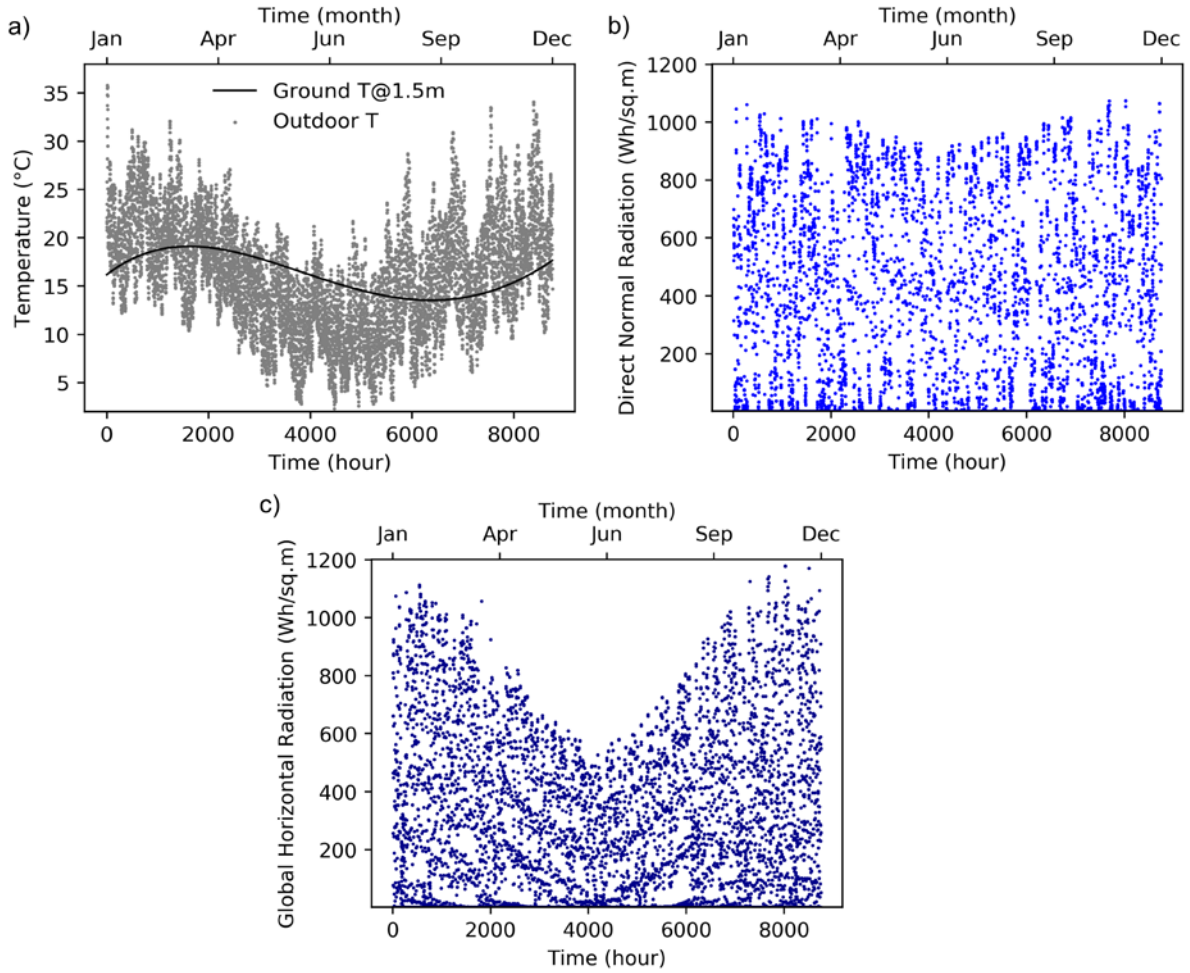


Figure 3-3 Weather data: (a) Hourly outdoor and ground temperature,(b) Hourly direct normal solar radiation, (c) Hourly global horizontal solar radiation.

For the solar radiation (Fig 3-3 b,c), the same trend as the temperature applies here. It can be seen that the maximum solar radiation happens in November, which is nearly double than the lowest in Jun. This change in radiation is mainly caused due to the global horizontal radiation, which is highly affected by the angle of the earth Polaris axis to the earth orbit around the sun.

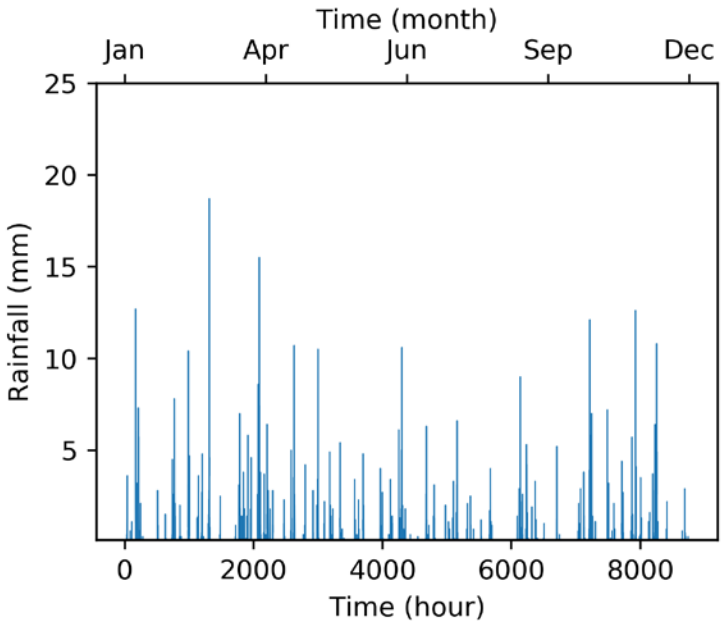


Figure 3-4 Rainfall by hour.

Additionally, rainfall can be an important factor that influencing the performance of GHEs as it changes the moisture content of the soil, which impacts the soil thermal conductivity. For the rainfall (Figure 3-4), it can be seen that the maximum rainfall happens in March, at about 19 mm per hour. In general, there are more rainfall at the beginning and end of the year than in the middle of the year. It should also be noted that detailed analysis between soil thermal conductivity and the moisture content can be further investigated by considering the rainfall duration and surface run-off.

Geologically, from the surface to the depth of about 1.5 to 2.0 m, the site of this farm is underlain by sand (79% according to Golder Associate Pty Ltd., see Appendix B, as shown in Figure 3-75, 3-6 and 3-7). Two test pits were excavated (within the GHE field, exact location not reported), and soil samples were taken and tested by Golder Associates Pty Ltd. The logging of the trench and soils was performed by Dr Stuart Colls, a Principle Engineer from Golder Associates Pty Ltd. The log report is included as Appendix B.

From this report, the topsoil goes from the earth surface to the depth of 0.5 m. Then the sand showed up until 2.5 m, where sandstone was hit (Figure 3-6 and 3-7). Three in-situ tests for the temperature and thermal conductivity are also conducted in the morning of 25th July 2017. It is shown that temperature goes from 13.59 °C at 0.7 m depth to 15.01 °C at 1.55 m depth and then to 15.73 °C at 2.20 m depth. The temperature distribution observed fits the knowledge that the ground temperature becomes higher and more stable when goes deeper. It is also close to the monthly mean temperature at 1.0 m in July, which is 14 °C.

Together with the ground temperature, the soil thermal conductivity is also recorded when conducting the in-situ test. It is shown that there is an increasing trend of the thermal conductivity, from 1.87 $WK^{-1}m^{-1}$ at 0.7 m depth to 2.44 $WK^{-1}m^{-1}$ at 1.55 m depth and then to 4.72 $WK^{-1}m^{-1}$ at 2.20 m depth. Followed by the in-situ test, a lab

test by Golder Associates Pty Ltd was also conducted to get more information of the soil. For the soil thermal conductivity, it shows a similar result as the in-situ test, as shown in detail later in Section 3.4.3. The reason that the thermal conductivity at 2.20 m seems very high could be the moisture at the depth is high. The detailed reports are attached as Appendix B.

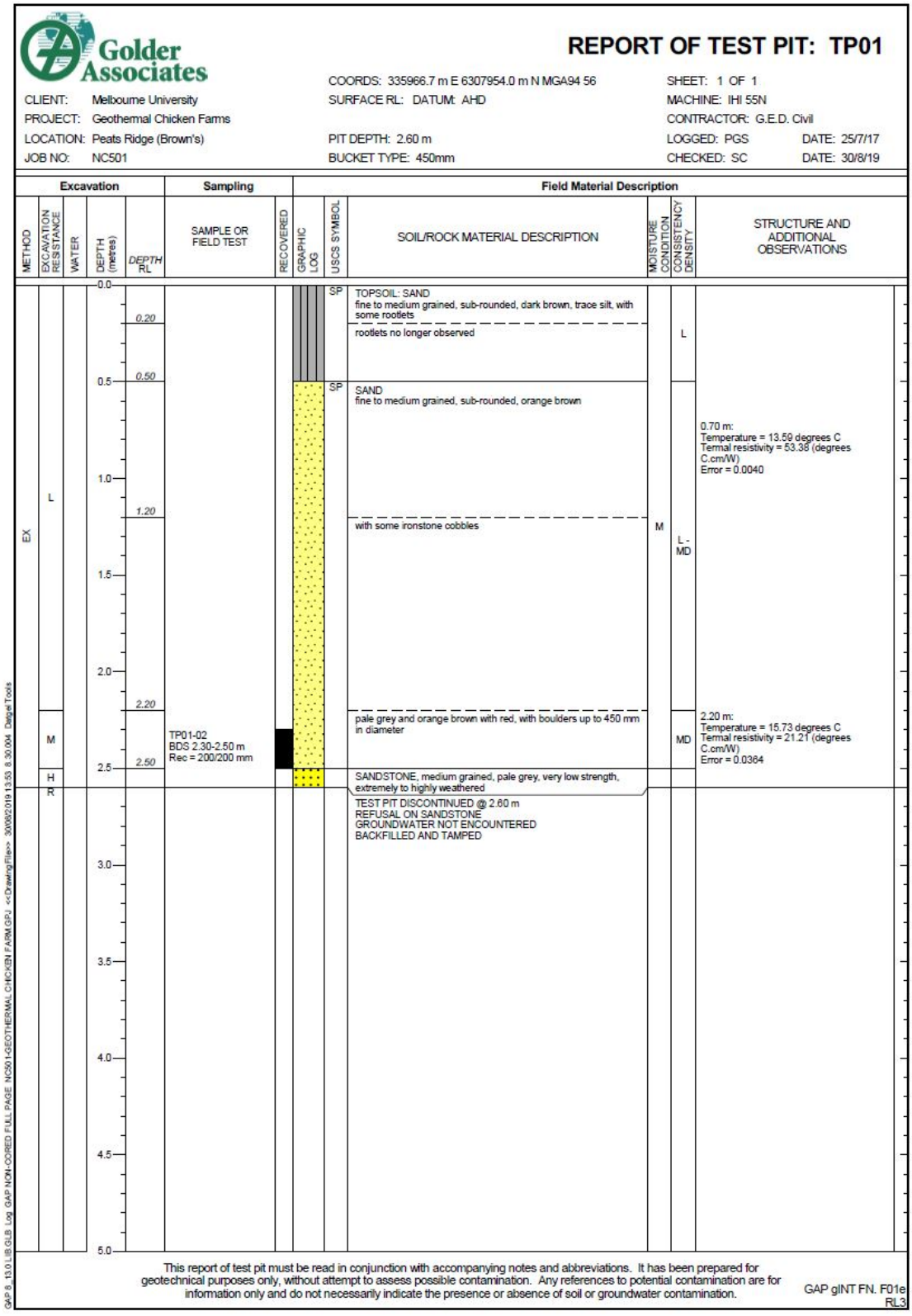


Figure 3-5 Soil report pit 1.

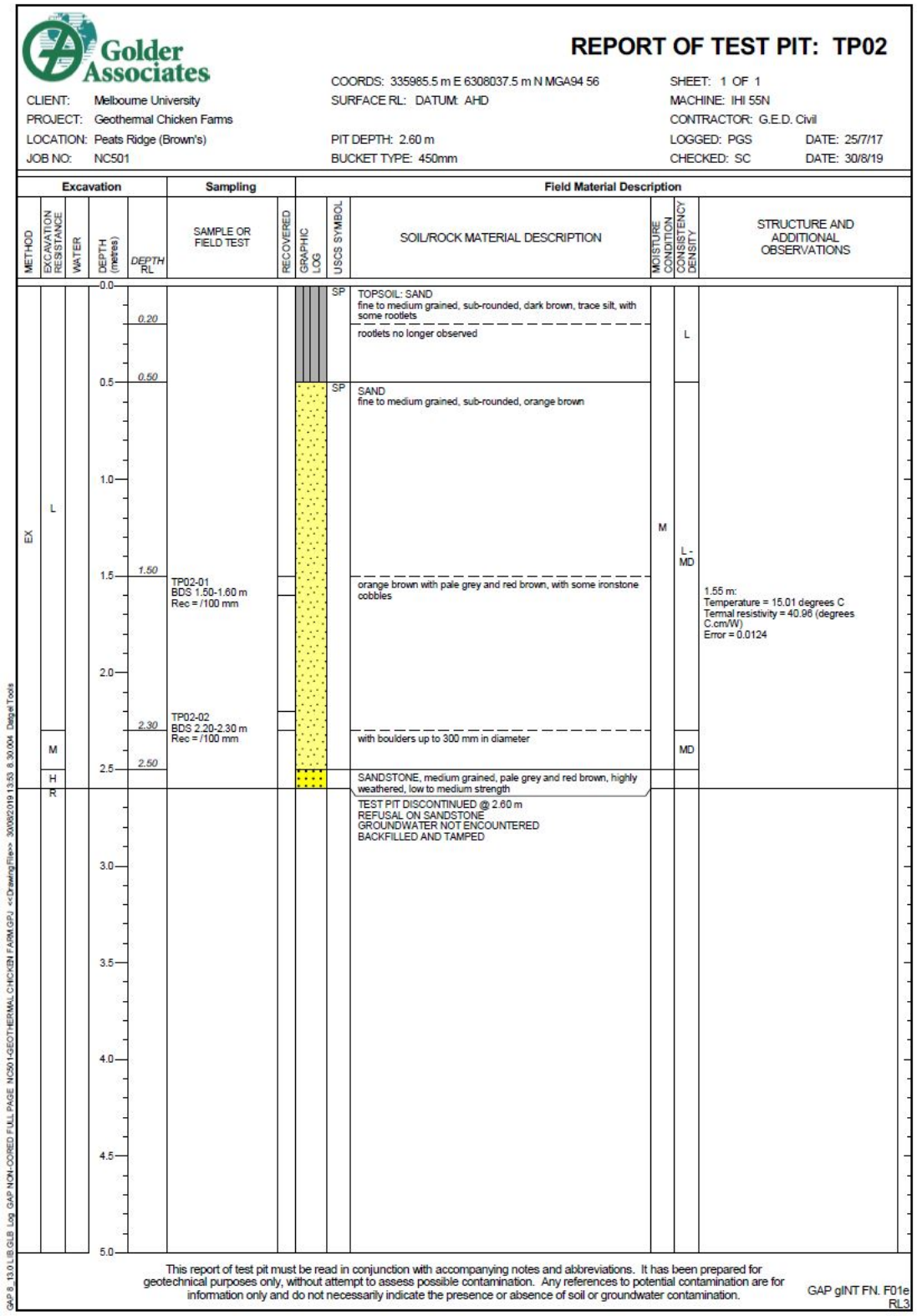


Figure 3-6 Soil report pit 2.

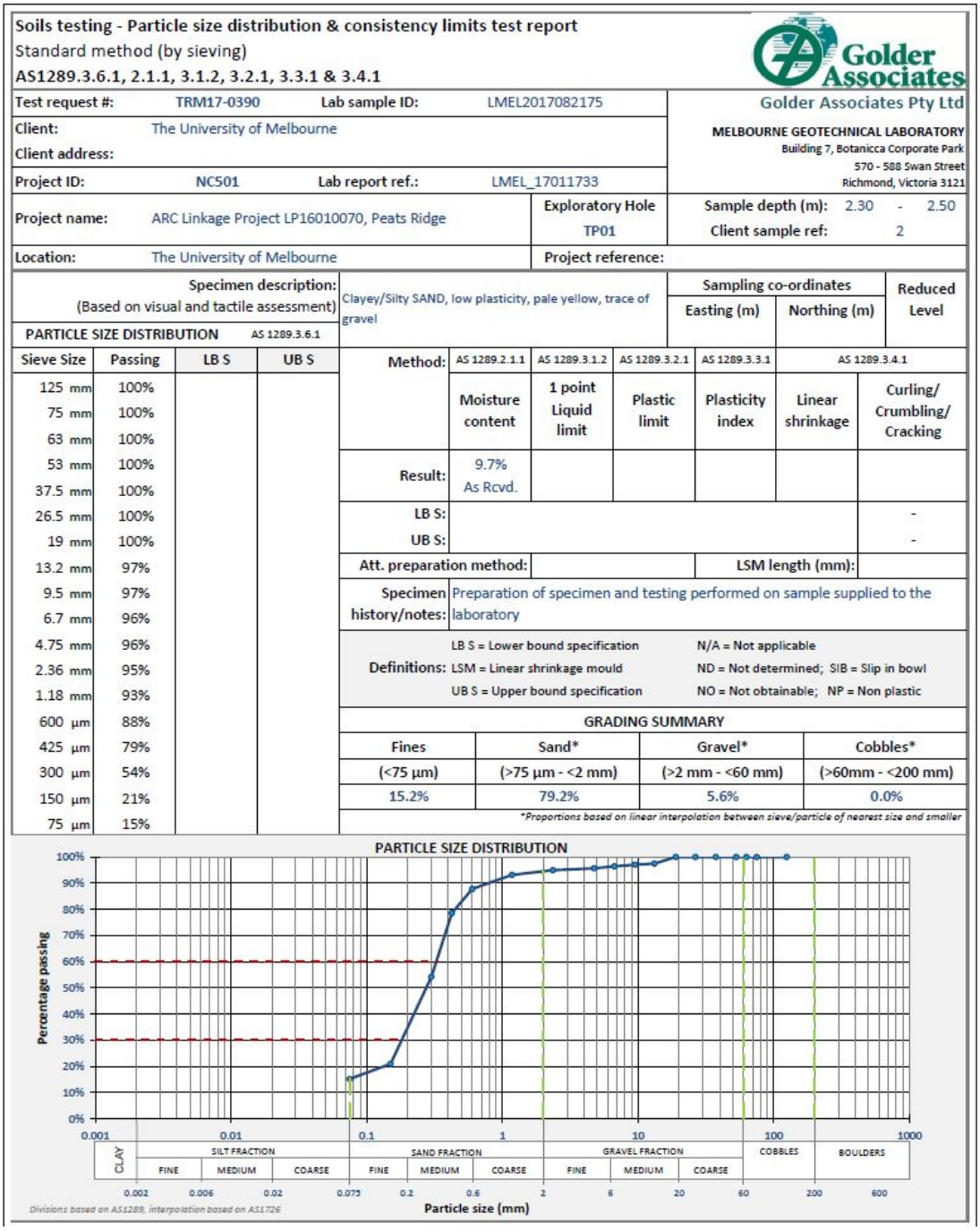

**Soils testing - Particle size distribution & consistency limits test report**
Standard method (by sieving)
AS1289.3.6.1, 2.1.1, 3.1.2, 3.2.1, 3.3.1 & 3.4.1

Golder Associates
Golder Associates Pty Ltd
MELBOURNE GEOTECHNICAL LABORATORY
Building 7, Botanicca Corporate Park
570 - 588 Swan Street
Richmond, Victoria 3121

| | | | |
|---|---|---|---|
| Test request #: | TRM17-0390 | Lab sample ID: | LMEL2017082175 |
| Client: | The University of Melbourne | | |
| Client address: | | | |
| Project ID: | NC501 | Lab report ref.: | LMEL_17011733 |
| Project name: | ARC Linkage Project LP16010070, Peats Ridge | Exploratory Hole | TP01 |
| Location: | The University of Melbourne | Project reference: | |

Sample depth (m): 2.30 - 2.50
Client sample ref: 2

Specimen description: (Based on visual and tactile assessment): Clayey/Silty SAND, low plasticity, pale yellow, trace of gravel

Sampling co-ordinates: Easting (m), Northing (m); Reduced Level

PARTICLE SIZE DISTRIBUTION AS 1289.3.6.1

| Sieve Size | Passing | LB S | UB S |
|---|---|---|---|
| 125 mm | 100% | | |
| 75 mm | 100% | | |
| 63 mm | 100% | | |
| 53 mm | 100% | | |
| 37.5 mm | 100% | | |
| 26.5 mm | 100% | | |
| 19 mm | 100% | | |
| 13.2 mm | 97% | | |
| 9.5 mm | 97% | | |
| 6.7 mm | 96% | | |
| 4.75 mm | 96% | | |
| 2.36 mm | 95% | | |
| 1.18 mm | 93% | | |
| 600 µm | 88% | | |
| 425 µm | 79% | | |
| 300 µm | 54% | | |
| 150 µm | 21% | | |
| 75 µm | 15% | | |

| Method: | AS 1289.2.1.1 | AS 1289.3.1.2 | AS 1289.3.2.1 | AS 1289.3.3.1 | AS 1289.3.4.1 | |
|---|---|---|---|---|---|---|
| | Moisture content | 1 point Liquid limit | Plastic limit | Plasticity index | Linear shrinkage | Curling/ Crumbling/ Cracking |
| Result: | 9.7% As Rcvd. | | | | | |
| LB S: | | | | | | - |
| UB S: | | | | | | - |
| Att. preparation method: | | | | LSM length (mm): | | |

Specimen history/notes: Preparation of specimen and testing performed on sample supplied to the laboratory

Definitions: LB S = Lower bound specification; LSM = Linear shrinkage mould; UB S = Upper bound specification; N/A = Not applicable; ND = Not determined; SIB = Slip in bowl; NO = Not obtainable; NP = Non plastic

GRADING SUMMARY

| Fines | Sand* | Gravel* | Cobbles* |
|---|---|---|---|
| (<75 µm) | (>75 µm - <2 mm) | (>2 mm - <60 mm) | (>60mm - <200 mm) |
| 15.2% | 79.2% | 5.6% | 0.0% |

*Proportions based on linear interpolation between sieve/particle of nearest size and smaller



Figure 3-7 Soil report lab test.

### 3.3.3. **Configuration of hybrid geothermal system**

The hybrid geothermal-solar-gas system installed in the poultry shed building is designed by the author in 2017, with the advises of supervisors and the help of the research team and industry partners. The details of all the configuration and instrumentation can be found in Appendix C.

Figure 3-8 shows the schematic diagram of the hybrid geothermal-solar-gas system. The primary heating power (80 kW) is delivered by four identical GSHPs, each with about 20 kW heating capacity (Mammoth J086), connected in parallel to a main header. Each

GSHP is coupled with a series of ground heat exchangers (GHEs). Upstream, the GSHPs are connected to a buffer tank to minimise the cycling of heat pump on and off. The buffer water tank, sized at 1.5 $m^3$, is also connected to three gas (LPG) boilers (Bosch 32) with 120 kW total heating capacity. The existing gas (LPG) boilers can top up heating when needed. The water buffer tank is then connected to a set of six fan coil units (custom made by Eastaway Services Pty Ltd in Sydney, each with about 33 kW heating capacity) in the shed to supply the heat. Additionally, there are two more backup heating sources to top up heating in extreme situations. The first on is the electric heating coils inside the water tank, which is connected to solar Photovoltaic (PV) panels on the roof of the mobile mechanical and control plant. During the day, the PV panels will generate electricity to heat the water in the tank. However, it can also be connected to the grid when situation requires. The second back up heating source is the existing gas burners inside the poultry shed. Together, this hybrid system can supply a total nominal heating capacity of 200 kW and can be boost to over 600 kW with existing gas burners when needed. According to the analysis in Chapter 3, this system is primarily driven by the operation of the GSHPs, which can supply over 80% of the heating required.

### 3.3.4. Ground Heat Exchangers

To study the impact of different pipe configurations on the performance of horizontal ground heat exchangers, there are twelve trenches (8 trenches are 75 m long, and 4 trenches are 38 m long, all at 1.5 m depth) and four pond loops in total. Each trench/loop consist of HDPE pipe, with a length of 300 m, with a 32 mm outside diameter (26 mm inner diameter, SRD11). These together make the total pipe length of 4.8 km, excluding the header pipes (Figure 3-9, 10, 11).

Table 3-1 Pipe and trench lengths for three pipe configurations.

| Configuration | Pipe Length (m) | Trench Length (m) | Loop Diameter/Pitch(cm) |
|---|---|---|---|
| Straight Pipe | 300 | 75 | N/A |
| Slinky | 300 | 75 | 90/137 |
| Dense Slinky | 300 | 38 to 40 | 90/46 |

The twelve trenches are grouped for every four trenches. The first four trenches (No. 1 to No. 4) contain horizontal straight pipes, which consists of four parallel pipes, at 30 cm spacing between each pipe in a 1.2 m wide, 1.5 m deep, 75 m long trench (Figure 3-10, 11), with 3.5 m spacing between each trench.

From trench no. 5 to trench no. 8 (Figure 3-10, 11), there are (extended) slinky pipes, these slinky pipes have a loop diameter of 0.9 m and a loop pitch at 1.37 m, which makes them have the same pipe length in the same length of trench comparing with the horizontal pipe (four m length of pipe in one m length of trench). These pipes are also buried at 1.5m deep within a 75m long trench as well, with 3.5 m spacing between each trench. By comparing the performance of the slinky trenches and the horizontal trenches, the impact of the different pipe layout on the on the performance of horizontal ground heat exchangers under the rural industries' condition can be studied.

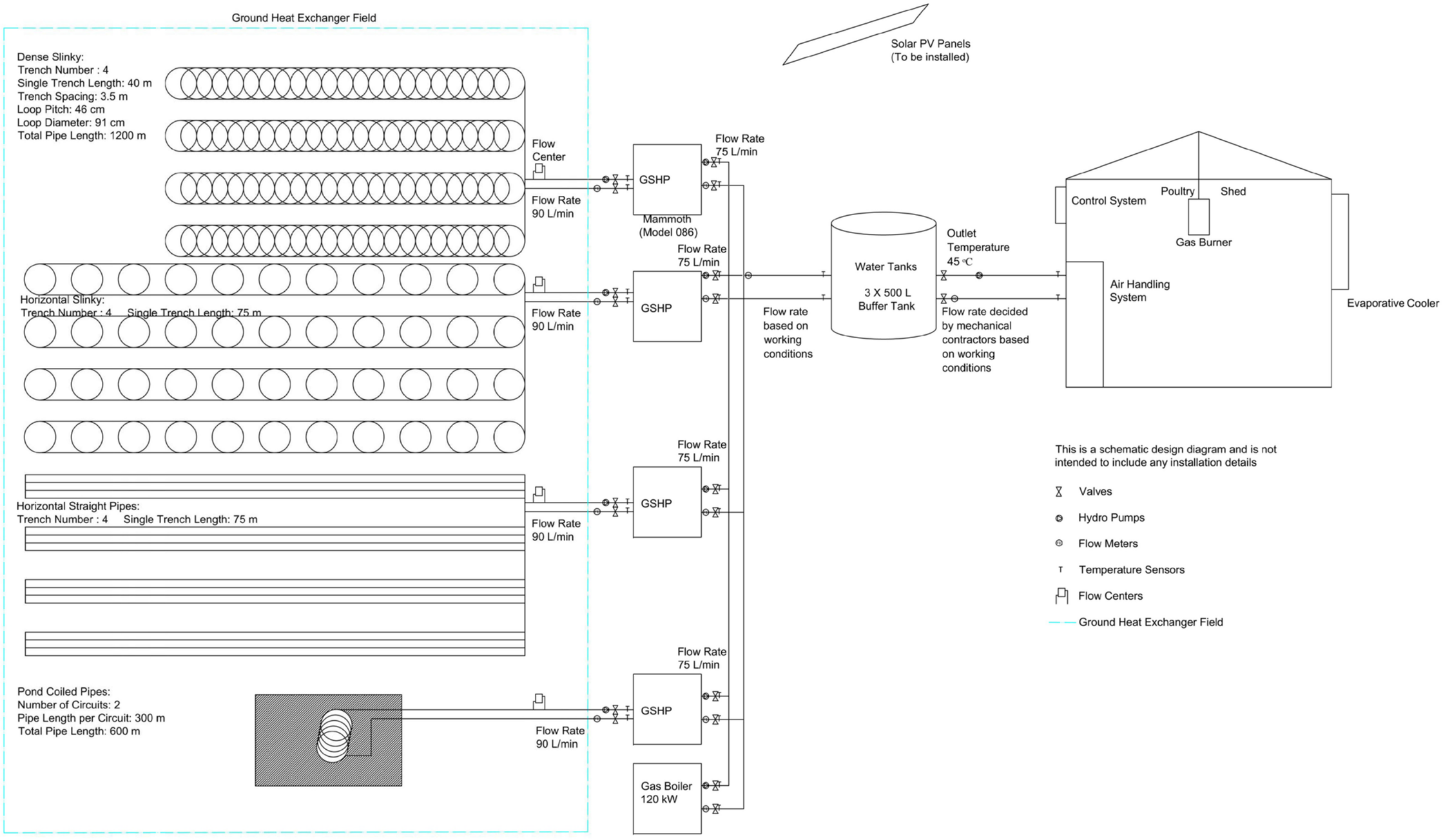


Figure 3-8 Schematic design drawing (for site pictures, see Figures 3-11, 3-16).

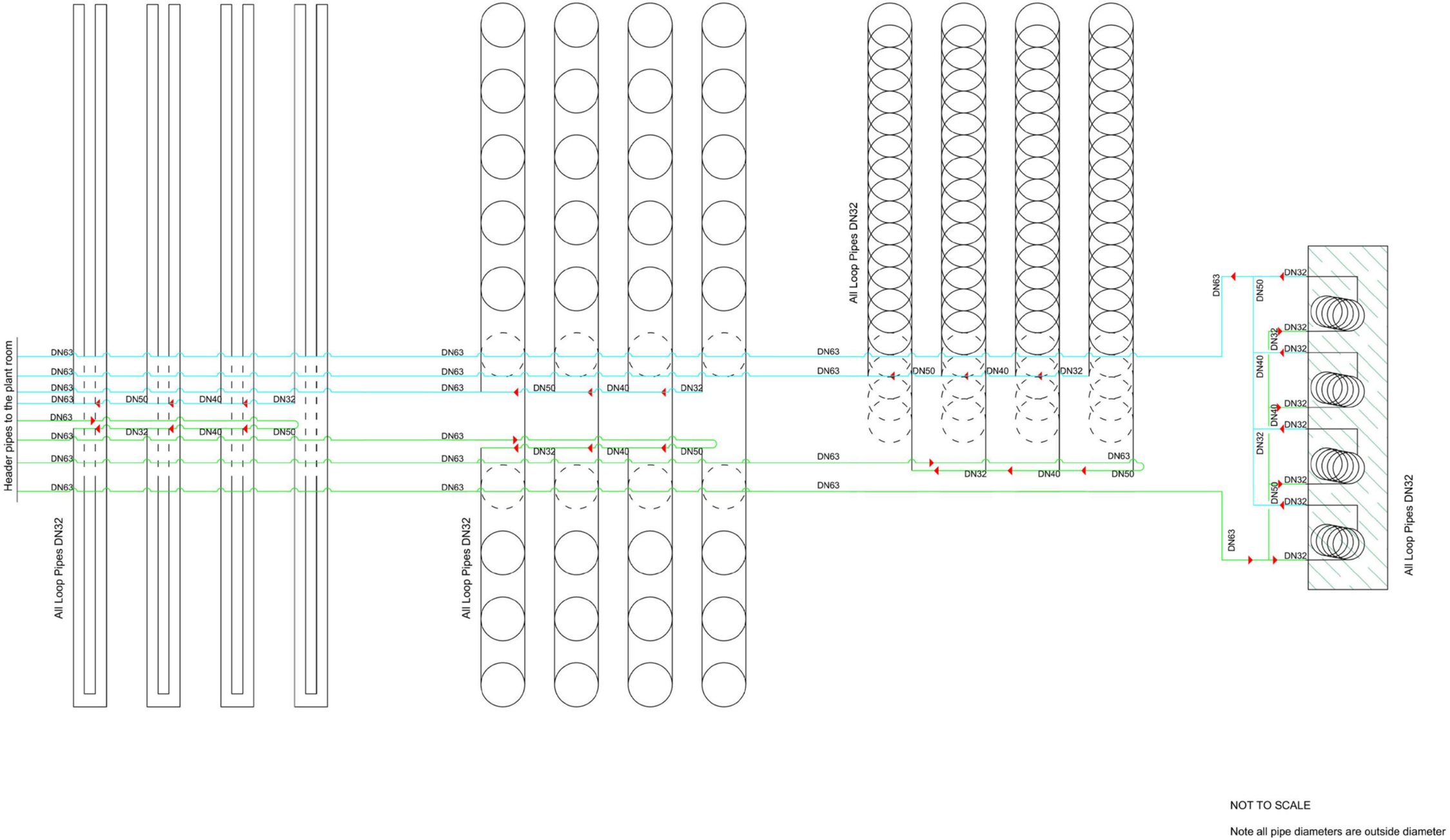


Figure 3-9 Hydraulic schematic drawing.

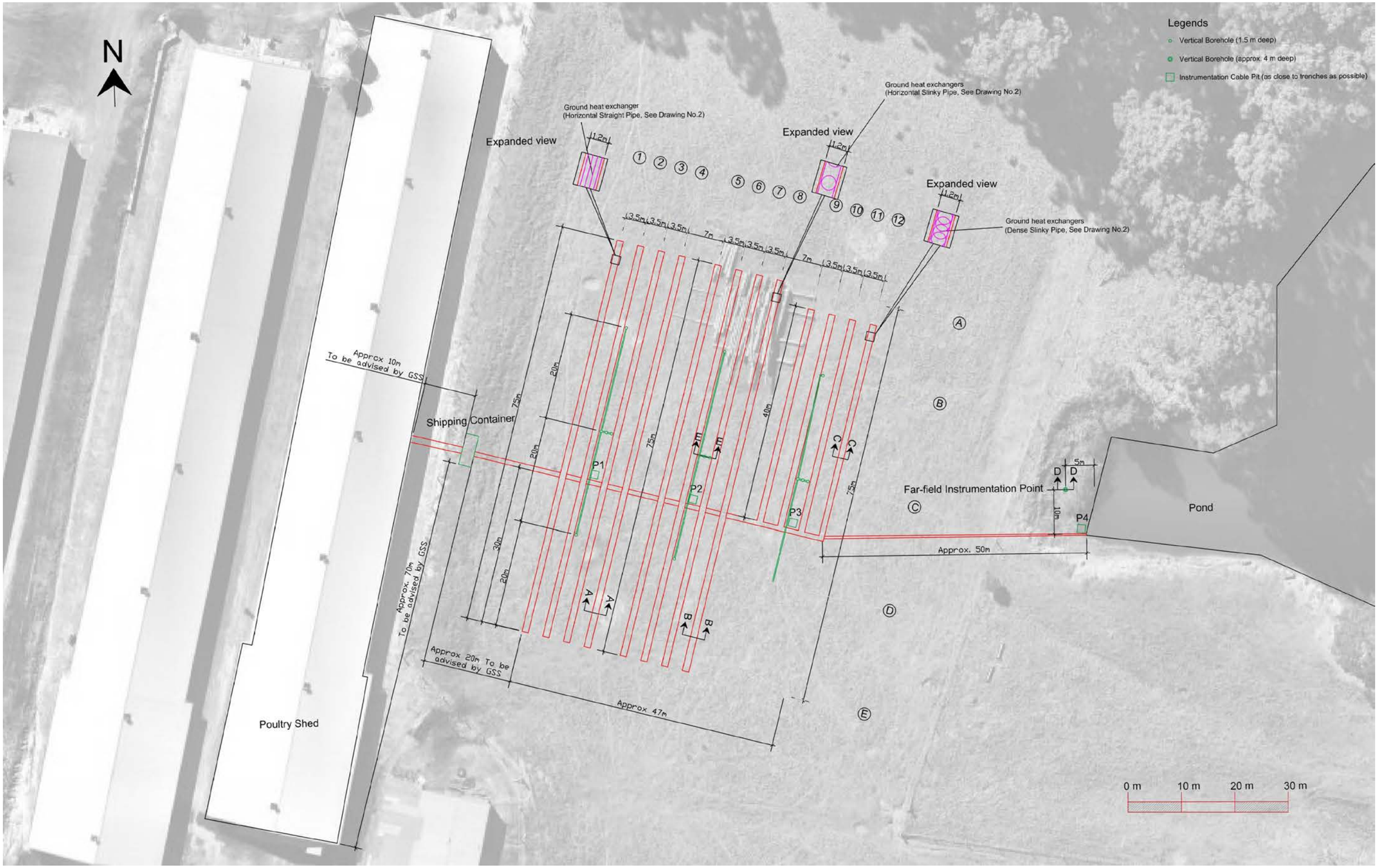


Figure 3-10 Construction drawing.

From the trench no. 9 to trench no. 12 (Fig 3-12, 13), there are dense slinky pipes with a diameter of 0.9 m and a loop pitch of 0.46 m, these make this configuration have doubled pipe length in the same length of trench comparing with the previous two configurations (eight m length of pipe in one m length of trench). The trench spacing remained the consistent with the other configurations (3.5 m). By comparing the performance of these two types of slinky trenches, the impact of the different pipe density on the on the performance of horizontal ground heat exchangers under the rural industries' condition can be studied.

Last but not least, in the east side of the field, there are four loops of heat exchangers inside the pond (Fig. 3-12). The pond has a depth of about 4 to 6 m and surface area at about 5,000 $m^2$, varying by seasons. To compare the performance of the pond loops and ground loops, each pond loop was also designed to have a pipe length of 300 m. However, due to the constructability, the length was reduced to 200m on site. The pipes of the pond loop are packed and laid on a customised frame at 0.3 m above the bottom of the pond.

Each group of the four loops has its own reverse return header pipes (Fig. 4-12). The outside diameter of the header pipe goes from 32 mm to 40 mm (32 mm inner diameter) and then to 50 mm (40 mm inner diameter) and finally reaches 63 mm (51 mm inner diameter). The details of the header pipes are shown in Figure 4-13. The depth the header pipe is 0.5 m and all the trenches were backfilled with the light compacted soil from original excavation.

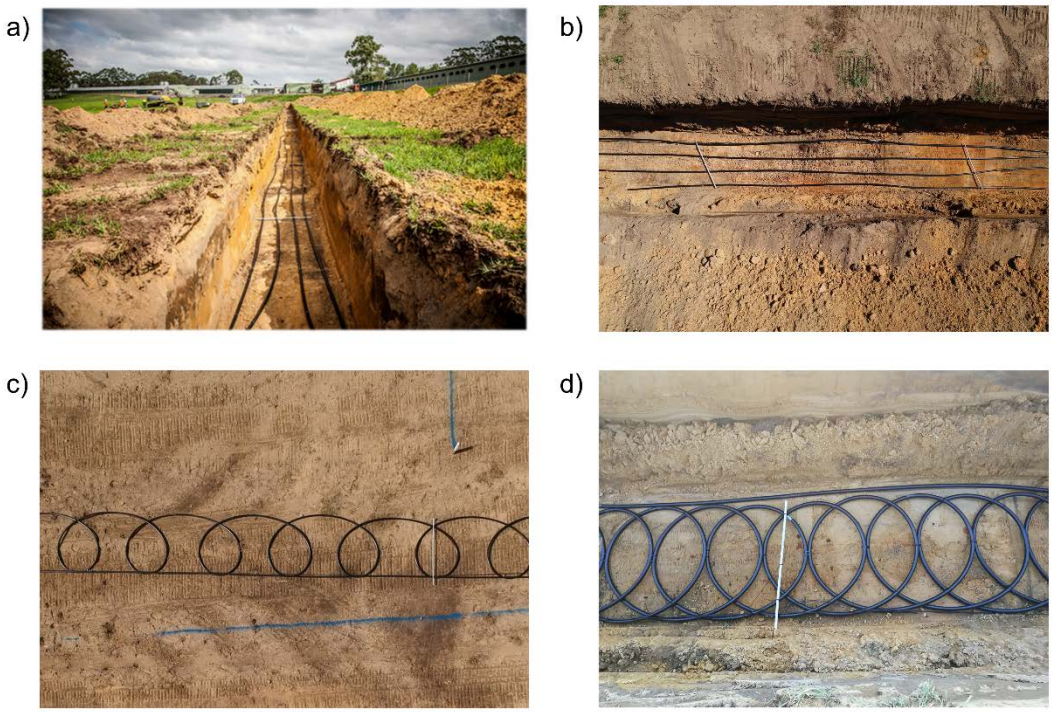


Figure 3-11 Ground Heat Exchangers (GHEs) configurations: a) Horizontal straight pipe in trench, b) horizontal straight pipe, c) slinky pipe, and d) "dense" slinky pipe.

### 3.3.5. Monitoring instrumentation

The hybrid geothermal system is immensely instrumented to monitor the performance and study the impact of the unique loads from the poultry shed building to the GHEs. There are over 170 temperature sensors were originally installed. Yet unfortunately, there are about 80

sensors that can still work in Oct. 2019. Even though it would be more beneficial to install even more sensors, it is not possible due to constructability and the constraints of time and cost.

In order to monitor the heating loads applied to the ground, each group of four loops is equipped with a water flow meter. As each group of four loops has an individual GSHP, there are water flow meters on the loading (building) side of each heat pump as well.

To monitor the ground temperature in the field at different depth, fifteen boreholes at 1.5 m depth were drilled (Figure 3-12). There are three temperature sensors in each borehole, at 0.5 m, 1.0 m and 1.5 m depth, and one soil moisture sensor in the middle borehole in the field. The moisture sensor has a length of 1.2 m, with 12 moisture sensors evenly spread for even 0.1 m (same as shown in Figure 3-14). The bottom of the moisture sensor was installed at the depth of 1.5 m.

To monitor the water temperature of the GHEs, six out of twelve trenches have been instrumented with temperature sensors, namely, all the even number trenches. As an example, Figure 3-13 shows that there are 15 sensors in one trench, ten of them are attached to the HDPE pipes and five of them are in the soil. The ten sensors attached to the pipe are in the pair of two, attached to five locations in the loop, namely, the inlet, outlet and every 75 m of pipe. The rest of the five sensors in soils are evenly spread in the middle line of the bottom of the trench (see Figure 3-13).

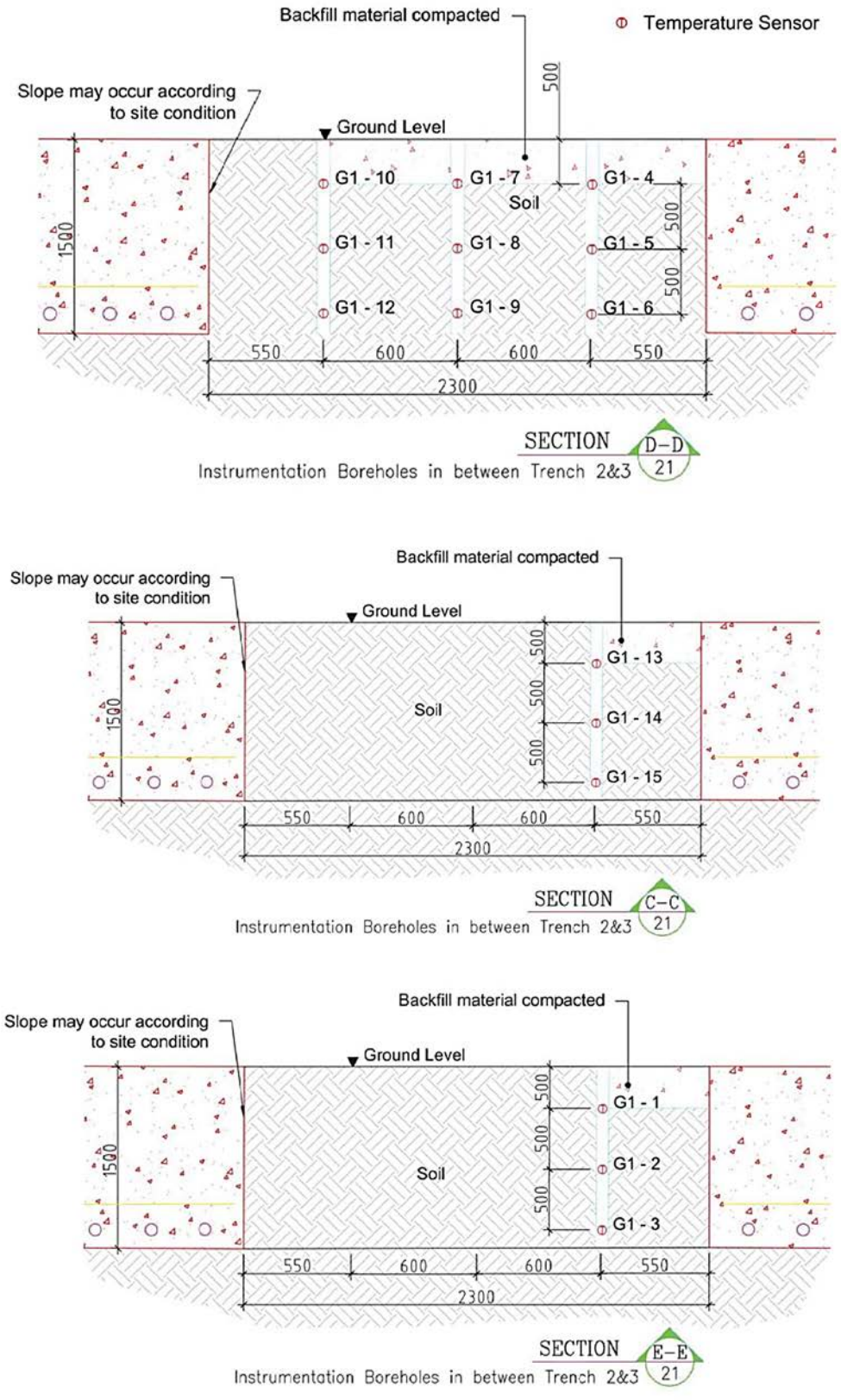


Figure 3-12 Instrumentation in between trenches (Dimensions in mm).

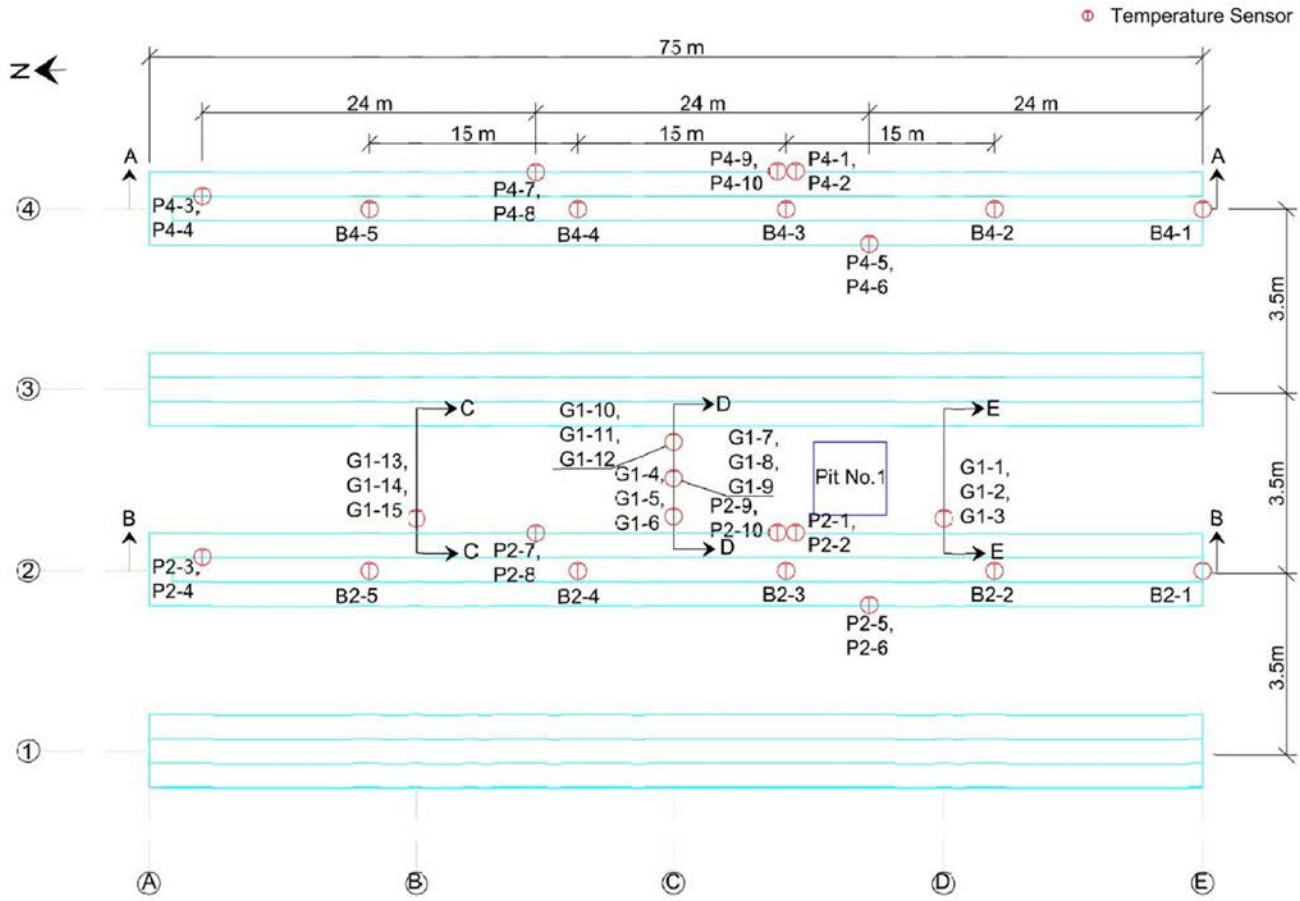


Figure 3-13 Instrumentation for horizontal loops. Pit No. 1 is used to connect all cables and channel them into the central datalogger.

Additionally, to monitor the far-field ground temperature, a 4-m-deep borehole was drilled, with 8 temperature sensors installed at 0.5 m distance to each other. This borehole is located on the east side of the farm and about 50 m away from the GHE field (Figure 3-10). There is also a soil moisture sensor as same as the on in the middle of the field installed in this borehole, with the bottom of the sensor at 1.5 m depth to monitor the far field soil moisture (see Figure 3-14).

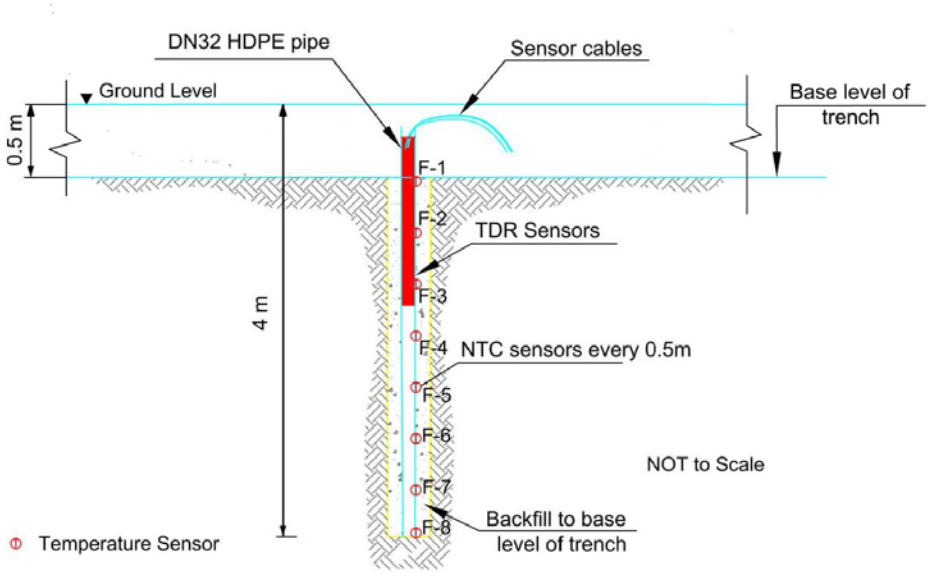


Figure 3-14 Instrumentation for far field borehole.

Finally, to monitor the temperature of the pond loops, there are fifteen temperature sensors installed for the pond loops. Eight of them were installed in the pair of two, at the inlets and outlets of two pond loops. Four of them were also installed at the inlet and outlet pipes of the pond loops, but very close to the pipes in the frame. The last three sensors were installed at the bottom, middle and top of one of the pond loop columns (See Figure 3-15).

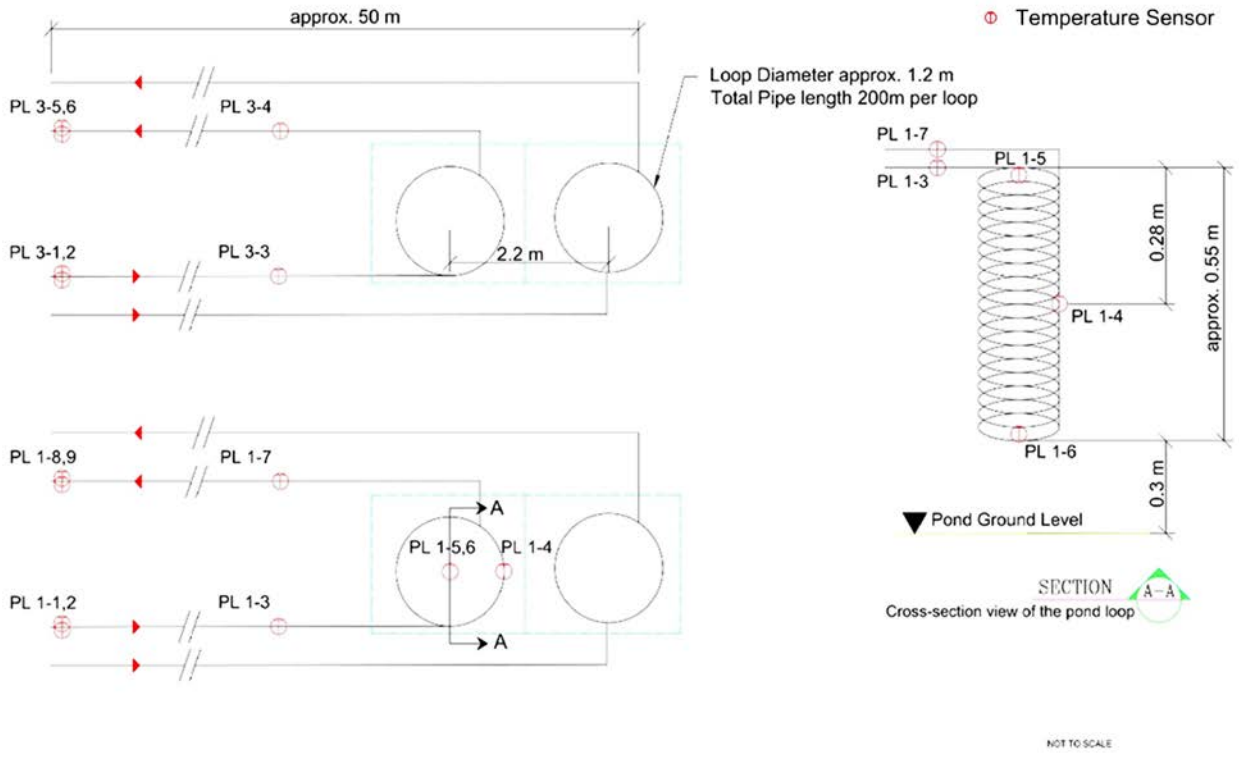


Figure 3-15 Instrumentation for pond loops.

### 3.3.6. Construction and Installation

The first stage of the installation commenced in March 2018 with all the GHEs (including pond loops) together with the temperature and soil moisture sensors installed in the field. The second stage of the installation then started from August 2018, with the mobile control and monitor plant been constructed and delivered to the site. The Final stage of this project started in March 2019, when the fan coil units were installed inside the poultry shed building. The selected image taken from various stages of the construction is shown in Figure 3-16.

Figure 3-16 Aerial views of the field while under construction as part of the research project (construction by industry partner Ground Source Systems and others).

## 3.4. Preliminary Experimental Results and Discussion

Unfortunately, due to an outbreak of Salmonella, the farm has been strictly regulated since Q2 2019 until the end of 2019. Therefore, no much GSHP operational data would be available until the end of this candidature. This section summarizes the currently available data which can be used to validate or verify the building energy and GHE models.

### 3.4.1. Monitoring Results of the Poultry Shed Building

Figure 3-17 shows the indoor temperature of the poultry shed from April 2018 to Mar 2019. From this figure, it can be identified that there are five cycles during this period, corresponding to five batches of raising chicken. This finding justified that six batches within a year is a reasonable assumption. Moreover, it can be seen that the indoor temperature has a good linear relationship versus time at the first two to three weeks of each batch, and then

begin to fluctuate at around 20 to 23 deg C. This observation can be explained by that at the beginning stage, heating is delivered via LPG gas burners, which maintained the indoor room temperature very close to the setpoint temperature. Later, when cooling is required, evaporative coolers will be in operation, yet it could only reduce the indoor temperature up to the dewpoint temperature, which results in the fluctuation.

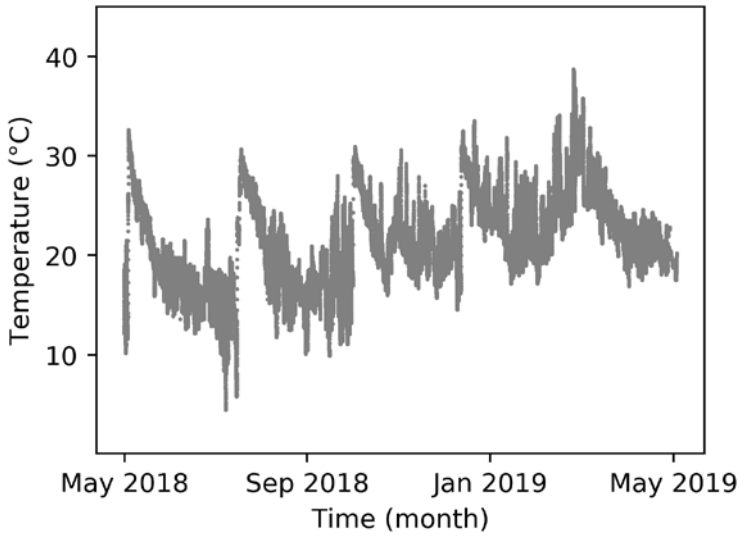


Figure 3-17 Monitored shed indoor temperature.

Figure 4-20 shows the indoor and outdoor temperatures from 19:00 02/04/19 until 8:00 03/04/19. The outdoor temperature was measured at the air inlet of the building (after the ventilation fans), hence can be representative as the inlet temperature of ventilation. It can be seen that the air gets cooled down when goes through the building during night. The explanation behind this observation is that the ground temperature is lower than the air temperature and the building losses heat due to heat radiation to the sky. A verification with the TRNSYS building model discussed in chapter 4 can further verify this explanation.

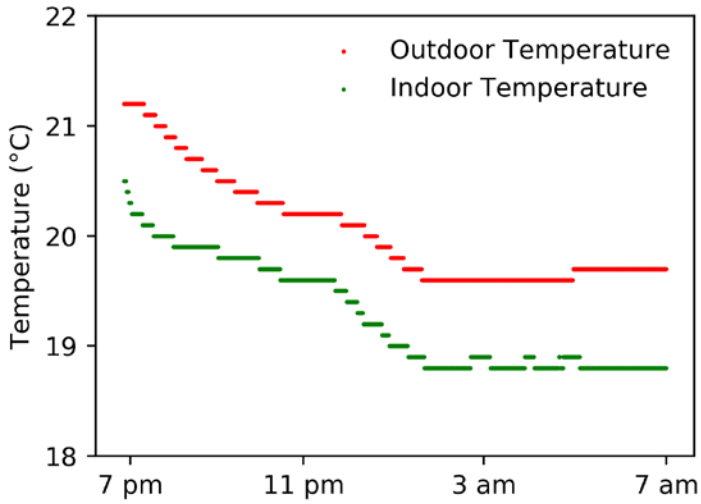


Figure 3-18 Monitored shed indoor and outdoor temperatures on 2nd April 2019 (HVAC system not in operation).

### 3.4.2. Instrumentation Results from the Horizontal GHEs

The instrumentation for the horizontal GHEs began in Mar. 2019. Even though the system was not in operation, the ground temperature data can still be recorded for important reference as boundary conditions for simulation. Later, test runs happened for two days in Oct. 2019 for one of the four heat pumps, which indicated the potential technical feasibility of this hybrid system. These data can also be used against validation of models. However, only some limited validations and verifications of models used in the thesis was possible due to time constrains (the experimental site just became fully operational towards the end of this thesis candidature. Nevertheless, the results for these data are reported as follows.

Figure 3-19 shows the ground temperature in the far-field temperature monitoring sensors from Apr. 2019 to Oct. 2019. The location of sensors is shown in Figure 4-14. It was observed that ground temperature at depths of 0.5 m to 2 m were highly subjected to seasonal variations and fluctuations whereas the ground temperature at depths of 2.5 m to 4 m had smaller fluctuation amplitudes. A TRNSYS simulation was conducted using the model to be discussed in Chapter 5 to verify the ground temperature at 1.5 m. With the TMY data used as boundary conditions, the results are in a reasonably good agreement (average difference less than 1 to 2 $^{o}$C which may be caused by yearly variation) with the measure data (Fig. 3- 19 b). This finding further verified the TRNSYS simulation model (using Type 997). A comparison with monthly mean ground temperature shown in Fig. 3-3 was also made (Fig. 3-19 b). The results show a good agreement with about 1 to 2 $^{o}$C difference as a variation to the TMY data.

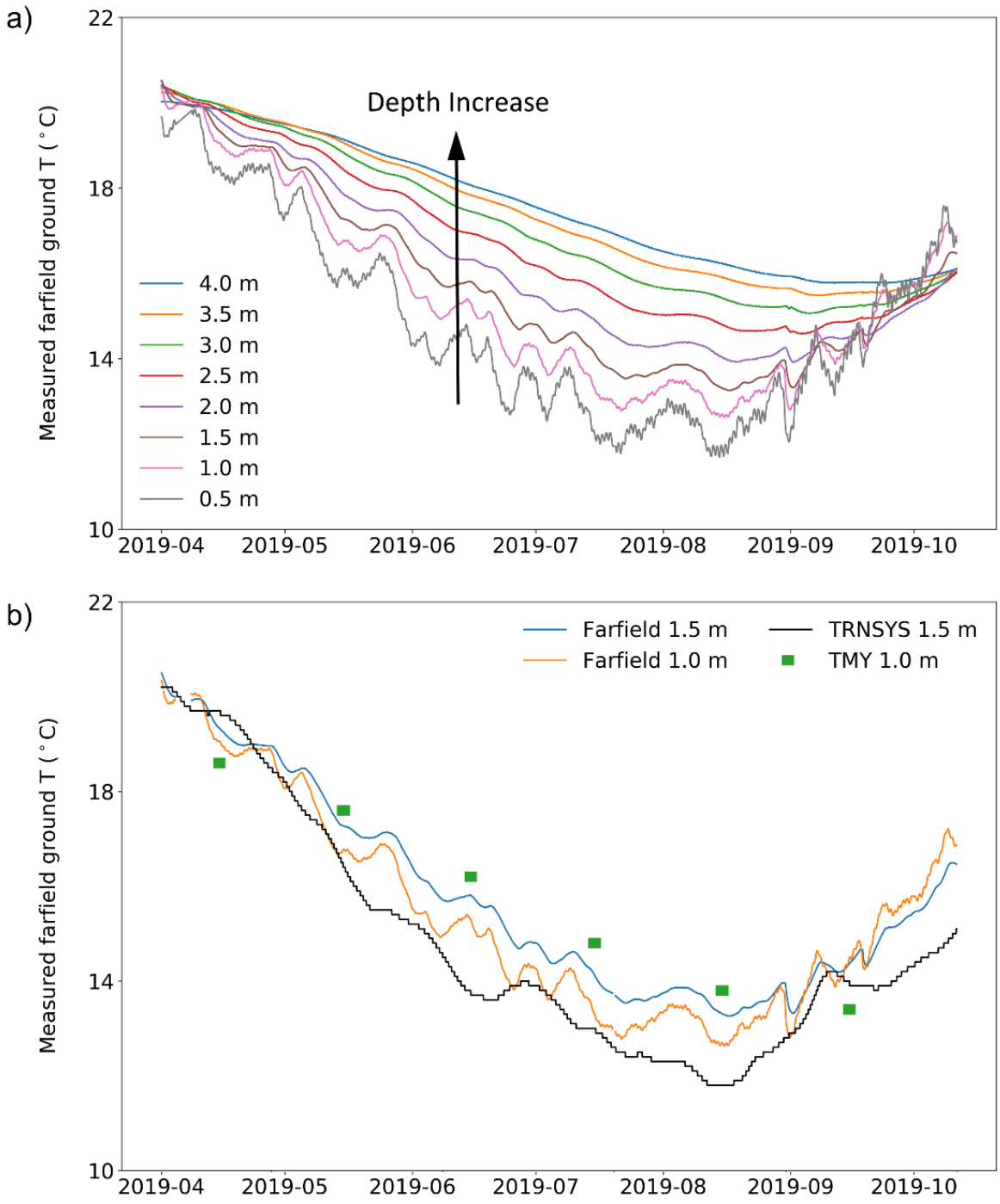


Figure 3-19 Monitored far-field temperatures: a) Far-field temperatures with depth, b) Far-field temperatures in comparison with TMY monthly mean and TRNSYS simulated temperatures.

The temperature of the ground adjacent to GHEs were monitored with the temperature sensors installed as shown in Figure 3-12. Similar to the far-field temperature, the temperatures were recorded from Mar. 2019 to Oct. 2019, (Figure 3-20). The ground temperature follows the similar trend with the far-field temperature (yet about 1 to 2 °C higher on average), the shallower sensors are more easily to be influenced by the seasonal variations. The monitored temperatures aim to provide general information about thermal influence of the operational GHE on the ground adjacent to them. However, given the relatively short running time, the influence of the operational GHE cannot be seen from the figure.

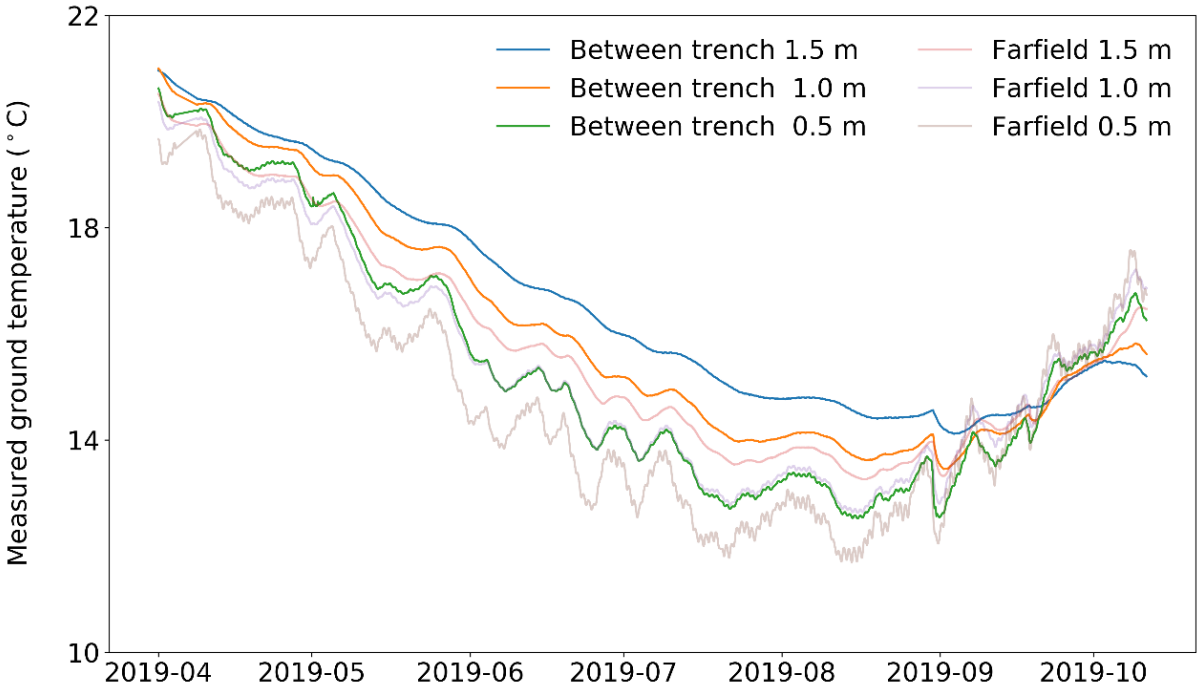


Figure 3-20 Monitored ground temperature at different depths (see legend) between Trench 10 & 11.

From 12:00 pm to 2:00 pm 13th April. 2019, a test run was conducted to test this hybrid system. Figure 3-21 shows the test run for the slinky horizontal GHE when the ground was stable. It is estimated that the average difference between inlet and outlet temperatures is about 2.7 °C when operating. The operation flow rate for the ground side is 1.7 L/s. Therefore, the calculated heat transfer rate is 20.6 k$W$. It should be noted that the temperature sensor P8-7 and P8-10 were damaged during monitoring and there are invalid recordings which are excluded for calculating mean temperature. It should also be noted that the mean fluid temperature was calculated based on temperature data recorded at five locations of the loop. While it is in between the inlet and outlet temperatures when operation, it may temporarily exceed this range due to switch on and off.

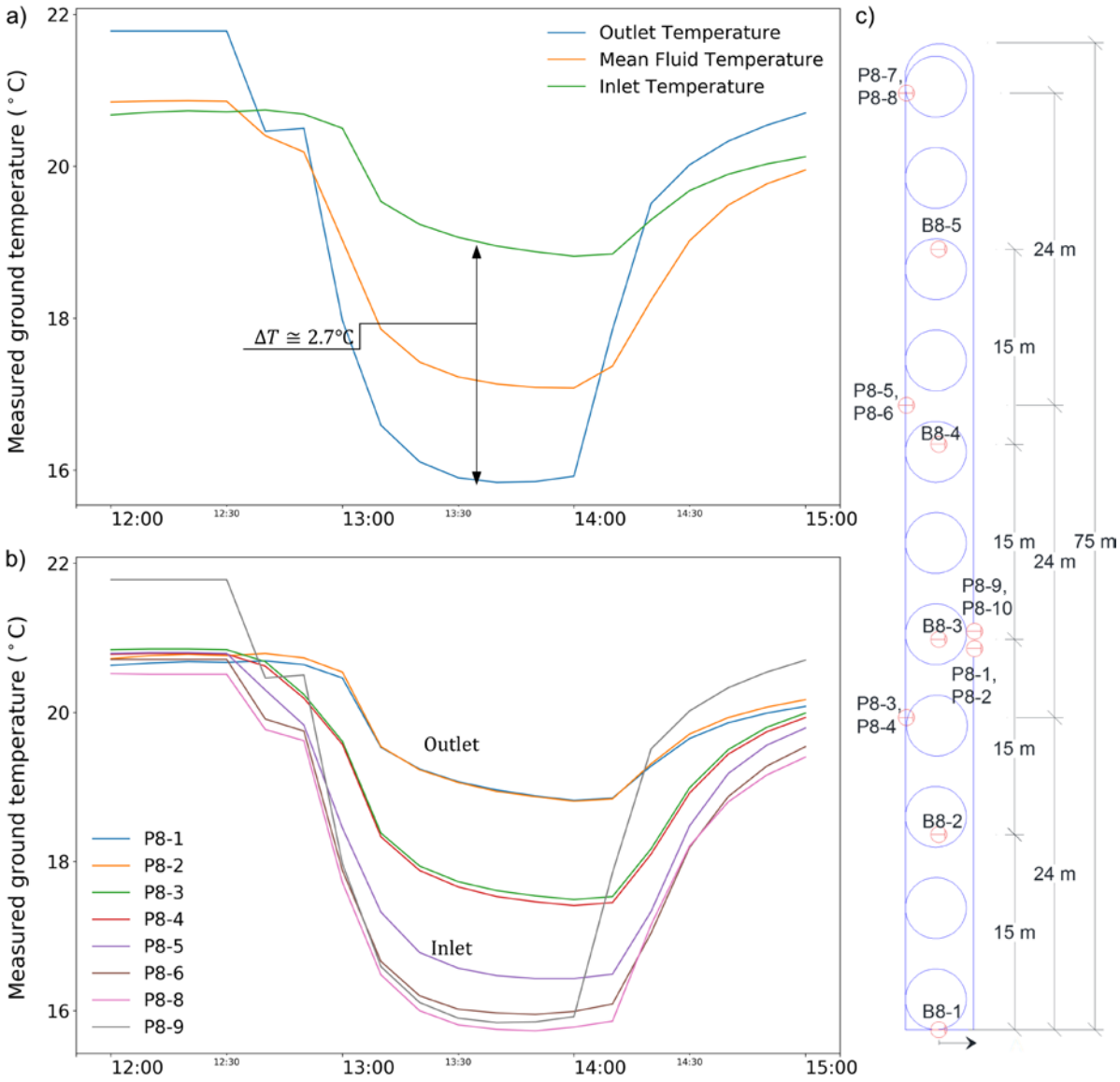


Figure 3-21 Temperatures recorded at the GHEs of GHE Trench No. 8 (Slinky): a) Inlet, outlet and mean fluid temperatures b) Temperature recorded by sensors attached to the pipe c) Location of sensors.

From 8th Oct. 2019 to 10th Oct. 2019, another test run was conducted to test the dense slinky loops and verify the feasibility of this hybrid system. Figure 3-22 shows the test run for the dense slinky horizontal GHE. The results show that the running lasts for 48 hours with some turn on and off. It is estimated that the average difference between inlet and outlet temperatures is 2.8 °C when operating, which is very similar to the slinky loops. The operation flow rate for the ground side is the same as 1.7 L/s. Therefore, the calculated heat transfer rate is 21.3k$W$, which is also very similar to the slinky loops. The results show that despite the difference in configuration, the heat transfer rate from the ground side is very similar as long as the total pipe length is the same. It should be noted that the temperature sensor P12-5 was damaged during monitoring and there are invalid recordings which are excluded for calculating average temperature. Given the turning on and off during the operation, the ground did not reach its steady state which leads to unstable temperature differences between inlet P12-1 & P12 -2 (Inlet temperature) and outlet P12-9 & P12 -10 (Outlet temperature).

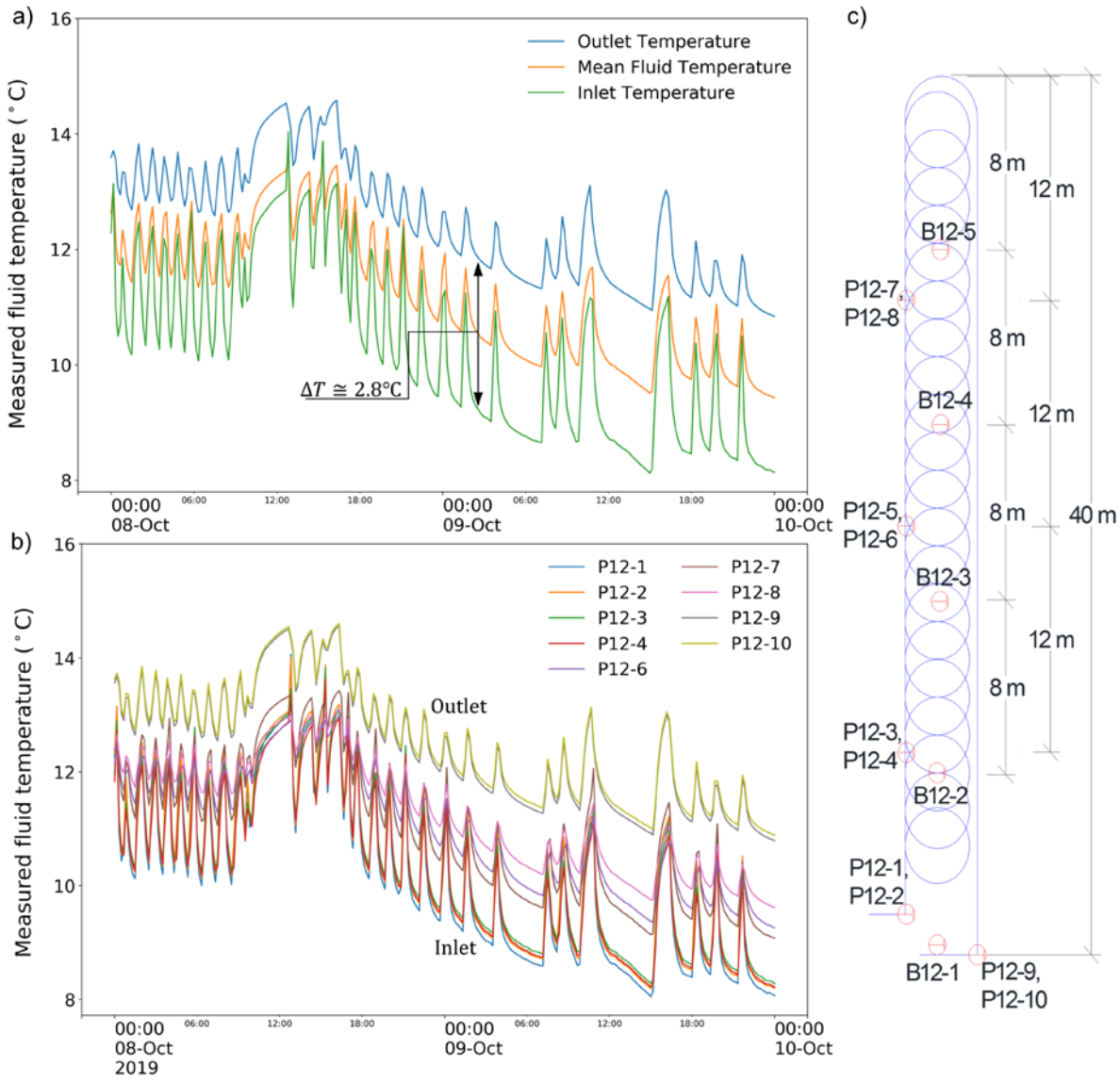


Figure 3-22 Temperatures recorded at the GHEs of Trench No. 12 (Dense slinky): a) Inlet, outlet and mean fluid temperatures b) Temperature recorded by sensors attached to the pipe c) Location of sensors.

Additionally, an analysis was conducted to interpolate the ground temperature distribution between the sensors and draw the temperature field accordingly. This figure intended to show the distance and area that this 2-day operation can impact. Longer running times would have seen greater radius of influence. Fig. 3-23 shows the temperature filed with time elapse. It can be seen that the operation of the GHEs can impact the sensors at 1.3 m from the trench centre. Corresponding to operation in Fig. 3-22, from 0 hr, 8$^{th}$ Oct. 2019 to 6 hr, 8$^{th}$ Oct. 2019, there is a minor decrease of the mean fluid temperature due to operation. Then, at 12 hr, 8$^{th}$ Oct. 2019, the mean fluid temperature recovered due to a two-hour break in operation.

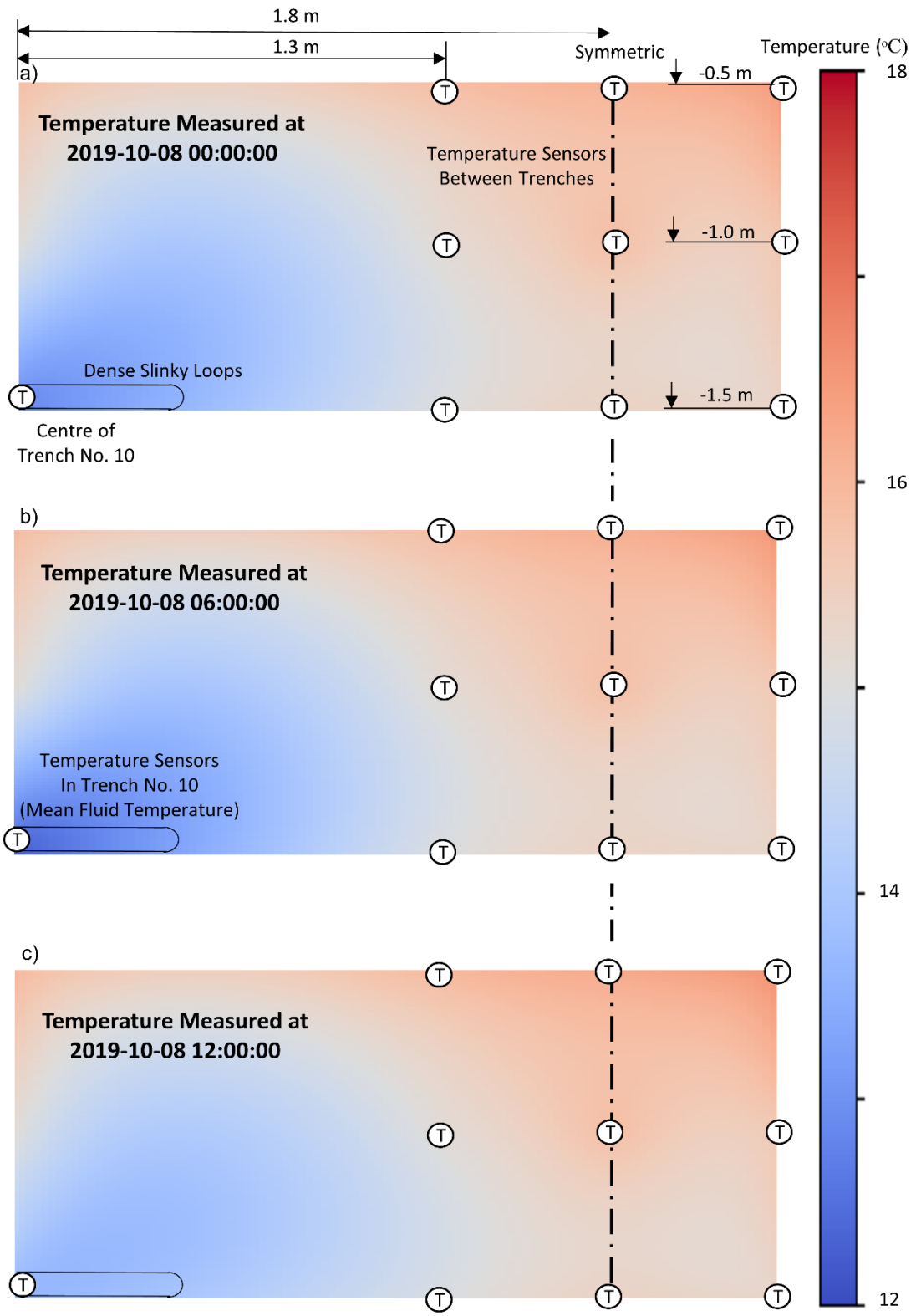


Figure 3-23 Temperatures recorded for Trench No. 10 (Dense slinky) and between Trench No. 10 & 11: a) Temperature measured at 2019-10-08 00:00:00, b) Temperature measured at 2019-10-08 00:00:00, c) Temperature measured at 2019-10-08 00:00:00.

### 3.4.3. Laboratory ground thermal cond. measurements

To further verify this study, laboratory tests were conducted to measure the thermal conductivity of the soil. The thermal needle probe (KD2pro by Decagon Devices Inc.) was used for the measurement. Two in situ test was conducted back in Oct. 2016 at the depth of about 1 m. Later, soil samples at similar depth were taken and tested in lab with the same thermal needle probe.

As expected, the tested soil thermal conductivities were proportionally increased with the moisture content as can be seen in Figure 4-27. From it, the thermal conductivities of the soil on Peats Ridge were tested and returned by Golder Associate under different moisture contents and dry density ratio compared to the maximum dry density under standard compaction. For both soil specimen, the thermal conductivities have increased 3 times from 0% to about 15% moisture content. It is noted that for higher compact density, soil have higher thermal conductivities under the same moisture content. The results reach a good agreement with the in-situ tests results mentioned in Section 3.3.2. It is also suggested that the 1.8 to 2.4 $WK^{-1}m^{-1}$ is a suitable range for the design (Appendix B). Based on this, 2.0 $WK^{-1}m^{-1}$ were used as the thermal conductivity in the design and simulation of this thesis.

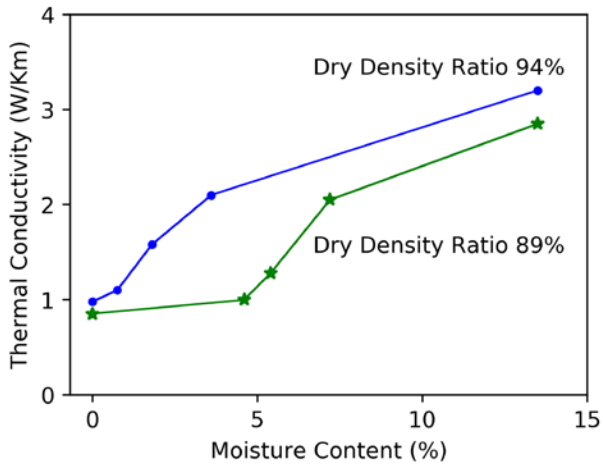


Figure 3-24 Thermal Conductivity Test Results from Golder Report (Appendix B).

## 3.5. Summary

This hybrid geothermal system with horizontal GHEs is believed to be a unique heavily instrumented full-scale system for the study of horizontal GHEs, under the unique rural industries' loading. The experimental set-up and monitoring instrumentation have been described in this chapter. The results of these tests verified the feasibility of the hybrid geothermal system under rural industries' unique loading condition. It is believed that future data comes from this experimental set-up can assist in validating simulation model and design tools for the horizontal GHEs.

## 3.6. Acknowledgement

The author would like to thank Dr Olga Mikhaylova and Mr Gregorius Aditya for their advice and help with system design and field work. The author acknowledges Ms Huiyan Qi and Ms Yi Zhang for helping analysing the field data during their final year IE project in semester one, 2019.

# 4. Improving energy efficiency of a typical poultry shed in Australia

This chapter has been submitted as a research article to Renewable and Sustainable Energy Reviews, in collaboration with Prof. Lu Aye and A/Prof. Guillermo A. Narsilio. Modifications have been made to the numbering of page numbers, sections, references, tables and figures to keep the consistency of the thesis. Preliminary results from a conference paper in related to this work are included as Appendices A.1. In this chapter, the primary focus is the operational costs, a more holistic approach of lifecycle costs (that includes capital costs amongst others) will be discussed in chapter 6.

*Acknowledgements*

The authors would like to thank the Australian Research Council for the funding of Linkage Project LP160100070 and FT140100227. The authors would also like to acknowledge the contribution Mr Adam Bittisnich made during his final year research project.

## 4.1. Abstract

Space heating and cooling is responsible for 40% of the global final energy use. With more energy efficient technologies, up to 10% of global energy consumption could be reduced. In agriculture industry, poultry sheds are used to raise poultry (broilers and layers). The range of acceptable indoor air temperature for poultry sheds is between 15°C and 25°C for mature birds, and higher temperatures are required for young birds depending on the stage of growth. It is recognised that the cost of heating, cooling and ventilating poultry sheds is a significant part of the chicken farm operating costs. Various potential improvements can be considered to reduce these costs considerably. They include better thermal performance of building envelopes, operational schedules, purging (ventilation strategy) and energy efficient HVAC systems. This investigation aims to reduce cooling and heating energy consumption by considering these four improvements. The heating and cooling demand cycles of a typical identical poultry sheds in three Australian states (NSW, QLD and VIC) have been simulated in detail by using TRNSYS 18. We found that operational schedule, ventilation strategies and HVAC systems have a significant influence on energy consumption. The building envelope has an opposite effect on the heating and cooling loads, when reducing one increase the other one. The maximum cost reduction by the building envelope optimisation is less than 0.5%. An optimised schedule can reduce about 2.0% to 3.7% of the heating and cooling cost, while a better ventilation strategy can reduce further up to 10.1% of the cooling cost. The selection of HVAC system is the most significant factor among all the other factors. Depending on the electricity and gas prices, up to 20% and on average 6% of the total heating and cooling operating cost can be reduced should the gas heating system be replaced by a geothermal system.

*Keywords:* Building energy simulation; Energy use; Poultry shed.

## 4.2. Introduction

The global annual energy consumption is about 544 EJ (13,000 Mtoe) [55], resulting in nearly 50 Gt $CO_2$-e Greenhouse Gas (GHG) emissions. It is widely accepted that our future energy supply could not highly rely on fossil fuels such as crude oil derivatives and natural gas. The reason is that these fossil fuels are finite, and more importantly the majority of GHG emission (65%) comes from burning them [2]. To provide our next generations with a sustainable energy future, alternative approaches must be adopted.

Space heating and cooling comprise a significant part (40%-50%) of the overall final energy use [56], resulting in 20 Gt $CO_2$-e GHG emissions. By using advanced technologies for space heating and cooling, up to 1,509 Mtoe of global annual energy consumption could be reduced by 2050 [57]. In order to improve energy efficiency in existing buildings, several approaches can be considered, which include improving the thermal performance of the building envelope, determining the most suitable operational schedule and purging (ventilation strategy) as well as increasing the energy efficiency of the Heating, Ventilation and Air-conditioning (HVAC) system.

The agriculture sector constitutes a significant part of Australia's economy. In financial year 2014/15; the overall sector was worth $51 billion, comprising 3% of Australia's total Gross Domestic Product (GDP) [58]. When further considering all the add-on processing industries, the overall contribution of the agriculture sector rises to 12% of the GDP [59]. Agriculture in Australia is responsible for over $1.04 \times 10^{11}$ MJ and 1.7% of the country's energy consumption annually [60-62]. Among these industries, nearly 600 million chickens per annum are raised for producing meat [7]. A typical shed provides about 200,000 chickens annually, which means there are currently around 3,000 poultry sheds for chicken meat production in Australia. The total annual cost of heating and cooling for chicken farms is estimated to be $80 million.

To raise chicken/broiler efficiently, poultry sheds are designed to meet the specific requirements for chickens during various growth stages. The indoor air temperature is a vital factor for the chicken to grow properly in an effective timeframe. Within each growing cycle, the indoor air temperature requirement changes from 33°C at the beginning to 21°C at the end, which results in a unique heating/cooling load cycle depending on the start date. Since outdoor air temperature changes throughout the day and throughout the year, a considerable amount of energy is sometimes needed to maintain the required indoor air temperature (i.e. to reach 33°C in winter).

Due to various climate conditions of the poultry sheds locations, it is essential to analyse the heating/cooling demands for local conditions. The aim of this paper is to reduce the energy consumptions for heating/cooling of an identical typical poultry sheds in three locations in Australia. They are Central Coast, New South Wales (NSW), Sunshine Coast, Queensland (QLD), and Mornington Peninsula, Victoria (VIC), as in these states about 74% of the chicken are raised. The reduction in energy consumptions can be achieved through improvements in building envelope, the adoption of energy efficient HVAC systems, applying appropriate operation schedules and ventilation. The next section presents the findings the current literature available.

## 4.3. Energy Efficiency Improvement Options

This section reviewed the key factors that can influence the heating and cooling energy consumptions for broiler production. First, the effects of building envelope insulation on heating and cooling loads were examined. Second, the effects of operational schedules and fourth the effects of night ventilation strategies were reviewed for poultry sheds. Third, the effects of alternative energy efficient HVAC systems and their implementations were investigated. The investigation includes geothermal, solar and biogas systems.

### 4.3.1. Building envelope

Researchers have conducted building energy simulations for poultry sheds considering heating/cooling load cycles in recent years. Kharseh and Nordell (2011) [10] estimated the heating and cooling loads for typical poultry shed in Syria in order to design a geothermal cooling and heating system for the shed. One of the assumptions made in [11] was "Heat release from chickens: 50 W $m^{-2}$ of floor area (varies with age)". This is not accurate enough to be generalise for estimating loads for other operations which may incrementally harvest the poultry. El Mogharbel et al. (2014) [63]developed a 3D computational simulation model for the heating system of a poultry shed in East Lebanon, with various factors taken into consideration. The model was based on the solar assisted heating system only and no annual performance data and cooling loads were reported. Rojano et al. (2015) [64] developed a 3D model using a CFD commercial software package, Fluent. In their study, the heat and mass transfer within poultry shed in the US is analysed in detail. However, the aim of their work was to analyse temperature, humidity and air quality in the shed. Hence, no heating and cooling loads were reported. Besides, owing to the complexity of the 3D model the computational time is long, thus applying their model for estimating annual heating and cooling loads is unlikely to be feasible. Hamilton et al. (2016) [65] developed a thermodynamic model for the thermal analysis of a poultry shed in Australia. Their model contributes to a theoretical analysis of chicken growth, heat generation, and water consumption during the cycle. Validation based on measured data was also made on the model. However, there were no direct data provided for heating and cooling loads. It was found that limited knowledge is available to derived shed's cooling and heating loads during growth cycles, particularly for specific local settings.

The building envelope of a poultry shed can be important due to the shed's indoor temperature requirements and closely related to its energy efficiency [66]. There are currently two major construction types of the poultry shed, i.e. ventilated poultry shed, and the tunnel shed [67-69]. Xin et al. (1993)[69] and Liang et al. (2013)[68] compare these two types of building envelopes and conclude that insulation in poultry shed is a requirement for energy load reduction. This may be a reason that in modern times the design of a single-story tunnel shape for the brooding of broiler chickens has become more common design option.

Mogharbel et al. (2014) [63] create a simulation of a modern poultry shed energy system in order to increase energy efficiencies. They applied a heat transfer coefficient (U-value) for the walls and ceiling to be 2 W $m^{-2}$ $K^{-1}$ indicating the rate in which energy is lost through the material, the larger the U-value, the more energy lost. Although this U-value may seem high, Hamilton et al. (2016) [65] reveal that in the past sheds were designed to have little insulation. It is only now; due to rising costs and research into the energy performance that farmers need to look into improving building envelops. In an agricultural centre in Canada, Hachem-Vermette and MacGregor cited the American Society of Heating, Refrigerating and Air-

conditioning Engineers' (ASHRAE) recommendation to utilise insulation of 1.74 W $m^{-2}$ $K^{-1}$ in commercial buildings [70]. The recommended value is lower as it offers better insulation. Beyond this recommended value, Missouri Poultry Farms applied U-values of 0.077 W $m^{-2}$ $K^{-1}$ for walls and 0.042 W $m^{-2}$ $K^{-1}$ for ceilings which result in savings of $1775 USD [71].

### 4.3.2. Operational schedule and ventilation

Local weather conditions (solar radiation, ambient air temperature, wind speed) have immense and direct impacts on the heating and cooling requirements in the already sensitive indoor temperature needed in poultry sheds [64, 72, 73]. Therefore, there is room for exploration of the timing of broiler growth cycles with local weather in an attempt to reduce heating and cooling loads. During summer, the temperature in the sheds are naturally high and less heating is required. Conversely, in the winter energy use for heating will need to counteract the infiltration of cold air outside in order to keep a stable and comfortable indoor temperature. The typical growth cycle of broilers ranges across the literature and the world anywhere from six to eight weeks [63] [74]. Previous study has found that after five weeks broilers reach harvest weight but may stay in the sheds to grow to larger weights commonly ending at eight weeks [8]. Ultimately the period of growth is dependent on market demand or producer constraints. This cycle period can decide the number of cycles able to be completed in a single year as a five-week cycle might result in eight to nine cycles in a year compared to live to six cycles per year at eight-week growth cycles.

Another operational procedure that is made in the production of broilers is the choice of broiler density (also known as stocking density). This determines the population of the broilers to be housed in any one house. Higher demand for poultry meat and inability to increase number of cycles possible per year or number of houses easily have resulted in increased broiler density in houses**.** A result of this higher density has meant increased heat generation by the flock and a reduction in heating loads but an increase in cooling loads later in the growth period. In order to grow RSPCA certified broilers the maximum broiler stocking density of 34 kg/$m^2$ [75]. Dawkins et al. (2004) [76]investigated how differing broiler densities can impact on animal welfare and growth rate. They determined that from a density of 30 kg/$m^2$ to 46 kg/$m^2$ the lowest density of 30 kg/$m^2$ was optimal in terms of having the highest growth rate and highest 'gait score' which assessed how well the broiler can move about the houses. However, they did not analyse any density lower than 30 kg/$m^2$ so it is inconclusive if this is the optimum density [76].

Other literature on this issue includes Bilgili & Hess (1995) [77], however their method of assessing levels of broiler densities is in the form of square foot per bird. This parameter is not as useful as it does not take into account the weight change of the bird during the cycle and as a result needs to be updated throughout growth stages. Regardless, their findings show that body weight increased, and mortality decreased at the lower density of 0.093 $m^2$/bird (equivalent to 1 $ft.^2$/bird); however, there was no exploration of densities lower than this for comparison. Feddes et al. (2002) [78] introduce a new method of measuring broiler density in the form of birds/$m^2$ and explore the effects of four different densities (23.8, 17.9, 14.3, 11.9 birds/$m^2$) on body weight. It was found that at 14.3 birds/$m^2$ the live weight was the highest.

Ventilation is also important in poultry shed operation to maintain a suitable indoor environment for the poultries to grow [79, 80]. It not only would remove the odour inside the building by providing the fresh air outside, but also can be helpful to reduce the cooling loading demand. Additionally, a well-defined ventilation strategy can also reduce the cooling loads of the building by providing passive cooling via night ventilation [81-89]. This method

is used to bring down the indoor temperature by circulating the night cool air during the evening when the building is not occupied. As the building is pre-cooled in the night, the cooling loads in the day can be reduced.

During poultry shed operation, the livestock is normally kept in the building all the time and the indoor temperature requirement is different from residential buildings. However, different ventilation strategy could still be utilised to reduce the cooling loads using similar concepts like night ventilation.

### 4.3.3. Energy efficient HVAC systems

In order to improve the energy efficiency of poultry sheds, it is important to examine the source of energy and system applied. For many farmers in Australia, the heat produced for use in poultry sheds is fuelled by either liquid petroleum gas (LPG) or natural gas [90]. The recent increased of gas prices, 262% over the past six years has forced farmers to explore alternative methods of generating heat for their poultry sheds [91]. One of these technologies is the utilisation of Ground Source Heat Pump (GSHP) system which utilize geothermal energy stored in the ground to heat poultry sheds. It is one of the renewable and highly efficient HVAC systems. Recent years have witnessed more and more applications of GSHP systems in the United States, Europe, Canada, China and Australia etc [15, 16, 21, 24, 26, 27, 92, 93]. For a well-designed GSHP system, it can typically operate with a coefficient of performance between three to four [9, 94, 95]. It means that for three to four kWh of energy removed/injected into the ground, one kWh electricity is consumed. The studies on geothermal systems in the residential sector have proven the technology to be feasible both in terms of performance and economy [21]. The study of twenty installed GSHP systems found that there may be a financial gain of $592 AUD per annum with a design life of 40 years [21].

In the case of farms, it is financially viable to install geothermal systems with horizontal ground heat exchangers at a shallow depth and take advantage of the large available land area [21]. For typical residential cases with vertical boreholes, the cost is reduced due to not requiring deep boreholes drilled which have been found to comprise over 50% of the total installation cost [21]. Furthermore, the larger heating requirements in the poultry shed may lead to shorter pay-back times. This is mainly due to the reduction of reliance on expensive and high quantity gas used to fuel the existing heating systems. Due to the heating and cooling loads of the poultry shed, there is a need for heating when the ambient air temperature is below the setpoint temperature, and a need for cooling when the ambient air temperature is above the setpoint temperature. This has traditionally required both a separate heating and cooling system which results in higher capital costs [21]. Choi et al (2012)[11] investigate the effects of using a GSHP for heating a poultry shed. They compared a GSHP system with a conventional heating system with diesel burners. They found that although electricity consumption increased during the 35-day cycle, the reduction in fuel consumption resulted in the total energy cost of heating was reduced by approximately ₩2.489 million won (~$2,487 AUD with 2010 exchange rate from Historic Exchange Rates - South Korean Won, 2018). This is a saving of 92% of the total energy cost when compared to the conventional system [11]. An additional benefit was the increase in the weight of chickens by 6.8% due to improved air quality in the geothermally heated shed. This finding was reaffirmed by the simulation study of Kharseh & Nordell (2010) [10] for a GSHP in the production of poultry. This is a case study in Syria where the weather is slightly different compared to South Korea. However, they both experience similar freezing periods during winter. Kharseh & Nordell (2010) [10] showed reduction in annual energy consumption by 57.2% by using GSHP instead

of conventional coal heating system by 6.8% mainly due to improved air quality conditions. A reduction of coal consumption by 107,600 t per annum was found. When compared to diesel system with an Air Source Heat Pump (ASHP) similar to the South Korea study, the annual operation costs could be reduced by 79.7%. In a slightly different application of geothermal energy; Tahersima et al. (2018) [96] experimented on a mass radiant floor system for a warehouse. The goal to maintain a constant temperature in relation to the freezing outside temperature within a 3000 $m^2$ warehouse using the concrete slab as heat storage is somewhat similar to the aims of heating for poultry sheds, albeit their target temperatures are slightly lower at the 21-23℃ range. They found that to operate the system for 12-hour durations (8 pm - 8 am) resulting in cheaper electricity costs by utilising off-peak prices. This method could potentially change the way HVAC is designed for use in poultry sheds as instead of heating from air pumped in then can opt for the warming of the floor creating an evenly distributed vertical temperature gradient up to 2.5 m high. Poultry shed flooring is normally comprised of ground or concrete similar to the study. Conversely, this would require large changes in current building design and regulations [96].

Although GSHP shows promising results in parts of the world with highly variable climates, it may not be applicable to all existing farms. As a result, there is a market another alternative for heating in biogas and solar systems. The litter produced during the broiler cycle is routinely removed and this waste can be used as fertiliser or sent to landfill. Due to efforts to reduce waste this litter can be utilised to produce biogas which can then be used for the system. This technology was studied for the Indian poultry industry by Begum et al. [97] where they successfully converted 1000 kg poultry litter into 68 $m^3$ of biogas per day. This resulted in daily generation of 89 kWh which was then be utilised on the farm allowing for less reliance on local power. On a much larger scale, Arshad et al. 2018 [98] calculated the possible energy generation by converting Pakistan's' twenty-five thousand poultry farm waste into biogas. From over one million tonnes of manure and other chicken waste, they estimate the potential daily electricity generation of 300 MWh. However, the infrastructure for this does not exist unless adopted in the countries renewable energy policy.

There is also the option of combining several energy efficient technologies to diversify farms energy security. There are studies that investigate the integration of solar and geothermal such as Carotenuto et al. (2017)[99] and Kharseh & Nordell (2010)[10] which show the benefits of the two technologies and how they interact. Kharseh & Nordell (2010) [10] combined solar collectors and ground heat exchangers in order to boost the amount of heating/cooling produced by the system. During winter the fluid is circulated through solar collectors to increase the temperature after passing through the ground heat exchangers. However, an issue with this is that the cooling load is higher during the summer months so heating the water should not be a priority. Although this technology may not seem ideal for use in Syria where winters result in low solar radiation, Australia has high solar radiation throughout the year so maybe more viable as average global solar radiation in Syria is about 2.3-2.5 kWh $m^{-2}$ $day^{-1}$ during winter compared to 2.8-3 kWh $m^{-2}$ $day^{-1}$ for Australia [100] [101]. Regardless Carotenuto et al. (2017) [99] propose a novel low temperature heating and cooling system for a city in Southern Italy which also combines solar and geothermal technology. They discover similar issues in winter where solar radiation is low so being annexed from the system during these periods to reduce heat loss. However, a study of solar-assisted localized ventilation system for poultry brooding by Fawaz et al. (2014) [102] has shown that solar technologies may still be practicable during winter months. A simulation of the heating load

was conducted, and a parabolic solar concentrator was sized to meet this requirement. This resulted in a reduction of energy needed by 74% compared to a conventional diesel system. Moreover, the concentrated solar system was efficient enough to cover 84% of the required load during the winter.

### 4.3.4. Summary of findings

From the brief review conducted by investigating the key parameters affecting heating and cooling loads, there are several key areas that require further investigation. These areas include the building envelope of the poultry shed which is responsible for regulating its internal temperature. The building envelope, focusing on the choice of building insulation is the key isolator between the internal and external temperatures of the poultry shed and as such dictates the required heating and cooling. The location and climate of the poultry shed also play a key role which either helps or hinders the constant temperature experienced within the poultry shed. The seasonality of the climate is especially important as the poultry production cycle occurs throughout the year. Later, the operational schedule, which indicates the starting and ending of the broiler growth cycles and when they occur during the year. The operational schedule and ventilation strategies are likely to be directly dependant on the local climate and discovering the optimum time to avoid extreme seasonal temperatures. Furthermore, the current reliance on gas heating for most Australian states results in a rising energy cost that is impacting the fiscal feasibility of broiler production. As such the review investigated energy efficient alternatives that are currently in use on small scales as well as emerging technologies that may change the face of the industry. To accelerate the uptake of these technologies, an appropriate investigation into the operation and feasibility need to be conducted with industry case studies and field measurements with the results of this to be made available to the industry.

## 4.4. Methods

Transient System Simulation Tool (TRNSYS) has been widely used for building energy performance simulations. In this paper, a TRNSYS model was developed and verified for a poultry shed. Other details of the methods employed are presented in this section.

### 4.4.1. Simulation parameters: location, construction, operation and climate

An existing typical poultry shed is take as a case study. It is located in the Central Coast Region, NSW, Australia (approximately 33.38861 S and 150.40250 E). Climate data are essential for building simulation. A typical meteorological year (TMY) data generated by an algorithm based on 20 years of the recorded dataset is widely used to predict the long-term performance of buildings. In this paper, the TMY file generated by Meteonorm 7.1 based on recorded climate data from 1990-2010 is utilised. An average error of 6% in year sum compared with the actual climate can be expected by using this method of hourly data generation [103].

Table 4-1 Poultry shed simulation parameters.

| | |
|---|---|
| Dimensions | Width:18.3 m, Length:138.7 m, Height: 2.7 to 4.3 m |
| Wall/Roof Material | No windows; Insulation with thin layers of metal cladding. Insulation thickness: 0.075 m , thermal conductivity: 0.039 $Wm^{-1}K^{-1}$ , density: 16 $kg\,m^{-3}$ , specific heat: 340 $Jkg^{-1}K^{-1}$ |

As shown in Table 4-1, this is only one zone within the shed. The building is constructed with 75 mm thick 'Coolroom' walls with no windows. A chicken usually attains 2.8 to 3 kg at the age of 8 weeks. The mass of chicken for the first 35 days is provided by Ground Source Systems Pty Ltd while the following 21 days data is generated through a quadratic function. Heat produced by a chicken is proportional to the metabolic weight, which is the unit of 0.75 power of kg [104]. The heat rate generated by an adult chicken is 160 $kcal\ d^{-1}W^{-1}$ (7.75 $W\ W^{-1}$) [105, 106].

In Australia, it usually takes about 50 days for a recently hatched chicken to develop fully for the market. Meat broilers reach the mass of harvest at the age of 35 days, and partial harvest of chicken happens up to three times in one batch on a chicken farm due to the different demand for light and heavy chicken meat. After that, there are 5 to 14 days for clean-up and preparation for the next batch [107]. The simulation in this paper is based on the operational schedule (raising batches of chicks) shown in Table 4-2. The data is in accordance with the chicken growing recommendations provided by the shed owner and operator.

Table 4-2 Chicken growth and metabolic heat generation.

| Day of growing cycle | Mass per chicken (kg) | Heat generation per chicken (W) | Number of chicken (-) | Indoor setpoint temperature (°C) |
|---|---|---|---|---|
| 1 | 0.054 | 0.82 | 50,000 | 31.0 |
| 7 | 0.180 | 2.02 | 50,000 | 28.6 |
| 14 | 0.438 | 3.93 | 50,000 | 26.1 |
| 21 | 0.829 | 6.34 | 50,000 | 23.7 |
| 28 | 1.337 | 9.08 | 50,000 | 21.2 |
| 35 | 1.897 | 11.80 | 50,000 | 19.0 |
| 42 | 2.444 | 14.27 | 35,000 | 19.0 |
| 49 | 2.873 | 16.11 | 25,000 | 19.0 |

Similar to the normal operation of the case study shed, 50,000 chickens were assumed at the beginning of each batch. Three harvests are expected in one batch, happening at the end of the fifth, sixth and seventh weeks of the cycle. The first harvest is assumed to be 15,000 chickens while the second one 10,000 chickens and the last harvest remaining 25,000 chickens. Mortality of chicken during growing cycles was not considered as it is negligible.

Table 4-3 Selected locations in Australia and their annual average outdoor air temperatures (°C) [109].

| **Location** | **Latitude (°)** | **Longitude (°)** | **Summer** | **Winter** |
|---|---|---|---|---|
| Central Coast, NSW | 33.38861 S | 150.40250 E | 25.1 | 11.5 |
| Mornington Peninsula, VIC | 35.28527 S | 145.09333 E | 31.7 | 15.3 |
| Sunshine Coast, QLD | 26.60621 S | 152.79397 E | 26.5 | 14.8 |

The location and its local climate may also have an impact on the heating and cooling loads. Three different locations: Central Coast, New South Wales (NSW); Sunshine Coast, Queensland (QLD) and Mornington Peninsula, Victoria (VIC) were considered. These locations are chosen based on the distribution of the chicken production in Australia [107,

108] and each location can be a good representative of its state. The three states account for over 74% of Australia's broiler production [7, 107, 108]. Table 4-3 summarises the differing climate patterns experienced around Australia. All factors besides the location of the poultry shed have been kept constant for this analysis.

### 4.4.2. Building envelope

The dimensions of this building can then be integrated into building energy simulation software, TRNSYS 18. As shown in Fig 4-1, the model consists of five components, including data input (weather data, ground temperature and operational schedules) mentioned above, building simulation (Type 56) and simulation output. The model allows sophisticated simulation for the heating and cooling loads of the building (poultry shed). It should be noted that the building envelope data as shown in Table 4-1 are inputted in Type 56.

To be specific, the TRNSYS project applied Type 56 multi-zone building model. For the building envelope section, the building material thickness, conductivity, density, specific heat can be specified. Since conductivity, density and specific heat are related to material and cannot be changed easily. This investigation aims to determine the most effective insulation by varying the thickness of the building envelope. By altering the thickness of the insulation walls, it affects the shed's ability to lose or gain heat. The higher the thickness, the less the material transfer heat. For the following analysis, it was assumed that the material is of a constant density, thermal conductivity, and specific heat.

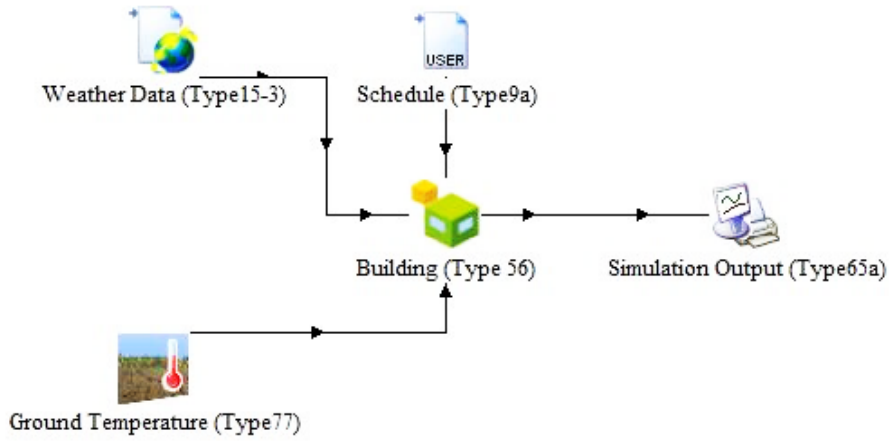


Figure 4-1 TRNSYS simulation model for heating and cooling loads.

### 4.4.3. Energy efficient HVAC systems

In this investigation, two different HVAC systems are considered. The first option is the gas burners for heating and evaporative coolers for cooling, which are typically equipped in current farms in Australia. The gas heaters were assumed to have an efficiency of 0.85 [9]. It was hard to determine the operating efficiency of evaporative coolers because their performance highly relies on the relative humidity and ambient air temperature. However, it is known that evaporative cooling usually saves around 75 to 85% of the cost compared with standard air conditioning [110]. This paper assumed one-sixth of the cost of air conditioners with a Coefficient of Performance (COP) of 2.5 [9, 21].

To further investigate the operational cost reduction with energy efficient systems, the state-of-the-art GSHP option is considered. However, an evaporative cooler is much more economical than conventional air conditioning systems. GSHP system will be used for heating only and cooling will still be provided by the evaporative coolers. The COP of a heat pump can vary under different operational conditions. In this investigation, the annual average COP of the heat pump was assumed to be 3.3 [9, 21]. The additional equipment electricity consumption, including the circulating pump, was assumed to be 10% of the heat pump electricity consumption. Apart from efficiency, energy prices are also key factors. Table 4-4 presents the energy prices used in this investigation. The energy prices in the reference farm in NSW were obtained from the current gas and electricity contracts of the farm owner. It should be noted that gas and electricity prices can differ from farm to farm depending on the contract with suppliers; electricity usage price for this farm is particularly competitive due to high fixed supply charge. The fixed supply charge for electricity and gas is not considered in the lifecycle analysis because the payment of the fixed charge is required, like the land tax or council rate, regardless of whether a hybrid system is installed or not. The average electricity and gas prices in NSW, QLD and VIC are obtained from Jacobs' and Alviss Consulting's reports as average prices for small and medium enterprise (SME) [111, 112].

Table 4-4 Energy prices for SME in Australia [111, 112].

| Location | Gas ($ $GJ^{-1}$) | Electricity (¢ $kWh^{-1}$) |
|---|---|---|
| NSW Farm contract | 19.5 (LPG) | 10.0 |
| NSW SME average | 26 | 31.2 |
| QLD SME average | 35 | 29.8 |
| VIC SME average | 18 | 24.3 |

### 4.4.4. Farm operations schedule and shed ventilation

A typical chicken growing batch takes seven weeks duration. It is almost impossible for a shed to run seven whole batches in one year due to the time required for cleaning and preparation. In this investigation, six batches were considered for one year. Assuming a minimum break of one week for cleaning and preparation, the possible intervals between each batch are one to six weeks. With at least a one-week break between the last batch and the first one, there are overall 1,092 possible operating schedules. In this paper, the costs of all of the 1,092 possible schedules have been estimated using a MATLAB code developed to find the one with minimum operational cost.

Various ventilation/purging scenarios are discussed to find the optimum ventilation method. When the ventilation rate becomes higher, the energy consumed to move the air will increase. The Ventilating Efficiency Ratio (VER) is used to describe the efficiency of the fan. This ratio is defined as the cubic feet of air moved per minute over the electricity consumed by the fan in Watts. The larger the number is, the higher the efficiency is. In this study, it is assumed that the VER of the ventilation fan is constant at 15 [113], which is within the range of the average performance of most fans. This paper reports both the reduction of the cooling loads and the electricity consumption of the fan when the ventilation rate is increased.

## 4.5. Results

The hourly heating and cooling loads were calculated using the TRNSYS model mentioned above. Estimation of costs based on the current HVAC system and Geothermal system have also been conducted.

### 4.5.1. Heating and cooling loads for different farm operational schedules

In order to determine the heating and cooling loads for the different starting dates, 52 batches starting at different weeks for one year were investigated. The first week starts on 1st of January, the first day in a year. As an example, Fig 4-2 depicts the indoor and outdoor temperatures (a) and hourly heading ad cooling loads (b) of a seven-week summer batch for a typical poultry shed in Central Coast, NSW, the first week of this batch starts on the 19th of December (corresponds to week 52 of the year). The indoor thermostat is set every day to meet the temperature requirement for raising broilers. During the growing batch, the heating load decreases as a result of increasing heat generated by the chickens. After that growth stage, the cooling load significantly increases during the following first five weeks. After each harvest, the internal gain (heat produced by chicken) reduces, which results in a reduction of the cooling load.

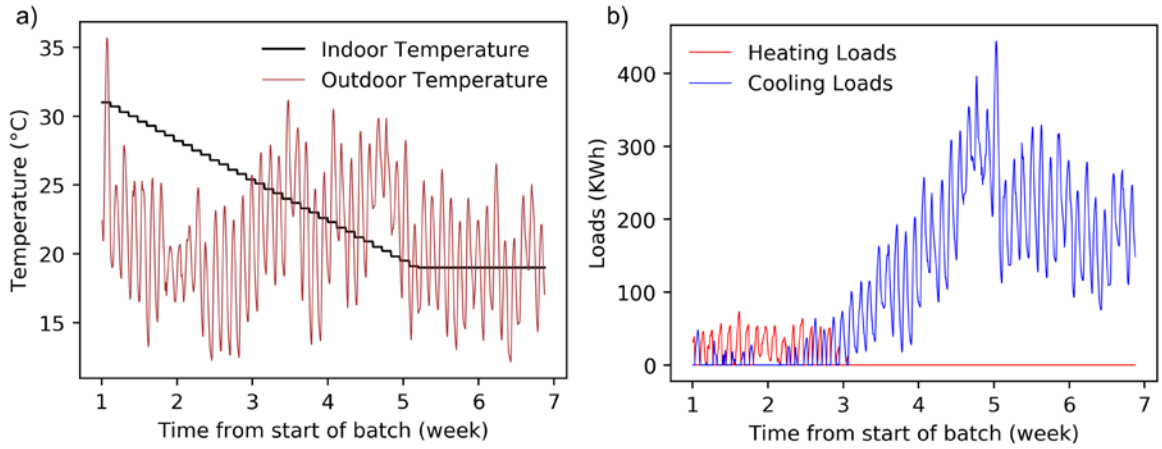


Figure 4-2 Seven-week summer batch for a typical poultry shed in Central Coast, NSW: (a) Hourly indoor and outdoor air temperatures, (b) Hourly heating and cooling loads.

### 4.5.2. Effect of the thickness of the building envelope

The basis of this section is an analysis of a poultry shed located in New South Wales using insulation materials of thickness 75 mm. The results from this simulation will consider how altering the thickness of the building envelope of the poultry shed will result in changes to its heating and cooling loads. From Fig. 4-3, it can be seen that thickness of the building envelope is showing an inverse relationship between heating and cooling loads.

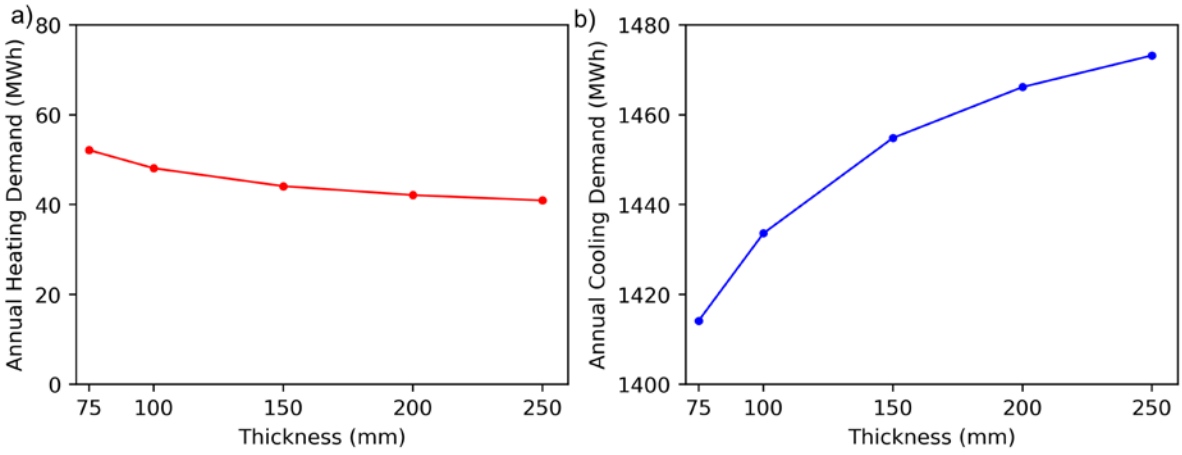


Figure 4-3 Effect of thickness of the building envelope for a typical poultry shed in Central Coast, NSW on (a) annual heating demand , and (b) annual cooling demand.

As thickness increased, the heating load reduces and conversely cooling loads increase. However, this tradeoff was not uniform as found by increasing the thickness 233% from 75 mm to 250 mm resulting in reduced heating loads of 21.4% and increased cooling loads by only 4.2%. Even though the reduction percentage for the heating is much higher than the increase percentage of the cooling, the actual reduced heating demand (11.2 MWh) is much less than the increased cooling demands (59.0 MWh). This is because the annual cooling demand (about 1,450 MWh) is much higher than the heating demand (about 50 MWh). Even though the evaporative cooler for cooling has a much higher efficiency comparing with GSHP or LPG/Gas burners for heating, the overall impact on the annual heating and cooling cost is marginal (less than 0.5%). Therefore, changing the thickness of the building envelope is not recommended for the improvement of the energy efficiency of the poultry shed.

### 4.5.3. Effect of ventilation/purging

Fig. 4-4 shows the hourly cooling loads for one week, starting from 1st April. Under 100%, 150% and 200% of the standard ventilation rate. To better perform the purging optimisation, this purging scenario was developed, considering only purging when the cooling is required, and the outdoor temperature is lower than the indoor temperature. In this scenario, it has been reported that the cooling loads are always no higher than the standard ventilation. Regarding the annual total cooling loads, 10.3% and 21.3% reduction compared with the standard ventilation has been observed under 150% and 200% ventilation rate, respectively. However, there is no reduction in the peak cooling loads as it happens when the outdoor temperature is higher than the indoor temperature, which is not suitable for purging.

As increasing the ventilation will also increase the energy required to operate the ventilation fans, it is necessary to also analyse the energy consumed by the fans. Table 4-5 shows the annual cooling and ventilation electricity consumption under different scenarios. Considering the annual total fan electricity consumption, the increase is 4.5 MWh and 9.2 MWh under 150% and 200% ventilation rate, respectively. By adding the cooling electricity consumption, the total electricity consumption has reduced by 4.8% and 10.1% under 150% and 200% ventilation rate, respectively. The maximum 200% of the standard ventilation rate is estimated based on the sizes of the ventilation and exhaustion fans. The same method can then be applied to the heating; however, the results have proved to be not significant (1 - 2%).

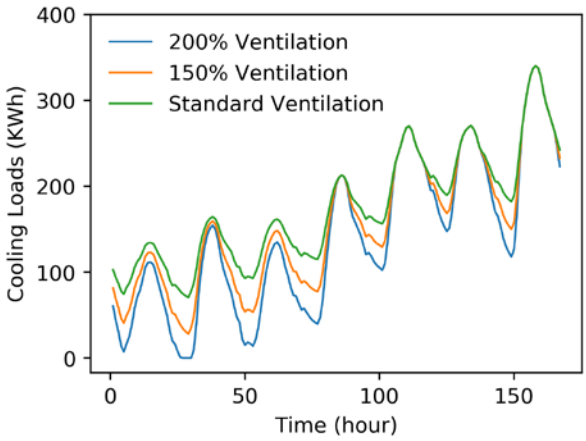


Figure 4-4 One-week cooling loads under discontinuing purging for a typical poultry shed in Central Coast, NSW starting 1st of April (week 14 of the year).

Table 4-5 Annual cooling and ventilation electricity consumption for a typical poultry shed in Central Coast, NSW.

| Ventilation | Cooling Loads (MWh) | Cooling Electricity Consumption (MWh) | Ventilation Electricity (MWh) | Total Electricity Consumption (MWh) |
|---|---|---|---|---|
| 100% | 1,414 | 94.3 | 13.3 | 107.6 |
| 150% | 1,269 | 84.6 | 17.8 | 102.4 |
| 200% | 1,113 | 74.2 | 22.5 | 96.7 |

### 4.5.4. Cost estimation for different HVAC systems

Different HVAC systems can have a significant effect on the energy expenditure. This section estimates the annual heating and cooling cost for a typical poultry sheds different locations with two different heating systems. Firstly, after hourly heating and cooling loads for 52 starting weeks were acquired, the overall energy consumption for each batch was obtained by summing up the heating and cooling loads. At the beginning of the year (summer), raising a batch requires much more cooling than heating (nearly eight times higher). Later, as the outdoor air gets colder, the heating loads increase while the cooling loads decrease. At the middle of July (winter), the heating load reach the peak for one batch, while the minimum cooling load. After the coldest periods of the winter, the heating load begins to reduce together with the increase of cooling demand. The highest cooling demand happens at the beginning of the year, corresponding to the minimum heating demand for one batch.

Based on the overall energy consumption for each batch starting at 52 different weeks in a year, the heating and cooling cost can be estimated. Fig. 3-5 shows the heating and cooling costs for the different starting week with two different heating options at three different locations. Since the evaporative cooler is cheaper to operate than GSHP systems, all the scenarios considered the evaporative coolers for cooling. For all the scenarios corresponding to the loads, the heating cost rises from minimum in the beginning to the peak in the mid-year while the cooling cost reduces from the peak to the bottom. After winter (mid-year), the heating cost decreases, and the cooling cost increases.

In general, the GSHP system has a lower heating expenditure than the LPG (gas) heating system (except the Mornington Peninsula, VIC case, where gas price is very low), as shown in Table 3-6. However, the amount and percentage of reduction in the heat cost by using GSHP systems depends on the energy price. In Central Coast, NSW, with their current contract price, the GSHP heating option can be nearly 60% cheaper than the LPG heating system on average. However, when the price is NSW state averaged price, this becomes slightly (5%) better. With the state averaged electricity and gas price, Sunshine Coast has the most benefit of GSHP heating system, where on average 33% of heating cost reduction can be expected. However, in the Mornington Peninsula, VIC case, the heating cost for GSHP system is even slightly higher (6%) than the gas heating system due to the cheap gas price. Based on the state averaged electricity and gas price, raising a chicken batch in Sunshine Coast, QLD is the most economical among all the cases investigated. The results also reveal that raising a chicken batch in autumn and early winter costs much less than the rest of the year. In general, the most cost-effective period for starting a batch is from late March (12$^{th}$ week) to June (29$^{th}$ week).

When considering the total cost saving by switching from LPG heating to GSHP heating, as shown in Table 4-7, there is also a high variation among different location and pricing

scenarios. The high reduction can be achieved is over 20%, in Central Coast, NSW, with their current contract price. For the rest of cases investigated, the saving can marginal, and may even be negative.

### 4.5.5. Operational optimisation under different climate conditions

Since the operational schedule can be impacted by the weather condition, it is important to evaluate the potential effective of the operational optimisation under different climate conditions. Two other locations in Sunshine Coast, QLD and Mornington Peninsula, VIC has been selected for this purpose. Based on the cost data this section investigates the effect of changing the starting weeks for raising a chicken batch. Fig. 4-6 shows that the annual costs for all operating schedules resemble the normal distribution pattern, with the average heating and cooling cost as summarised in Table 4-6. The Maximum Likelihood Estimation (MLE) is used in this investigation. MLE is a method that estimates parameters of statistical models based on given data. The distribution has also passed the Kolmogorov-Smirnov test in MATLAB, a hypothesis test for normal distribution, at a 1% significance level [114].

As shown in Fig. 4-6 and summarised in Table 4-6, there are over 1000 different combinations of operational schedule analysed in each case. In these cases, the minimum heating and cooling cost are 2.0% to 3.7% less than the average cost of all the combinations, with a 2.9% average reduction. The case in Sunshine Coast, QLD seems to be least impacted and the case in Central Coast, NSW seems to be most impacted by the operational schedule.

When further considering the optimum schedules where the minimum heating and cooling costs occur, it can be seen that the results are reasonably consistent despite the difference in location and heating options (Table 4-8). On average, by starting at 5$^{th}$, 13$^{th}$, 21$^{th}$, 29$^{th}$, 38$^{th}$, and 46$^{th}$ week of the year, the most economical schedule costs can be achieved, which is on average 2.9% less than the average cost. These results show only minor differences between the optimised schedules even though the climate conditions have changed. This could be caused by that climate differences for east coast of Australia are not significant enough to result in profound changes of the operational schedule.

Table 4-6 Heating and cooling cost summary for optimum schedules for GSHP and LPG (gas) heating options in different locations.

| | | Heating (AU$) | Cooling (AU$) | Total (AU$) | Average (AU$) | Saving (%) |
|---|---|---|---|---|---|---|
| GSHP | Central Coast, NSW | 1,927 | 9,018 | 10,944 | 11,276 | **2.94** |
| | Central Coast, NSW (SME Pricing) | 6,012 | 28,135 | 34,146 | 35,180 | **2.94** |
| | Sunshine Coast, QLD | 2,884 | 33,814 | 36,698 | 37,454 | **2.02** |
| | Mornington Peninsula, VIC | 5,872 | 19,717 | 25,589 | 26,397 | **3.06** |
| LPG/Gas | Central Coast, NSW | 4,398 | 9,214 | 13,612 | 14,131 | **3.68** |
| | Central Coast, NSW (SME Pricing) | 6,325 | 28,135 | 34,459 | 35,496 | **2.92** |
| | Sunshine Coast, QLD | 3,956 | 34,061 | 38,017 | 38,910 | **2.29** |
| | Mornington Peninsula, VIC | 5,543 | 19,717 | 25,260 | 26,063 | **3.08** |
| | | | | | Average | **2.87** |

Table 4-7 Comparison for the average cost saving by switching LPG (gas) to GSHP in different locations.

| | LPG Average (AU$) | GSHP Average (AU$) | Saving (%) |
|---|---|---|---|
| Central Coast, NSW | 14,131 | 11,276 | **20.2** |
| Central Coast, NSW (SME) | 35,496 | 35,180 | **0.9** |
| Sunshine Coast, QLD | 38,910 | 37,454 | **3.7** |
| Mornington Peninsula, VIC | 26,063 | 26,397 | **-1.3** |

Table 4-8 Optimum start week schedules for GSHP and LPG (gas) heating options in different locations.

| Batch ➔ | | 1 | 2 | 3 | 4 | 5 | 6 |
|---|---|---|---|---|---|---|---|
| GSHP | Central Coast, NSW | 5 | 14 | 22 | 30 | 38 | 46 |
| | Central Coast, NSW (SME Pricing) | 5 | 14 | 22 | 30 | 38 | 46 |
| | Sunshine Coast, QLD | 5 | 13 | 21 | 29 | 37 | 45 |
| | Mornington Peninsula, VIC | 5 | 14 | 22 | 30 | 38 | 46 |
| LPG/Gas | Central Coast, NSW | 4 | 12 | 20 | 28 | 38 | 46 |
| | Central Coast, NSW (SME Pricing) | 5 | 14 | 22 | 30 | 38 | 46 |
| | Sunshine Coast, QLD | 4 | 12 | 20 | 28 | 36 | 45 |
| | Mornington Peninsula, VIC | 5 | 14 | 22 | 30 | 38 | 46 |
| Average | | 5 | 13 | 21 | 29 | 38 | 46 |

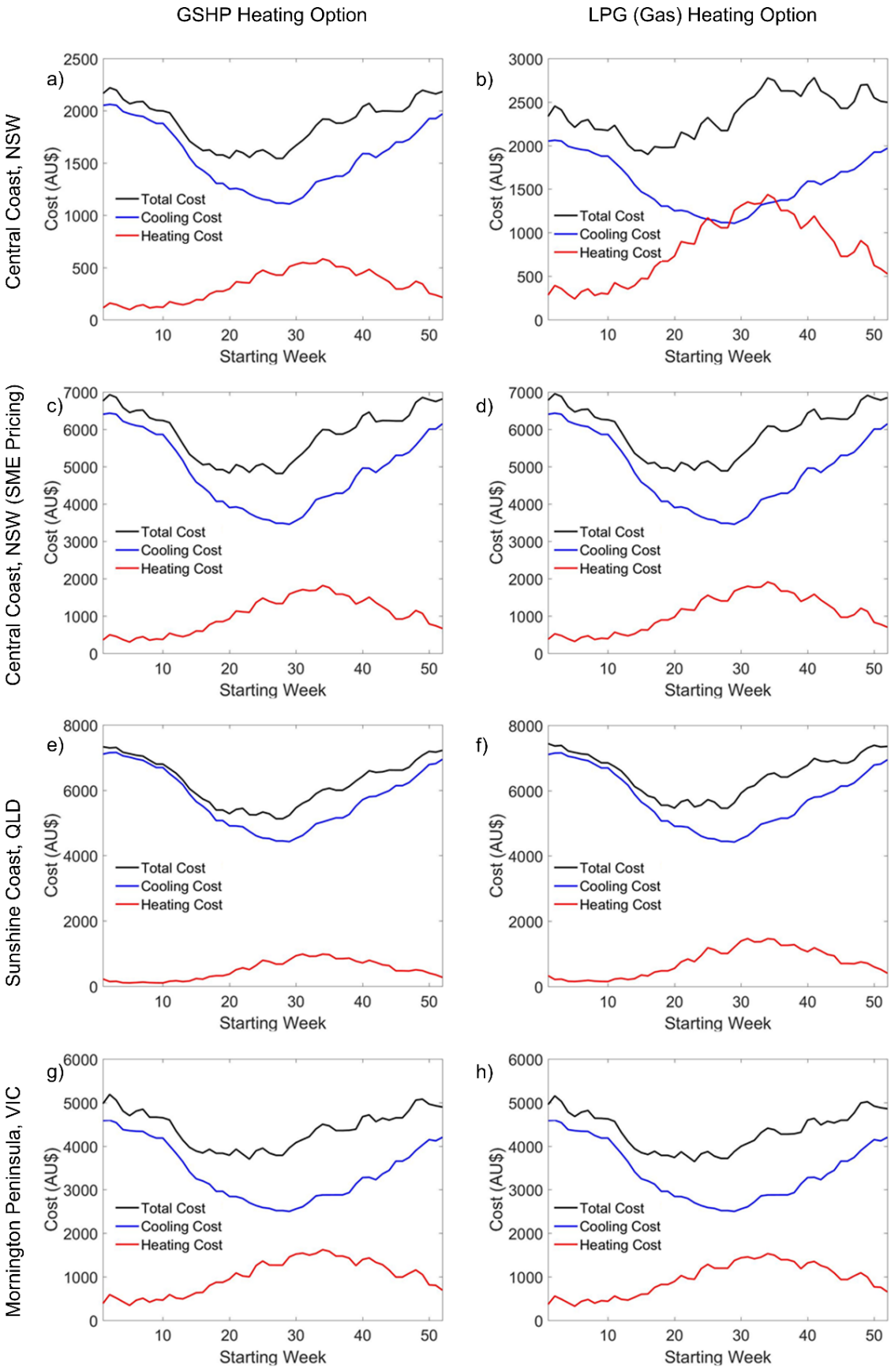


Figure 4-5 Operational heating and cooling cost with different heating options and locations.

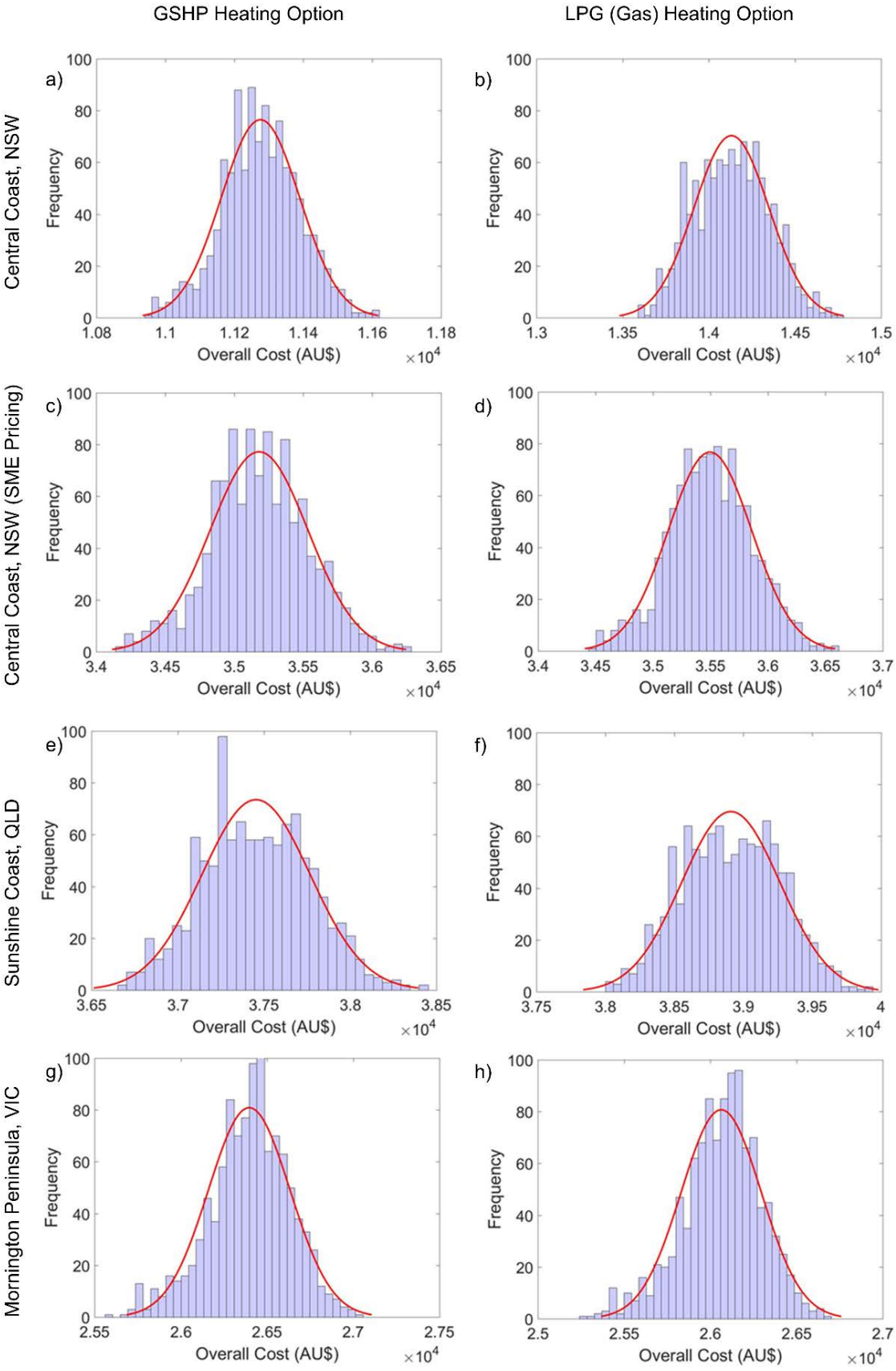


Figure 4-6 Annual operational heating and cooling cost distribution with different heating options and locations.

## 4.6. Discussion

From the results of the energy model output, it was determined that building envelope can impact the heating and cooling loads yet its impacts on the operational heating and cooling cost seem minor. This is because that reducing the heating loads will inevitably increase the cooling loads when varying the thickness of the building envelope. Moreover, for the building investigated, by reducing 1 kWh of the heating loads, about 5 kWh of the cooling loads will be generated. Even though cooling can be relatively economically supplied by evaporative coolers, there is no room to reduce operational cost by changing the thickness of the building envelope.

For the ventilation operation optimisation, it is observed that the cooling loads have highly decreased under higher ventilation rates during night-time (over 21% reduction under 200% ventilation rate). However, the total electricity consumption for both cooling and ventilation does not reduce significantly when the ventilation rate is increased. One potential reason behind this is that since the evaporative coolers are economical to use, though the reduction of cooling loads is high, the reduction of the operational expenditure for cooling is not significant enough to overweigh the increased ventilation cost much.

It was observed that the choice of HVAC system has a high impact on the operating cost, yet it is subject to the electricity and gas price. When switching from LPG gas heaters to a GSHP system, up to 60% of the heating operation expenditure and 20% of the combined heating and cooling operation cost (in Central Coast, NSW) can be saved. However, in Mornington Peninsula, VIC, switching to a GSHP heating system will increase the heating operating cost. The reason behind this is that the gas in VIC is much cheaper than the electricity. In this investigation, it is determined that the critical electricity to gas price ratio is 3.53. This means that when the electricity price (per kWh) is more than 3.53 times more expensive than gas, operating a GSHP system would be more expensive than the gas heating system. In Mornington Peninsula, VIC, the electricity is 3.75 times expensive than the gas. Therefore, switching from gas heating to GSHP heating is not financially feasible in Mornington Peninsula, VIC under this cost structure.

It should also be noted that though the operational cost reduction from an energy efficient HVAC system can be high, the installation of such GSHP system may cost much more than traditional gas/LPG systems. This can be further investigated via life cycle cost analysis to determine the most economical combination of the GSHP system and gas/LPG systems. However, here we focus on operational costs, yet worth to be recommended for future further studies.

Furthermore, the optimum operational schedule has been observed to be reasonably consistent under different location and heating options. This can be explained by the period of year when starting a batch is most economical late March ($12^{th}$ week) to June ($29^{th}$ week). This period coincides with the relatively low outdoor air temperature. The low air temperature results in low cooling demands, which can contribute to over 70% of the energy expenditure for combined heating and cooling. It can be observed that for the optimum schedule, half of the batches start within this period, which maximised the cost reduction.

## 4.7. Summary and conclusions

This paper investigated the energy efficient solution to reduce the heating and cooling loads of a typical poultry shed in Central Coast, NSW; Mornington Peninsula, VIC and Sunshine

Coast, QLD; where 74.4% of the Australian chicken meat is produced. The heating and cooling demand cycles of the poultry sheds have been investigated in detail by using TRNSYS, a widely used building energy simulation software. The TRNSYS model considered the chicken growth rate and metabolic heat generation, operating schedules, building envelop materials, orientation and climate conditions. It is found that the heating and cooling demand cycle of poultry industry can be highly different from common practice in residential or other commercial buildings. These unique characteristics include energy imbalance, sharp peak demands as well as shortly alternating heating and cooling cycles.

Based on the unique heating and cooling loads simulated, this paper then investigated the building envelope, operational schedule, ventilation strategies, and different HVAC systems to reduce the heating and cooling energy consumption and expenditure. The building envelope has been found to be the least impact factor as the it cannot reduce the heating and cooling loads at the same time. The operational schedule is the third most important influencing factor. Between 2.0 to 3.7 % of the operational cost can be saved on average if the operational schedule is optimised. The night ventilation strategies turn to be the second influencing factor. Even though increasing the ventilation rate at night can reduce the cooling loads significantly, the total electricity cost reduction is about 5 to 10% due to the increase in fan electricity consumption. The increase of ventilation rate for heating has been found to be minor due to the outdoor temperature is lower than the indoor temperature for the majority of the time when heating is required.

It is found that the HVAC system selection can have the highest impact on cooling and heating energy consumption, subject to lower electricity and gas prices. By switching from an LPG heating system to GSHP heating system, up to 60% of the heating operation cost and up to 20% of the combined heating and cooling cost can be saved. A limitation worth noting is that this study considers only the operational cost of the HVAC systems. When switching from a traditional system to a highly efficient system, installation costs will typically occur. These costs can sometimes be significant and should be considered in lifecycle analysis. Chapter 6 of this thesis will discuss this in detail.

# 5. Artificial neural networks for the performance of horizontal ground heat exchangers under rural industries' loading conditions

This chapter is submitted as a research article to Applied Energy, in collaboration with A/Prof. Guillermo A. Narsilio, Dr Nikolas Makasis, Prof. Kenichi Soga from the University of California, Berkeley and Prof. Lu Aye. Modifications have been made to the numbering of page numbers, sections, references, tables and figures to keep the consistency of the thesis. Preliminary results from a conference paper in related to this work are included as Appendices A.2.

*Acknowledgements*

The authors would like to thank the Australian Research Council for the funding of Linkage Project LP160100070 and FT140100227. The authors would also like to acknowledge the effort that Ms Yuqi Kuai made during her final year IE project.

## 5.1. Abstract

A Ground Source Heat Pump (GSHP) system is a highly efficient heating, ventilation, and air conditioning (HVAC) system which utilizes the ground as the heat source when heating and as the heat sink when cooling. This paper investigates GSHP systems with horizontal Ground Heat Exchangers (GHEs) for poultry (chicken) sheds in Australia, exemplifying the technology's promising application in the rural industry. In addition, a key aim of this investigation is to provide an Artificial Neural Network (ANN) model which can be used for GSHP design at different locations and with different climate conditions. To this extent, a TRNSYS model with a typical horizontal GHE within a rural farm in Australia has been developed and validated. Using this model, over 700,000 hourly performance data have been obtained, covering over 80 different yearly loading patterns under three different climate conditions. The simulated performance data is then used to train the ANN. We found that the trained ANN is able to predict the performance of GSHPs systems with identical (multiples of) GHEs, even under climatic conditions (and locations) that has not been specifically trained for. Unlike other works, this ANN model has shown to be accurate even with limited types of input data, showing a high accuracy (no more than 5% error in most cases tested). The presented ANN is 100 times computationally faster than TRNSYS simulations and 10,000 times faster than FEM models.

*Keywords:* ground-source heat pumps, horizontal ground heat exchangers, TRNSYS simulation, artificial neural networks

## 5.2. Introduction

Ground Source Heat Pump (GSHP) systems are renewable and highly efficient Heating Ventilation and Air Conditioning (HVAC) systems that utilise the ground to exchange heat. The ground acts as the heat source when delivering heating and as a heat sink when providing cooling. Recent years have witnessed more and more applications of GSHP systems in the United States, Europe, Canada, China, Korea and Australia [15, 16, 21, 24, 26, 27, 92, 93]. To exchange the heat with the ground, Ground Heat Exchangers (GHEs) are typically used, comprising high density polyethylene (HDPE) pipes with a carrier fluid. GHEs can take many forms, including vertical boreholes, horizontal trenches, energy piles, energy retaining walls and energy tunnels [25]. Among them, vertical boreholes and horizontal trenches are the two most commonly utilised GHEs. While vertical boreholes can be installed under almost any ground and site conditions, horizontal trenches are typically utilised in suburban and rural areas, at a depth between one to two m below the surface, as it normally requires a large field of land to install them in but costs less than drilling vertical boreholes. Due to the heat exchangers being close to the ground surface, their thermal performances can be impacted by the daily and seasonal variation of the air temperature [115, 116] and soil moisture content, the latter affecting thermal conductivity of the ground [48, 117]. A well-designed GSHP system with horizontal GHEs can typically operate at a coefficient of performance (COP) between three and five [13, 39, 94, 95, 118-120]. The COP is defined as the ratio of heating (or cooling) supplied to the energy required to operate the GSHP. This means that for three to five kWh of energy removed/injected into the ground, only one kWh energy of electricity is consumed by the GSHP. Drawbacks of GSHP systems include high upfront construction costs, mainly caused by the GHE installation costs (drilling/earthworks), as well as the embodied energy and associated GHG emissions. However, these can be reduced by coupling GSHPs with other energy sources to form a hybrid system [18, 19]. Previous studies indicated that a hybrid GSHP system could not only be financially attractive, but also help to balance the thermal loads in the ground [22-24].

Current applications of GSHP systems span over a wide range of end uses including commercial office buildings, residential buildings, schools, hospitals and underground metro stations [15, 16, 21, 24, 26, 27, 92, 93].. However, there is very limited focus on applying this relatively new technology into the rural industry, which could potentially be largely beneficial. In Australia, the agriculture and all its related processing industry contributes to 12 % of the national Gross Domestic Product [5]. As an example, within the Australian agriculture sector, this paper will primarily focus on the poultry industry. Within the poultry industry, over 600 million chicken are raised yearly [7]. One of the major costs for poultry farmers and to the environment is the energy required to heat and cool large poultry breeding houses (estimated at A$80 million per year) [121]. The uniqueness of the heating and cooling load profiles of chicken brooder houses (a.k.a., sheds), together with the high risk of storing high volume of combustible gas as well as the lack of access to (cheap) natural gas in rural areas where these houses are located, make the GSHP or shallow geothermal alternative a very attractive option. Its adoption can transform the poultry farming industry by significantly reducing energy consumption (and energy bills to farmers), greenhouse gas (GHG) emissions, odours and volatile compounds (e.g., ammonia gas production, hydrogen sulphide, mercaptans), chicken mortality, and thus notably impacting on the economics and environmental performance of the Australian poultry industry. As the rural industries' unique loading patterns can be highly

different from residential, commercial and public buildings, detailed analyses are required to achieve an appropriate design of GSHP systems specifically for the rural industry.

Currently, commercial software packages including Ground Loop Design (GLD) and GLHEPRO (stands for ground loop heat exchanger) have been widely used in the analysis and design of GSHP systems [17]. Understanding the hourly performance of the GSHP systems is important when detailed design or analysis are required. While hourly performance calculations are available for GSHP systems with vertical boreholes in both GLD and GLHE pro, such function is not yet available for GSHP systems with horizontal GHEs (only annual averages are outputted). One possible explanation for this limitation could be that commercial software normally use simpler analytical models (for vertical GHEs) to provide quick calculations. While infinite line source, infinite cylindrical source and finite line source models are popular in modelling vertical GHEs, these models cannot be directly used for horizontal GHEs. Hence, the applications of such similar sophisticated analytical methods in horizontal GHEs are currently limited and can be more difficult to be applied in commercial softwares [122-124].. This is mainly because the performance of the horizontal GHEs is highly affected by the configuration of the pipes and climate and geological conditions which are difficult to be covered by a generalised analytical model [125].

When a detailed analysis is required, researchers have developed numerical simulation models to analyse GSHP systems with horizontal GHEs. As an example, Transient System Simulation Tool (TRNSYS) simulations are widely used in various types of building energy simulations [126-128] as well as to predict the performance of the GSHPs and GHEs [129]. By using full implicit finite difference methods to solve three-dimensional meshed soil and GHE models, this approach can be implemented in common practice of GSHPs with vertical or horizontal GHEs, as well as be modified to simulate the complex GSHPs applications like GSHPs with dual sources or solar assisted GSHPs [38, 130, 131]. Apart from TRNSYS, researchers have also developed other numerical simulation models and approaches, including Finite Element Modelling and Computational Fluid Dynamics [36, 45, 94, 95, 118, 120, 132, 133]. Numerical simulation results can be in good agreement with the respective experiments and hence contribute to the optimum design of horizontal GHEs. However, current numerical simulation models, including TRNSYS simulations, are usually time consuming, resource demanding and case specific, which could limit their application in engineering practice.

Statistical and machine learning models represent potential approaches to accelerate the simulation, with only a marginal compromise on accuracy. As summarized in Table 5-1, recent years have witnessed a wide range of applications of statistical and machine learning models in energy systems, specifically Artificial Neural Networks (ANNs) [134-141]. Well designed and properly trained ANNs can provide reasonably accurate results almost instantly, when applied in GSHP systems. As shown in Table 5-1, different types of neural networks and machine learning tools have been tested on GSHP systems, including Feedforward neuron networks (FFNN), Adaptive neuro fuzzy inference systems (ANFIS), Nonlinear autoregressive exogenous models (NARX) and Extreme learning machine. While FFNN has been identified as the best performing tools for the performance prediction of GSHPs, NARX is very good in time series predictions, including predicting temperature and load series. However, there is very limited research currently available for the application of ANNs in GSHP systems with horizontal GHEs with none found that is considering rural industries' unique loading

conditions. Moreover, current ANN applications in GSHP systems are mostly based on case-specific studies, meaning they cannot be generalised and applied to different cases than those they were created for.

Table 5-1 Summary of published research regarding ANN for GSHP systems.

| System type | Reference | Notes | Usage | Best performing tool |
|---|---|---|---|---|
| Geothermal district heating system | Keçebaş & Yabanova, 2012[142] | 6 plate heat exchangers | Energy and exergy efficiencies and exergy destructions for thermal optimization | FFNN |
| | Şahin & Yazıcı, 2012[143] | 6 plate heat exchangers | Energy and exergy analysis | FFNN |
| | Keçebaş et al., 2012[144] | Geothermal well | Exergy prediction | FFNN |
| | Keçebaş et al., 2013[145] | 6 plate heat exchangers | Energy analysis | FFNN |
| | Arat & Arslan, 2017[146] | Aided by geothermal heat pump | Prediction and optimization | FFNN |
| Ground source heat pump | Esen et al., 2008[140] | *Horizontal GHEs* | Performance prediction | ANFIS |
| | Xie et al., 2008[147] | Ground-water heat pump | Performance prediction | FFNN |
| | Esen & Inalli, 2009[136] | Vertical GHE (30m to 90m deep) | Performance prediction | ANFIS |
| | Wang, 2013[148] | Ground-coupled heat pump | Performance prediction | ANN based on improved Radical Basis Function |
| | Fannou et al., 2014[149] | Direct expansion geothermal heat pump | Performance prediction | FFNN |
| | Sun et al., 2015[150] | Geothermal well (54m deep) | Performance prediction | ANFIS |
| | Benli, 2016[151] | Vertical GHE (60m deep), *horizontal GHE (246m long)* | Performance prediction | FFNN |
| | Makasis et al., 2018[135] | Energy pile design | Exergy prediction | Multiple linear regression |
| | Park et al., 2018[152] | Vertical GHE (200m deep) | Performance prediction | Multiple linear regression |
| | Zhang et al., 2018[153] | Distributed thermal response test, vertical GHE | Thermal conductivity prediction | FFNN |
| Hybrid ground | Gang & Wang, 2013[31] | Cooling tower, vertical GHE (60m deep) | Temperature prediction | FFNN |

| | | | | |
|---|---|---|---|---|
| source heat pump | Gang et al., 2014[154] | Cooling tower, vertical GHE (60m deep) | Performance prediction | FFNN |
| | Esen et al., 2017[36] | *Horizontal* and vertical slinky GHE, solar assisted | Performance prediction | ANFIS |
| Other systems | Bassam et al., 2010[155] | Geothermal borehole | Temperature prediction | FFNN |
| | Arslan, 2011[156] | Kalina cycle system for geothermal fields of low and medium enthalpy | Pump power prediction | FFNN |
| | Morales et al., 2015[157] | Absorption heat transformer | Prediction and optimization | FFNN |
| | Hamdan et al., 2016[158] | Flat-plate solar air collector | Temperature prediction | NARX |
| | Qi et al., 2016[159] | Shower cooling tower | Performance prediction | Wavelet neural network |
| | Shojaeefard et al., 2017[160] | Compact heat exchanger | Performance prediction | Recurrent neural network |
| | Islam & Morimoto, 2017[161] | Pillar cooler system | Inside air temperature prediction | FFNN |
| | Alhamid et al., 2018[162] | Absorption chiller | Performance prediction | FFNN |
| | Guo et al., 2018[139] | Building heating system | Energy demand prediction | Extreme learning machine |
| | Aghadavoodi & Shahgholian, 2018[163] | Combustion loop control system | Closed loop identification | NARX |
| | Koschwitz et al., 2018[164] | Non-residential building | Load prediction | NARX |

Within the handful of pioneering ANN studies dealing with horizontal GHEs currently available in the literature, Esen et al. and Benli 's ANN models are the only ones that can predict COP of water to air GSHPs with horizontal GHEs with pre-processed input data [36, 151, 165]. Their results show the ANN can predict the COP well when enough input data are given. Their methodologies require three to five types of input data, including at least the inlet air, outlet air and ground temperatures. In their most recent work Esen et al. [36], utilize ground temperatures at seven different depths, inlet air, outlet air, ambient air, tank water, inlet water and outlet temperatures as inputs to the predictive model. However, these input data cannot be acquired easily, and more importantly, it would be arguably simpler and faster to find the COP via the heat pump specifications if these data are accessible. Moreover, the input data required by current ANNs can be typically part of the output needed for GSHP system design, making these works of limited use for in practice. Lastly, the ANNs found in the literature have limited applicability for wider utilisation, as their validity is mostly shown for the case they were studied/trained with.

This study aims to provide an ANN methodology that can predict and tremendously accelerate the design of GSHPs with horizontal GHEs (using numerical simulations) under

rural industries' loading conditions and with limited input data types. A Transient System Simulation Tool (TRNSYS) model for a typical horizontal GHE field arrangement (details in Section 5.4.1) has been developed (and verified) and the resulting simulated performance data are used to train the ANNs. The trained ANNs are then used to predict the performance of GSHPs with identical GHEs (but varying number of GHEs) in other locations that are not in the training dataset to showcase its applicability for wider utilisation.

## 5.3. Rural Industries' Heating Loads Patterns and Locations

As mentioned in the introduction, since the rural industries' thermal loading pattern can be highly different from commercial and residential building applications, the GSHP design requires careful and detailed analysis. As an example of these unique rural industries' loading patterns and to exemplify the study for temperate climate regions, in this investigation a chicken shed building located in Peats Ridge, NSW, Australia is adopted. The schematic drawing of the typical test broiler house (or shed) with a hybrid GSHP system can be seen in Figure 5-1.

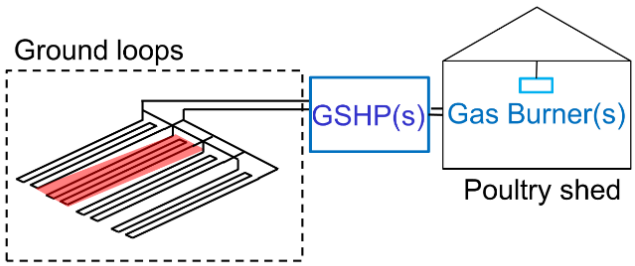


Figure 5-1 Diagram of hybrid geothermal systems for poultry shed. Each trench is 75 m long and contains ~300 m of HDPE pipe (highlighted in red).

A building energy simulation model was developed for the shed using numerical simulation software TRNSYS 18, which simulates the heating and cooling loads for the shed. The location and parameters used for the simulation is summarized in Table 5-2. For this study, the shed is used for six chicken raising cycles per year (from chicks to chicken for meat) as per typical broiler house operation, with the first raising cycle for the chickens assumed to start on 1st of January. Each cycle is assumed to last seven weeks with two weeks break time in between batches [39].

Table 5-2 Typical broiler house dimensions and temperate climate case study location.

| | |
|---|---|
| **Dimensions** | Width:18.3 m, Length:138.7 m, Height: 2.7 to 4.3 m |
| **Wall/Roof Material** | No windows; Insulation with thin layers of metal cladding. Insulation thickness: 0.075 m, thermal conductivity: 0.039 $Wm^{-1}K^{-1}$, density: 16 $kg\ m^{-3}$, specific heat: 340 $Jkg^{-1}K^{-1}$ |
| **Orientation** | Long axis (Length) across North-South |
| **Location** | Peats Ridge, NSW, Australia (33°23'49"S, 150°24'09"E) |
| **Climate Data** | Typical Meteorological Year (TMY) data [54] |

A previous study has identified that although there is a high cooling demand, cooling can be economically provided via evaporative coolers [121]. Hence, the primary focus of this work is on providing heating via a GSHP (or hybrid GSHP) systems. Figure 5-2 shows the simulated *heating* power demand of the shed based on the building energy consumption model developed. It was estimated that the annual heating energy of the shed is 58,477 kWh with a

peak heating power demand of 208 kW. During each heating cycle, the heating demand is usually at its maximum at the start of each cycle when the least metabolic heat is generated by chickens and, at the same time, the required indoor temperature is at its maximum (typically 31 °C). The heating demand decreases later in each cycle due to the increase in metabolic heat generated by chickens and lower indoor temperature requirement corresponding to the age of the cycle (typically to a minimum of 19°C within 21 days of the start of the cycle).

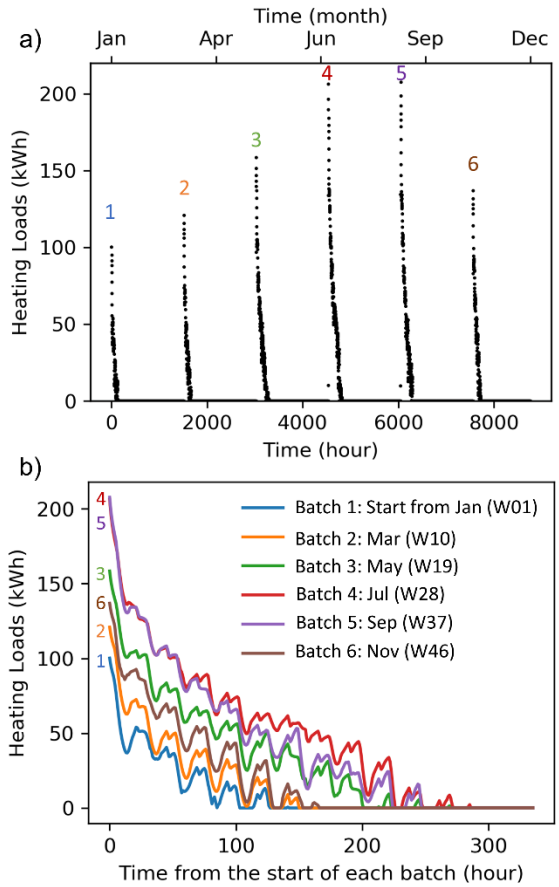


Figure 5-2 Hourly heating demand of the chicken shed: a) yearly loading pattern showing the six batches b) detail of these six heating cycles over one year.

To provide the heating loads demand for the building, a hybrid GSHP system with horizontal GHEs is employed. As the initial installation cost of GHEs can be relatively high, a hybrid geothermal-gas system is chosen to reduce the capital cost while maintaining most benefits of the geothermal (GSHP) technology. In this hybrid system, the heating is delivered by several identical GSHPs connected in parallel to a main header pipe. Each GSHP is coupled to a series of GHEs. The LPG gas burners installed in the shed can top up the heating when needed. A 'shave factor' S is used to describe the capacity portion of the GSHP in the hybrid system. It is defined as the ratio of the installed capacity of the GSHP of the system to the peak heating demand of the load to be satisfied by the hybrid system [30, 32]:

$$S = \frac{\text{Installed capacity of GSHP}}{\text{Peak heating load}} \times 100\% \qquad \text{(Eq. 5-1)}$$

In this study, a 0% shave factor represents a full gas system and 100% a full GSHP system. A shave factor of 40% in this GSHP-gas hybrid system (208 kW peak load) means that the installed capacity of the GSHPs is 208 kW × 40% = 83 kW, and the installed capacity of a gas burners will be the difference between the peak heating load and the GSHP installed capacity, that is, 125 kW, only operational when the demand exceeds 83 kW.

To further investigate this hybrid system, two other locations across Australia under different climate conditions are analyzed following similar approaches. Together with the one mentioned above, these three locations are representatives of conditions in Queensland (QLD), New South Wales (NSW) and Victoria (VIC) (Figure 5-3). The three states analysed in this study account for 74.4% of Australia's overall broiler production with different climate conditions [53, 108]. The peak heating loads and annual energy demand are 228 kW and 73,456 kWh for Mornington Peninsula, VIC and 164 kW and 34,149 kWh for Sunshine Coast, QLD.

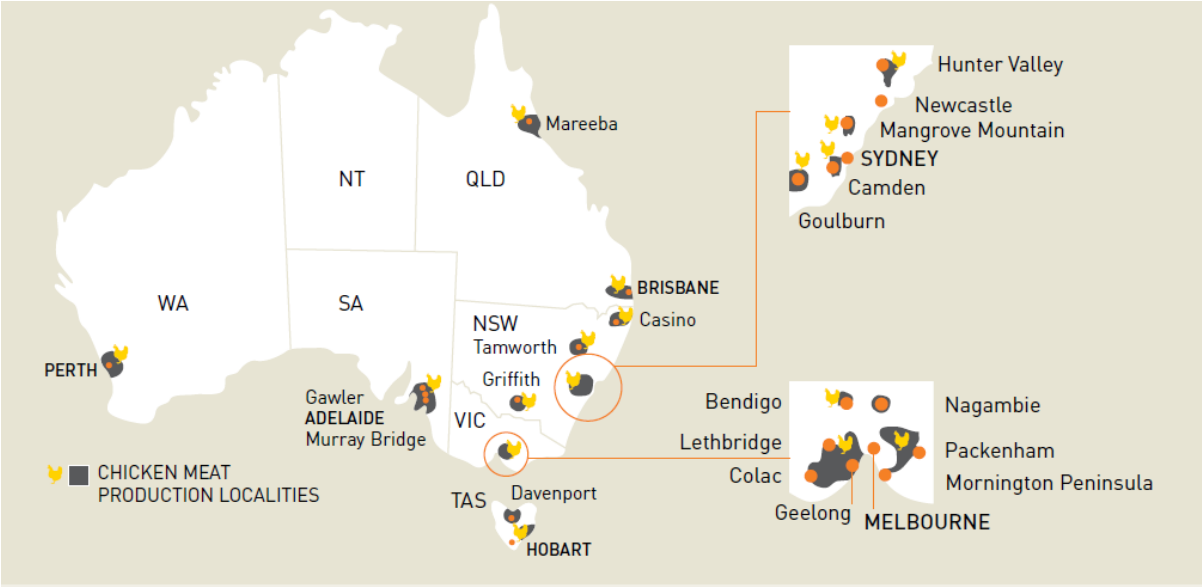


Figure 5-3 Chicken industry profile in Australia [108].

The latest average annual temperatures (maximum, minimum and average) are summarised in Table 5-3. For the building side, all other factors besides the climatic conditions associated with the different locations, such as shed envelope, orientation, and ventilation conditions, are kept constant in this study to ensure a representative comparison between them.

Table 5-3 Simulation locations and key climate data [166].

| Location | Coordinates | Annual mean maximum temperature (℃) | Annual mean minimum temperature (℃) | Undisturbed ground temperature (℃) |
|---|---|---|---|---|
| Central Coast, NSW | **33°23'49"S 150°24'09"E** | **21.9** | **11.6** | **16.1** |
| Mornington Peninsula, VIC | **38°17'7"S 145°5'36"E** | **18.9** | **10.1** | **14.4** |
| Sunshine Coast, QLD | **26°51'36"S 152°57'36"E** | **25.3** | **17.0** | **19.9** |
| Warracknabeal, VIC (Test case) | **36° 6' 7" S 142° 40' 12" E** | **22.4** | **8.7** | **14.5** |
| Murray Ridge, SA (Test case) | **35° 7' 1.2" S 139° 16' 1.2" E** | **23.0** | **9.9** | **15.8** |
| Gaborone, Botswana (Test case) | **24° 39′ 29″ S 25° 54′ 44″ E** | **29.0** | **13.4** | **20.6** |

In addition to the three discussed locations for training (and testing), three additional test cases, one in Warracknabeal (Victoria), one in Murray Ridge (South Australia) and an extra one in Gaborone (Botswana, annual average temperature 20.6 ℃) have also been adopted to further check accuracy of the ANN model results and flexibility to accommodate different site conditions. The data relating to these test cases are not part of the training dataset (Table 5-3) and can therefore be used to evaluate the accuracy of the prediction ANN model, after it has been trained.

## 5.4. TRNSYS Simulation

In this study, a developed TRNSYS simulation model for the poultry industry is utilised to simulate over 700,000 hourly performance data, covering over 80 different yearly thermal loading patterns (by varying the shave factors) under three different climate conditions. The simulation data from the completed TRNSYS models are then used to train the ANNs.

### 5.4.1. TRNSYS Simulation Model

To generate data to train the ANN, a typical poultry shed in Australia equipped with a hybrid GSHP system to provide the heating required is utilised [39]. As mentioned in section 5.3, the hybrid system consists of several identical GSHPs with horizontal GHEs and gas burners. The sizing and configuration of the GSHPs and the gas burners within the hybrid system varies based on the thermal demand (and the different shave factors determining it). The TRNSYS model is used to evaluate the hourly performance of the GSHPs for each of these cases of different thermal load and configurations. A Typical Meteorological Year (TMY) dataset was used as the boundary condition of the soil surface. The soil is meshed three-dimensionally, and a fully implicit finite difference method is utilised in the modelling. For

all the models, a sandy clay soil is assumed, with an average thermal conductivity of about 2 $WK^{-1}m^{-1}$.

In the modelled systems several identical single speed GSHPs with 20 kW heating capacity are utilised to provide the required thermal energy. Each heat pump has a fixed ground heat exchanger field configuration formed by four horizontal trenches. Each trench is dug at the depth of 1.5 m below the ground surface and there are four pipes in each trench, at 300 mm separation between each pipe. The length for each trench is 75 m, rendering a pipe length of about 300 m per trench. As an example of an overall system, to provide 208 kW peak heating in total at a shave factor of 38% (therefore requiring 80 kW), four 20 kW heat pumps are installed, each with its own ground heat exchanger field in four trenches (i.e., 16 trenches in total). For simplicity, the thermal conductivity of the soil was assumed the same for different locations, however the ground temperature reflects that of each site (see Table 5-3). It is also assumed that all trenches are placed sufficiently apart from each other to minimise any thermal interference between them.

The operation of the heat pumps is controlled by the hourly loading demands. When the operation of a new heat pump is required, the one with the lowest accumulated hours of operation will start. For example, in the 208-kW total capacity case above (with 80kW provided by the GSHPs, i.e. S=38%), when the loads increase from 19 kW to 35 kW, the operation of a second 20 kW heat pump is required. At this time, the system will compare the accumulated hours of operation from the three heat pumps that are not operating and turn on the one with the lowest accumulated hours of operation. In this way, the loads can be relatively evenly divided amongst all the heat pumps throughout the life of the system. For heating demands in excess of 80kW, all four GSHPs will be in operation and the gas burners will provide the balance of the required load.

The diagram below shows the configuration of the TRNSYS model (Figure 5-4) for each GSHP. This model simulates one water to water GSHP (Type 927) with a short distance (5 m) buried head pipe (Type 951) and a horizontal ground heat exchanger (Type 997) composed of the four 75 m long trenches (recall Figure 5-1). The thermal loads generated from TRNSYS are imported to the water heat exchanger (Type 682) to simulate the loading from the building. A control unit (Type 1502) together with the Typical Meteorological Year TMY weather data (Type 15-6) generated from Meteonorm, a widely used weather analysis software [77], complete the TRNSYS model of the smallest GSHP component (20kW) of the hybrid system.

In this TRNSYS model, only one heat pump is simulated with fixed loads input (heating loads are inputted from outside files with data generated). However, it is worth noting that for one particular scenario each of the GSHP involved receives a unique loading pattern based on the system's operation. For example, when the shave factor is 100% in the NSW training case, 208kW peak loads needs to be covered by 11 GSHPs (of 20kW capacity each).

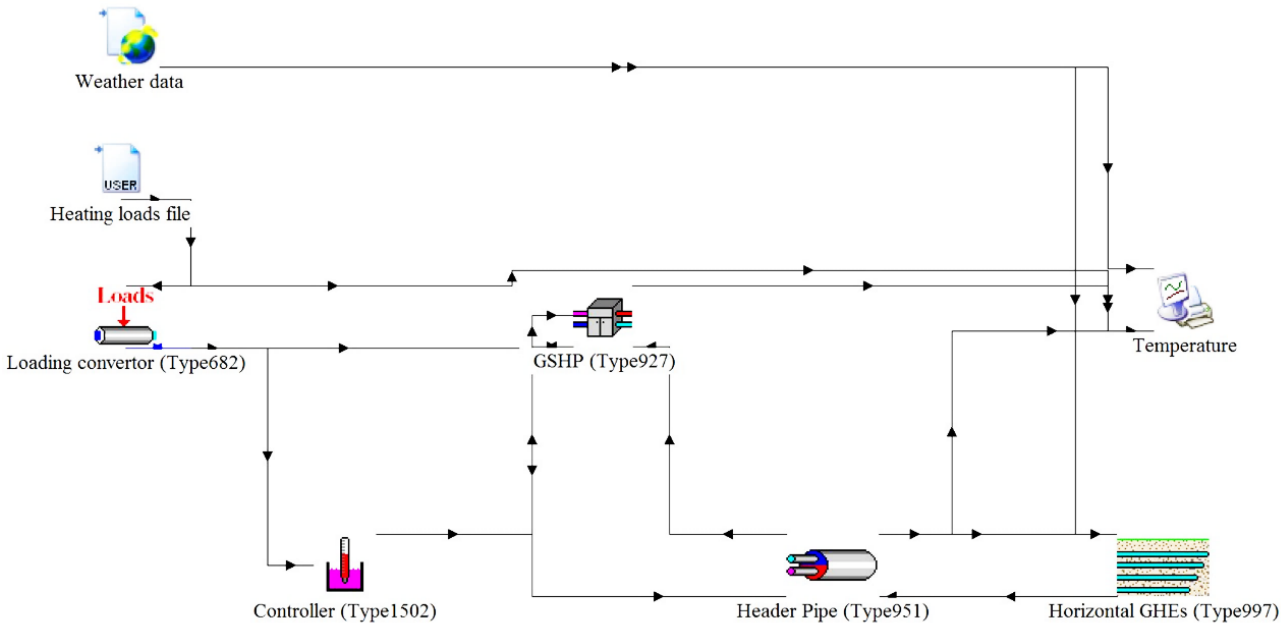


Figure 5-4 Schematic drawing of TRNSYS model.

Accordingly, 80 different loading patterns for the GSHP are generated as inputs, depending on when each heat pump needs to be turned on or off. Therefore, considering that simulations have been conducted for different shave factors and locations and for each shaved factor multiple GSHPs might be needed with different loading patterns, over 30 simulations are considered for the training case in NSW, and 25 for each of the training cases in VIC and QLD. Therefore, in total more than 80 simulations (each with unique loading patterns/conditions) and over 700,000 hours simulation data are generated and will be used to train the ANNs as explained in Section 5.5.

### 5.4.2. Simulation Results from TRNSYS

Following the discussion on the methodology and data mentioned above, this section presents the simulation results from TRNSYS. These results are used in the prediction model both as inputs as well as outputs (to train the prediction model as well as compare the results to evaluate its accuracy). These include a loading pattern as an example for the inputs and simulated hourly COP and inlet and outlet temperatures of the GHEs as examples for the outputs.

In TRNSYS, over 80 different loading patterns in the three locations are simulated. For example, Figure 5-5 shows one loading pattern of one GSHP (connected to a set of four trenches, the GHE field) in a hybrid GSHP-gas system in NSW with a shave factor of 25% (or 52 kW of GSHP capacity for a total peak demand of the whole system being 208 kW – see Section 5.3).

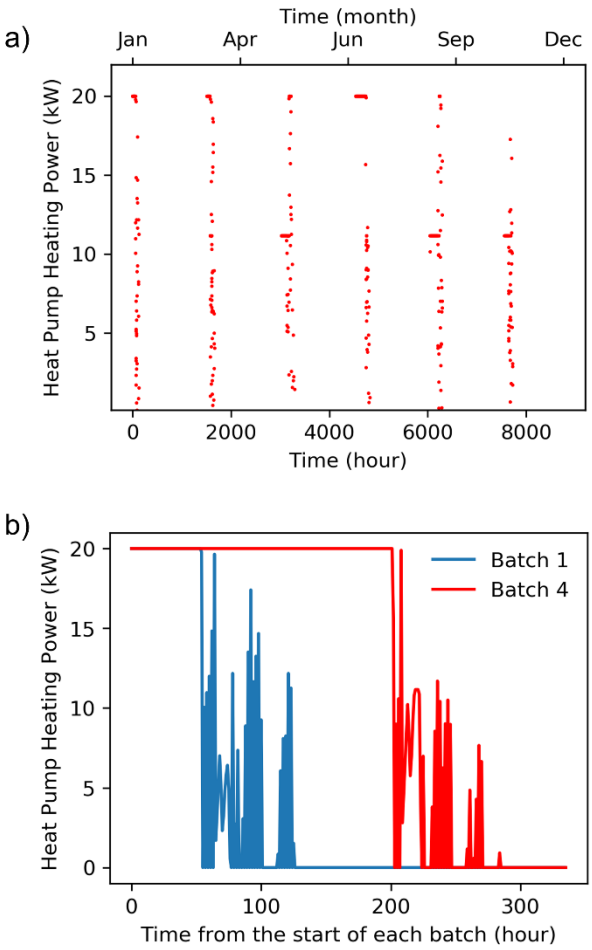


Figure 5-5 One hourly heating loads pattern example for a 20-kW capacity ground source heat pump (GSHP): (a) overall yearly load, and (b) detail of the lowest (Batch 1, Jan) and highest (Batch 4, July) GSHP run fraction batch loads.

Figure 5-6 shows the results of the simulation based on the loading pattern in Figure 5-5 and weather conditions in Central Coast, NSW. As it can be seen, the GHE inlet and outlet temperatures (or LWT and EWT[1] respectively) vary with the loading and seasons as expected. The maximum is about 20.3 °C and the minimum is about 5.8 °C. When there is loading, the GHE outlet temperature is higher than the GHE inlet temperature by one to two Celsius degrees. The resulting $COP_{GSHP_{hr}}$ is about 4 under full loading conditions (Figure 5-6). However, when it is under partial loading, there is a decrease in the $COP_{GSHP_{hr}}$ to about 2, which is expected.

[1] EWT = Entering water temperature (into the GSHP from the GHEs); LWT = Leaving water temperature (out of the GSHP and to the GHEs)

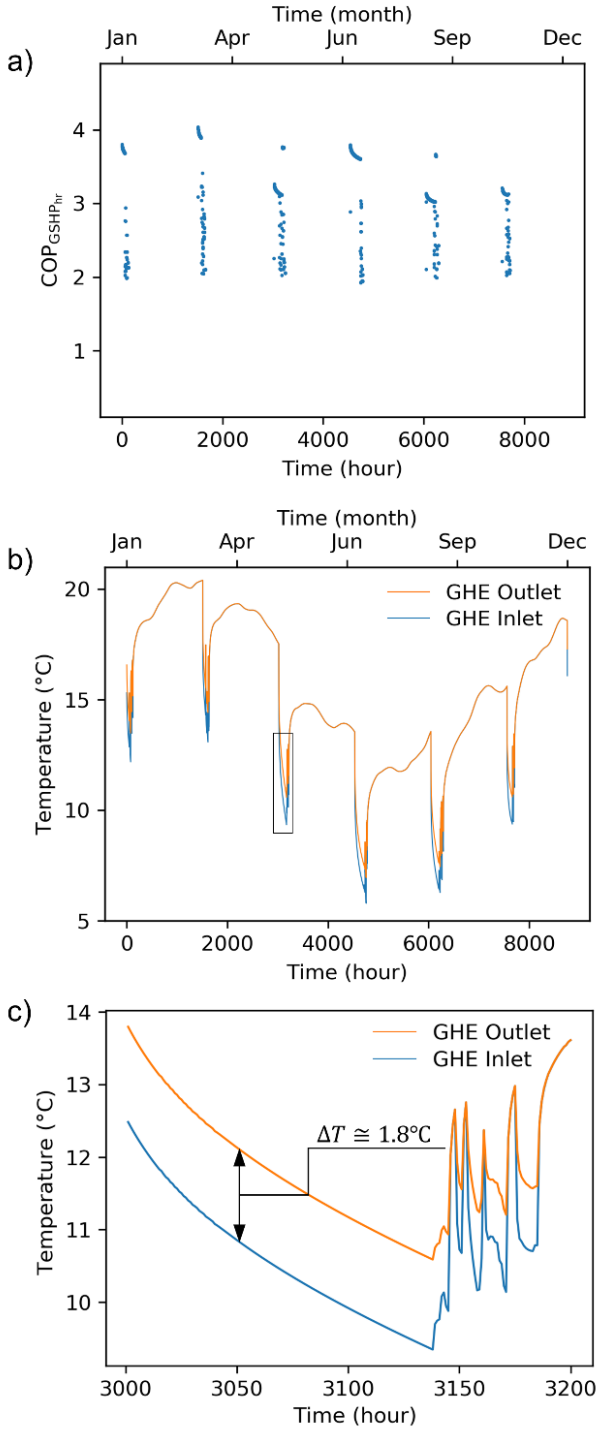


Figure 5-6 Typical TRNSYS simulation results: (a) hourly COP of an individual heat pump, (b) GHE inlet and outlet temperatures, (c) temperatures for the starting of the third batch.

The simulations used within this work model one year of operation of the system using the TMY data. In order, however, to test that the tools and insights from this work are also representative for a long-term performance analysis, a longer 10-year simulation was also undertaken using annually repeating TMY data. The results show that the $COP_{GSHP_{hr}}$ and the GHE inlet and outlet temperature profiles are identical for each year of simulation (Figure 5-7). Therefore, one-year simulation results are used throughout this study and are considered representative of the long-term system's performance. These results are different from typical

vertical systems, as imbalanced loads will have long term accumulated effects on the ground, which could impact the performance of GSHP systems with vertical GHEs. A more thorough discussion of this observation is provided in Section 5.6.

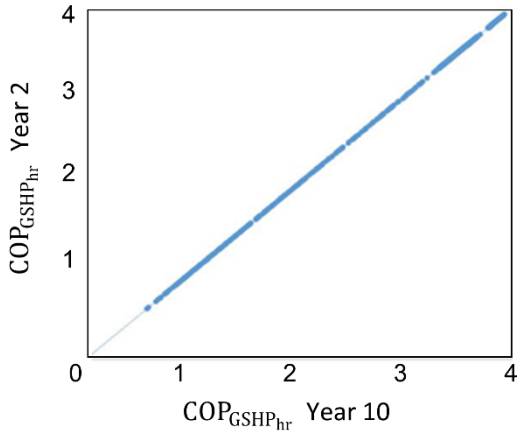


Figure 5-7 Correlations between a 2nd year and 10th year.

The next section will present the ANN models (which use the above results from TRNSYS for training, validation and testing) and their simulation results, including $COP_{GSHP_{hr}}$ and inlet and outlet temperature for the GHEs.

## 5.5. ANN Models of the GSHPs and GHEs

An artificial neural network (ANN) is a mathematical approach that simulates a network of artificial neurons to mimic the human brain. With a well-trained ANN, the computer can be taught to solve problems, including generalisation, classification, forecasting and even decision making [83]. In this study, two ANN models are developed and implemented using MATLAB: i) an FFNN (feedforward artificial neural network) is used to predict the performance of the GSHPs in terms of $COP_{GSHP_{hr}}$, and ii) a NARX (nonlinear autoregressive network with exogenous inputs) network is used to predict the inlet and outlet temperatures of the horizontal GHEs. In this study, the term ANN is used as a general description of this method and FFNN/NARX refer to the specific model, which can be replaceable in most cases. The training input data only include three types of input: the loads, accumulated loads and the outdoor temperature. Yet, the trained ANN can still predict the performance of the GSHPs and horizontal GHEs reasonably well, which can significantly reduce the need for time consuming numerical simulations. Details of these models are included next.

### 5.5.1. Modelling of the GSHPs with FFNN

The FFNN statistical model, also referred to as multilayer perceptron (MLP), or simply artificial neural network (ANN) in some studies, is by far the most popular machine learning tool used in energy-related fields. It is versatile and may be used to model complex systems with great accuracy, including but not limited to geothermal district heating systems [142, 145, 146], geothermal walls [155], GSHP or hybrid GSHP systems [151]. In this work, an FFNN is developed to predict the COP of the GSHPs ($COP_{GSHP_{hr}}$), as shown schematically in Figure 5-10.

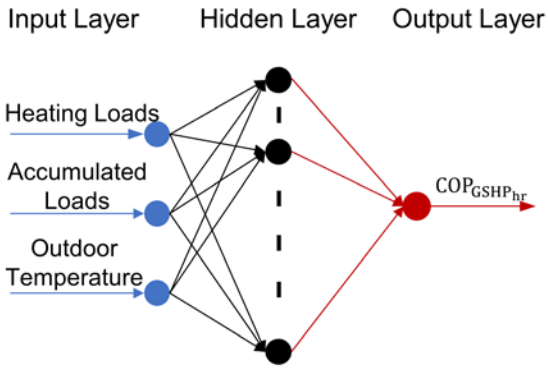


Figure 5-8 Structure of the FFNN model to calculate the COP of a 20 kW GSHP.

**The input layer (Feature Variables)**

Although various types of datasets can be set as feature variables, such as the inlet air, outlet air (on the building side of the GSHP), ground, inlet and outlet GHE water temperatures (on the ground side of the GSHP), the complexity of acquiring them may make the FFNN not practically usable in engineering practice. Instead, in this study, the input layer consists of three neurons, which represents the three easy to acquire influencing factors for the performance of the GSHPs: the hourly loads (which are typically known), the hourly accumulated loads and the moving average monthly outdoor temperature (which can be easily obtained from the Typical Meteorological Year (TMY, Meteonorm) when designing a system or via weather stations or sensors when optimising scheduling of the system dynamically).

*Hourly heating loads:* The simulated hourly heating loads from TRNSYS that will be delivered by the GSHPs to the building. As explained in sections 5.3 and 5.4, these hourly loads between GSHPs vary based on the control strategy, the shave factor adopted and the operating conditions of each GSHP.

*Adjusted accumulated heating loads:* Since the continuing heating operation of the heat pumps can have an impact on the performance, hourly loads, showing the demand at a specific point in time, are not enough to fully capture the problem and train the network. Thus, the accumulated thermal loads are introduced to represent the short-term effects of heating the ground and its recovery. In this study, this value is estimated based on the hourly heating loads and the ground conductive heat flux [167-169]. As the GHE pipes are buried 1.5 m deep, the conductive heat flux is the primary heat flux at this depth and can range from 6 to 14 W/m$^2$ depending on the moisture content of the soil [168]. In this study, the ground heat flux $f_g$ is assumed to be 10 W/m$^2$. Since the area of the GHE trench field in this study is about 1,500 m$^2$ (4 trenches per GSHP), the estimated heat flux is 15,000 W.

$$AQ_{i+1} = \begin{cases} AQ_i + Q_i - fg, AQ_i + Q_i - fg > 0 \\ 0, \quad AQ_i + Q_i - fg \leq 0 \end{cases} \qquad \text{(Eq. 5-2)}$$

where, $AQ_i$ is the adjusted accumulated loads in i$^{th}$ hour, and $Q_i$ is the heating loads in i$^{th}$ hour.

*Outdoor ambient air temperature:* This input represents the variation introduced to the performance of the heat pumps due to seasonality. The air temperature can be used some

delay to represent the ground temperature (and therefore the neutral ground condition [170, 171]. In this work, a *moving average monthly* outdoor temperature is introduced to very simply but effectively represent the effects of the daily and seasonal variation. By applying a two weeks delay, the moving average monthly outdoor temperature has shown a reasonably good correlation to the TRNSYS simulated ground temperature at 1.5 m deep.

**The hidden layer**

The hidden layer is used as an intermediary between input and output to enable the predictions and transformation of input to output. In this study, the hidden layer consists of one layer of ten neurons of a feedforward network. The transfer functions in the hidden layer are sigmoid functions, which are most commonly utilised throughout the literature and make it possible to solve nonlinear problems. As shown in Section 5.5.5, ten is found to be the optimum number for the neurons in the hidden layer.

**The output layer**

The aim of the FFNN is to predict the performance of each GSHP. In this case, the output layer has only one neuron which carries the hourly COP of the modelled GSHP ($COP_{GSHP_{hr}}$) (Figure 8). This output is important for design assessment and optimisation of GSHP systems.

### 5.5.2. Modelling of the horizontal GHEs with NARX

The NARX architecture is well suited for circumstances with the presence of long-term dependencies, performing better than certain variations of recurrent neural networks [172], which can be advantageous in many time series prediction problems. As a result, NARX networks work well in prediction problems, in which temporal patterns may be present and negatively influence some of the other models.

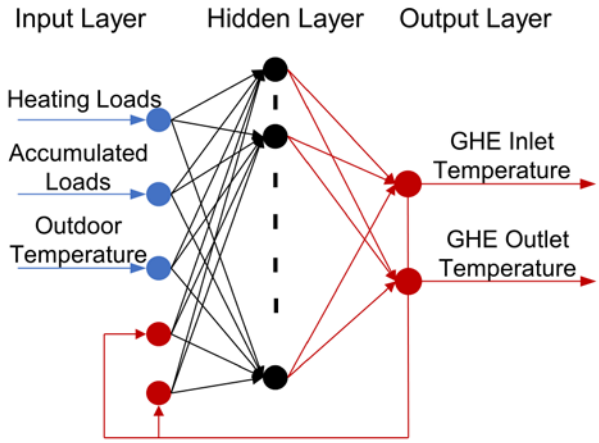


Figure 5-9 Structure of the NARX model for GHE.

**The input layers**

The input variables are the same as the input variables in the NARX for GSHPs.

**The hidden layer**

The hidden layer consists of one layer of ten neurons of a NARX network. As the base architecture of the NARX network is a feedforward network, this layer also follows the same reasoning as for the FFNN model of section 5.1, with also ten neurons and sigmoid transfer functions.

**The output layer**

The aim of the NARX network is to predict the inlet and outlet temperatures of the GHEs. In this case, the output layer has two neurons representing the hourly inlet and outlet temperatures of the GHEs (Figure 5-9). The values of these parameters are used in each following iteration of the NARX calculations for the time series (i.e. the temperatures for time t are used to compute the temperatures for time t+1) and there These results are important for evaluate the design length of GHEs and can directly impact the COP of GSHPs.

### 5.5.3. Learning algorithm, training and testing samples

There are different learning algorithms that are available in MATLAB to train and test the FFNN and NARX, including Levenberg-Marquardt and BFGS Quasi-Newton [173]. In this study, the Levenberg Marquardt method is selected due to its popularity and high speed. The simulated data from TRNSYS simulation are used to train and test both the FFNN and NARX models. As explained in Section 5.4, there are different thermal loading conditions for heat pumps under different shave factors and climate conditions. This covers in total over 80 different operational conditions across three locations in Australia (Table 5-3). The trained FFNN and NARX models are then tested by several different operational conditions in other three locations (Table 5-3). The RMSE (Root Mean Square) metrics are used to quantify the performance of these models.

### 5.5.4. Prediction Results from ANNs

Based on the models and algorithm mentioned above, this section presents the prediction results from the two ANN networks. The first FFNN model predicts the $COP_{GSHP_{hr}}$ and the second NARX model, the hourly inlet and outlet temperature of the corresponding horizontal GHEs (GHE inlet, GHE outlet) in many other untrained test locations (Table 5-3).

### 5.5.5. COP prediction from FFNN

This section presents the results comparing the FFNN predictions with the respective time-consuming TRNSYS simulations. As an example, Figure 5-10 shows this comparison for the test case in VIC and 100% shave factor (Case 4 in Table 5-4). The results from the FFNN prediction of the $COP_{GSHP_{hr}}$ compare reasonably well with the simulation results from TRNSYS. Apart from the data points when the heat pump is not in operation (when $COP_{GSHP_{hr}}$ is zero), 84% of data points fall within the ±10 % error band. These results suggest that the FFNN model may not be able to understand the impact of weather condition on $COP_{GSHP_{hr}}$ extremely well at this stage. A more holistic view of the testing results, considering eleven other cases (and including both FFNN and NARX results discussed later), can be seen in Table 5-4, showing the RMSE (Root Mean Square Error) and MAE (Mean Absolute Square Error). The results are reasonably consistent in all the test cases. Moreover, Figure 5-11 a shows the $COP_{GSHP_{hr}}$ distribution of the all the variations (changes in S) for the three testing locations. Similar to Case 4, the results are in a reasonable agreement with TRNSYS simulation, with about 80% of the data have an error less than ±10%.

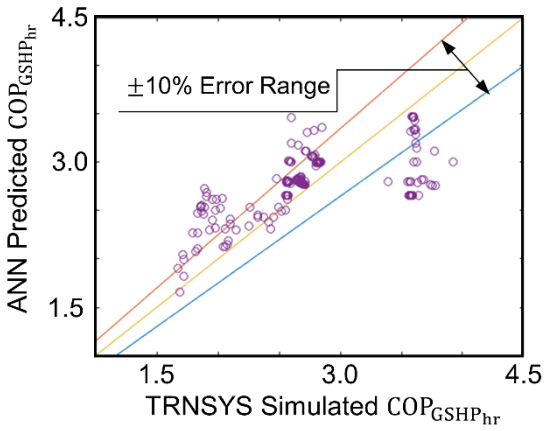


Figure 5-10 Hourly COP from TRNSYS simulation vs ANN prediction (100% shave factor test case in VIC).

Table 5-4 RMSE and MAE for test cases.

| Test Cases | | | $COP_{GSHP_{hr}}$ | | GHE Inlet | | GHE Outlet | |
|---|---|---|---|---|---|---|---|---|
| No. | Location | Shave Factor | RMSE ( - ) | MAE ( - ) | RMSE (°C) | MAE (°C) | RMSE (°C) | MAE (°C) |
| 1 | Victoria | 25% | 0.085 | 0.061 | 0.287 | 0.069 | 0.150 | 0.038 |
| 2 | | 50% | 0.112 | 0.080 | 0.359 | 0.097 | 0.184 | 0.050 |
| 3 | | 75% | 0.072 | 0.056 | 0.411 | 0.116 | 0.210 | 0.058 |
| 4 | | 100% | 0.069 | 0.053 | 0.437 | 0.124 | 0.224 | 0.061 |
| 5 | South Australia | 25% | 0.107 | 0.076 | 0.279 | 0.064 | 0.146 | 0.036 |
| 6 | | 50% | 0.086 | 0.066 | 0.344 | 0.087 | 0.177 | 0.044 |
| 7 | | 75% | 0.078 | 0.062 | 0.391 | 0.102 | 0.201 | 0.051 |
| 8 | | 100% | 0.076 | 0.061 | 0.483 | 0.120 | 0.256 | 0.058 |
| 9 | Botswana | 25% | 0.079 | 0.054 | 0.298 | 0.061 | 0.155 | 0.031 |
| 10 | | 50% | 0.091 | 0.070 | 0.339 | 0.076 | 0.176 | 0.038 |
| 11 | | 75% | 0.079 | 0.063 | 0.362 | 0.082 | 0.188 | 0.040 |
| 12 | | 100% | 0.074 | 0.058 | 0.372 | 0.084 | 0.192 | 0.040 |
| Average | | | 0.084 | 0.063 | 0.364 | 0.090 | 0.188 | 0.045 |

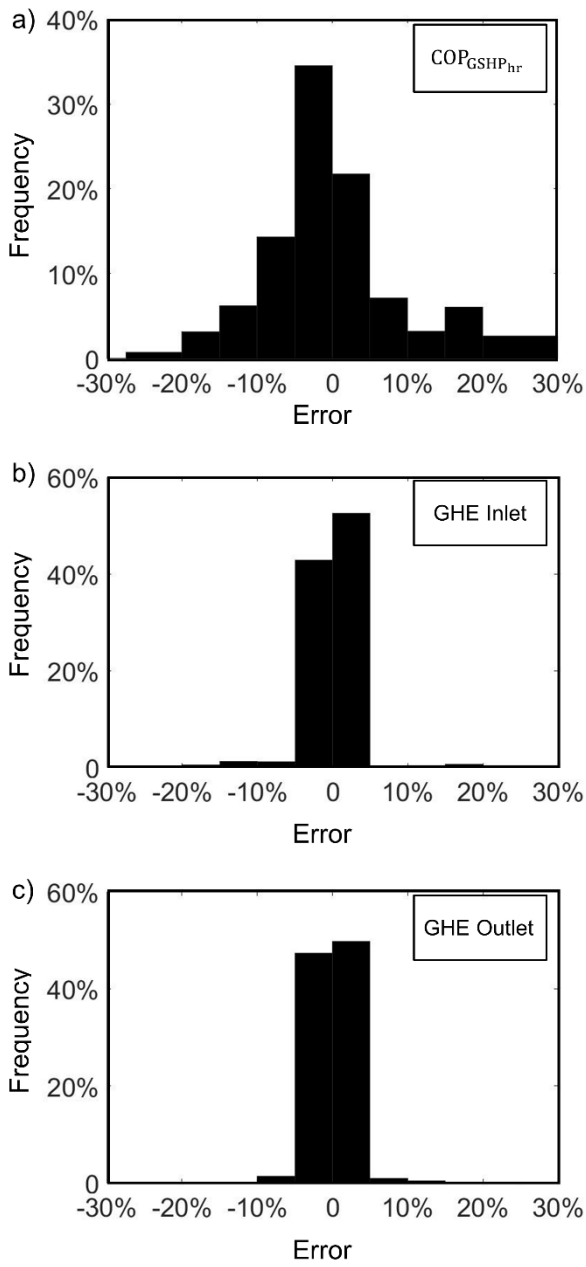


Figure 5-11 Error distribution for all the testing cases: (a) $COP_{GSHP_{hr}}$, (b) GHE inlet temperature, (c) GHE outlet temperature.

All the results presented here are based on 10 neurons in the hidden layer. Figure 5-12 shows the RMSE with the number of neurons in the hidden layer for all the cases, showing that the optimum number of neurons that minimises the error, is about 10.

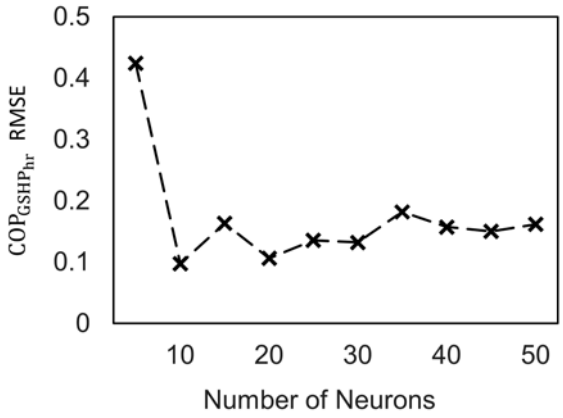


Figure 5-12 RMSE for different number of neurons in the hidden layer.

### 5.5.6. Temperature predictions from NARX

The results for the temperature predictions using NARX are overall very promising. As shown in Figure 5-13 a (Case 5 - 25% shave factor test case in SA), the prediction results of the GHE inlet temperature from the NARX models compares well with the simulation results from the TRNSYS simulations for the test farm in VIC. The results are in a reasonable agreement with TRNSYS simulation, with about 95% of the data have an error less than ±5%. Moreover, when considering the all testing cases, 98% of the results have an error of less than 1 °C and 96.3% of data points fall into the ±5 % error range as depicted in Figure 5-11 b, which shows the GHE inlet error distribution of the all the testing cases. The results also show a reasonably consistency in all the test cases, with slightly lower error when the shave factor is low (Table 5-4).

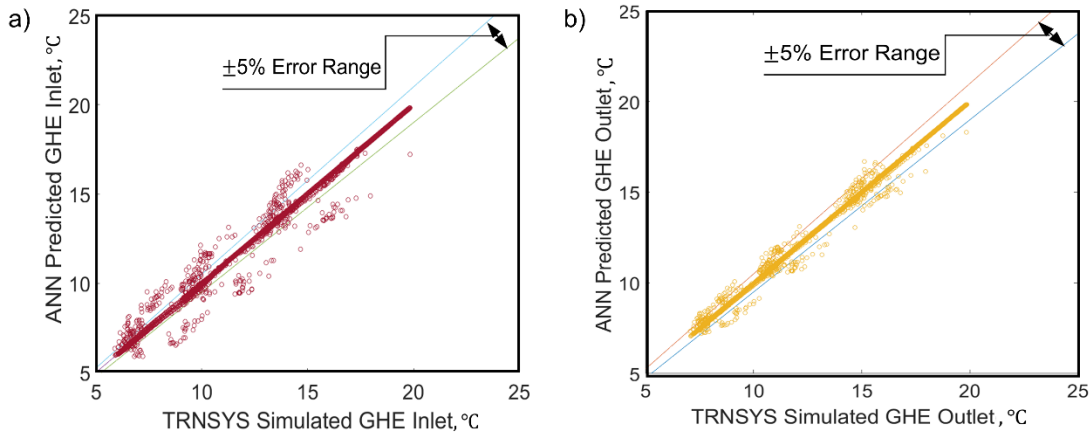


Figure 5-13 Hourly GHE temperatures from TRNSYS simulation and ANN: a) GHE inlet b) GHE outlet.

Figure 5-13 b presents the analogous results for the GHE outlet temperature (Case 5 - 25% shave factor test case in SA), showing that the prediction results of the from the NARX prediction compare very well with those obtained via the TRNSYS simulation. About 99% of the results have an error of less than 1 °C and about 98% of the data points fall into the ±5 % error range. When considering the overall analysis and all other testing cases (Table 5-4), the results also show reasonably consistency, with slightly lower error when the shave factor is low. Figure 5-11 c shows the GHE outlet error distribution of the all these twelve testing cases.

## 5.6. Discussions

Following the results presented above, this section further discusses the key findings, limitations and highlights of this study.

The two ANN prediction models can be used to obtain the COP (FFNN model), GHE inlet and outlet temperatures (NARX model) of hybrid GSHP systems with horizontal GHEs in rural industries. The models only require three input parameters and have shown to perform reasonably well.

Looking at the results closely, an interesting observation is that there seems to be a trend for the FFNN to underestimate the COP during the peak of winter when the heat pump is under full loading. This is possibly caused by the limited sets of feature variables. As the performance of GSHPs is determined by inlet and outlet temperatures of the building side and the ground side, the feature variables may not contain enough information for a perfect prediction. If the inlet and outlet temperatures are used as inputs, the prediction of the performance of the GSHPs could be improved. However, this will make the FFNN less practical as GHE inlet and outlet temperatures are normally not easy to obtain.

Another highlight of this work is that the ANNs have been tested with a broad selection of cases. Trained with the simulated dataset in three locations from TRNSYS, the ANNs can predict the performance of the GSHPs and the horizontal GHEs in other untrained locations reasonably well. This suggests a generalisation ability for the ANN model that can potentially be widely used in prediction, optimisation and control problems. Even though one limitation is that the ANN is only for a 75-m-long trench with 300 m of pipes, it can still benefit the designers as a comparison metric or by comprising the loops for one heat pump by a combination of several 75 m trenches. Since hourly simulation data for horizontal GHES are not available in any commercial software at this stage, the results from this ANN can provide the designers with some confidence.

Furthermore, even though the $COP_{GSHP_{hr}}$ can possibly be estimated from the GSHP technical specification sheets given the temperature difference between the inlet and outlet to the GHEs and the loads, the estimation results are inaccurate as the errors can be significantly exaggerated during the calculation process (compounding errors). As an example, the errors in inlet and outlet temperature can be 1°C. However, the temperature difference between inlet and outlet is normally only one to two degree. Therefore, an error of only 3-5% in inlet and outlet temperatures (1°C), can result in 50-100% error (1-2°C) in the temperature difference (GHE outlet minus GHE inlet). This 50-100% error will be transferred to the $COP_{GSHP_{hr}}$, causing a 50-100% error. Given the reason above, the use of two different ANN models, the first one for the prediction of $COP_{GSHP_{hr}}$ and the second one for the temperatures, seems to be a better alternative.

Finally, a comparison between the computational time of the ANN, TRNSYS simulation and finite element simulation are shown in Table 5-5. This table summarised the computational time of one-year simulation (time step in one hour) for the inlet and outlet temperature of horizontal GHEs. A typical personal computer was used to run these simulations (Windows 7, i7-5600U CPU, 16 GB of RAM), for a fair comparison and to showcase the methodology's accessibility. The ANN and TRNSYS model were as described previously in this paper.

The Finite Element Modelling (FEM) model was developed in COMSOL Multiphysics [174] and is based on the coupling of the governing equations of heat transfer (energy balance) and fluid flow (momentum and continuity) in a similar fashion as in [115, 116], but with horizontal GHEs. The heat transfer mechanism in this model is primarily the heat conduction in the soil, the pipe walls and partly in the carrying fluid and the heat convection in the carrying fluid. The FEM model is solved with similar boundary conditions as the TRNSYS model (i.e., adiabatic conditions on four side of the field, The outdoor temperature on the top and the undisturbed ground temperature at the bottom). The details of the FEM model can be found in Appendix D.

The computational time for FEM is estimated based on simulation for 48-hour actual time. It can be seen that the ANN resulted almost 100 times faster than TRNSYS simulation and 10,000 times faster than the FEM model in COMSOL Multiphysics.

Table 5-5 Computational time comparison for ANN, TRNSYS and FEM simulation.

| One Year Simulation | Computational Time (mins) |
|---|---|
| ANN | 0.5 to 1 |
| TRNSYS | 80 to 100 |
| FEM in COMSOL Multiphysics | 8,000 to 10,000 (estimated) |

## 5.7. Conclusions

This paper presented an investigation on the applicability of a hybrid GSHP system with horizontal GHEs in rural industries with unique heating dominant thermal load requirements. A TRNSYS simulation model for the performance of the system was developed and utilised to benchmark the investigation. Statistical machine learning approaches (Artificial Neural Networks, ANN) were adopted and fine-tuned to speed up computational times.

In horizontal GSHP systems, no annual accumulative effects are observed since the natural thermal recharge of the horizontal GHEs is enough to restore the ground to its initial state, even under extremely imbalanced loading conditions. This allows the simulation of only one year of operation to provide insights for long-term system performance. It is also observed that there is a decreasing trend of the performance of the GSHP component when the shave factor is increasing. It may be counterintuitive, but it has been proven to be the effect of the partial loading of the heat pump. This observation also suggests that when design a hybrid geothermal system, the sizing of the GSHP needs to be analysed in detailed.

Since hourly simulation data for horizontal GHEs are not available in commercial software at this stage and numerical approaches including TRNSYS simulations or FEM can be computationally expensive, two different ANNs for the prediction of the performance of GSHPs and horizontal GHEs are developed and presented. Trained with the simulated dataset from the TRNSYS results for three different locations, the ANNs can predict the performance of the GSHPs in other untrained (previously unseen) locations reasonably well (less than 5% COP error in most cases) and the performance of horizontal GHEs reasonably well (less than 3% GHE water temperature error in most cases). This suggests that the ANN models developed here can potentially be widely used in prediction, optimisation and control problems for similar sites and conditions.

A computational time comparison of the ANN predictions and TRNSYS and FEM simulations has been presented. The results show that ANNs can do the prediction reasonably well and 100 times faster than TRNSYS simulations and approximately 10,000 times faster than FEM simulations.

Overall, it is believed that this work will contribute to the wider application of ANN for the GSHP systems.

# 6. Minimising lifecycle cost and greenhouse gas emissions of hybrid geothermal-solar (PV)-gas heating systems

This chapter has been submitted as a research article to Energy Conversion and Management, in collaboration with A/Prof. Guillermo A. Narsilio, Dr Asal Bidarmaghz from the University of New South Wales, Prof. Kenichi Soga from the University of California, Berkeley and Prof. Lu Aye. Modifications have been made to the numbering of page numbers, sections, references, tables and figures to keep the consistency of the thesis. Preliminary results from conference papers in related to this work are included as Appendices A.3 and A.4.

*Acknowledgements*

The authors would like to thank the farm owners for providing the detailed information relevant to the chicken sheds. The authors would also like to thank the Australian Research Council for the funding of Linkage Project LP160100070 and FT140100227, and industry partners Ground Source Systems Pty Ltd. and Golder Associates Pty Ltd.

## 6.1. Abstract

Poultry sheds have unique indoor air temperature requirements to raise poultry (chickens: broilers and layers, turkeys, and ducks), and these determine their heating and cooling demand cycles. While low cost cooling can be achieved with evaporative coolers, effective heating options are required to minimise the lifecycle cost and greenhouse gas (GHG) emissions. There are no previous detailed studies available for heating options of typical poultry sheds for broilers. In this paper, we investigated various options under different climate conditions, including case studies across Australia under conditions similar to those encountered around the world. The operation of the sheds involves six heating and cooling cycles (seven weeks each) per year. To minimise the life cycle cost and GHG emissions of heating the sheds, hybrid geothermal-solar (PV)-gas heating systems with various configurations have been proposed. The baseload heating demand is satisfied by ground source heat pumps (GSHPs), with solar photovoltaic panels providing the electricity needed. LPG gas burners satisfy the rest of the heating demand. They are integrated with the GSHPs to reduce the overall installation costs of the heating system. The primary focus of this investigation is on the reduction of costs and GHG emissions for heating poultry sheds with these hybrid systems, considering three different electricity offsetting scenarios. We found that a considerable reduction in the lifecycle cost (up to 55%) and GHG emissions (up to 50%) can be achieved when hybrid systems are used for heating. The Pareto front solutions for the systems were also determined. By comparing the Pareto front solutions under different scenarios, it was found that the shave factor, a measure of the GSHP proportion of the overall system, significantly influenced the lifecycle cost, while the size and utilisation of solar PV panels significantly affect the lifecycle GHG emissions.

*Keywords:* multi-objective optimisation, building performance simulation, poultry sheds, geothermal energy, solar PV.

## 6.2. Introduction

A ground source heat pump (GSHP) system can provide lower carbon footprint space heating by extracting thermal energy from the ground when operating [13]. It comprises a ground heat exchanger (GHE) field (i.e., high-density polyethylene pipes embedded into the ground), a heat pump, and a distribution system. GSHP systems have been used for a number of applications worldwide, including both residential and commercial buildings [26, 27]. Adoption of the GSHP technology is relatively high in the United States, Canada, Sweden, Austria, and China [15, 16, 22, 23, 26, 27, 31, 95, 132, 141, 175], and it has been introduced for the heating of poultry sheds in recent years [10, 11]. Drawbacks of GSHP systems include high upfront construction costs, typically the GHE installation costs, as well as the embodied energy and associated GHG emissions. However, these can be reduced by coupling GSHPs with other energy sources to form a hybrid system [18-21]. Previous studies indicated that a hybrid geothermal system could not only be financially attractive, but also help to balance the thermal loads in the ground [22-24, 30, 32, 33, 154]. One potential area where hybrid geothermal system can be applied to reduce the energy consumption and GHG emission, is in agriculture. This is because agriculture contributes almost 5 trillion U.S dollars to the global economic (~6.4% of the GDP), with a significant amount of energy been consumed and emissions produced [176].

While a wide range of applications regarding the hybrid geothermal system have been investigated[22-24, 30, 32, 33, 154], they are mainly for residential and commercial buildings, which have quite different thermal load patterns compared to rural industries. This difference in load pattern can have a significant impact on the performance of hybrid geothermal systems. There are no detailed analyses currently available regarding the optimisation of hybrid geothermal systems under rural industries' loading condition. This work aims to redress this issue and to contribute to the widespread of the application of hybrid geothermal systems.

The research herein covers a range of climatic conditions encountered around the world for typical poultry sheds envelops and is exemplified using case studies from the poultry industry from across Australia. Agriculture and the associated processing industry contribute 12% to the Australian national gross domestic product [58, 59]. Within the poultry industry, it is estimated that approximately 600 million chickens are raised nationwide annually [7]. The scale of this industry results in significant energy consumption, primarily for heating and cooling the poultry sheds, as well as greenhouse gas (GHG) emissions. An estimation by Zhou et al. [8] suggested that approximately AU$80 million is spent annually by this industry and significant amount (approx. $1.8 \times 10^9$ kg $CO_2e$) of GHG emissions are produced. With the adoption of energy efficient and renewable heating and cooling systems, the operating costs of farming, as well as the energy bills, could be reduced. As existing cooling systems for chicken sheds can be cost-effective to operate and generate relatively low GHG emissions (for example, if evaporative cooling systems are used), the primary focus of this investigation is on the reduction of costs and GHG emissions for heating poultry sheds.

Network-piped natural gas and bottled liquefied petroleum gas (LPG) are the primary energy sources for heating in Australia [61] and many other parts of the world. These fossil fuels are not only expensive to utilise, but also produce a significant amount of GHG emissions when combustion occurs (approximately 0.186 kg $CO_2$-e per kW·h) [177]. Through new built and refurbishment and partial replacement of current gas heating systems with high-performance

equipment that uses renewable and more sustainable energy sources, a reduction in lifecycle costs and GHG emissions can be achieved. To further reduce the operating costs of GSHP systems, renewable solar PV systems can be utilised to offset the electricity consumed by the GSHP systems, which will also help reduce GHG emissions. From previous studies, even though the solar thermal collectors are commonly used to boost the performance of the GSHP by up to 10% [20, 33, 35-38], the benefits are significantly less than for the solar PV (up to 100% operating cost savings) [9]. Therefore, in this study, only the involvement of solar PV will be employed and analysed. By combining these three sources of energy, reduced costs and GHG emissions can be achieved [40, 41]. The hybrid geothermal-solar (PV)-gas heating systems could potentially significantly reduce the operating and lifecycle heating costs, as well as the GHG emissions associated with operation [9]. This study further investigates the influence of different sizing of the components of these systems (GSHPs, solar PV, and gas burners) to determine the optimum system configurations.

This investigation minimises the lifecycle cost and life cycle GHG emissions (in other words it identifies the Pareto front solutions) of hybrid geothermal-solar (PV)-gas heating systems. In particular, it discusses optimisation of the systems for typical chicken sheds in Central Coast, New South Wales (NSW), Sunshine Coast, Queensland (QLD), and Mornington Peninsula, Victoria (VIC), where greater than 74% of the Australian chicken meat is produced and a range of climatic conditions are encountered; thus covering situation similar to those found around the world where chicken meat is produced. Building energy simulation model of the typical shed(s) was developed using TRNSYS 18 and verified against the current energy consumptions. Based on this building performance simulation, a 40-year lifecycle analysis, and an optimisation of the installed capacities of different components of the geothermal-solar (PV)-gas hybrid heating systems was performed. The expected lifetime of ground heat exchangers is at least 40 years, and sheds are typically expected to be utilised for 40 years and, therefore, a 40 years lifetime is considered in this study.

## 6.3. Data and Methodology

### 6.3.1. Poultry Shed: Location, Construction, Operation and Climate

In this case study, a poultry shed, located in Peats Ridge, NSW, Australia, was first investigated as an example in a temperate climate region. The primary parameters of the shed are presented in Table 6-1. A TRNSYS building energy simulation model was developed for the shed. The energy model simulated the heating and cooling loads for the shed. The performance data of components (GSHP, and Solar PV) were based on the equipment currently available on the market in Australia.

Table 6-1 Poultry shed parameters.

| | |
|---|---|
| Dimensions | Width:18.3 m, Length:138.7 m, Height: 2.7 to 4.3 m |
| Wall/Roof Material | No windows; Insulation with thin layers of metal cladding. Insulation thickness: 0.075 m, thermal conductivity: 0.039 $Wm^{-1}K^{-1}$, density: 16 $kg\ m^{-3}$, specific heat: 340 $Jkg^{-1}K^{-1}$ |
| Orientation | Long axis (Length) across North-South |
| Location | Peats Ridge, NSW, Australia (33°23'49"S, 150°24'09"E) |
| Climate Data | Typical Meteorological Year (TMY) data [103] |

Zhou et al. (2017) reported that the operating schedule significantly influences the heating energy consumption of chicken sheds [4]. They estimated that as much as a 20% variation in the annual energy consumption can be expected for different starting dates of batches (growing cycles for young chicks from hatching to the market, which typically is 7–8 weeks in Australia). For this study, the first batch is assumed to start on the 1st of January and that the shed is used for six batches per year. Each batch is assumed to take 7 weeks, with a 2-week break between batches.

For the normal operation of the case study shed, 50,000 chickens are assumed at the beginning of each batch. Three harvests are expected from each batch: midnight at the end of the fifth (15,000 chickens), sixth (10,000 chickens), and seventh (25,000 chickens) weeks of the cycle. This reflects typical shed harvesting practices. Chicken mortality during growing cycles is not considered as no detailed reliable mortality data are available.

The chicken weight gain and metabolic heat generation data applied in each cycle are presented in Table 6-2. These data are in accordance with the chicken growing recommendations provided by the shed owner and operator.

Table 6-2 Chicken growth and metabolic heat generation.

| Day of growing cycle | Mass per chicken (kg) | Heat generation per chicken (W) | Number of chicken (-) | Indoor setpoint temperature (°C) |
|---|---|---|---|---|
| 1 | 0.054 | 0.82 | 50,000 | 31.0 |
| 7 | 0.180 | 2.02 | 50,000 | 28.6 |
| 14 | 0.438 | 3.93 | 50,000 | 26.1 |
| 21 | 0.829 | 6.34 | 50,000 | 23.7 |
| 28 | 1.337 | 9.08 | 50,000 | 21.2 |
| 35 | 1.897 | 11.80 | 50,000 | 19.0 |
| 42 | 2.444 | 14.27 | 35,000 | 19.0 |
| 49 | 2.873 | 16.11 | 25,000 | 19.0 |

The case study shed is currently heated by LPG burners. The energy consumption model developed was calibrated and verified with LPG purchase receipts for two years provided by the farm owner. To match the actual LPG consumption, we adjusted the ventilation rate (air exchange rate with the outdoor environment). The calibrated ventilation rate of $1.04 \times 10^{-4}\, m^3 \cdot s^{-1} \cdot kg^{-1}$ [79] was applied to closely match the actual and calculated annual heating costs.

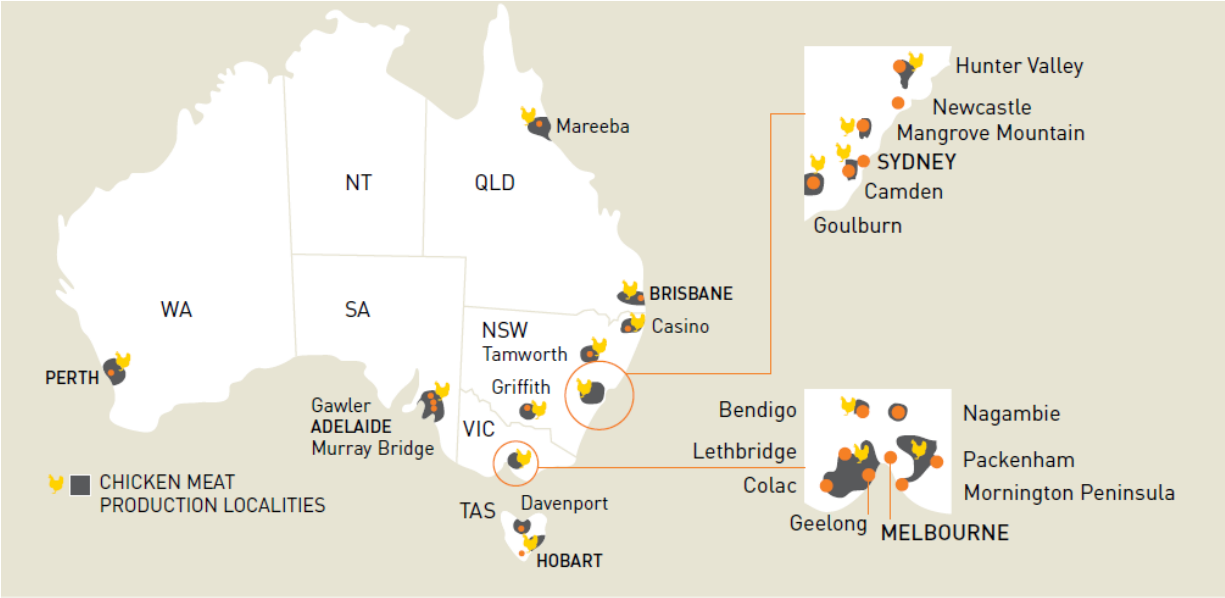


Figure 6-1 Chicken industry profile in Australia [108].

To further investigate this hybrid system, two other locations across Australia, under different climatic conditions, are analysed following the same approaches. The three locations are representative of Queensland (QLD), New South Wales (NSW), and Victoria (VIC) (Figure 6-1). These three states account for 74.4% of the overall Australian broiler production [108] and covers the humid subtropical and temperate oceanic climate conditions, which can be suitable for raising poultries [108, 178-180]. The coordinates and latest average yearly summer and winter temperatures are presented in Table 6-3. The undisturbed ground temperature is estimated based on the annual mean outdoor temperature. All factors for each location are held constant in this study.

Table 6-3 Simulation locations and key climate data for Australia [103, 109].

| Location | Coordinates | Annual mean maximum temperature (℃) | Annual mean minimum temperature (℃) | Undisturbed ground temperature (℃) |
|---|---|---|---|---|
| Central Coast, NSW | **33°23'49"S 150°24'09"E** | **21.9** | **11.6** | **16.1** |
| Mornington Peninsula, VIC | **38°17'7"S 145°5'36"E** | **18.9** | **10.1** | **14.4** |
| Sunshine Coast, QLD | **26°51'36"S 152°57'36"E** | **25.3** | **17.0** | **19.9** |

### 6.3.2. Hybrid System: Shave Factor

The 'Shave factor' S is used to describe the capacity portion of the GSHP in the hybrid system. It is defined as the ratio of the installed capacity of the GSHP system to the estimated peak heating demand of the load to be satisfied (Eq. 6-1) by the hybrid system [30, 32]. In this study, a 0% shave factor represents a full gas system and 100% a full GSHP system.

$$S = \frac{\text{Installed capacity of GSHP}}{\text{Peak heating load}} \times 100\% \qquad \text{Eq.6-1}$$

For example, a shave factor of 40% in a geothermal-gas hybrid system with 208 kW peak load demands means that the installed capacity of a GSHP system within a hybrid system is 208 kW × 40% = 83 kW, and the installed capacity of gas burners will be the difference between the peak heating load and the GSHP installed capacity (125 kW).

### 6.3.3. Hybrid System: Configuration

Figure 6-2 shows the system configuration. The heating is delivered by several identical GSHPs connected in parallel to the main header pipe. Each GSHP is coupled to a series of ground heat exchangers (GHEs). Upstream, the GSHPs are connected to a buffer tank to minimise heat pump on and off cycling. The existing LPG burners installed in the shed can top up the heating when needed. In this case, this is a hybrid geothermal-solar (PV)-gas heating system.

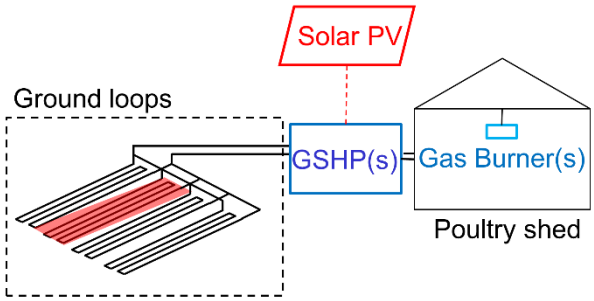


Figure 6-2 Schematic representation of a hybrid geothermal-solar (PV)-gas system.

### 6.3.4. Hybrid System Components: Efficiency, Pricing and Embodied Emissions

To perform the cost and emission optimisation of the hybrid system(s), information regarding energy efficiency, pricing, and GHG emissions for each primary component of the proposed hybrid system is required. Table 6-4 presents the energy pricing used in the optimisation. The energy prices in NSW were obtained from the current gas and electricity contracts of the NSW farm owner. It is noted that gas and electricity prices can differ from farm to farm depending on contracts with suppliers, and the electricity usage cost for this farm is particularly competitive because of high fixed supply charges. The fixed supply charge for electricity and gas is not considered in the lifecycle analysis because the fixed charge should be paid regardless of whether a hybrid system is installed or not, and it is similar to land taxes or council rates. The average electricity price in QLD and VIC are obtained from reports by Jacobs and Alviss Consulting as average prices for Small and Medium Enterprises (SME) [111, 112]. The annual average efficiency of LPG gas burners was assumed based on the equipment currently available on the market in Australia. The coefficient of performance (COP) of heat pumps can vary significantly under different operating conditions. Therefore, a simulation model in TRNSYS was developed to elaborate the hourly variation of the GSHP COP.

Table 6-4 Energy prices of gas and electricity for investigated systems.

| | NSW | NSW SME | QLD SME | VIC SME |
|---|---|---|---|---|
| Electricity Price, c/(kW·h) | 10 | 31.2 | 29.8 | 24.3 |
| Gas Price, $/GJ | 19.5 (LPG) | 26 | 35 | 18 |

Solar PV modules convert solar radiation into electricity. In this study, it is proposed that solar PV modules are installed to provide electricity to the shed heating system. The hourly electricity generated per square m of solar PV panels is calculated based on TMY (Typical Meteorological Year) weather data. Three different scenarios are considered regarding the usage of the electricity generated from solar PV: a) no electricity storage scenario, b) farm offset scenario, and c) grid selling scenario, these are detailed in Section 6.3.6. Various-sized PV arrays were investigated to determine the optimum-sized PV panels under these three situations. These scenarios will be discussed in detail in Section 6.3.6. The embodied GHG emission for 1 $m^2$ of solar PV is estimated as 42 kg/$m^2$ [181-183].

The GSHPs (and associated circulation pumps driving fluid thought the GHEs), consume electricity for their operation. The GHG emission is estimated at 0.82 kg $CO_2$e per kW·h of electricity consumed in NSW [177]. In this study we assumed a 1% annual reduction in the GHG emission factor for electricity generation. This assumption is based on the commitment of the Australian government to reduce the GHG emissions by 26% to 28%, below the 2005 levels, by 2030, which represents an approximate GHG emission reduction of 1% per year [184]. In 2017, the GHG emission factor for LPG use in NSW was 0.186 kg $CO_2$e per kW·h of energy consumption [177]. As opposed to electricity, the GHG emissions for LPG is assumed to be constant in this study.

Table 6-5 Initial GHG emission and lifetime for different components.

| | GSHP Above Ground Components (Including GSHP, water tank, air handling units) | GSHP Under Ground Components (Including ground loops, trenching and backfilling) | Solar PV | LPG Burner |
|---|---|---|---|---|
| Initial GHG Emission, kg $CO_2$e per kW | 67 | 93.8 | 42 kg/$m^2$ | 10.2 |
| Initial Cost, (AU$/kW) | 750 | 750 | AU$1,245 per kW of PV capacity | 100 |
| Lifecycle, years | 20 | 40 | 20 | 10 |

From the information summarised above, the calculated initial embodied GHG emission of solar PV for one kW capacity of the GSHP system is summarised in Table 6-5. The data for initial GHG emission of GSHPs and gas burners are calculated based on a lifecycle analysis undertaken for a typical 10 kW heating system in Australia [17].

### 6.3.5. Lifecycle Analysis and Objective Functions

As discussed in the previous section, with the adoption of the hybrid geothermal–solar (PV)–gas heating system, significant operating cost reductions can be expected. With electricity offset from solar PV modules, the operating costs can be reduced even further (up to 100%). However, high operating cost savings are typically related to high capital system investment costs.

In order to balance the initial investment with future financial returns (operating cost savings), a number of financial metrics and methods can be employed to objectively make investments decisions, these include simple payback period, discounted payback period, internal rate of return, external rate of return, and lifecycle cost analysis (LCCA) [21]. In this study, LCCA is used to guide the optimisation of the sizing of different components of hybrid heating systems.

An LCCA is a financial analysis that evaluates the financial feasibility of a project over a long period [185]. This analysis considers the net present values of the capital investment cost, operation, maintenance, and the final disposal cost. In this study, the life cycle cost of the heating system is the first objective function and is calculated as follows [43]:

$$LCC = C + \sum_{n=1}^{t} C_r \left( \frac{1}{1+d} \right)^n \qquad \text{Eq.6-2}$$

where C is the initial capital cost, $C_r$ is the recurring cost in a time period, d is the real discount rate, and t is the project lifetime in years.

The initial capital costs and lifetimes of different components applied in the analysis are presented in Table 6-5. These figures are estimated based on average current market data for the various system components. The costs of LPG heaters, GSHPs, and GHEs are calculated per unit heating capacity. The cost of solar PV modules is calculated per installed peak electricity generation capacity of solar PV, while the overall installed capacity of the solar PV panels is based on the annual electricity consumed by the system. The sizing of these components is discussed in Section 6.3.4. The current energy prices and the energy efficiency of different components of heating systems were assumed to be similar to those presented in Table 6-4.

In this analysis, the price escalation rate for LPG was assumed to be the same as for natural gas, which is 6.14%, and the price escalation rate for electricity was assumed to be 6.20% [17]. It is noted that these rates were estimated based on the actual fuel prices in Australia from 2000 to 2015. As this is considered to be a low risk project, the actual discount rate in this study is set to 5.08%, which was derived from the typical current business loan rates of the major banks in Australia.

In addition, regarding the environmental aspects, the lifecycle GHGs were investigated as the second objective function with a similar approach:

$$LGE = ME + \sum_{n=1}^{t} OE_n \qquad \text{Eq.6-3}$$

where LGE is the lifecycle GHG emission, $ME$ is the manufacturing GHG emission, $OE_n$ is the operating GHG emission in year n, and $t$ is the project lifetime in years. The initial GHG emissions and lifetime of the different components were discussed in Section 6.3.4 and presented in Table 6-5.

### 6.3.6. Different Scenarios for Multi-Objective Optimisation

Using the data and methodology discussed above, three different scenarios are considered to determine the Pareto front solutions of the hybrid geothermal-solar (PV)-gas system. The Pareto front solutions are identified based on the two objective functions discussed earlier (i.e. the lifecycle cost, and lifecycle GHG emissions).

**Scenario 1 – No Solar Electricity Storage**

In this case, there is no other equipment or system on the farm that consumes or stores the electricity generated by the solar PV panels, apart from GSHP systems. Therefore, solar

electricity cannot be sold to the grid for profit. This means that the extra electricity generated by the solar PV panels that is not consumed by the GSHP systems will be wasted.

**Scenario 2 – Farm Offset**

Poultry farms in Australia are typically large and have more than one poultry shed and includes at least a farmhouse. Therefore, it is assumed that the extra electricity generated by the solar panels can be consumed by other equipment or systems on the farm. It is assumed that the farm has a minimum constant electricity consumption of 10 kWh, which means that this is the limit (in our scenarios) that the excess solar electricity can be consumed. This number is estimated based on the electricity bill of the reference farm. The minimum monthly average hourly demand is 20 kWh (in July). Considering the solar electricity generation only happens during the day, we assume at least 50% of the average demand are always required. However, in this scenario, the electricity still cannot be sold back to the grid, resulting in a waste of electricity generated if it exceeds the demand of the farm.

**Scenario 3 – Excess Solar Grid Selling**

In this scenario, it is assumed that a contract between the farmer and the electricity supplier is established, allowing the farmer to sell electricity to the grid at a market-related or minimum governmental regulated feed-in prices, which are currently 10 c/kWh, 12 c/kWh and 10 c/kWh in NSW, VIC and QLD [44] respectively. In this case, the electricity generated by the solar PV panels is first consumed by the GSHP systems, and excess electricity will be sold to the grid. The profit of selling the electricity will then be used to pay for the operation and maintenance costs of the hybrid system.

## 6.4. Results and Discussions

Results and discussion are summarised next. We present in detail results for a single case to then summarise the multiple realisations of the thermal loads and climatic conditions investigated.

### 6.4.1. Heating Cycles of Poultry Sheds in different locations

Figure 6-3 shows the simulated heating power demand of the Central Coast, NSW shed based on the verified energy consumption model developed. It was estimated that the annual heating energy of the shed is 58,477 kWh with a peak heating demand of 208 kW. During each heating cycle, the heating demand is at its maximum at the start of the cycle when the least metabolic heat is generated by the chickens; simultaneously, the required indoor temperature is at maximum (Table 6-2). The heating demand decreases later in each cycle because of the increase in metabolic heat generated by chickens and lower indoor temperature requirement corresponding to the age of the batch (Table 6-2). The heating load cycles in Sunshine Coast, QLD and Mornington Peninsula, VIC exhibit similar patterns, with peak loads of 164kW and 228 kW, and heating demands of 34,149 kWh and 73,456 kWh respectively.

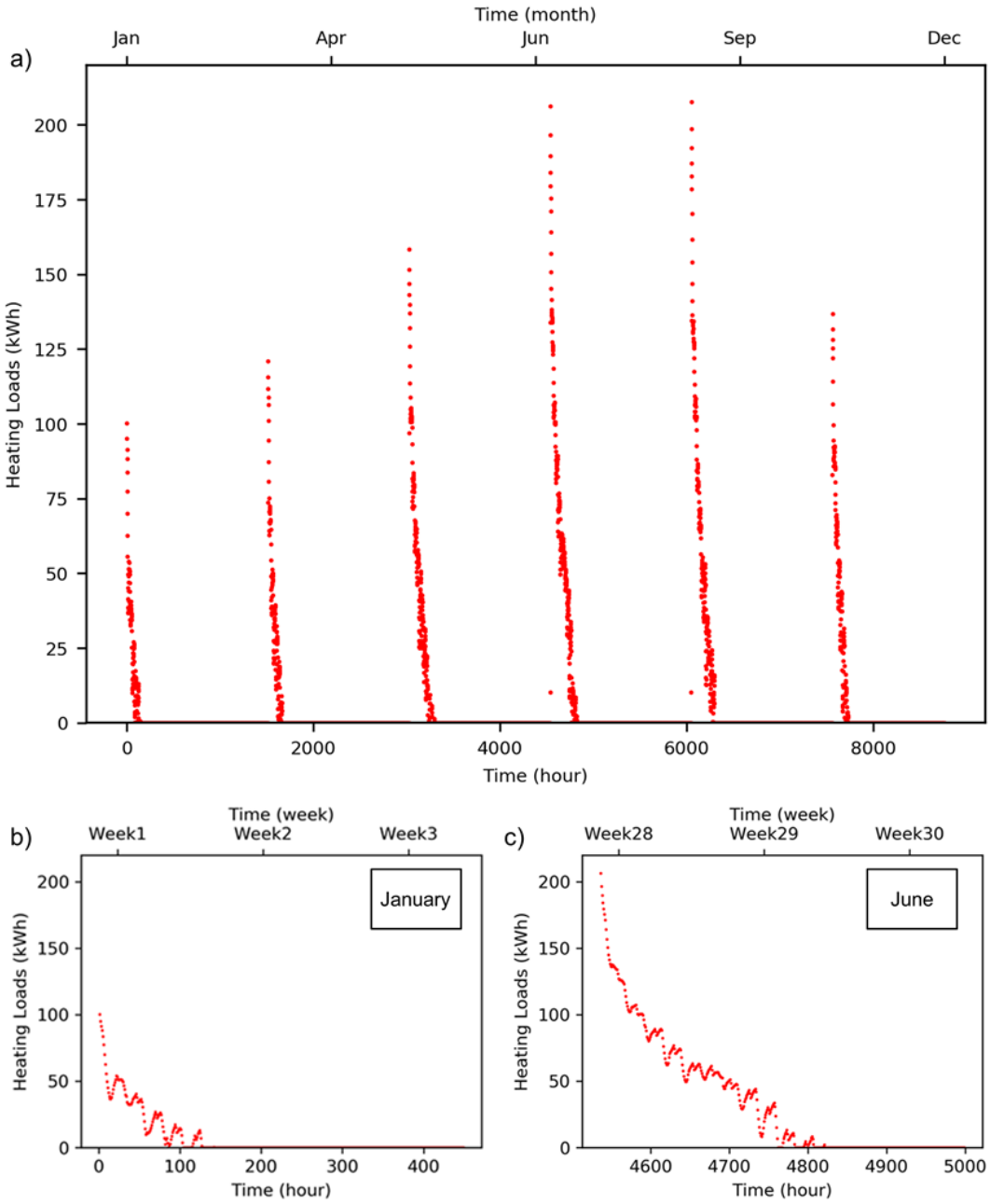


Figure 6-3 Hourly heating demand of the poultry shed at Central Coast, NSW: a) Annual heating demand b) Heating demand for the first cycle c) Heating demand for the fourth cycle.

It is noted that the heating demand of the shed is lower than 80 kW for over 80% of the time (Figure 6-3). This means that, if a hybrid heating system with an installed GSHP capacity of approximately 40% (~80 kW) of the peak heating power demand (208 kW) is used for heating (i.e., S=40%), more than 90% of the annual heating energy can still be satisfied by the GSHP. This indicates the advantage of a hybrid heating system, as it could satisfy the bulk of the heating requirements with cost-effective and renewable energy resources, with a relatively lower initial capital cost (much less trenching needed for the GHEs). The next section discusses the efficiency of the components of hybrid systems that could achieve such potential operating cost savings, and objective ways to determine best shave factors.

### 6.4.2. Hourly Coefficient of Performance of the GSHPs

As the heating loads vary from hour to hour, the COP of the GSHPs will also vary. A simulation model in TRNSYS was developed to evaluate the hourly performance of GSHPs under different shave factors and loading conditions. In this system, several identical single speed GSHPs with 20 kW heating capacity are utilised. Each heat pump has a fixed ground heat exchanger field configuration formed by four horizontal trenches. The trench is dug at the depth of 1.5 m below the ground surface and there are four straight pipes in each trench, at 30 cm separation between each pipe, similar to the one depicted in Fig. 6-4). The length for each trench is 75 m, rendering a pipe length of 300 m per trench. The system is formed by several identical GSHPs to meet the required heating capacity. For example, to provide 208 kW peak heating in total at a shave factor of 50%, there would be six 20 kW heat pumps installed, each with its own ground heat exchanger field in four trenches (i.e., 16 trenches in total).

The operation of the heat pumps is then controlled by the hourly loading demands. When the operation of a new heat pump is required, the one with the lowest accumulated hours of operation will start. In the 208kW total capacity example above (with 104kW provided by the GSHPs, i.e. S=50%), when the loads increase from 19 kW to 35 kW, the operation of a second heat pump is required. At this time, the system will compare the accumulated hours of operation from the three heat pumps that are not operating and turn on the one with the lowest accumulated hours of operation. In this case, the loads can be relatively evenly divided among all the heat pumps throughout the life of the whole system. For heating demands in excess of 104kW, all the GSHPs will be in operation and the gas burners provide the balance of the required load.

For the NSW case study thermal loading condition corresponding to a shave factor of 50% or 104 kW of GSHP capacity, six heat pumps each with 20 kW heat capacity were simulated. Since the loads are distributed relatively evenly among these heat pumps, the differences in the performances among these six heat pumps are not major. Yet, when evaluating the performance of the whole GSHP system, the six heat pumps are needed to be considered as a whole. Therefore, the hourly *system* COP of the heat pumps is then calculated based on Equations 6-4. The hourly *system* COP is representative of the performance of whole GSHP system and can be used to calculate electricity consumed by all the heat pumps, hour by hour:

$$COP_{Geo_{hr}} = \frac{\sum_{i=1}^{n} HPQ_i}{\sum_{i=1}^{n} \frac{HPQ_i}{COP_{GSHP_{hr}i}}} \qquad \text{Eq.6-4}$$

where $n$ is the number of heat pumps (e.g., n=11 for the Central Coast, NSW shed case study) $HPQ_i$ is the hourly heating loads covered by each *one ($i^{th}$)* heat pump in kWh, $COP_{GSHP_{hr}i}$ is the hourly COP for that *one ($i^{th}$)* heat pump. The electricity consumed by all the heat pumps is then calculated based on the hourly system COP as Eq. 6-4 here. A factor of 10% is then added to consider the electricity consumed by other equipment, such as the circulating pumps [35, 92, 94].

Figure 6-4 Images of a full-scale hybrid system being installed in Central Coast, NSW: a) A pipe and trench configuration b) A view of the GHE field c) A top view of the farm.

As an example, Figure 6-5 shows the $COP_{GSHP_{hr}}$ for the shave factor 50% in Central Coast, NSW. Corresponding to the loading pattern shown in Fig. 6-3, there are six operational cycles in a year. The first cycle in the year has the shortest hours of operation (Fig. 6-5 b) and the fourth cycle in the year has the longest hours of operation (Fig. 6-5 c).

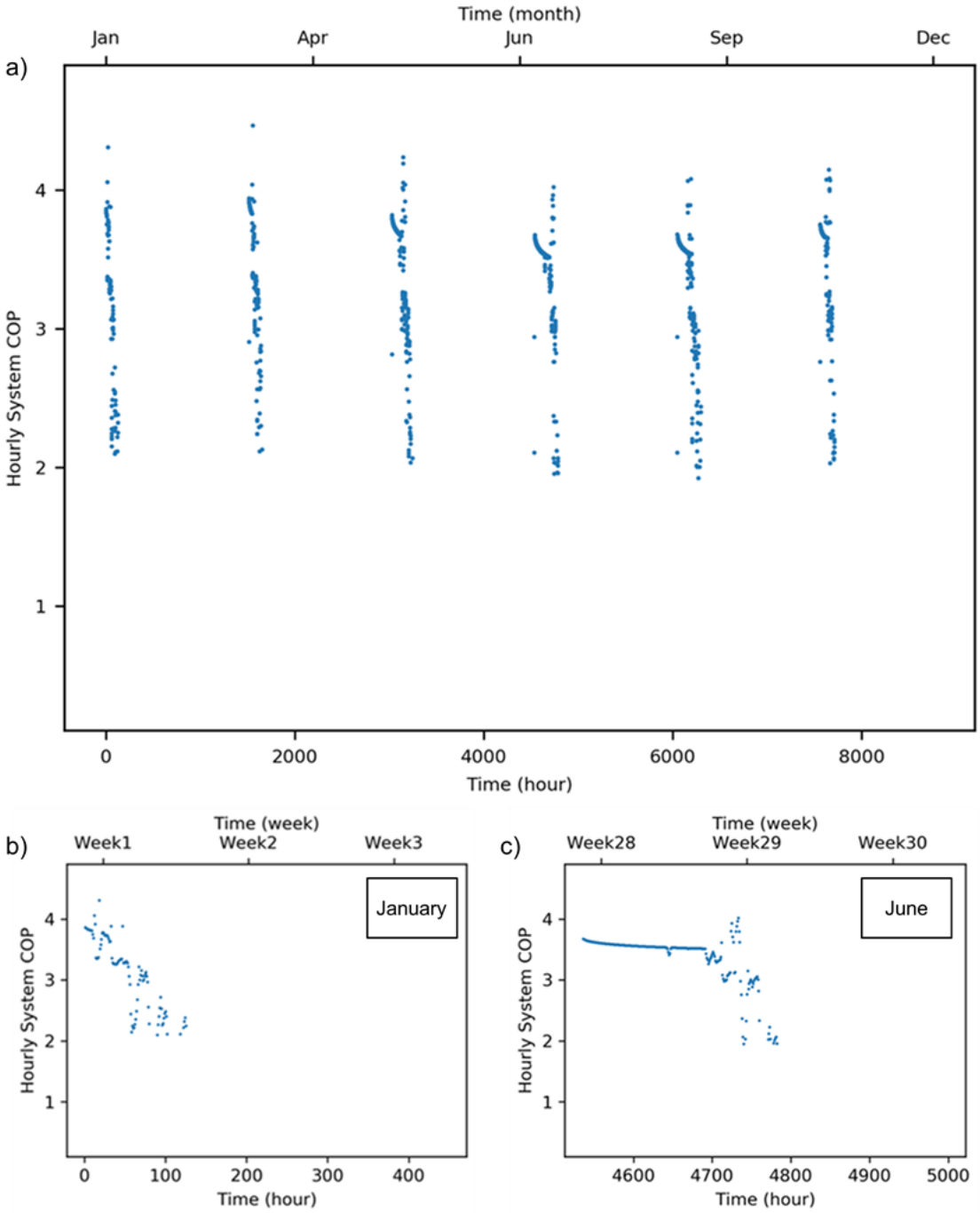


Figure 6-5 Hourly system COP for 50% shave factor in Central Coast, NSW: a) Hourly system COP for the whole year b) Hourly system COP for the first cycle in a year c) Hourly system COP for the fourth cycle in a year.

We then use the total hourly ($t^{th}$ hour in the year) heating demand for the GSHP system component, $TQ_t$, together with the hourly system COP, $COP_{Geo_{hr}}$ to estimate the average *annual* COP of the GSHP (geothermal) component COP of the whole hybrid system,

$$COP_{Geo_{annual}} = \frac{\sum_{t=1}^{8760} TQ_t}{\sum_{t=1}^{8760} \frac{TQ_t}{COP_{Geo_{hr}t}}} \quad \text{Eq. 6-5}$$

Then, the simulations are conducted for four different shave factors (i.e. 25%, 50%, 75%, 100%, 100%). The hourly system COP under the full range of shave factors (from 1% to 100%), which

is not simulated, is estimated via second order polynomial functions generated from these four data points. Subsequently, the annual system $COP_{Geo_{annual}}$ is calculated based on these hourly system COPs ($COP_{GSHP_{hr}}$) (Eq. 6-5), as shown in Figure 6-6, where it can be seen that, with increasing shave factor, there is a decrease in the overall COP. The trend observed is counterintuitive, one would expect an increase in overall COP with an increasing percentage use of a more efficient HVAC system (the GSHPs). The decrease rate also tends to be slower as the shave factor becomes higher. Based on the heating loads presented in Section 6.4.1, this decreasing COP is caused by the increasing overall running time but chances of partial loading of the heat pumps as the shave factor increases. The partial loading condition significantly reduces individual heat pump COP [186-188].

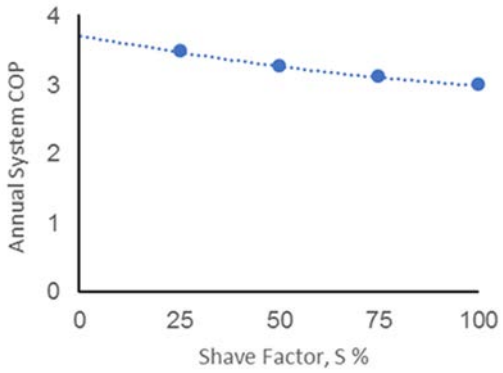


Figure 6-6 Annual system COP under the full range of shave factors for the NSW shed case study.

### 6.4.3. Hourly Solar PV Panel Electricity Generation

In order to calculate the electricity generated hourly by the solar PV panels, the following equations were used. The primary part of the calculation is to determine the irradiation on the sloped surface of the solar PV panel $I_T$, which is calculated as follows [34]:

$$I_T = RI = \left[\frac{I_b}{I}R_b + \frac{I_d}{I}\left(\frac{1+cos\beta}{2}\right) + \rho_g\left(\frac{1-cos\beta}{2}\right)\right]\cdot I \qquad \text{Eq.6-6}$$

where R is the ratio of total radiation on the sloped surface to that on a horizontal surface; I is total hourly irradiation on a horizontal surface in MJ·$m^{-2}$ ·$h^{-1}$, which equals $I_b + I_d$; $I_b$ is hourly beam irradiation on a horizontal surface in MJ·$m^{-2}$ ·$h^{-1}$; $I_d$ is hourly diffuse irradiation on a horizontal surface in MJ·$m^{-2}$ ·$h^{-1}$ ; β is the slope in degrees; $\rho_g$ is the dimensionless reflectance of ground (ground albedo) [189]; and $R_b$ is the ratio of beam radiation on a slope surface to that on the horizontal plane, and it can be calculated as [34]:

$$R_b = \frac{\cos(\emptyset+\beta)cos\delta cos\omega+\sin(\emptyset+\beta)sin\delta}{cos\emptyset cos\delta cos\omega+sin\emptyset sin\delta} \text{ (for North facing surfaces)} \qquad \text{Eq.6-7}$$

where ∅ is the Latitude in degrees; β is the slope in degrees as mentioned above; $\delta$ is the declination angle in degrees, which represents the angular position of the sun at noon with respect to the plane of the equator; $\omega$ is the hour angle in degrees, which represents the angular displacement of the sun east or west of the local meridian due to rotation of the earth on its axis.

The equations show that the electricity generation from solar PV panels is a function of the slope of the solar PV panel. The weather data used in this analysis is the same as Meteonorm

data explained in the previous sections. The optimum slope for the solar PV panel is determined. By varying the slope from 0° to 90° degrees in 0.1° steps, the total annual electricity generation from 5 $m^2$ (1.2 kW capacity) were calculated, using the parameters of the solar PV panels summarised in Table 6-6. For example, the optimum slope for the Central Coast site in NSW is determined to be 39°. The optimum slopes for Mornington Peninsula, VIC and Sunshine Coast, QLD are 34° and 26° respectively. Then, equation 6-8 can be used to calculate the instantaneous array efficiency of the solar PV panels [34]:

$$\eta = \eta_r[1 - \beta_t(t_c - t_r)]\eta_{pt} \qquad \text{Eq.6-8}$$

where $\eta_r$ is the cell packing factor times the cell reference efficiency; $\beta_t$ is the temperature coefficient of efficiency; $t_c$ is the cell temperature; $t_r$ is the reference temperature; $\eta_{pt}$ is the efficiency of power tracking equipment.

Table 6-6 Parameters for solar PV panel used in this investigation.

| | | |
|---|---|---|
| NOCT | 45 | Nominal operating cell temperature, °C |
| $\eta_r$ | 0.122 | Cell packing factor x cell packing efficiency |
| $\eta_{pt}$ | 1 | Efficiency of power tracking equipment |
| $\beta_t$ | 0.0065 | Temperature coefficient of efficiency |
| $t_r$ | 25 | Reference temperature, °C |

Fig. 6-7 shows hourly solar radiation on the surface (from TMY data) and the hourly electricity generation by the PV panels discussed above (see Table 6-6). It can be seen from the figure that the solar radiation is higher in the summer (peak radiation of 7.5 MJ·$m^{-2}$ ·$h^{-1}$ in February) than in winter (the highest radiation in July is only approximately 5.5 MJ·$m^{-2}$·$h^{-1}$). However, the amount of electricity generated in the different seasons differs only marginally. As the solar PV panels typically have an optimum temperature at about 25 ℃ (when above and below this temperature, the efficiency of the solar PV panel decreases), this marginal difference between summer and winter solar PV power generation could possibly be because in summer, the higher outdoor air temperature reduces the efficiency of the solar PV panels [34].

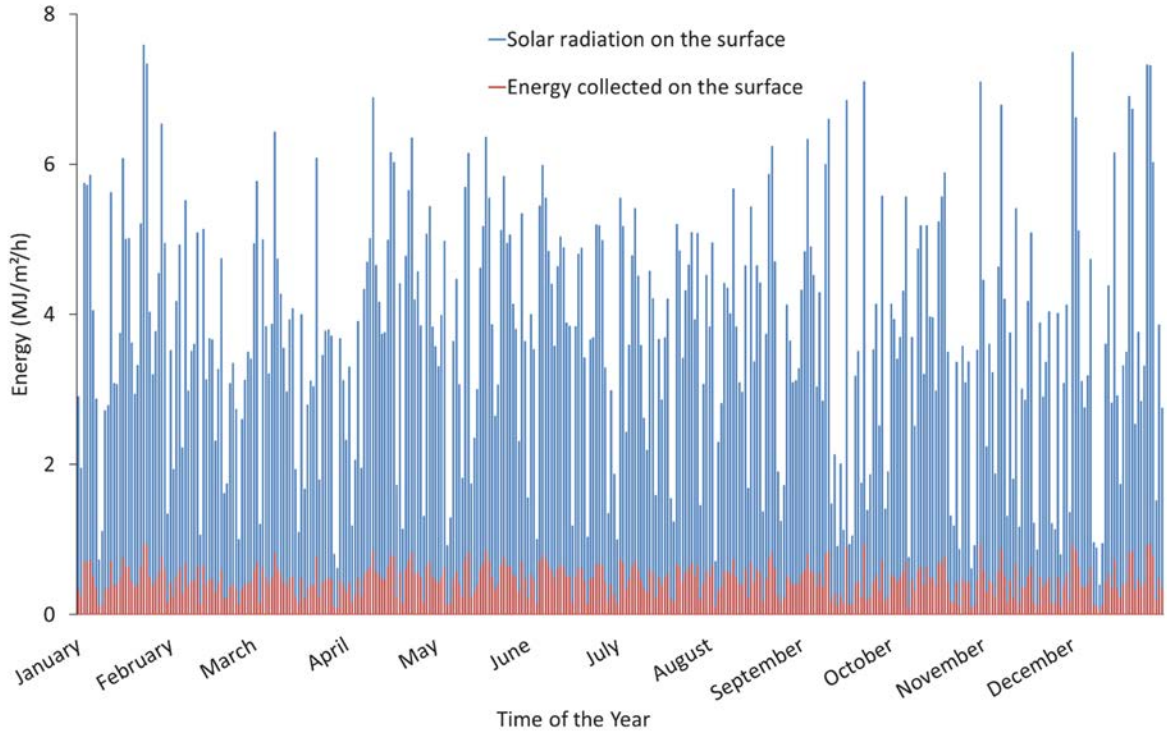


Figure 6-7 Hourly radiation and electricity generation from solar PV panels in Central Coast, NSW.

### 6.4.4. Lifecycle Analysis: Cost and GHG Emission

Using the data and methodology discussed above, the three different scenarios are discussed to determine the Pareto front solutions of the hybrid geothermal-solar (PV)-gas system.

**Scenario 1 – No Solar Electricity Storage**

In the first scenario, there is no other equipment or system in the farm that can consume (or can store) the electricity generated by the solar PV panels, apart from the GSHP systems.

For the lifecycle cost arising from equation 2 on the case study in Central Coast, NSW (Figure 6-8 a), it can be seen that the shave factor has a greater impact than the solar PV size. The optimum shave factor is approximately 20% to 25% and the optimum solar PV size under this condition is approximately 0 to 50 $m^2$. For the lifecycle GHG emission (Figure 6-8 b), the solar PV size becomes more important when the shave factor is greater than 20%. The optimum shave factor here is approximately 30% to 35%, however, the optimum solar PV size has increased to 220 to 245 $m^2$.

**Scenario 2 – Farm Offset**

In this scenario (Figure 6-8 c, d), for the lifecycle cost, the shave factor still has a greater impact than the solar PV size. The optimum shave factor remains approximately 20% to 25%. However, the optimum solar PV size under this condition is increased to approximately 0 to 100 $m^2$. For the lifecycle GHG emission, the solar PV size is critical when the shave factor is high. The optimum shave factor is approximately 30% to 35% and the optimum solar PV size, 230 to 245 $m^2$.

**Scenario 3 – Excess Solar Grid Selling**

In this scenario (Figure 6-8 e, f), for the lifecycle cost, the optimum shave factor remains similar to the previous two at approximately 20 to 30%. However, the optimum solar PV size under this condition is approximately 150 to 245 $m^2$. For the lifecycle GHG emission, the optimum shave factor is lower than the previous two, at approximately 25 to 30%, and the optimum solar PV size is 245 $m^2$.

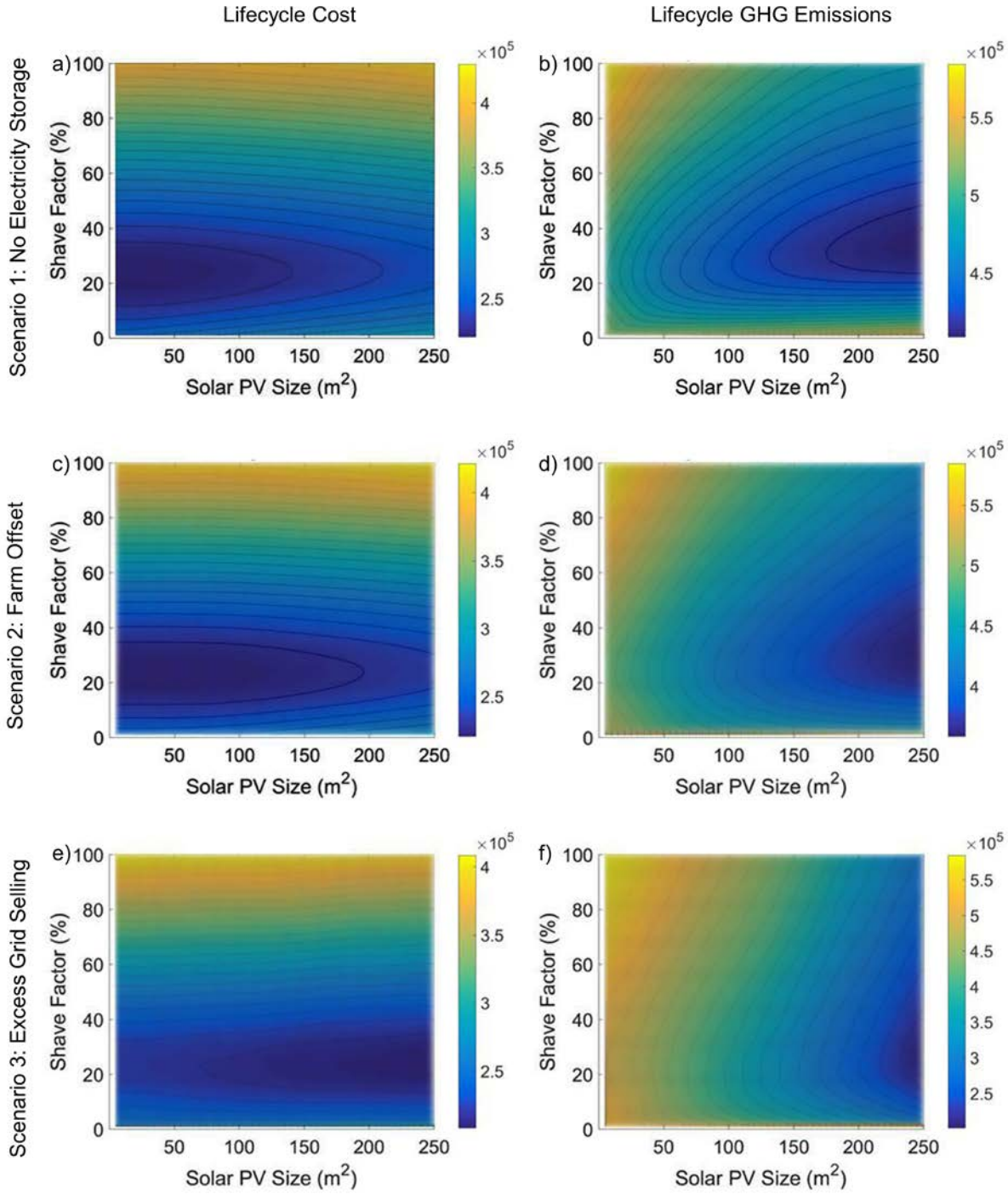


Figure 6-8 Lifecycle cost and GHG emission for three scenarios in Central Coast, NSW.

To summarise, the optimum range for the shave factor under different scenarios are around the range of 20 to 30%. However, the optimum range for the shave factor can vary highly

among different scenarios and even between the minimum lifecycle cost case and minimum lifecycle GHG emission case. In general, a larger solar PV size is preferred when the goal is to minimise lifecycle GHG emission. When minimise lifecycle cost, a larger solar PV size is preferred when the solar PV can be utilised more (Scenario 3 > Scenario 2 > Scenario 1).

### 6.4.5. Multi-objective Optimisation: Pareto Front Solutions

With the lifecycle cost and GHG emission results from the above section, multi-objective optimisation can be undertaken by identifying the Pareto optimum front. This section will present the Pareto optimum front solutions for the three scenarios mentioned in section 6.3.6 and for the three different climatic conditions encountered in the regions with the highest poultry meat production in Australia.

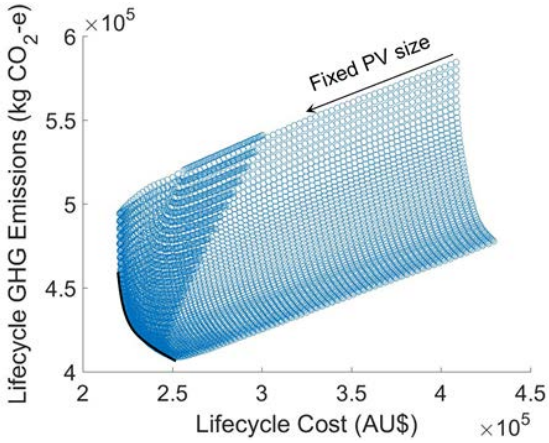


Figure 6-9 Pareto optimum solutions for Scenario 1 (no electricity storage, no grid sells) in Central Coast, NSW.

Fig. 6-9 shows the lifecycle cost and the lifecycle GHG emissions of scenario one for the reference farm in NSW. In this scenario, it is assumed that there is no storage for the electricity generated from solar PV panels. The horizontal and vertical axis represent the two objective functions, i.e. the lifecycle cost and the lifecycle GHG emissions, with the results data from Fig. 6-8. The different line formed by the points in the upright of Fig. 6-9 shows the results while fixing the PV size but changing the shave factor. As can be seen, the data points are denser on the left than on the upright section of the plot, which is because the low lifecycle cost and GHG emission can be achieved by a large number of combinations of shave factors and PV size. The Pareto optimum solutions, in this case, are defined as follows: The relationship between the lifecycle cost and GHG emission on this line cannot be expressed in a simple formula. At a shave factor of 22% and PV size of 0 $m^2$, the minimum lifecycle cost is AU$220,651, with a lifecycle GHG emission of 490,658 kg $CO_2$e. At a shave factor 32% and PV size of 245 m$^2$, the minimum lifecycle GHG emission is 405,520 kg $CO_2$e, with a lifecycle cost of AU$251,686. The dark line between these two points then forms the Pareto optimum front.

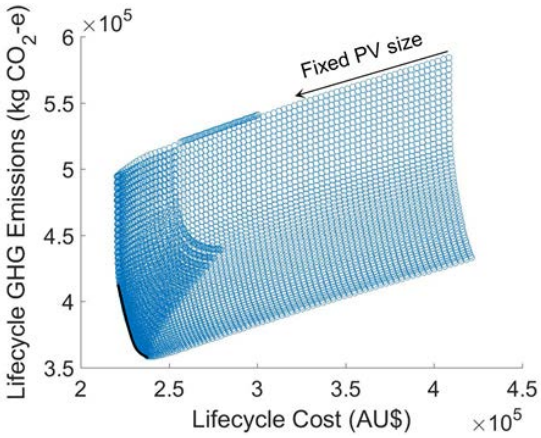


Figure 6-10 Pareto optimum solutions for Scenario 2 (farm offset) in Central Coast, NSW.

Fig. 6-10 shows the lifecycle cost and the lifecycle GHG emissions of scenario two for the reference farm. In this scenario, it is assumed that the electricity generated by the solar PV can be offset by equipment in the farm for up to 10 kW. The trend is very similar to scenario 1. The Pareto optimum solutions, in this case, are defined as follows:

For the minimum lifecycle cost, it is the same as Scenario 1. At a shave factor 30% and PV size of 245 $m^2$, the minimum lifecycle GHG emission is 355,975 kg $CO_2$e, with a lifecycle cost of approximately AU$240,484. The line between these two points then forms the Pareto optimum front.

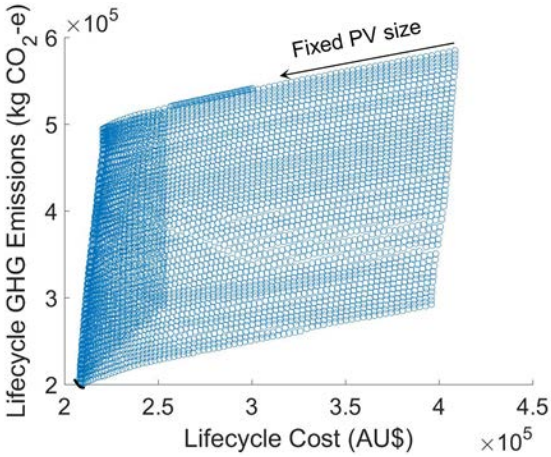


Figure 6-11 Pareto optimum solutions for Scenario 3 (grid sells) in Central Coast, NSW.

Fig. 6-11 shows the lifecycle cost and the lifecycle GHG emissions of scenario three for the reference farm. In this scenario, it is assumed that the electricity generated by the solar PV can be sold back to the grid at market price. The trend is very similar to both scenarios 1 and 2. The Pareto optimum solutions, in this case, are defined as follows:

At a shave factor 22% and PV size of 245 $m^2$, the minimum lifecycle cost is AU$208,029, with a lifecycle GHG emission of 201,716 kg $CO_2$e. At a shave factor of 28% and PV size of 245 $m^2$, the minimum lifecycle GHG emission is 201,184 kg $CO_2$e, with a lifecycle cost of approximately AU$210,421. The short line between these two points then forms the Pareto optimum front (the difference is minor).

To summarise, considering the lifecycle cost and GHG emission results from section 6.4.4, the range for the optimum shave factor is similar for all the scenarios tested under NSW weather and pricing structure conditions (about 20% to 30%). However, the optimum range for the solar PV panels are different for these scenarios. The scenario 3 has the highest optimum solar PV sizes (245 $m^2$), while scenario 2 has a higher one than scenario 1. This can be explained by that the electricity generated by solar PV can be fully utilised in scenario 3 (selling to the grid), partially used in scenario 2 (offset by other equipment in the farm) and minorly used in scenario 1. When the solar PV panels are better used, the capital and maintenance cost of the solar PV panels can be better justified. Hence, the optimum range of the solar PV panels become higher.

When showing the Pareto Optimum Front for three scenarios in the same scale (Fig. 6-12), it can be clearly seen that the scenario 3 has the best solution among them, which is due to the full utilisation of the solar PV panels. The optimum lifecycle GHG emission of scenario 3 is about 40% less than scenario 1, and 60% less the gas only system. The results reveal that the solar PV panels are essential components, particularly in reducing the GHG emission.

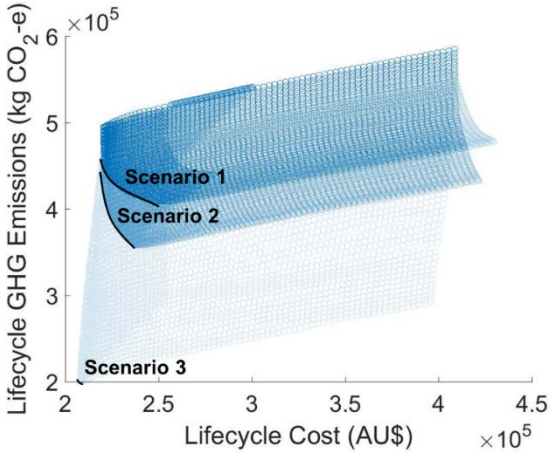


Figure 6-12 Pareto optimum solutions for three scenarios in Central Coast, NSW.

### 6.4.6. Pareto Front Solutions for other location and pricing scenarios

With the same methods and approaches mentioned above, this study extended the investigation to state average energy pricing cases for the reference farm in NSW as well as two other locations, including two locations in QLD and VIC. The results (Figure 6-13 and Table 6-7) from these cases are illustrated as follows:

For all these three scenarios, the scenario 3 shows the best Pareto optimum solution among them, which is due to the full utilisation of the solar PV panels. Considering the optimum lifecycle cost, all the scenarios for the three cases shows about 45% to 55% savings with respect to the gas only system. For the optimum lifecycle GHG emissions, scenario 3 for all the three cases show a significant advantage. For the NSW case, the optimum lifecycle GHG emission for scenario 3 is about 60% lower than scenario 1 and 40 % lower than scenario 2. For the VIC case, the optimum lifecycle GHG emission for scenario 3 is about 75% less than scenario 1 and 60 % less than scenario 2. For the QLD case, the optimum lifecycle GHG emission for scenario 3 can even be reduced to negative value, which is due to the relatively low heating demand and high amount of solar electricity selling to the grid from QLD. It should be noted that when selling to green electricity to the grid, there is a negative GHG

emission (uptake) added to the calculation. This is because the same emission generated from the grid can be saved. Overall, the results confirm that the solar PV panels are essential in reducing the GHG emission.

When considering the shave factor and solar PV size under optimum conditions, it shows similar patterns as the case discussed in section 6.4.5. The optimum shave factors range from about 20% (VIC) to 35% (QLD) for these cases. For the optimum solar PV size, almost all the cases ask for the highest size in scenario 3 (245 $m^2$), less in scenario 2 (100 to 245 $m^2$) and least in scenario 1 (0 to 125 $m^2$). These are also in good agreement with the findings in section 6.4.5.

Table 6-7 Optimum lifecycle cost and GHG emissions under different scenarios and locations.

| Scenarios | | 1: No Storage | | 2: Farm Offset | | 3: Grid Selling | |
|---|---|---|---|---|---|---|---|
| | | Optimum Cost Case | Optimum Emissions Case | Optimum Cost Case | Optimum Emissions Case | Optimum Cost Case | Optimum Emissions Case |
| Central Coast, NSW | Cost, AU$ | 220,651 | 251,686 | 220,651 | 240,484 | 208,029 | 210,421 |
| | Emission, $CO_2e$ | 490,658 | 405,520 | 490,658 | 355,975 | 201,716 | 201,184 |
| Central Coast, NSW (SME Pricing) | Cost, AU$ | 333,003 | 371,334 | 311,542 | 336,202 | 309,609 | 322,982 |
| | Emission, $CO_2e$ | 467,775 | 405,520 | 404,303 | 355,975 | 208,819 | 201,184 |
| Mornington Peninsula, VIC | Cost, AU$ | 297,705 | 355,100 | 276,575 | 324228 | 257,411 | 191,595 |
| | Emission, $CO_2e$ | 652,185 | 505,297 | 571,395 | 435708 | 244,230 | 286,375 |
| Sunshine Coast, QLD | Cost, AU$ | 228,752 | 259,588 | 211,119 | 230,261 | 212,088 | 216,462 |
| | Emission, $CO_2e$ | 242,179 | 233,320 | 192,615 | 169,725 | 4,179 | -15,847 |

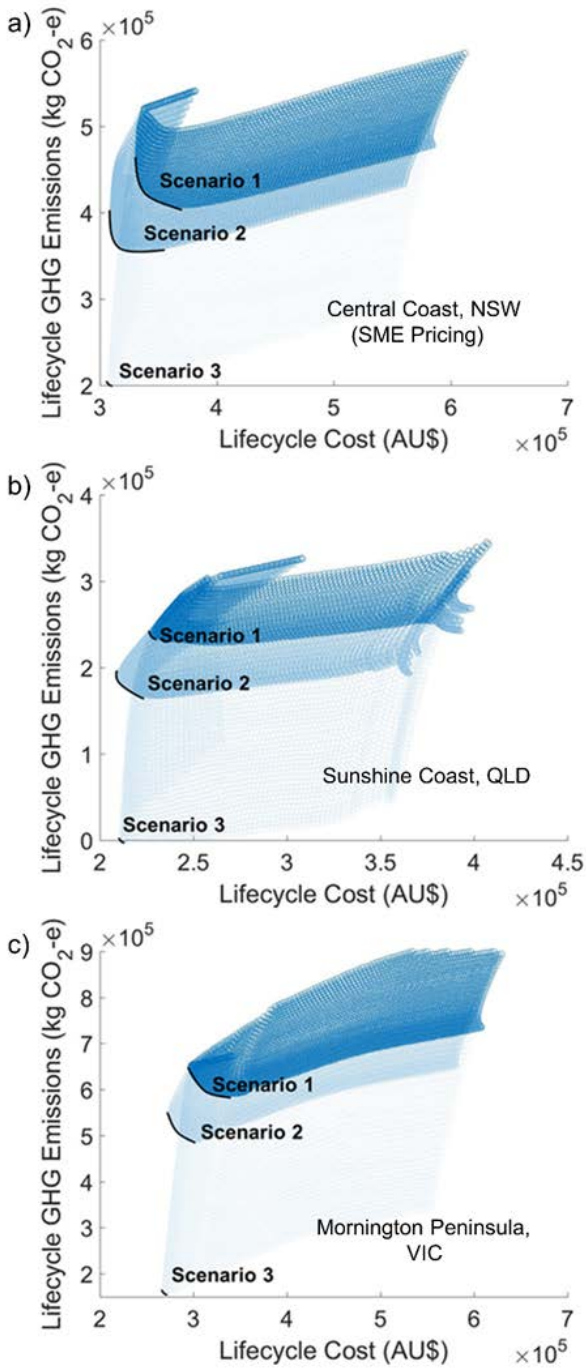


Figure 6-13 Pareto optimum solutions for average pricing cases in: a) Central Coast, NSW b) Sunshine Coast, QLD c) Mornington Peninsula, VIC. Please note different axis scales for each case.

### 6.4.7. Applicability of results to other worldwide locations within similar climate zones

As mentioned before, the locations of the three case studies investigated fall into humid subtropical (Sunshine Coast, QLD and Central Coast, NSW) and temperate oceanic (Mornington Peninsula, VIC) climate zones of the Köppen classification [21]. As this classification is based on threshold values and seasonality of monthly ambient air temperature and precipitation, the temperature and solar radiation patterns can be reasonably similar within one climate zone [190, 191]. As shown in Figure 6-14, these two climate zones includes Western Europe, south-eastern parts of United States, China, Africa and Australia, as well as isolated locations elsewhere. The key findings of this research can be potentially applied to the poultry industry within these regions.

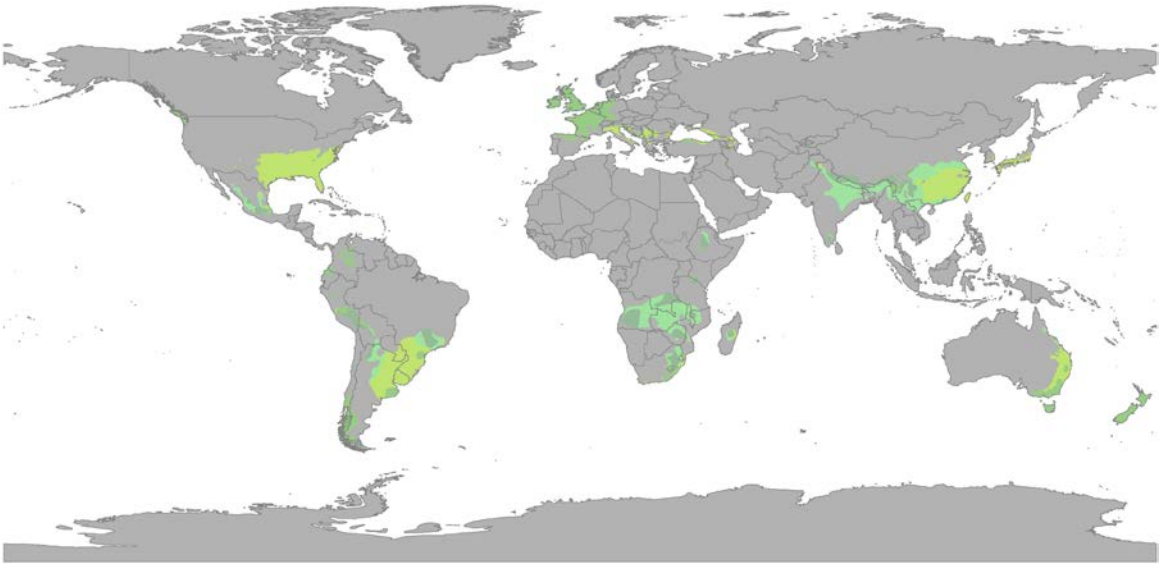

Figure 6-14 World climate map for humid subtropical and temperate oceanic regions [178, 192].

## 6.5. Conclusions

This investigation evaluated the unique annual heating load pattern of typical poultry sheds in humid subtropical and temperate oceanic climate zones. These were exemplified with case studies in the Central Coast (NSW), Sunshine Coast (QLD) and Mornington Peninsula (VIC) in Australia. These regions cover and account for more than 74.4% of the national chicken meat production. A hybrid geothermal-solar (PV)-gas system was proposed as an energy-efficient and cost-effective heating system for the sheds. Based on verified simulated hourly heating loads by TRNSYS, the hybrid heating system was analysed for various sizes of components, by varying the shave factor and size of solar PV panels. To quantify the annual performance of the system, hourly COPs of the GSHPs were simulated by the TRNSYS project developed. The annual electricity generated from the solar PV panels was calculated based on the analysed optimum slopes of the panels.

Lifecycle cost and GHG emission analyses were performed to optimise the sizes of the components of the hybrids and determine the most cost-effective and the lowest GHG emissions configuration of a hybrid geothermal system. Multi-objective optimisations (minimum lifecycle cost and GHG emissions) were conducted to identify the Pareto front solutions under three different scenarios. As the search feasible region was relatively small, a full enumeration method was used.

It was found that hybrid geothermal-solar (PV)-gas systems can be financially better and environmentally friendlier than the original gas-only shed heating systems for 40 years shed lifetime. Within the two parameters, the shave factor can contribute more to reducing the lifecycle costs, and the solar PV size can contribute more to reducing the lifecycle GHG emissions.

# 7. Conclusions and Recommendations

This thesis focuses on hybrid geothermal heating systems and aims to contribute to the utilisation, modelling and optimisation of such systems for poultry industry. Firstly, this work investigated the unique heating and cooling loads and discussed energy efficient solutions for the poultry industry. To do so, a building simulation model in TRNSYS was developed and verified for a poultry shed. Various HVAC systems, building envelopes, ventilation strategies and operational schedules were analysed. The optimum ventilation strategies and operational schedules were also proposed. Later, the experimental set-ups of the hybrid GSHPs with horizontal GHEs in Peats Ridge, NSW, Australia were presented. The explanation and discussion were made on dataset that are currently available. The findings verified the feasibility of this study.
Following, detailed numerical simulation of the GSHPs and horizontal GHEs were conducted. A TRNSYS projected was firstly developed to investigate the performance of GSHPs and horizontal GHEs under various conditions. Different Artificial Neural Networks (ANNs) were then developed and trained with simulated dataset from TRNSYS, which significantly speed up the simulation time. The performance and computational speed of the ANNs were then evaluated. Finally, this work presents a multi-objective optimisation of the hybrid geothermal-solar-gas systems. Two objective functions, i.e. the lifecycle cost and lifecycle GHG emissions, were considered for 40-year project lifetime. The Pareto optimum solutions for these systems are then presented while considering three different scenarios for the usage of electricity generated by Solar PV panels.

## 7.1. Conclusions

Main conclusions drawn from each chapter are presented as followed.

### 7.1.1. Experimental Set-ups for hybrid geothermal heating systems

A full-scale experimental rig of a hybrid geothermal system with horizontal GHEs was constructed. This hybrid geothermal system with horizontal GHEs believed to be a unique fully instrumented full-scale system for the study of horizontal GHEs, applied for poultry sheds. A 200-kW hybrid system (80 kW from Geothermal Energy and 120 kW from LPG) for an existing poultry shed building located at Peats Ridge, NSW, Australia was designed and selected as an experiment for this study. In this system, a total 4.8 km of HDPE pipes were buried as heat exchangers in 12 horizontal trenches, each at 1.5 m depth below the ground surface and 4 groups of loops in a pond nearby, at the depth of about 4 to 6 m below the water surface (actual depth varying by season due to the change of water level). The monitoring results from the instrumentation have been discussed. The results of these tests verified the feasibility of the hybrid geothermal system under rural industries' unique loading condition. It is believed that future data comes from this experimental set-up can assist in validating simulation model and design tools for the horizontal GHEs.

### 7.1.2. Unique heating and cooling loads for poultry sheds

The heating and cooling loads of the poultry sheds have been investigated in detail by using TRNSYS (a widely used building energy simulation software). The TRNSYS model considered the chicken growth rate and metabolic heat generation, operating schedules, building envelop materials, orientation and climate conditions. The results revealed unique loading characteristics including energy imbalance, sharp peak demands as well as shortly alternating heating and cooling. In detail, there are six heating and cooling demand cycles within a year,

each last for seven weeks. Within each cycle, the heating load decreases as a result of the increasing heat generated by the chickens due to growth. After the initial stage, the cooling load significantly increases. It was also found that even though the cooling load is much higher than the heating load, the priority should be focused on the reduction of heating load and expenditure. This is because the current evaporative coolers already have good efficiency with low cost.

#### 7.1.3. Energy efficient solutions for poultry sheds

Within various energy efficient solutions investigated to reduce the heating and cooling energy consumption and expenditure, the building envelope has been found to be the least impact as the it cannot reduce the heating and cooling loads simultaneously. Then, the operational schedule is the third most influencing factor. Between 2.0 to 3.7 % of the operational cost can be saved on average if the operational schedule is optimised. The night ventilation strategy is the second influencing factor. Increasing the ventilation rate at night can reduce the cooling loads significantly. However, the total electricity cost reduction is about 5 to 10% due to the increase in fan electricity consumption. The increase ventilation rate for heating has been found to be minor due to the outdoor temperature is lower than the indoor temperature for the majority of the time when heating is required. Lastly, it was found that HVAC system selection can have the highest impact on cooling and heating energy consumption, subject to lower electricity and gas prices. By switching from an LPG heating system to GSHP heating system, up to 60% of the heating cost and up to 20% of the heating and cooling cost can be saved.

#### 7.1.4. Numerical simulation of GSHP systems with horizontal GHEs in TRNSYS

The TRNSYS simulation model for the performance of GSHPs and horizontal GHEs under rural industries' unique loading condition was developed and presented. As can be seen from a ten-year simulation, the results show that there is a yearly repeating pattern for the inlet and outlet temperatures of the horizontal GHEs as well as the heat pump COP. This pattern means that natural recharge to the horizontal GHEs is enough even under extremely imbalance loading condition. Thus, one-year simulation can be representative to the horizontal GHE case studies. High shave factor in the hybrid system results in low COP. The reason is that with a higher shave factor, there is more time that the heat pump is operating under partial loads, which leads to lower COP.

#### 7.1.5. Machine learning predictions of the GHEs and GSHPs

Hourly simulation data for horizontal GHEs are not available in commercial softwares at this stage and numerical approaches including TRNSYS simulation also can be computationally expensive. Therefore, two different ANNs for the prediction of the performance of GSHPs and horizontal GHEs were developed and presented. Trained with the TRNSYS simulated dataset in three locations, the ANNs can predict the performance of the GSHPs in other untrained location reasonably well (less than 10% error in most cases) and the performance of horizontal GHEs even better (less than 5% error in most cases). This indicated that the ANN model has a generalisation ability that can potentially be widely used in prediction, optimisation and control when site conditions are similar. A computational time comparison of the ANN, TRNSYS simulation and finite element simulation was conducted. ANN can predict reasonably well while 100 times faster than TRNSYS simulations and approximately 10,000 times faster than finite element model simulations.

#### 7.1.6. Lifecycle analyses and multi-objective optimisation of hybrid geothermal-solar-gas systems

Based on hourly heating loads from TRNSYS, the hybrid heating system was analysed for various sizes of components, by varying the shave factor and size of solar PV panels. To quantify the annual performance of the system, hourly COPs of the GSHPs simulated by the TRNSYS project were used. The annual electricity generated from the solar PV panels was calculated based on the optimum slopes of the panels. Lifecycle cost and GHG emission analyses were performed to optimise the sizes of the components of the hybrids and determine the most cost-effective and the lowest GHG emissions configuration of a hybrid geothermal system. Multi-objective optimisations (minimum lifecycle cost and minimum GHG emissions) were conducted to identify the Pareto front solutions under three different scenarios. As the search feasible region was relatively small, a full enumeration method was used. It was found that hybrid geothermal-solar (PV)-gas systems can be financially better and environmentally friendlier than the original gas-only shed heating systems for 40 years shed lifetime. Within the two parameters, the shave factor can contribute more to reducing the lifecycle costs, and the solar PV size can contribute more to reducing the lifecycle GHG emissions.

### 7.2. Recommendations for future works

#### 7.2.1. Further investigation of indoor environment of rural industry

The primary aspects considered in this thesis is the heating and cooling loads and the heating associated lifecycle cost and GHE emission. However, the indoor environment might have impacts on the mortality and growth rate of the animals and can be further investigated. The first step can be a more detailed thermal loading analysis distinguishing in sensible and latent loads. The analysis can identify cases where humidification or dehumidification is required so that relative humidity can be preserved to provide a better indoor environment for the animals.

Going further to the issue above, it deserves to be further investigated in the future the use of heat pumps for cooling. As presented in the thesis, the cooling loads are much higher compared to the heating ones and it is challenging to counterbalance them in view to achieve desirable indoor conditions. Evaporative pads are widely applied for poultry houses cooling due to its low operational cost. However, their capability of establishing all year-round optimal indoor conditions is limited (e.g. hot and very humid periods). An analysis of heating loads would most probably reveal that in most of the cases of cooling especially during hot and humid periods, dehumidification or even reheating would be necessary to achieve desirable indoor conditions. The two last processes are feasible only by using heat pumps. Apparently, we talk about conditions strongly diversified from common applications of heat pumps such as in residential or commercial buildings.

#### 7.2.2. Further validation of horizontal GHE models against future observations

High quality dataset which is suitable for model validation is rare and difficult to acquire. This is mainly due to the costs of the design, construction and instrumentation of hybrid geothermal systems with GHEs are high. This thesis presents the ground temperature in the trenches and the short test results of the horizontal GHEs. Even though the author has made great effort for the experiment set-up, the outbreak of Salmonella prohibits the further observation of the system until December 2019. Therefore, only limited dataset was obtained to verify the models and justify the findings from this study. When future data become available from the instrumentation, further validation of models can be made. The specific

parameters that can be further validated in relation to the works in this thesis include the effective soil thermal conductivity, carrier fluid temperatures and COP of the heat pumps. Needless to say, new data can be used for other models and further verifications.

### 7.2.3. Verification for various climate and ground conditions

The investigation was primarily conducted for five locations in four states in Australia, which represents over 90% of the Australian poultry industry. There five cases were selected to clearly demonstrate the proposed methods discussed in Chapter 3 to Chapter 6. Using these methods, various energy efficiency solutions have been proposed, followed by the numerical simulation and optimisation of the system. As next step, though great efforts have been made to verify this study in different climate and geological conditions, further verifications beyond these locations can still be made to strengthen the applicability of this work. The further verification can take places in other climate zones around the world. This would allow the evaluation of the hybrid geothermal systems under different climate, geological, energy price and emission conditions.

### 7.2.4. Application in different industries

Although the application of this research is for the poultry industry, due to limit of time and resources, the primary cases studies are for Australia. Though great efforts have been made to make this study as general as possible, further verifications beyond the poultry industry can still be made to strengthen the wider applicability of this work. The potential industries and end-users include farms for dairy and swine as well ice rooms, which may share unique loading characteristics investigated (an even larger energy imbalance and sharp peak demands) in this research.

# 8. References

[1] International Energy Agency. KeyWord Statistics 2015. International Energy Agency, 31-35 rue de la Fédération, 75739 Paris Cedex 15 France2015.
[2] Pachauri RK, Allen MR, Barros V, Broome J, Cramer W, Christ R, et al. Climate change 2014: synthesis report. Contribution of working groups I, II and III to the fifth assessment report of the intergovernmental panel on climate change: IPCC; 2014.
[3] IEA. Renewables for Heating and Cooling. 2007.
[4] Internatinal Energy Agency. Technology Roadmap Energy-efficient Buildings: Heating and Cooling Equipment. 2011.
[5] National Famer's Federation. NFF Annual Review 2014-15. 2016.
[6] NFF. Farm Facts. 2012.
[7] Australian Bureau of Statistics. 7215.0 - Livestock Products, Australia, March 2016. 2016.
[8] Zhou Y, Bidarmaghz A, Narsilio G, Aye L. Heating and Cooling Loads of a Poultry House in Central Coast, NSW, Australia. World Sustainable Built Environment Conference 2017. Hong Kong 2017.
[9] Zhou Y, Mikhaylova O, Bidarmaghz A, Donovan B, Narsilio GA, Aye L. Hybrid geothermal-gas and geothermal-solar-gas heating systems for poultry sheds. Zero Energy Mass Custom Home 2018. Melbourne2018. p. 545-54.
[10] Kharseh M, Nordell B. Sustainable heating and cooling systems for agriculture. International Journal of Energy Research. 2011;35:415-22.
[11] Choi H, Salim H, Akter N, Na J, Kang H, Kim M, et al. Effect of heating system using a geothermal heat pump on the production performance and housing environment of broiler chickens. Poultry science. 2012;91:275-81.
[12] Hepbasli A. A key review on exergetic analysis and assessment of renewable energy resources for a sustainable future. Renewable and sustainable energy reviews. 2008;12:593-661.
[13] Johnston IW, Narsilio GA, Colls S. Emerging geothermal energy technologies. KSCE Journal of Civil Engineering. 2011;15:643-53.
[14] Rybach L. The future of geothermal energy and its challenges. Proceedings World Geothermal Congress2010.
[15] Lund JW, Boyd TL. Direct utilization of geothermal energy 2015 worldwide review. Geothermics. 2016;60:66-93.
[16] Self SJ, Reddy BV, Rosen MA. Geothermal heat pump systems: Status review and comparison with other heating options. Applied Energy. 2013;101:341-8.
[17] Q. Lu. Shallow geothermal system: Feasibility and design practices in Melbourne, Australia [PhD Thesis]: University of Melbourne; 2018.
[18] Eslami-Nejad P, Bernier M. Coupling of geothermal heat pumps with thermal solar collectors using double U-tube boreholes with two independent circuits. Applied Thermal Engineering. 2011;31:3066-77.
[19] Kjellsson E, Hellström G, Perers B. Optimization of systems with the combination of ground-source heat pump and solar collectors in dwellings. Energy. 2010;35:2667-73.
[20] Weeratunge H, Narsilio G, de Hoog J, Dunstall S, Halgamuge S. Model predictive control for a solar assisted ground source heat pump system. Energy. 2018;152:974-84.
[21] Lu Q, Narsilio GA, Aditya GR, Johnston IW. Economic analysis of vertical ground source heat pump systems in Melbourne. Energy. 2017;125:107-17.
[22] Kuzmic N, Law YLE, Dworkin SB. Numerical heat transfer comparison study of hybrid and non-hybrid ground source heat pump systems. Applied Energy. 2016;165:919-29.
[23] Man Y, Yang H, Wang J. Study on hybrid ground-coupled heat pump system for air-conditioning in hot-weather areas like Hong Kong. Applied Energy. 2010;87:2826-33.
[24] Yi M, Hongxing Y, Zhaohong F. Study on hybrid ground-coupled heat pump systems. Energy and Buildings. 2008;40:2028-36.

[25] Narsilio GA, Aye L. Shallow Geothermal Energy: An Emerging Technology (Chapter 18),. In: Sharma A, Shukla, D., and Aye, L., editor. Low Carbon Energy Supply: Green Energy and Technology,: Springer Nature Singapore Pte Ltd.; 2018.
[26] Han C, Yu XB. Performance of a residential ground source heat pump system in sedimentary rock formation. Applied Energy. 2016;164:89-98.
[27] Zhou Z, Zhang Z, Chen G, Zuo J, Xu P, Meng C, et al. Feasibility of ground coupled heat pumps in office buildings: A China study. Applied Energy. 2016;162:266-77.
[28] Bayer P, Saner D, Bolay S, Rybach L, Blum P. Greenhouse gas emission savings of ground source heat pump systems in Europe: a review. Renewable and Sustainable Energy Reviews. 2012;16:1256-67.
[29] Saner D, Juraske R, Kübert M, Blum P, Hellweg S, Bayer P. Is it only CO2 that matters? A life cycle perspective on shallow geothermal systems. Renewable and Sustainable Energy Reviews. 2010;14:1798-813.
[30] Alavy M, Nguyen HV, Leong WH, Dworkin SB. A methodology and computerized approach for optimizing hybrid ground source heat pump system design. Renewable energy. 2013;57:404-12.
[31] Gang W, Wang J. Predictive ANN models of ground heat exchanger for the control of hybrid ground source heat pump systems. Applied Energy. 2013;112:1146-53.
[32] Mikhaylova O, R. Choudhary, K. Soga, Johnston IW. Benefits and Optimisation of District Hybrid Ground Source Heat Pump Systems. Energy Geotechnics. 2016.
[33] Woo N-S, Kim Y-J, Jo Y-D, Hwang I-J. Performance investigation of the hybrid-renewable energy system with geothermal and solar heat sources for a residential building in South Korea. Journal of Solar Energy Engineering. 2013;135:021005.
[34] Duffie JA, Beckman WA. Solar engineering of thermal processes: John Wiley & Sons; 2013.
[35] Bakirci K, Ozyurt O, Comakli K, Comakli O. Energy analysis of a solar-ground source heat pump system with vertical closed-loop for heating applications. Energy. 2011;36:3224-32.
[36] Esen H, Esen M, Ozsolak O. Modelling and experimental performance analysis of solar-assisted ground source heat pump system. Journal of Experimental & Theoretical Artificial Intelligence. 2017;29:1-17.
[37] Si Q, Okumiya M, Zhang X. Performance evaluation and optimization of a novel solar-ground source heat pump system. Energy and Buildings. 2014;70:237-45.
[38] Trillat-Berdal V, Souyri B, Achard G. Coupling of geothermal heat pumps with thermal solar collectors. Applied Thermal Engineering. 2007;27:1750-5.
[39] Zhou Y, Olga Mikhaylova, Asal Bidarmaghz, Brad Donovan, Guillermo Narsilio, Aye L. Hybrid geothermal-gas and geothermal-solar-gas heating systems for poultry sheds. Zero Energy Mass Custom Home 2018. Melbourne2018. p. 545-54.
[40] Sarbu I, Sebarchievici C. General review of ground-source heat pump systems for heating and cooling of buildings. Energy and buildings. 2014;70:441-54.
[41] Hong B, Howarth RW. Greenhouse gas emissions from domestic hot water: heat pumps compared to most commonly used systems. Energy Science & Engineering. 2016;4:123-33.
[42] Gurney K. An introduction to neural networks: CRC press; 2014.
[43] Markvart T. Solar Electricity, University of Southampton UK, John Wiley and Sons Ltd. Baffin's lane, Chichester. 1994.
[44] İnallı M, Esen H. Experimental thermal performance evaluation of a horizontal ground-source heat pump system. Applied thermal engineering. 2004;24:2219-32.
[45] Wu Y, Gan G, Verhoef A, Vidale PL, Gonzalez RG. Experimental measurement and numerical simulation of horizontal-coupled slinky ground source heat exchangers. Applied Thermal Engineering. 2010;30:2574-83.
[46] Wu Y, Gan G, Gonzalez RG, Verhoef A, Vidale PLJIJoL-CT. Prediction of the thermal performance of horizontal-coupled ground-source heat exchangers. 2011;6:261-9.
[47] Kim M-J, Lee S-R, Yoon S, Go G-H. Thermal performance evaluation and parametric study of a horizontal ground heat exchanger. Geothermics. 2016;60:134-43.
[48] Demir H, Koyun A, Temir G. Heat transfer of horizontal parallel pipe ground heat exchanger and experimental verification. Applied thermal engineering. 2009;29:224-33.

[49] Xuedan Z, Yiqiang J, Yang Y. Improved method and case study of ground-coupled heat pump system design. Energy Procedia. 2012;14:849-54.
[50] Naili N, Attar I, Hazami M, Farhat AJJECTC. Experimental analysis of horizontal ground heat exchanger for Northern Tunisia. 2012;2:44-51.
[51] Naili N, Attar I, Hazami M, Farhat AJEc, management. First in situ operation performance test of ground source heat pump in Tunisia. 2013;75:292-301.
[52] Valizadeh Kivi A. Development of design tools for direct geothermal systems. Melbourne, Australia: the University of Melbourne 2015.
[53] The Bureau of Meteorology, CSIRO. State of the Climate 2016. The Bureau of Meteorology; 2016.
[54] Meteotest. Meteonorm Handbook. 2016.
[55] International Energy Agency. KeyWord Statistics 2015. Paris, France: IEA PUBLICATIONS; 2015.
[56] International Energy Agency. Renewables for Heating and Cooling. Paris, France: IEA PUBLICATIONS; 2007.
[57] Internatinal Energy Agency. Technology Roadmap Energy-efficient Buildings: Heating and Cooling Equipment. Paris, France: IEA PUBLICATIONS; 2011.
[58] National Farmer's Federation. NFF Annual Review 2014-15: National Farmer's Federation; 2016.
[59] National Farmer's Federation. Farm Facts: National Farmer's Federation; 2012.
[60] Allison Ball, Justin Billing, Caitlin McCluskey, Pam Pham, Owen Pittman, Sean Lawson, et al. Australian Energy Update 2018. Canberra: Department of the Environment and Energy; 2018.
[61] Allison Ball, Shamim Ahmad, Caitlin McCluskey, Pam Pham, Inja Ahn, Lauren Dawson, et al. Australian Energy Update 2016. Canberra: Department of the Environment and Energy; 2016.
[62] Allison Ball, Shamim Ahmad, Caitlin McCluskey, Pam Pham, Owen Pittman, Andrew Starr, et al. Australian Energy Update 2017. Canberra: Department of the Environment and Energy 2017.
[63] El Mogharbel O, Ghali K, Ghaddar N, Abiad MG. Simulation of a localized heating system for broiler brooding to improve energy performance. International Journal of Energy Research. 2014;38:125-38.
[64] Rojano F, Bournet P-E, Hassouna M, Robin P, Kacira M, Choi CY. Modelling heat and mass transfer of a broiler house using computational fluid dynamics. Biosystems Engineering. 2015;136:25-38.
[65] Hamilton J, Negnevitsky M, Wang X. Thermal analysis of a single-storey livestock barn. Advances in Mechanical Engineering. 2016;8.
[66] Natephra W, Yabuki N, Fukuda T. Optimizing the evaluation of building envelope design for thermal performance using a BIM-based overall thermal transfer value calculation. Building and Environment. 2018;136:128-45.
[67] Liang Y, Kidd M, Watkins S, Tabler G. Effect of commercial broiler house retrofit: A 4-year study of live performance. Journal of Applied Poultry Research. 2013;22:211-6.
[68] Liang Y, Tabler GT, Watkins SE, Xin H, Berry IL. Energy use analysis of open-curtain vs. totally enclosed broiler houses in northwest Arkansas. Applied engineering in agriculture. 2009;25:577-84.
[69] Xin H, Berry I, Barton T, Tabler G. Sidewall effects on energy use in broiler houses. Journal of Applied Poultry Research. 1993;2:176-83.
[70] Hachem-Vermette C, MacGregor A. Energy Optimized Envelope for Cold Climate Indoor Agricultural Growing Center. Buildings. 2017;7:59.
[71] Marney A, Kendrick J, Robertson B. Top money-saving practices on Missouri dairy farms. 2015.
[72] Rojano F, Bournet P-E, Hassouna M, Robin P, Kacira M, Choi CY. Computational modelling of thermal and humidity gradients for a naturally ventilated poultry house. Biosystems Engineering. 2016;151:273-85.
[73] Bustamante E, Calvet S, Estellés F, Torres AG, Hospitaler A. Measurement and numerical simulation of single-sided mechanical ventilation in broiler houses. Biosystems Engineering. 2017;160:55-68.
[74] Okonkwo W, Akubuo C. Trombe wall system for poultry brooding. International journal of poultry science. 2007;6:125-30.

[75] Royal Society of Prevention of Cruelty to Animals. RSPCA APPROVED FARMING SCHEME STANDARDS. ACT: Royal Society of Prevention of Cruelty to Animals; 2013.
[76] Dawkins MS, Donnelly CA, Jones TA. Chicken welfare is influenced more by housing conditions than by stocking density. Nature. 2004;427:342.
[77] Bilgili S, Hess J. Placement density influences broiler carcass grade and meat yields. Journal of Applied Poultry Research. 1995;4:384-9.
[78] Feddes J, Emmanuel E, Zuidhoft M. Broiler performance, body weight variance, feed and water intake, and carcass quality at different stocking densities. Poultry Science. 2002;81:774-9.
[79] Vest L, Tyson B. Key factors for poultry house ventilation. Bulletin-Cooperative Extension Service, University of Georgia, College of Agriculture (USA). 1991.
[80] Gurdil GA. Numerical Simulation of Natural Ventilation Rates in Laying Hen Houses. Journal of Animal and Veterinary Advances. 2009;8:624-9.
[81] Geros V, Santamouris M, Tsangrasoulis A, Guarracino G. Experimental evaluation of night ventilation phenomena. Energy and Buildings. 1999;29:141-54.
[82] Kolokotroni M, Aronis A. Cooling-energy reduction in air-conditioned offices by using night ventilation. Applied energy. 1999;63:241-53.
[83] Kolokotroni M, Webb B, Hayes S. Summer cooling with night ventilation for office buildings in moderate climates. Energy and buildings. 1998;27:231-7.
[84] Pfafferott J, Herkel S, Wambsganß M. Design, monitoring and evaluation of a low energy office building with passive cooling by night ventilation. Energy and buildings. 2004;36:455-65.
[85] Seppanen O, Fisk WJ, Faulkner D. Cost benefit analysis of the night-time ventilative cooling in office building. 2003.
[86] Solgi E, Fayaz R, Kari BM. Cooling load reduction in office buildings of hot-arid climate, combining phase change materials and night purge ventilation. Renewable Energy. 2016;85:725-31.
[87] Wang Z, Yi L, Gao F. Night ventilation control strategies in office buildings. Solar Energy. 2009;83:1902-13.
[88] Yang L, Li Y. Cooling load reduction by using thermal mass and night ventilation. energy and buildings. 2008;40:2052-8.
[89] Heijmans N, Wouters P. Pilot study report: Probe, Limelette, Belgium. Principles of Hybrid Ventilation. 2002.
[90] McGahan E, Davis R, Poad G. Quantifying On-Farm Energy Usage in the Australian Meat Chicken Industry. Barton, ACT: Australian Government.; 2014.
[91] Australian Energy Regulator. 2018.
[92] Omer AM. Ground-source heat pumps systems and applications. Renewable and sustainable energy reviews. 2008;12:344-71.
[93] Rees S. Advances in Ground-Source Heat Pump Systems: Woodhead Publishing; 2016.
[94] Colangelo G, Congedo P, Starace G. Horizontal heat exchangers for GSHP. Efficiency and cost investigation for three different applications. ECOS2005 e 18th International conference on efficiency, cost, optimization, simulation and environmental impact of energy systems Norway2005.
[95] Go G-H, Lee S-R, Yoon S, Kim M-J. Optimum design of horizontal ground-coupled heat pump systems using spiral-coil-loop heat exchangers. Applied Energy. 2016;162:330-45.
[96] Tahersima M, Tikalsky P, Revankar R. An experimental study on using a mass radiant floor with geothermal system as thermal battery of the building. Building and Environment. 2018;133:8-18.
[97] Begum S, Ahuja S, Anupoju GR, Kuruti K, Juntupally S, Gandu B, et al. Process intensification with inline pre and post processing mechanism for valorization of poultry litter through high rate biomethanation technology: A full scale experience. Renewable Energy. 2017;114:428-36.
[98] Arshad M, Bano I, Khan N, Shahzad MI, Younus M, Abbas M, et al. Electricity generation from biogas of poultry waste: An assessment of potential and feasibility in Pakistan. Renewable and Sustainable Energy Reviews. 2018;81:1241-6.
[99] Carotenuto A, Figaj RD, Vanoli L. A novel solar-geothermal district heating, cooling and domestic hot water system: Dynamic simulation and energy-economic analysis. Energy. 2017;141:2652-69.

[100] Al-Mohamad A. Global, direct and diffuse solar-radiation in Syria. Applied Energy. 2004;79:191-200.
[101] Monthly Mean Daily Global Solar Exposure. Monthly Mean Daily Global Solar Exposure. 2018.
[102] Fawaz H, Abiad MG, Ghaddar N, Ghali K. Solar-assisted localized ventilation system for poultry brooding. Energy and Buildings. 2014;71:142-54.
[103] Meteotest. Meteonorm Handbook2016.
[104] Bender DA. A dictionary of food and nutrition: OUP Oxford; 2009.
[105] Shannon D, Brown W. A calorimetric estimate of the efficiency of utilisation of dietary energy by the growing cockerel. British poultry science. 1970;11:1-6.
[106] Fuller H, Dale N, Smith C. Comparison of heat production of chickens measured by energy balance and by gaseous exchange. The Journal of nutrition. 1983;113:1403-8.
[107] Australian Chicken Meat Federation (ACMF) Inc. Growing Meat Chickens. 2013.
[108] Australian Chicken Meat Federation (ACMF) Inc. An Industry in Profile. North Sydney2016.
[109] Department of Meteorology. Australian Climate Data. 2018.
[110] Egg J, Howard BC, Bass J, Otte N, Hassman K. Geothermal HVAC. [electronic resource] : green heating and cooling: New York : McGraw-Hill, [2011]; 2011.
[111] Alviss Consulting, Energy Consumers Australia. Analysis of small business retail energy bills in Australia. 2017.
[112] JACOBS, Australian Energy Market Operator. Retail electricity price history and projected trends. Melbourne, Australia: Australian Energy Market Operator; 2017.
[113] Shelton DP, Bodman GR. G95-1244 Ventilation Fans: Efficiency and Maintenance. 1995.
[114] Hollander M, Wolfe DA, Chicken E. Nonparametric statistical methods: John Wiley & Sons; 2013.
[115] Bidarmaghz A, Narsilio GA, Johnston IW, Colls S. The importance of surface air temperature fluctuations on long-term performance of vertical ground heat exchangers. Geomechanics for Energy and the Environment. 2016.
[116] Jensen-Page L, Narsilio GA, Bidarmaghz A, Johnston IW. Investigation of the effect of seasonal variation in ground temperature on thermal response tests. Renewable Energy. 2018;125:609-19.
[117] Beier RA, Holloway WA. Changes in the thermal performance of horizontal boreholes with time. Applied Thermal Engineering. 2015;78:1-8.
[118] Congedo PM, Colangelo G, Starace G. CFD simulations of horizontal ground heat exchangers: A comparison among different configurations. Applied Thermal Engineering. 2012;33-34:24-32.
[119] Esen H, Inalli M, Esen M. Numerical and experimental analysis of a horizontal ground-coupled heat pump system. Building and Environment. 2007;42:1126-34.
[120] Tarnawski VR, Leong WH, Momose T, Hamada Y. Analysis of ground source heat pumps with horizontal ground heat exchangers for northern Japan. Renewable Energy. 2009;34:127-34.
[121] Zhou Y, Asal Bidarmaghz, Guillermo Narsilio, Aye L. Heating and Cooling Loads of a Poultry House in Central Coast, NSW, Australia. World Sustainable Built Environment Conference 2017. Hong Kong 2017.
[122] Bandos TV, Montero Á, Fernández E, Santander JLG, Isidro JM, Pérez J, et al. Finite line-source model for borehole heat exchangers: effect of vertical temperature variations. Geothermics. 2009;38:263-70.
[123] Zeng H, Diao N, Fang Z. A finite line - source model for boreholes in geothermal heat exchangers. Heat Transfer—Asian Research: Co - sponsored by the Society of Chemical Engineers of Japan and the Heat Transfer Division of ASME. 2002;31:558-67.
[124] Philippe M, Bernier M, Marchio D. Validity ranges of three analytical solutions to heat transfer in the vicinity of single boreholes. Geothermics. 2009;38:407-13.
[125] Yuan Y, Cao X, Sun L, Lei B, Yu N. Ground source heat pump system: A review of simulation in China. Renewable and Sustainable Energy Reviews. 2012;16:6814-22.
[126] Webb M, Aye L, Green R. Simulation of a biomimetic façade using TRNSYS. Applied Energy. 2018;213:670-94.

[127] Magnier L, Haghighat F. Multiobjective optimization of building design using TRNSYS simulations, genetic algorithm, and Artificial Neural Network. Building and Environment. 2010;45:739-46.
[128] Safa AA, Fung AS, Kumar R. Performance of two-stage variable capacity air source heat pump: Field performance results and TRNSYS simulation. Energy and Buildings. 2015;94:80-90.
[129] Ruiz-Calvo F, Montagud C, Cazorla-Marín A, Corberán JM. Development and experimental validation of a TRNSYS dynamic tool for design and energy optimization of ground source heat pump systems. Energies. 2017;10:1510.
[130] Chargui R, Sammouda H, Farhat A. Geothermal heat pump in heating mode: modeling and simulation on TRNSYS. International journal of refrigeration. 2012;35:1824-32.
[131] Chargui R, Sammouda H. Modeling of a residential house coupled with a dual source heat pump using TRNSYS software. Energy Conversion and Management. 2014;81:384-99.
[132] Chong CSA, Gan G, Verhoef A, Garcia RG, Vidale PL. Simulation of thermal performance of horizontal slinky-loop heat exchangers for ground source heat pumps. Applied Energy. 2013;104:603-10.
[133] Tarnawski V, Leong W. Computer analysis, design and simulation of horizontal ground heat exchangers. International Journal of Energy Research. 1993;17:467-77.
[134] Kalogirou SA. Applications of artificial neural-networks for energy systems. Applied energy. 2000;67:17-35.
[135] Makasis N, Narsilio GA, Bidarmaghz A. A machine learning approach to energy pile design. Computers and Geotechnics. 2018;97:189-203.
[136] Esen H, Inalli M. Modelling of a vertical ground coupled heat pump system by using artificial neural networks. Expert Systems with Applications. 2009;36:10229-38.
[137] Wang J, Chen Y, Dou C, Gao Y, Zhao Z. Adjustable performance analysis of combined cooling heating and power system integrated with ground source heat pump. Energy. 2018;163:475-89.
[138] Afram A, Janabi-Sharifi F, Fung AS, Raahemifar K. Artificial neural network (ANN) based model predictive control (MPC) and optimization of HVAC systems: A state of the art review and case study of a residential HVAC system. Energy and Buildings. 2017;141:96-113.
[139] Guo Y, Wang J, Chen H, Li G, Liu J, Xu C, et al. Machine learning-based thermal response time ahead energy demand prediction for building heating systems. Applied energy. 2018;221:16-27.
[140] Esen H, Inalli M, Sengur A, Esen M. Predicting performance of a ground-source heat pump system using fuzzy weighted pre-processing-based ANFIS. Building and Environment. 2008;43:2178-87.
[141] Cai B, Liu Y, Fan Q, Zhang Y, Liu Z, Yu S, et al. Multi-source information fusion based fault diagnosis of ground-source heat pump using Bayesian network. Applied Energy. 2014;114:1-9.
[142] Keçebaş A, Yabanova I. Thermal monitoring and optimization of geothermal district heating systems using artificial neural network: A case study. Energy and Buildings. 2012;50:339-46.
[143] Şahin AŞ, Yazıcı H. Thermodynamic evaluation of the Afyon geothermal district heating system by using neural network and neuro-fuzzy. Journal of Volcanology and Geothermal Research. 2012;233:65-71.
[144] Keçebaş A, Yabanova İ, Yumurtacı M. Artificial neural network modeling of geothermal district heating system thought exergy analysis. Energy Conversion and Management. 2012;64:206-12.
[145] Keçebaş A, Alkan MA, Yabanova İ, Yumurtacı M. Energetic and economic evaluations of geothermal district heating systems by using ANN. Energy policy. 2013;56:558-67.
[146] Arat H, Arslan O. Optimization of district heating system aided by geothermal heat pump: A novel multistage with multilevel ANN modelling. Applied Thermal Engineering. 2017;111:608-23.
[147] Xie H, Liu L, Ma F. Performance prediction of ground-water heat pump system using artificial neural networks. 2008 3rd International Conference on Intelligent System and Knowledge Engineering: IEEE; 2008. p. 880-5.
[148] Wang G, Zhang Y, Wang R, Han G. Performance prediction of ground-coupled heat pump system using NNCA-RBF neural networks. 2013 25th Chinese Control and Decision Conference (CCDC): IEEE; 2013. p. 2164-9.

[149] Fannou J-LC, Rousseau C, Lamarche L, Kajl S. Modeling of a direct expansion geothermal heat pump using artificial neural networks. Energy and Buildings. 2014;81:381-90.
[150] Sun W, Hu P, Lei F, Zhu N, Jiang Z. Case study of performance evaluation of ground source heat pump system based on ANN and ANFIS models. Applied Thermal Engineering. 2015;87:586-94.
[151] Benli H. Performance prediction between horizontal and vertical source heat pump systems for greenhouse heating with the use of artificial neural networks. Heat and Mass Transfer. 2016;52:1707-24.
[152] Park SK, Moon HJ, Min KC, Hwang C, Kim S. Application of a multiple linear regression and an artificial neural network model for the heating performance analysis and hourly prediction of a large-scale ground source heat pump system. Energy and Buildings. 2018;165:206-15.
[153] Zhang Y, Zhou L, Hu Z, Yu Z, Hao S, Lei Z, et al. Prediction of layered thermal conductivity using artificial neural network in order to have better design of ground source heat pump system. Energies. 2018;11:1896.
[154] Gang W, Wang J, Wang S. Performance analysis of hybrid ground source heat pump systems based on ANN predictive control. Applied energy. 2014;136:1138-44.
[155] Bassam A, Santoyo E, Andaverde J, Hernández J, Espinoza-Ojeda O. Estimation of static formation temperatures in geothermal wells by using an artificial neural network approach. Computers & Geosciences. 2010;36:1191-9.
[156] Arslan O. Power generation from medium temperature geothermal resources: ANN-based optimization of Kalina cycle system-34. Energy. 2011;36:2528-34.
[157] Morales L, Conde-Gutiérrez R, Hernández J, Huicochea A, Juárez-Romero D, Siqueiros J. Optimization of an absorption heat transformer with two-duplex components using inverse neural network and solved by genetic algorithm. Applied Thermal Engineering. 2015;85:322-33.
[158] Hamdan M, Abdelhafez E, Hamdan A, Haj Khalil R. Heat transfer analysis of a flat-plate solar air collector by using an artificial neural network. Journal of Infrastructure Systems. 2014;22:A4014004.
[159] Qi X, Liu Y, Guo Q, Yu S, Yu J. Performance prediction of a shower cooling tower using wavelet neural network. Applied Thermal Engineering. 2016;108:475-85.
[160] Shojaeefard MH, Zare J, Tabatabaei A, Mohammadbeigi H. Evaluating different types of artificial neural network structures for performance prediction of compact heat exchanger. Neural Computing and Applications. 2017;28:3953-65.
[161] Islam M, Morimoto T. Non-linear autoregressive neural network approach for inside air temperature prediction of a pillar cooler. International journal of green energy. 2017;14:141-9.
[162] Alhamid MI, Saito K. Hot water temperature prediction using a dynamic neural network for absorption chiller application in Indonesia. Sustainable Energy Technologies and Assessments. 2018;30:114-20.
[163] Aghadavoodi E, Shahgholian G. A new practical feed-forward cascade analyze for close loop identification of combustion control loop system through RANFIS and NARX. Applied Thermal Engineering. 2018;133:381-95.
[164] Koschwitz D, Frisch J, van Treeck C. Data-driven heating and cooling load predictions for non-residential buildings based on support vector machine regression and NARX Recurrent Neural Network: A comparative study on district scale. Energy. 2018;165:134-42.
[165] Esen H, Inalli M, Sengur A, Esen M. Forecasting of a ground-coupled heat pump performance using neural networks with statistical data weighting pre-processing. International Journal of Thermal Sciences. 2008;47:431-41.
[166] DOM. Australian Climate Data,. 2018.
[167] Carslaw H, Jaeger J. Conduction of heat in solids: Oxford Science Publications: Oxford, England; 1959.
[168] Larwa B. Heat Transfer Model to Predict Temperature Distribution in the Ground. Energies. 2018;12:1-16.
[169] Wang J, Bras R. Ground heat flux estimated from surface soil temperature. Journal of hydrology. 1999;216:214-26.

[170] Kusuda T, Achenbach PR. Earth temperature and thermal diffusivity at selected stations in the United States. National Bureau of Standards Gaithersburg MD; 1965.
[171] Baggs SA. Remote prediction of ground temperature in Australian soils and mapping its distribution. Solar Energy. 1983;30:351-66.
[172] Lin T, Horne BG, Tino P, Giles CL. Learning long-term dependencies in NARX recurrent neural networks. IEEE Transactions on Neural Networks. 1996;7:1329-38.
[173] Martinez WL, Martinez AR. Computational statistics handbook with MATLAB: Chapman and Hall/CRC; 2015.
[174] Bidarmaghz A. 3D Numerical Modelling of Vertical Ground Heat Exchangers. PhD Thesis the Unversity of Melbourne, Parkville, Vic, Australia. 2015.
[175] Genchi Y, Kikegawa Y, Inaba A. CO 2 payback–time assessment of a regional-scale heating and cooling system using a ground source heat–pump in a high energy–consumption area in Tokyo. Applied Energy. 2002;71:147-60.
[176] Central Intelligence Agency. The World Factbook 2019. Washington, DC: Central Intelligence Agency; 2019.
[177] Australian Government. Dept. of the Enviroment. National Greenhouse Accounts Factors. Australian National Greenhouse Accounts2017.
[178] Kottek M, Grieser J, Beck C, Rudolf B, Rubel F. World map of the Köppen-Geiger climate classification updated. Meteorologische Zeitschrift. 2006;15:259-63.
[179] Singh H. Optimizing delivery of genetic merit in subtropical climates through advanced reproductive technologies. Poultry science. 1999;78:453-8.
[180] Rowlinson P. Adapting livestock production systems to climate change–temperate zones. Livestock and global change. 2008:61-3.
[181] Krauter S, Rüther R. Considerations for the calculation of greenhouse gas reduction by photovoltaic solar energy. Renewable Energy. 2004;29:345-55.
[182] Leckner M, Zmeureanu R. Life cycle cost and energy analysis of a Net Zero Energy House with solar combisystem. Applied Energy. 2011;88:232-41.
[183] Nawaz I, Tiwari G. Embodied energy analysis of photovoltaic (PV) system based on macro-and micro-level. Energy Policy. 2006;34:3144-52.
[184] Department of the Environment and Energy. Powering forward: A better energy future for Australia: Department of the Environment and Energy,; 2017.
[185] Kirk SJ, Dell'Isola AJ. Life cycle costing for design professionals1995.
[186] Magraner T, Montero Á, Quilis S, Urchueguía J. Comparison between design and actual energy performance of a HVAC-ground coupled heat pump system in cooling and heating operation. Energy and buildings. 2010;42:1394-401.
[187] In S, Cho K, Lim B, Lee C. Partial load performance test of residential heat pump system with low-GWP refrigerants. Applied Thermal Engineering. 2015;85:179-87.
[188] Waddicor DA, Fuentes E, Azar M, Salom J. Partial load efficiency degradation of a water-to-water heat pump under fixed set-point control. Applied Thermal Engineering. 2016;106:275-85.
[189] Gueymard CA. Direct and indirect uncertainties in the prediction of tilted irradiance for solar engineering applications. Solar Energy. 2009;83:432-44.
[190] Belda M, Holtanová E, Halenka T, Kalvová J. Climate classification revisited: from Köppen to Trewartha. Climate research. 2014;59:1-13.
[191] Panagiotidou M, Aye L, Rismanchi B. Solar driven water heating systems for medium-rise residential buildings in urban mediterranean areas. Renewable Energy. 2020;147:556-69.
[192] Peel MC, Finlayson BL, McMahon TA. Updated world map of the Köppen-Geiger climate classification. Hydrology and earth system sciences discussions. 2007;4:439-73.

# Appendix A Original publications

## A.1 Conference paper related to chapter 4

This appendix contains the author-accepted manuscript of conference paper of Proceedings of World Sustainable Built Environment Conference 2017 related to chapter 4. The published manuscript is:

Zhou Y, Bidarmaghz A, Narsilio G, Aye L (2017), Heating and Cooling Loads of a Poultry House in Central Coast, NSW, Australia, Proceedings of World Sustainable Built Environment Conference 2017, ISBN 978-988-77943-0-1; pp. 2127-2133, 5-7 June 2017, Hong Kong, China

# Heating and Cooling Loads of a Poultry Shed in Central Coast, NSW, Australia


## ABSTRACT

Space heating and cooling comprises 40% of the global final energy use. With more energy efficient technologies in heating and cooling, up to 10% of global energy consumption could be saved. In agriculture, poultry sheds are used to shelter poultry (broilers and layers) for the production of meat and eggs, sources of animal protein for most people. The range of acceptable indoor air temperature for poultry sheds is 15°C to 25°C for mature birds, and higher temperatures are required for young birds depending on the stage of growth. It is recognised that the costs of heating, cooling and ventilating poultry sheds constitutes a significant portion of the chicken farm operating costs. Various aspects can be considered to reduce these costs considerably. The potential improvements include better thermal performance of building envelopes, energy efficiency of HVAC systems and operational schedules or timing of the production cycle. This paper aims to reduce the cooling and heating energy consumption by identifying the most suitable operational plan. The heating and cooling demand cycles of a poultry shed in the Central Coast region has been investigated in detail by using building energy simulation software tools. This paper reveals that the operational schedule (i.e. begin dates of the cycles of production) has profound influence on energy consumption. The optimised operational schedule can save an average of 12% of overall energy expenditure and 20% on heating.



*Keywords: Building energy simulation; Energy use; Poultry shed.*


## 1. INTRODUCTION

The global annual energy consumption is about 13,000 Mtoe (~544 EJ) [1], resulting in nearly 50 Gt $CO_2$-e Greenhouse Gas (GHG) emissions. It is widely accepted that our future energy sources could not highly rely on fossil fuel such as oil and gas since these resources are finite, and more importantly the majority of GHG emission (65%) comes from them [2]. To provide our next generations with a sustainable energy future, alternative approaches must be adopted as soon as possible.

Space heating and cooling comprises a significant part (40%-50%) of the overall final energy use [3], resulting in 20 Gt $CO_2$-e GHG emissions. By using advanced technologies for space heating and cooling, up to 1,509 Mtoe of global annual energy consumption could be reduced by 2050 [4]. In order to develop sustainable buildings and improve energy efficiency in existing buildings, several approaches can be considered, which include improving the thermal performance of the building envelope, increasing the energy efficiency of HVAC system and determining the most suitable operational schedule.

The agriculture sector constitutes a significant part of Australia's economy. In year 2014/15; the overall sector was worth $51 billion, comprising 3% of Australia's total gross domestic product (GDP) [5]. However, when considering all the add-on processing industries, the overall contribution of the agriculture sector rises to 12% of the GDP [6]. Among these industries, nearly 600 million chickens are raised every year for producing meat [7] and a typical shed provides about 200,000 chickens annually, which means there are currently around 3,000 poultry sheds for chicken meat production in Australia. The overall costs of heating and cooling for chicken farms are estimated to be $80 million per year.

To raise chicken/broiler efficiently, poultry sheds are designed to meet the specific requirement for chickens during different growth stages. The indoor temperature is a vital factor for the chicken to grow properly in an effective timeframe. Within each growing cycle, the indoor air temperature requirement changes from 33°C at the beginning to 21°C in the end, which results in a unique heating/cooling load cycle depending on the start date. Since outdoor air temperature changes throughout the year, a considerable amount of energy is sometimes needed to maintain the required indoor air temperature (i.e. to reach 33°C in winter).

Researchers have conducted building simulations for poultry sheds for heating/cooling load cycles in recent years. Kharseh and Nordell (2011) estimated the heating and cooling loads for a typical poultry shed in Syria in order to design a geothermal cooling and heating system for the shed [8]. However, the assumption made for the chicken is not enough to describe the heat generation due to the growth of chicken, which may result in an inaccuracy of the heating and cooling loads. El Mogharbel et al. (2014) developed a 3D computational simulation model for the heating system of a poultry shed in East Lebanon, with various factors taken into consideration [9]. However, this model is based on the solar assisted heating system only. At the same time, no annual data and cooling loads has been reported. Rojano et al. (2015) developed a 3D model using a CFD commercial software package, Fluent [10]. In their study, the heat and mass transfer within a poultry shed in the US is analysed in detail. However, the aim of their work is to analyse temperature, humidity and air quality in the shed. Hence, no heating and cooling loads were reported. Besides, owing to the complexity of this 3D model computational time is long, thus a detailed model for annual heating and cooling loads is unlikely to be feasible. Hamilton et al. (2016) developed a thermodynamic model for the thermal analysis of a poultry shed in Australia [11]. This model contributes to a theoretical analysis of chicken growth, heat generation, and water consumption during the cycle. Validation based on measured data was also made on the model. However, no models were derived in this article and there were no direct data for heating and cooling loads. From the review of the literature, it follows that limited knowledge is available to derived sheds load cycles, particularly of local settings.

Due to the different agricultural standards encountered among countries (i.e. construction materials, operational schedules) and the various climate conditions of the poultry sheds, it is essential to analyse the heating/cooling demands for local conditions, in the case presented herein, for Australia. The aim of this paper is to estimate the heating/cooling load for a specific poultry shed in NSW, Australia, as representative of current practice in the area. The estimated costs base on the current HVAC system is also reported. An optimisation of growing cycle start date for the minimum cost is investigated.

## 2. BUILDING SIMULATION MODELS

EnergyPlus is widely used for building energy performance simulations. In this paper, an EnergyPlus model was developed for a poultry shed in Central Coast, NSW. Other details of the methodology employed are included in this section.

### 2.1. Simulation Parameters

The poultry shed investigated in this investigation is located in the Central Coast Region, NSW, Australia (approximately at 33°23'49"S and 150°24'09"E). Climate data are essential for the building simulation. A typical meteorological year (TMY) data generated by an algorithm based on 20 years of recorded dataset is widely used to predict the long term performance of buildings. In this paper, the TMY file generated by Meteonorm 7.1 based on recorded climate data from 1990-2010 is utilised. An average error of 6% in year sum comparing with the actual climate can be expected by using this method of hourly data generation [12].

Table 8: Poultry Shed Simulation Parameters

| Time/Days | Weight/kg | Metabolic Weight/w | Power/W | Population of Chicken | Size of Shed | Required Temperatue/°C |
|---|---|---|---|---|---|---|
| 1 | 0.04 | 0.09 | 0.68 | 40,000 | Small | 33.0 |
| 7 | 0.16 | 0.25 | 1.82 | 40,000 | Small | 30.7 |
| 14 | 0.42 | 0.52 | 3.82 | 40,000 | Small | 27.5 |
| 21 | 0.84 | 0.88 | 6.43 | 40,000 | Large | 24.8 |
| 28 | 1.39 | 1.28 | 9.36 | 40,000 | Large | 22.0 |
| 35 | 1.97 | 1.66 | 12.13 | 40,000 | Large | 21.0 |
| 42 | 2.43 | 1.95 | 14.21 | 30,000 | Large | 21.0 |
| 49 | 2.74 | 2.13 | 15.55 | 20,000 | Large | 21.0 |
| 56 | 2.90 | 2.22 | 16.23 | 10,000 | Large | 21.0 |

As shown in Table 1, there are two building models to meet the different space requirements as chickens grow. The small area within the shed is for the first three weeks of growth with dimensions of 18x18x3 $m^3$. Later, the bigger chickens are redistributed into a larger space within the shed, with dimensions of 18x160x3 $m^3$. The building is constructed with 75 mm 'Coolroom' walls (thickness: 0.075m, thermal conductivity: 0.039 W $m^{-1}{\cdot}K^{-1}$, density: 16 kg $m^{-3}$, specific heat: 340 J $kg^{-1}{\cdot}K^{-1}$) with no windows. A chicken usually attains 2.8 to 3 kg at the age of 8 weeks. The mass of chicken for the first 35 days is provided by our industry partner (Ground Source Systems Pty Ltd) while the following 21 days data is generated through a quadratic function. Heat produced by a living creature is proportional to the metabolic weight, which is the unit of 0.75 power of kg [13]. The heat rate generated by an adult chicken is 160 kcal $d^{-1}$ $w^{-1}$ (7.75 W $w^{-1}$) [14, 15].

### 2.2. Operational Schedules

In Australia, it usually takes about 55 to 60 days for a recently hatched chicken to develop fully for the market. Meat broilers reach the mass of harvest at the age of 5 weeks, and partial harvest of chicken happens up to four times in one batch on a chicken farm due to the different demand for light and heavy chicken meat. After that, there are 5 to 14 days for clean-up and preparation for the next batch [16]. The simulation in this paper is based on the operational schedule shown in Table 1.

As shown in Table 1, during the first 21 days, chicks are kept in a small area with controlled temperature inside the shed to save energy. At the 22nd day of each batch, the shed is expanded to the full area. At the 35th day, the average mass of a chicken reaches about 2 kg, meeting the requirement for the market. The first harvest happens in the midnight of the 35th day, when one-fourth of the overall population, which is 10,000 chickens, are taken away. Later, in every following week chickens are taken away at different stages in order to suit the demand of the market. The partial harvesting significantly decreases the internal heat gain, hence influencing the heating and cooling loads. The final harvest happens at the end of the eighth week, followed by two weeks of clean-up and preparation for the next batch.

## 3. HEATING/COOLING LOADS AND COSTS ESTIMATION

By utilising 'Ideal Air Load' option in EnergyPlus, the hourly heating and cooling loads were estimated. The algorithm applied is the third order backward difference method [17]. Estimation of costs based on the current HVAC system has also been conducted.

### 3.1. Heating and Cooling Loads for Different Starting Dates

In order to determine the heating and cooling loads for the different starting dates, 52 batches starting at different weeks for one year were investigated. The first week starts at 3rd of January, the first working day in a year in Australia. As an example, Figure 1 and Figure 2 describe a typical eight-week batch starting at the 19th of December. The indoor temperature requirement is set every day to meet the temperature requirement for raising broilers. During this batch, the heating load decreases as a result of increasing heat generated by the chickens. After that growth stage, the cooling load significantly increases during the following first five weeks. After each harvest, the internal gain (heat produced by chicken) reduces, which results in a reduction of cooling loads.

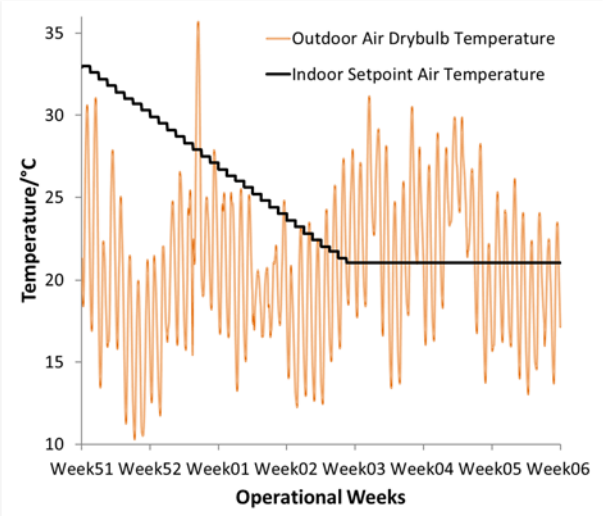


Figure 15: Indoor and Outdoor Air Temperature

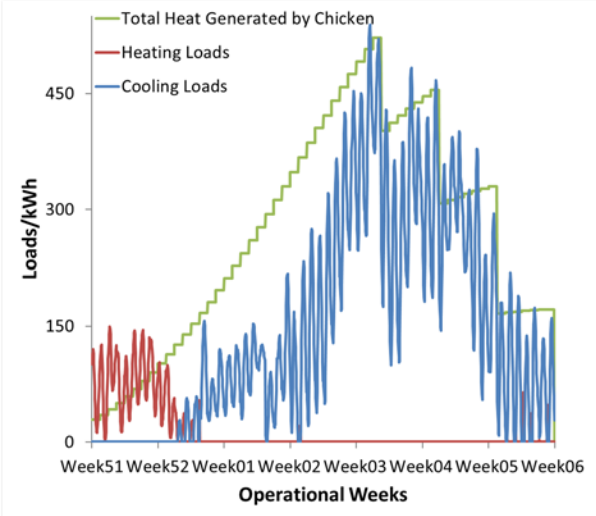


Figure 2: Hourly Heating and Cooling Loads

After hourly heating and cooling loads for 52 starting weeks were acquired, the overall energy consumption for each batch was obtained by summing up the heating and cooling loads. As shown in Figure 3, at the beginning of the year (summer), raising a batch requires much more cooling than heating (nearly eight times higher). Later, as the outdoor air gets

colder, the heating loads increase while the cooling loads decrease. At the middle of July (winter), the heating load reach the peak (105,108 kWh) for one batch, while the minimum cooling load, 23,366 kWh, appears in the 24th week. After the coldest periods of the winter, the heating load begins to reduce together with the boost of cooling demand. The highest cooling demand happens at the end of the year, corresponding to the minimum heating demand of only 11,575 kWh for one batch.

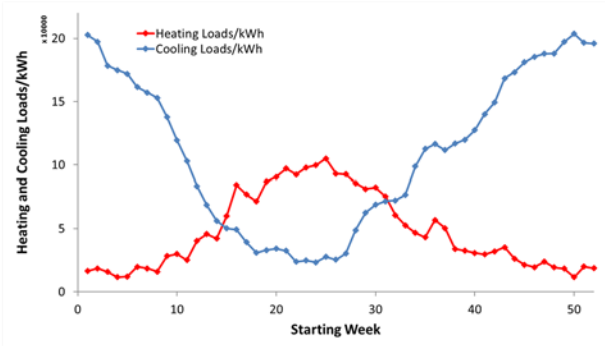


Figure 3: Loads for Different Starting Weeks

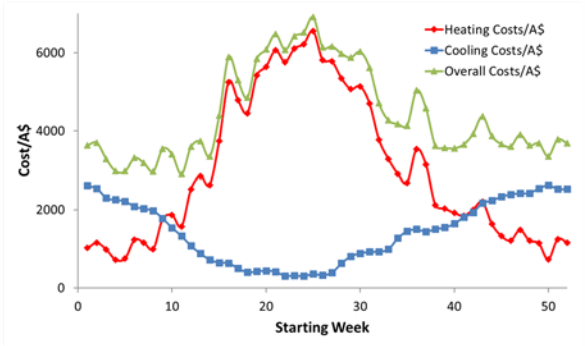


Figure 4: Costs for Different Starting Weeks

## 3.2. Estimation of Costs

Chicken sheds are typically equipped with gas heaters for heating and evaporative coolers for cooling in NSW. The gas heaters were assumed to have an efficiency of 0.85. It was hard to determine the operating efficiency of evaporative coolers because their performance highly relies on the relative humidity and ambient air temperature. However, it is known that evaporative cooling usually saves around 75% of the cost compared with standard air conditioning [18]. This paper assumed one-fourth of the cost of air conditioners with COP of 2.5 as estimation. The prices of energy applied for the analysis are 12.9 c/kWh for electricity and 5.3 c/kWh for gas [19].

Figure 4 shows the heating and cooling costs for the different starting week. Corresponding to the loads, the heating cost rises from AU$ 722 to more than AU$ 6,500 in the mid-year while the cooling cost reduces from AU$ 2,614 to AU$ 301. After winter, the heating cost decreases and the cooling cost increases. Since the evaporative cooler is cheaper to operate, the cooling cost is much less than heating in the year total, despite the nearly doubled cooling load's peak. The results also show that raising a batch in winter costs much more than in summer. The most cost-effective period for starting a batch is from late September to early April.

# 4. OPERATIONAL OPTIMISATION

As fully-grown chickens generate large amounts of heat, i.e. 40,000 chickens in a shed could generate heat up to 600 kW, raising a batch in summer consumes a large amount of energy for cooling. In winter, due to the low outdoor temperature and the relatively high initial temperature requirement (33°C on the first day), the heating loads could also be large. By avoiding raising chicks in the coldest time of winter as well as adult chickens during the hottest weather in summer, a suitable yearly operational schedule reduces the heating loads in winter and the cooling loads in summer.

A typical batch takes eight weeks duration. It is almost impossible for a shed to run six whole batches in one year due to the time required for cleaning and preparation. In this paper, five batches were considered for one year. Assuming a minimum break of one week for cleaning and preparation, the possible intervals between each batch are one to six weeks. Assuming at least a one week break between the last batch and the first one, there are overall 3,248 possible operating schedules. In this paper, the costs of all of the 3,248 possible schedules have been estimated using a Matlab code developed.

Figure 5 shows that the annual costs for all operating schedules resemble the normal distribution pattern, with an average of AU$ 22,126 and the standard variations of AU$ 852, which is calculated with the Maximum Likelihood Estimation (MLE). MLE is a method that estimates parameters of statistical models based on given data. The distribution has also passed the Kolmogorov-Smirnov test in Matlab, a hypothesis test for normal distribution, at a 1% significance level [20].

In statistics, for the normal distribution, the three standard deviation (sigma) rule treats the values within the region of the distance of three times of the standard deviation to the mathematical expectation as a practical certainty. By starting at 5$^{th}$, 14$^{th}$, 28$^{th}$, 39$^{th}$ and 48$^{th}$ week of the year, the most economical schedule costs only AU$ 19,514, which is out of the three-sigma region (AU$ 19,570 to AU$ 24,681). This result reveals the significance of the optimisation because it is improbable for a farmer to operate the chicken shed with the minimum cost if the optimised schedule identified is applied.

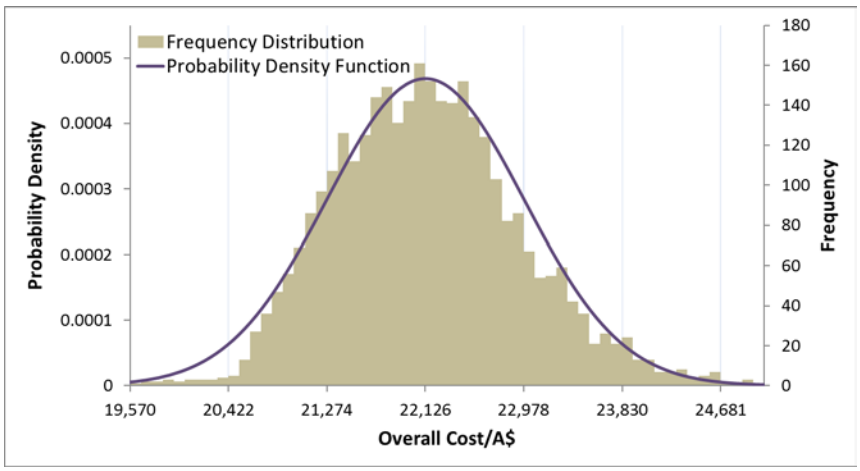


Figure 5: Costs Distribution for all Operating Schedules

More specifically, the optimised schedule costs are AU$ 11,972 for heating and AU$ 7,542 for cooling. Although the cooling cost is 5.5% higher than average, this schedule nevertheless consumes 11.8% lower than the overall average and saves more than 20% on heating. Since gas heaters produce GHG emissions, adopting this schedule would also reduce the GHG emissions. For the typical poultry shed investigated, approximately 10 t $CO_2$-e would be reduced annually, equivalent to the removal of two cars or the planting of more than 600 trees per year [21].

## 5. CONCLUSIONS

This paper investigated the heating and cooling load cycles of a typical poultry shed in Central Coast Region, NSW, Australia by using EnergyPlus simulation engine. The

simulations considered the chicken growth rate and metabolic heat generation, operating schedules, building envelop materials, orientation and climate conditions.

The two vital factors that influence the energy consumptions for heating and cooling the chicken shed are internal gains from the metabolic heat of chickens and the climate conditions. The energy consumption could be reduced by changing the operating schedules. By evaluating the heating/cooling load profiles for batches starting at 52 different weeks throughout a year, the relationship between energy consumption and operating schedule has been discussed. The results reveal that the period from late September to early April is the most economical time for starting a batch.

Considering the estimated cost based on the current HVAC system, an operational optimisation for the minimum cost is suggested. The results show that operational optimisation would significantly reduce the heating/cooling loads as well as the costs for heating and cooling. By applying the lowest cost schedule, on average 20% of the heating cost and 12% in total cost could be saved.

## ACKNOWLEDGEMENTS

The authors would like to thank Mr. Brad Donovan from Ground Source Systems Pty Ltd and Mr. Brad Brown for kindly providing information regarding the poultry house.

## REFERENCES

[1] International Energy Agency,2015, *KeyWord Statistics 2015*. International Energy Agency, 31-35 rue de la Fédération, 75739 Paris Cedex 15 France.
[2] Pachauri, R.K., et al.,2014, *Climate change 2014: synthesis Report. Contribution of working groups I, II and III to the fifth assessment report of the intergovernmental panel on climate change*. IPCC.
[3] IEA,2007. *Renewables for Heating and Cooling.*
[4] IEA,2011. *Technology Roadmap Energy-efficient Buildings: Heating and Cooling Equipment.*
[5] National Famer's Federation,2016. *NFF Annual Review 2014-15.*
[6] NFF,2012. *Farm Facts.*
[7] Australian Bureau of Statistics,2016. *7215.0 - Livestock Products, Australia, March 2016.*
[8] Kharseh, M. and B. Nordell,2011. *Sustainable heating and cooling systems for agriculture.* International Journal of Energy Research, **35**(5): p. 415-422.
[9] El Mogharbel, O., K. Ghali, N. Ghaddar, and M.G. Abiad,2014. *Simulation of a localized heating system for broiler brooding to improve energy performance.* International Journal of Energy Research, **38**(1): p. 125-138.
[10] Rojano, F., P.-E. Bournet, M. Hassouna, P. Robin, M. Kacira, and C.Y. Choi,2015. *Modelling heat and mass transfer of a broiler house using computational fluid dynamics.* Biosystems Engineering, **136**: p. 25-38.
[11] Hamilton, J., M. Negnevitsky, and X. Wang,2016. *Thermal analysis of a single-storey livestock barn.* Advances in Mechanical Engineering, **8**(4).
[12] Meteotest,2016. *Meteonorm Handbook.*
[13] Bender, D.A.,2009, *A dictionary of food and nutrition*. OUP Oxford.
[14] Shannon, D. and W. Brown,1970. *A calorimetric estimate of the efficiency of utilisation of dietary energy by the growing cockerel.* British poultry science, **11**(1): p. 1-6.
[15] Fuller, H., N. Dale, and C. Smith,1983. *Comparison of heat production of chickens measured by energy balance and by gaseous exchange.* The Journal of nutrition, **113**(7): p. 1403-1408.
[16] Australian Chicken Meat Federation (ACMF),2013. *Growing Meat Chickens.*
[17] U.S. Dept. of Energy,2016. *Energyplus Engineering Reference.*

[18] Egg, J., B.C. Howard, J. Bass, N. Otte, and K. Hassman,2011, *Geothermal HVAC. [electronic resource] : green heating and cooling*. McGraw-Hill's AccessEngineering. New York : McGraw-Hill, [2011].
[19] Ison, N., J. Rutovitz, and S. Harris,2011. *NSW Business Energy Prices To 2020.* Sidney, Australia: Institute for Sustainable Futures, University of Technology, Sydney prepared for the NSW Office of Environment and Heritage.
[20] Hollander, M., D.A. Wolfe, and E. Chicken,2013, *Nonparametric statistical methods*. John Wiley & Sons.
[21] Australian Government. Dept. of the Enviroment,2015, *National Greenhouse Accounts Factors*, in *Australian National Greenhouse Accounts*.

## A.2 Conference paper related to chapter 5

This appendix contains the author-accepted manuscript of conference paper of Proceedings of XVI Panamerican Conference on Soil Mechanics and Geotechnical Engineering related to chapter 5. The published manuscript is:

Zhou Y, Narsilio G, Makasis N, Aye L (2019), A machine learning approach for the performance of GSHPs with horizontal ground heat exchangers, XVI Panamerican Conference on Soil Mechanics and Geotechnical Engineering, 17-20 November 2019, Cancún, Mexico

# A machine learning approach for the performance prediction of GCHPs with horizontal ground heat exchangers

Yu ZHOU[a], Guillermo NARSILIO[a,2], Nicolas MAKASIS[a] and Lu AYE[a]
[a] *Department of Infrastructure Engineering, Melbourne School of Engineering, the University of Melbourne, Vic 3010, Australia*

**Abstract.** This study aims to provide a machine learning approach to predict the performance of Ground Coupled Heat Pumps (GCHPs) with horizontal Ground Heat Exchangers (GHEs). Specifically, an ANN model was developed for this purpose which can potentially be generally applied to similar sites at different locations and climate conditions, with even limited types of input data. In this example, a TRNSYS model regarding a typical horizontal trench within a rural farm in Australia, has been developed and verified, covering over 50 different yearly loading patterns under 3 different climate conditions. The simulated performance data is then used to train the artificial neural network. As results, the trained ANN is able to predict the performance of GSHPs systems with identical GHEs even under climatic conditions (and locations) that has not been specifically trained for. With only limited input data, the presented ANN shows no more than 5% error in most cases tested.

**Keywords.** Ground coupled heat pumps, artificial neural networks, performance prediction

[2] Corresponding Author, A/Prof. Guillermo Narsilio, Department of Infrastructure Engineering, the University of Melbourne, Vic 3010, Australia
E-mail: narsilio@unimelb.edu.au

## a) Background & Aim

Ground Coupled Heat Pump (GCHP) systems are a type of highly efficient device which utilizes the ground as the heat source when heating and as the heat sink when cooling. Ground Heat Exchangers (GHEs) are usually applied to transfer the heat between the working fluid and ground. There are many forms of ground heat exchangers, including vertical boreholes, horizontal trenches, energy piles, retaining walls etc. While vertical boreholes are the most common practice, horizontal trenches are cheaper options when land and space permit due to its low construction capital investment [1]. The design of the horizontal GHEs is challenging and time consuming as various factors such as thermal loadings and climate conditions affect the performance. Simulation tools based on phenomenological models have been developed and applied to predict the performance of the GCHPs and GHEs. However, modelling and computing time may be resource intensive and prohibitive for optimization runs of a site-specific case study. Previous studies [2, 3] have identified that Artificial Neural Network (ANN) can reduce the computing time significantly. However, no ANN has yet been available to predict the performance of GCHPs with horizontal GHEs under the rural industries' thermal loading conditions. This investigation aims to provide an ANN to predict the performance of the GCHPs with horizontal GHEs under rural industries' loading condition. The presented ANN is computationally fast and able to deal with limited input data.

## b) Method

A TRNSYS model regarding a typical horizontal trench has been developed and verified. Using this model, over 400,000 hourly performance data have been obtained via simulations, covering over 50 different yearly loading patterns in the rural industry under three different climate zone conditions. The performance data is then used to train the ANN. The ANN network is a feedforward network with an input layer of three neurons, carrying three inputs, i.e. hourly loads, accumulated hourly loads and outdoor ambient air temperature, a hidden layer of 30 neurons and an output layer of a neuron for the COP.

## c) Results and Discussions

As shown in Figure 1, the results from the ANN prediction is reasonably agree well with the simulation results from the TRNSYS model. Apart from the data points when the heat pump is not in operation (when COP is zero), 80.7% of data points fall into the ±5 % error band. The ANN results show a slight under-estimation when the heat pump is at full load condition (i.e. in winter). This means that the ANN developed was not able to estimate the impact of weather conditions on COP extremely well at this stage.

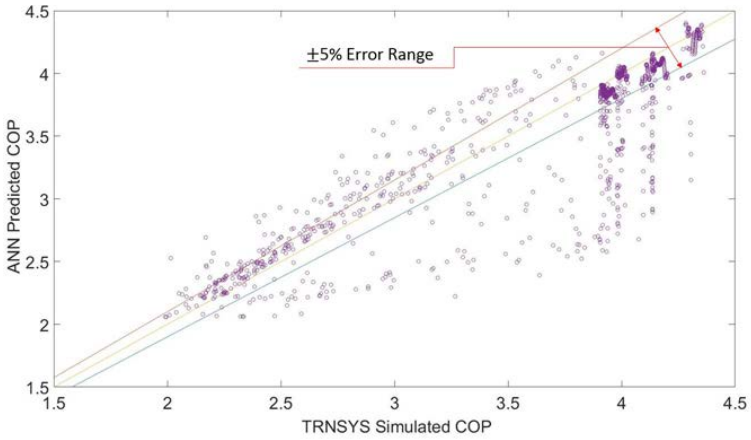


**Figure 1.** Hourly COP from TRNSYS simulations vs ANN predictions

## d) Conclusions

For rural industries' heating load patterns, the ANN developed is able to predict the performance of GCHPs with horizontal ground heat exchangers reasonably well even with limited input data. However, there is a trend that ANN underestimates the COP during winter when the heat pump is under full load.

## References


[1] Zhou, Y., Olga Mikhaylova, Asal Bidarmaghz, Brad Donovan, Guillermo Narsilio, and L. Aye. *Hybrid geothermal-gas and geothermal-solar-gas heating systems for poultry sheds*. in *Zero Energy Mass Custom Home 2018*. 2018. Melbourne.

[2] Kalogirou, S.A.,2000. *Applications of artificial neural-networks for energy systems.* Applied energy, **67**(1-2): p. 17-35.

[3] Makasis, N., G.A. Narsilio, and A. Bidarmaghz,2018. *A machine learning approach to energy pile design*. Computers and Geotechnics, **97**: p. 189-203.

## A.3 Conference paper 1 related to chapter 6

This appendix contains the author-accepted manuscript of conference paper of Proceedings of Building Simulation and Optimisation 2018 related to chapter 6. The published manuscript is:

Zhou Y, Narsilio G, Aye L, Mikhaylova O, Bidarmaghz A, Soga K (2018), Optimisation of a hybrid geothermal-solar-gas system: A case study for a typical poultry shed in New South Wales, Australia, Proceedings of Building Simulation and Optimisation 2018; pp. 358-365, 11-12 September 2018, Cambridge, United Kingdom

# Optimisation of a hybrid geothermal-solar-gas system: A case study for a typical poultry shed in New South Wales, Australia

Yu Zhou[1], Guillermo Narsilio[1], Lu Aye[1], Olga Mikhaylova[2], Asal Bidarmaghz[3], Kenichi Soga[4]
[1]Department of Infrastructure Engineering, The University of Melbourne, Vic 3010, Australia
[2]Golder Associates Pty Ltd, Sydney, Australia
[3]Department of Engineering, University of Cambridge, Cambridge, UK
[4]University of California-Berkeley, Berkeley, CA, USA

## Abstract

Poultry sheds are used to raise poultries (chickens, turkeys and ducks), and have a unique heating and cooling demand pattern. A significant amount of energy is consumed for the heating and cooling of poultry sheds to maintain an indoor air temperature suitable for the growth and comfort of the poultries according to their age. This energy consumption results in a considerably high greenhouse gas (GHG) emissions and energy expenditure for the poultry shed operation. Previous studies have shown that a large amount of operational and lifecycle cost of heating can be reduced with the adoption of hybrid geothermal-solar-gas systems. In addition to the costs, GHG emissions should also be considered when heating equipment is selected. This paper presents an environmental analysis and optimisation for the sizing of components of a hybrid geothermal-solar-gas system for a typical poultry shed located in Peats Ridge, NSW, Australia. The results reveal that up to 100% of the operational emissions and up to 95% of the lifecycle GHG emissions can be reduced if the current gas heating system is replaced by the hybrid geothermal-solar-gas system. By also considering the lifecycle cost, the Pareto front solutions for this hybrid geothermal-solar-gas heating system has been found.

Keywords: Building simulation, poultry sheds, geothermal energy, solar energy.

## Introduction

In Australia, agriculture and the associated processing industry contribute 12% to the national Gross Domestic Product (National Farmer's Federation 2016; NFF 2012). Within the poultry industry, it is estimated that approximately 600 million chickens are raised nationwide (Australian Bureau of Statistics 2016). The scale of this industry results in a significant amount of energy consumption, as well as greenhouse gas (GHG) emissions, primarily for heating and cooling the poultry sheds. An estimation by Zhou et al. (2017) suggested that about A$80 million is spent annually for this purpose and a significant amount of GHG emissions is produced. Since existing cooling systems for chicken sheds can be cost-effective to operate and generate relatively low GHG emissions (for example, if evaporative cooling systems are used), the primary focus of this investigation is on the reduction of costs and GHG emissions for heating poultry sheds.

Network piped natural gas and bottled liquefied petroleum gas (LPG) are the primary energy sources for heating in Australia (Allison Ball et al. 2016). The combustion of these fossil fuels results in a significant amount of GHG emissions (0.186 kg $CO_2$-e per kWh) (Australian Government. Dept. of the Enviroment 2017). Through refurbishment and partial replacement of current heating systems with high-performance equipment that uses renewable and more sustainable energy sources, lifecycle cost and GHG emission reductions could be potentially achieved. Zhou et al. (2018) has illustrated that both hybrid geothermal-gas heating systems and hybrid geothermal-solar-gas heating systems can reduce the operational and lifecycle heating costs significantly. This paper investigates these systems while further considering the environmental aspect as well.

A Ground Coupled Heat Pump (GCHP) system provides low-carbon outcome for space heating and cooling, extracting thermal energy from the ground when operating in heating mode, and rejecting heat into the ground when in cooling mode (Johnston, Narsilio & Colls 2011). If the systems are used for heating, utilising only the ground as the heat source, they are termed Ground Source Heat Pump (GSHP) systems. They comprise a ground heat exchanger (GHE) field (i.e., high density polyethylene (HDPE) pipe embedded into the ground), a heat pump, and a distribution system. GSHP systems have been used for various applications worldwide. They are especially popular in the United States, Canada, Sweden, Austria and China (Lund & Boyd 2016). GSHP systems have also been introduced for the heating of poultry sheds in recent years (Kharseh & Nordell 2011). Some drawbacks of GSHP systems include the high upfront construction costs, typically responsible for the GHEs installation, as well as the embodied energy and associated GHG emissions. However, these can be reduced by coupling GSHPs with other energy sources to form a hybrid system (Eslami-Nejad & Bernier 2011; Kjellsson, Hellström & Perers 2010). For example, gas boilers and gas burners have relatively low installation costs and can be integrated with GSHP systems. To further boost the heating efficiency of GSHP systems, renewable solar thermal systems can also be coupled to form solar-assisted GSHP systems, which will help in the

reduction of GHG emissions. By combining these three sources of thermal energy, lower costs and lower GHG emissions can be achieved (Sarbu & Sebarchievici 2014; Hong & Howarth 2016).

This investigation primarily focuses on environmental benefits of a geothermal-solar-gas hybrid heating system for poultry sheds in Australia. In particular, it discusses optimisation of a hybrid geothermal-solar-gas heating system for a typical chicken shed in Peats Ridge, NSW, Australia. Based on a building energy simulation model of the shed developed in EnergyPlus (Zhou et al. 2018), a 40-year lifecycle analysis, an optimisation of the installed capacities of different components of the geothermal-gas-solar hybrid heating system was performed to minimise the operational GHG emissions of the hybrid system, as well as the lifetime GHG emissions of heating. The expected lifetime of ground heat exchangers is at least 40 years and sheds are typically expected to be utilised for the next 40 years, thus the 40-year lifetime is considered in this study. The two objective functions to be minimised are: the total operational GHG emissions and the lifecycle cost.

## • Heating cycles of a chicken shed

In this investigation, a chicken shed located in Peats Ridge, NSW, Australia was examined to exemplify the optimisation study for temperate climate regions around the world. Details of the EnergyPlus simulation model of this shed can be found in Zhou et al. (2018). The shed has been heated by LPG burners. The energy model developed was calibrated and verified against two-year LPG consumptions provided by the farm owner.

The model estimated that the annual heating energy of the shed is 143,811 kWh with a peak heating power demand of 195 kW. The chicken growing cycles are six times a year, leading to repeated heating cycles within a year. The heating demand is at its maximum at the beginning of each heating cycle, when the least metabolic heat is generated by the chickens and the required indoor temperature is at a maximum. The heating demand decreases later in each cycle due to the increase in metabolic heat generated by the chickens and lower indoor temperature requirement corresponding to the age of the batch (Zhou et al. 2018).

It should be noted that 86% of the time when heating is needed, the peak demand of the shed is lower than 80 kW. This means that if a hybrid heating system with an installed GSHP capacity of about 40% (~80 kW) of the peak heating power demand (195 kW) is used for heating, about 86% of the annual heating energy can still be satisfied by the GSHPs. This illustrates the advantage of a hybrid heating system, as it could satisfy most heating requirements with cost-effective, renewable energy resources and a lower initial capital cost (since a significantly reduced GHE field would be needed). The next section of the paper introduces variations of such hybrid systems.

## • Hybrid geothermal-solar-gas system: efficiency, pricing and embodied emissions

Figure 1 shows the schematic diagram of the hybrid geothermal-solar-gas system under study. The heating is delivered by several identical GSHPs connected in parallel to a main header. Each GSHP is coupled with a series of ground heat exchangers (GHEs). The GSHPs are assisted by Flat Panel Solar Collectors (FPSCs) connected to the GHEs. The FPSCs are designed to complement the heat extracted from the ground, as well as to recharge the ground. Upstream, the GSHPs are connected to a buffer tank to minimise the cycling of heat pump on and off. The existing gas (LPG) burners installed in the shed can top up heating when needed. Solar Photovoltaic (PV) panels offset electricity consumption of the hybrid system, primarily driven by the operation of the GSHPs.

'Shave factor' $S$ is used to describe the capacity portion of the GSHP in the hybrid system. It is defined as the ratio of the installed capacity of the GSHP system to the peak heating demand of the load to be satisfied by the hybrid system (Alavy et al. 2013; Mikhaylova et al. 2016). For example, 0% of the shave factor means a full gas heating system and 100% shave factor means a full geothermal system, noting that the 'solar' components are tied to the GSHPs in this investigation.

$$S = \frac{Installed\ Capacity\ of\ GSHPs}{Peak\ Heating\ Loads} \times 100\% \qquad (1)$$

To perform the optimisation, energy efficiency, price and GHG emissions for each main component of the proposed hybrid system are required. Table 1 presents the system component efficiencies and assumptions used in the optimisation.

*Table 1 Energy Efficiency and Prices of Gas and Electricity for the Systems Investigated*

| | **LPG Burner (G)** | **GSHP (Eg)** | **Hybrid GSHP+FPSC (Eg+S)** | **Hybrid GSHP+FPSC and Solar PV (Es+S)** |
|---|---|---|---|---|
| System energy efficiency, % | 85 | 300* | 320+ | 320 |
| Energy source price, c/kWh | 7 | 10 | 10 | 10 |
| Solar offset, % | Nil | Nil | Nil | 100 |

Notation: G = Gas; Eg = Electricity from grid; Es = Electricity from solar PV; S = Solar (assumed price = Nil); *COP = 3; +COP of GSHP integrated with FPSC = 3.2 (based on Kjellsson et al 2010)

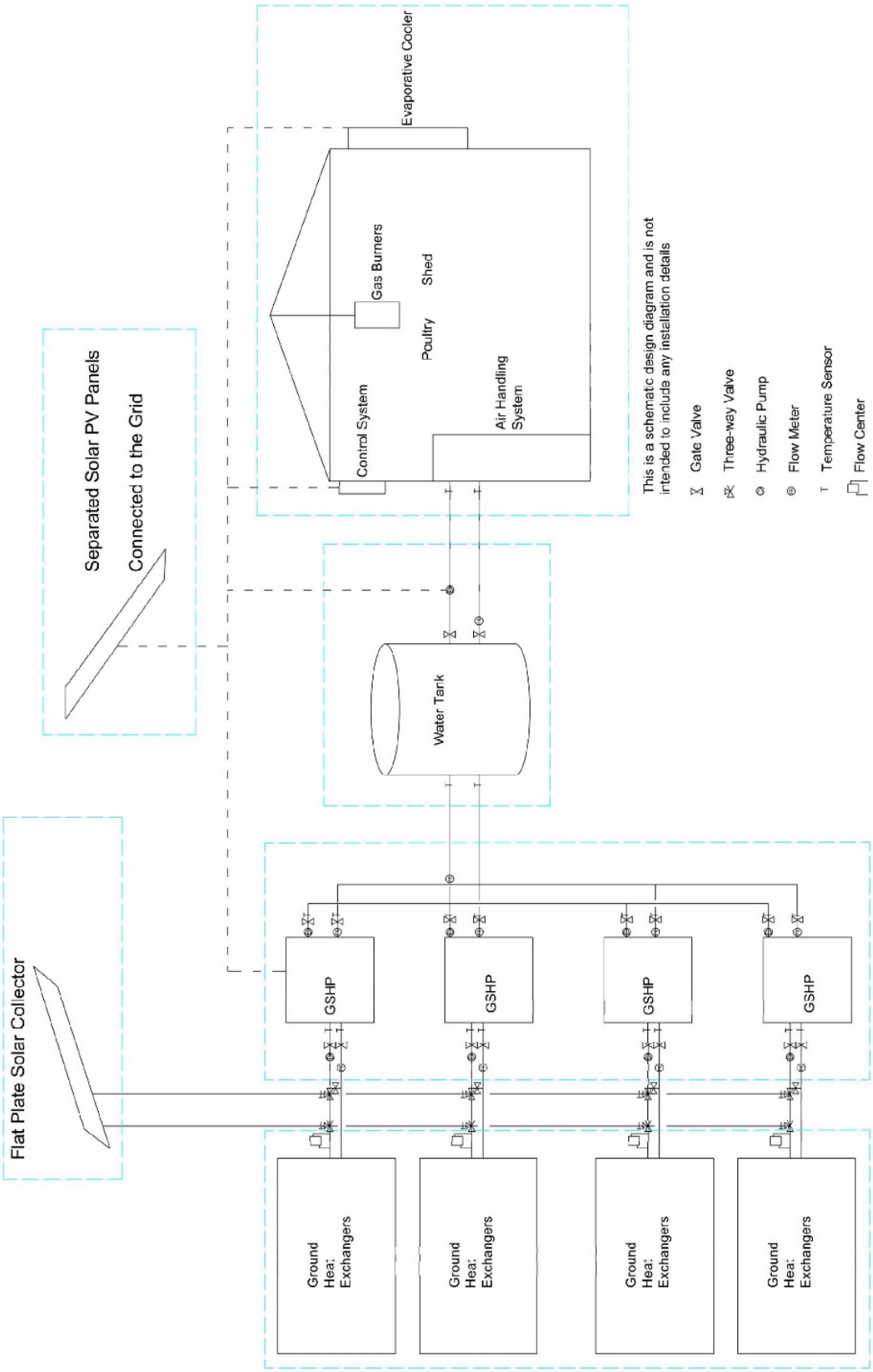


*Figure 1 Schematic Drawing for the Hybrid Geothermal-Solar-Gas System*

The energy prices used in this study were obtained from the current gas and electricity contracts of the farm owner in NSW (note that gas and electricity prices can differ from farm to farm depending on contracts with suppliers, pricing for this farm is particularly competitive). Annual average system energy efficiency of each equipment was assumed based on the equipment currently available on the market in Australia.

It is important to note that for GSHP systems, the energy efficiency is usually expressed via a Coefficient of Performance (COP), which is defined as the ratio of output heat power to the input electric power. To be consistent with the LPG system, whose efficiency is approximately 85%, the performance of GSHP systems are expressed in energy efficiency, where 300% of energy efficiency means a COP of 3.0.

Flat plate solar collectors (FPSCs) are cost-effective solar thermal collectors that utilise solar energy for heating. Previous studies (Eslami-Nejad & Bernier 2011; Kjellsson, Hellström & Perers 2010) confirmed that with the integration of FPSCs, the performance of the GSHPs can be improved at least by between 5% and 10%. In this study, it was assumed that the system heating coefficient of performance (HCOP) of solar-assisted GSHPs increases from 3.0 to 3.2 with the installation of 7.5 $m^2$ of FPSCs per 5 kW of heat pump nominal heating capacity (no FPSC optimisation was undertaken in this investigation). The addition of FPSC reduces the electricity consumption of the overall system by improving the COP of the heat pump.

Solar PV modules convert solar radiation into electricity. In this investigation, it is proposed that solar PV modules are installed to offset grid electricity consumption of the heating system for the shed. The PV array is sized to provide the amount of electricity equivalent to all the electricity used by the hybrid heating system in annual basis (no PV sizing optimisation was undertaken in this investigation). As the shed investigated located in large farm with eight sheds, it was assumed that in during the day, the solar PV provides electricity to all (hybrid and non-hybrid) sheds, and during the night, the electricity from the grid is used. With the utilisation of the solar PV array, the cost of electricity for the shed heating system can be completely offset. It was assumed 1 $kW_p$ installed capacity of solar PV requires 7 $m^2$ of PV panels and generates 3.9 kWh of electricity daily on average in NSW.

Regarding embodied GHG emission of the various components of the hybrid Geothermal-Solar-Gas system, the following information is used.

GSHPs (and associated circulation pumps driving fluid thought the GHEs), consumes electricity for their normal operation. The GHG emission is estimated at 0.83 kg $CO_2$-e per kWh of electricity consumed in NSW (Australian Government Dept. of the Environment 2017). This investigation assumed a reduction in GHG emission factor for electricity generation of 1% per year. This assumption is based on the Australian government's commitment to reduce the GHG emissions by 26 % to 28 % below the 2005 levels, by 2030, which represents about 1 % GHG emission reduction per year (Department of the Environment and Energy (2017)).

In 2017, the GHG emission factor for LPG use in NSW was 0.186 kg $CO_2$-e per kWh of energy consumption (Australian Government Dept. of the Environment 2017). Unlike for electricity, the GHG emissions for LPG is assumed to be constant over time in this investigation.

Regarding the solar components of the hybrid system, the embodied GHG emissions for 1 $m^2$ of FPSC is estimated as 21.28 kg/$m^2$ (Krauter & Rüther 2004; Leckner & Zmeureanu 2011; Nawaz & Tiwari 2006). The calculated initial GHG emissions of FPSC for one kW capacity of the GSHP system is shown in Table 2. The embodied GHG emissions for 1 $m^2$ of solar PV is estimated as 42 kg/$m^2$ (Krauter & Rüther 2004; Leckner & Zmeureanu 2011; Nawaz & Tiwari 2006).

From the information summarised, the initial embodied GHG emissions of Solar PV for one kW capacity of the GSHP system is estimated and shown in Table 2. The information for initial GHG emissions of GSHPs and gas burners are calculated based on a lifecycle analysis undertaken for a typical 10 kW heating system in Australia (Lu 2018).

## • Annual GHG emissions analysis of hybrid heating systems

Annual operational GHG emissions of shed heating by the hybrid system (Geothermal-Solar-Gas) with different shave factors were calculated using the annual heating demand estimated from the verified EnergyPlus model (Zhou et al., 2018) and the assumptions shown in Table 1.

- *Table 2 Initial GHG Emission and Lifetime for Different Components*

.

| | **GSHP Above Ground Components (Including GSHP, water tank, air handling units)** | **GSHP Under Ground Components (Including ground loops, trenching and backfilling)** | **Solar PV** | **FPSC** | **LPG Burner** |
|---|---|---|---|---|---|
| Initial GHG Emission, kg $CO_2$-e per kW GSHP capacity | 67 | 93.8 | 170.9 | 31.9 | 10.2 |
| Lifecycle, years | 20 | 40 | 20 | 20 | 10 |

Figure 2 shows the annual operational energy consumption and GHG emissions of the hybrid geothermal-solar-gas heating system with different shave factors (and for adjusted FPSC and PV panels whose size are tied to the size of the GSHPs), as well as the portions of the heating energy provided by the GSHP system in each sizing combination of the hybrid system. It is apparent from the figure that the maximum and the minimum annual energy investment and GHG emissions are expected when the gas-only and the GSHP-only heating systems are used for the shed, respectively.

Even though there are significant benefits in the reduction of annual operational energy consumption and GHG emissions comparing with original LPG heating system, the construction and installation of the hybrid geothermal-solar-gas system would result in high initial capital cost and GHG emissions. The next section analyses the lifecycle GHG emissions.

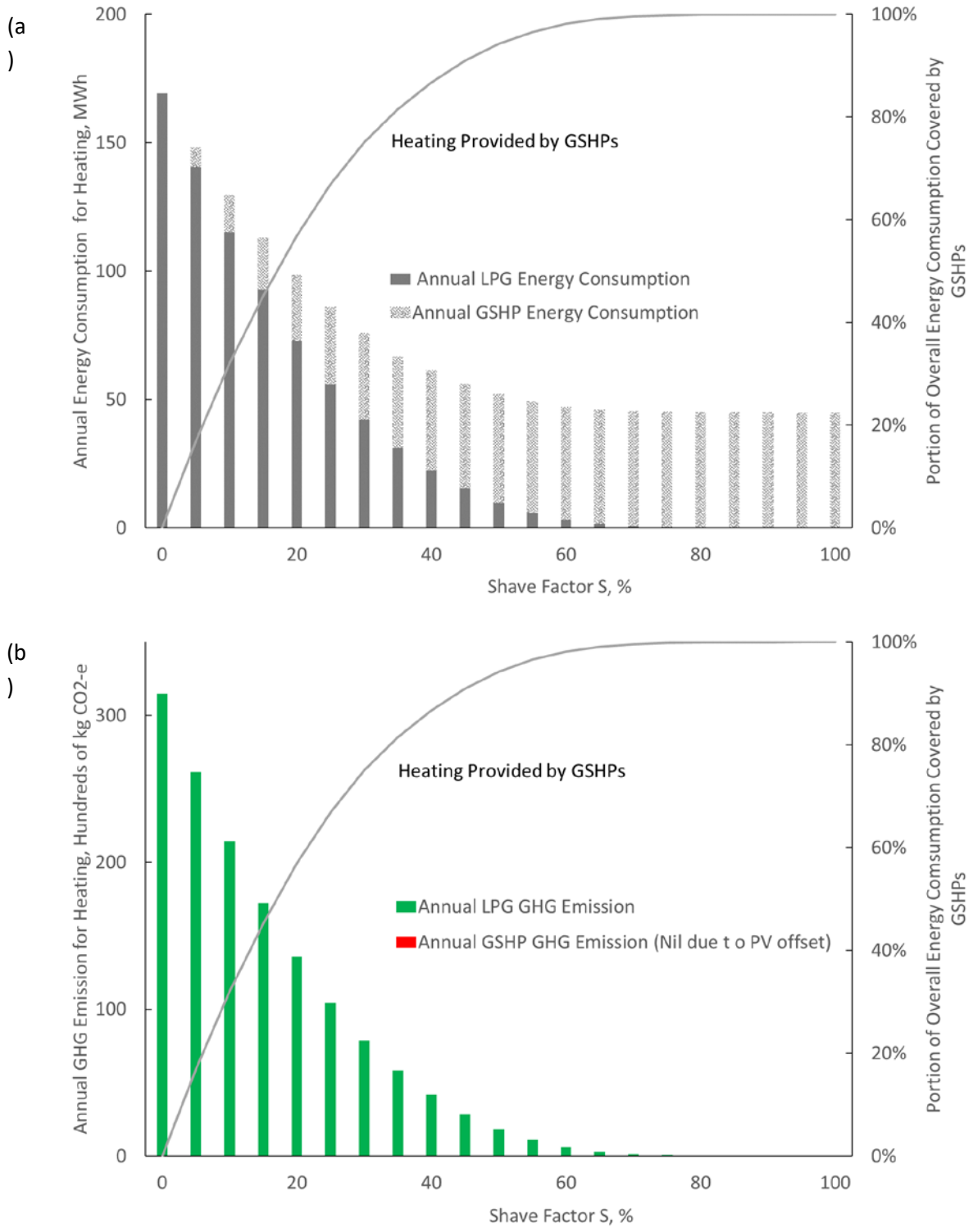


*Figure 2 Hybrid Geothermal-Solar-Gas System: (a) Annual Energy Consumption; and (b) Annual GHG Emission*

- **Analysis for lifecycle GHG emissions of hybrid heating systems**

As the GSHP system, FPSC and Solar PVs have higher embodied GHG emissions comparing to gas heating Figure 3 shows the lifecycle GHG emissions with different shave factors, shown in grams of $CO_2$ equivalent per kWh of heating energy provided. The lifecycle cost shown here is the same one from a previously published study (Zhou et al 2018). It can be seen that the GHG emissions are reduced significantly with an increasing shave factor until it reaches around 75%. Based on a more detailed analysis, the minimum lifecycle GHG emission system, it is important to take them into account by conducting a lifecycle analysis. The lifetime considered in this study is 40 years. The data used in this analysis are shown in Table 1 and Table 2.

(11.38 g $CO_2$-e per kWh) is found to exist at shave factor 73%, which is 95% less than the normalised emissions of that of a gas-only (LPG burners) heating system. However, when considering the design of this system, it is important to take both lifecycle cost and life cycle GHG emissions into account. The next section contains a brief discussion regarding these two objectives.

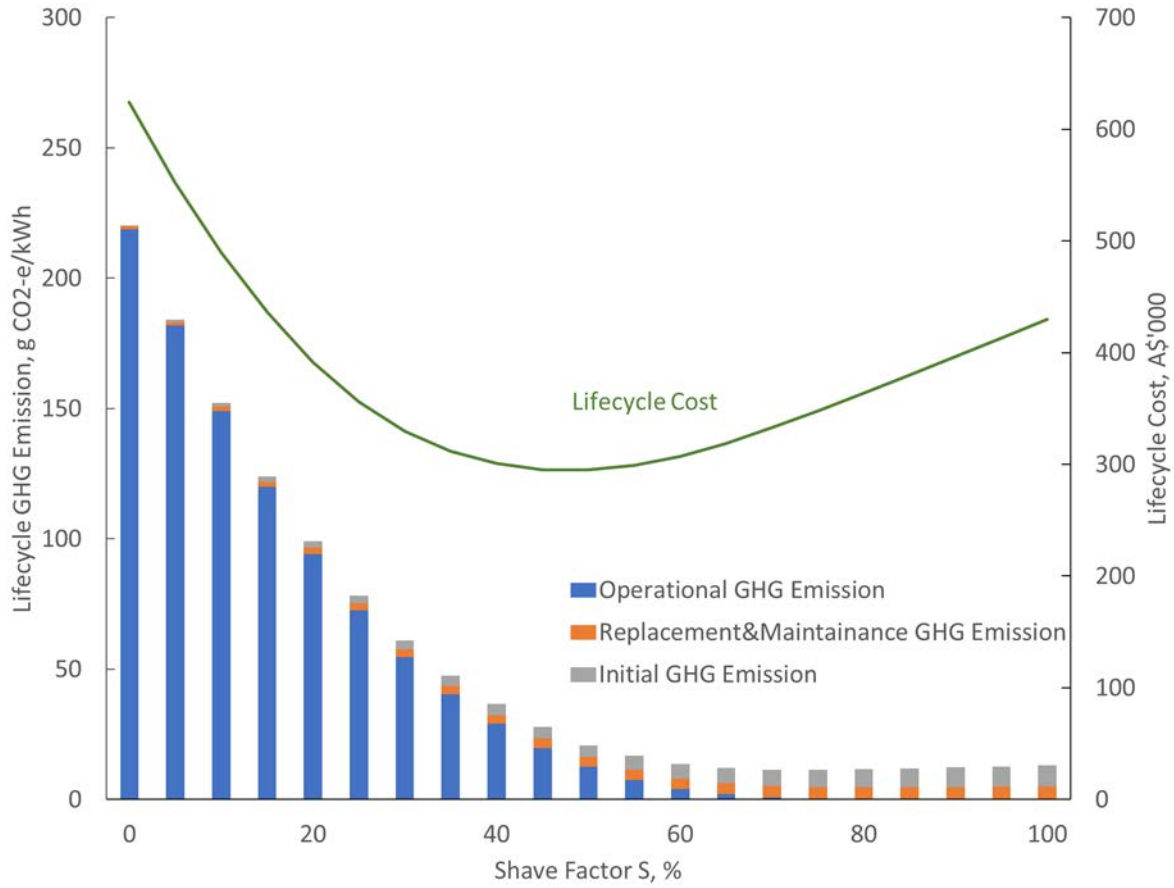


*Figure 3 Lifecycle GHG Emissions and Cost for Hybrid Geothermal-Solar-Gas System*

- **Pareto front solutions and discussion**

By employing an excel macro program, the lifecycle cost and GHG emissions have been calculated for a number of cases where the shave factors varied from 0 % to 100 %. Based on the minimum lifecycle cost approach. The optimum shave factor is found at 48% with a cost of A$294,358 and GHG emission of 23.84 g $CO_2$-e per kWh. On the other hand, based on the minimum lifecycle GHG emission approach, the optimum shave factor is found to be at 73%with a cost of A$342,090 and GHG emission of 11.38 g $CO_2$-e per kWh.

Hence, the design objectives need to be considered throughout the design process as different optimisation point exists for these hybrid design approach. Since the lifecycle cost increases and the GHG emissions decrease between the shave factors of 48% and 73%, there is no way to minimise either of them without the increase of another. As shown in Figure 4, the values corresponding with shave factors from 48% to 73% has Pareto front for this investigation.

At this stage, a trade-off can be made to balance these two objectives, but it is beyond the scope of this investigation. The authors are developing a full scale experimental monitoring facility to validate the results of this investigation.

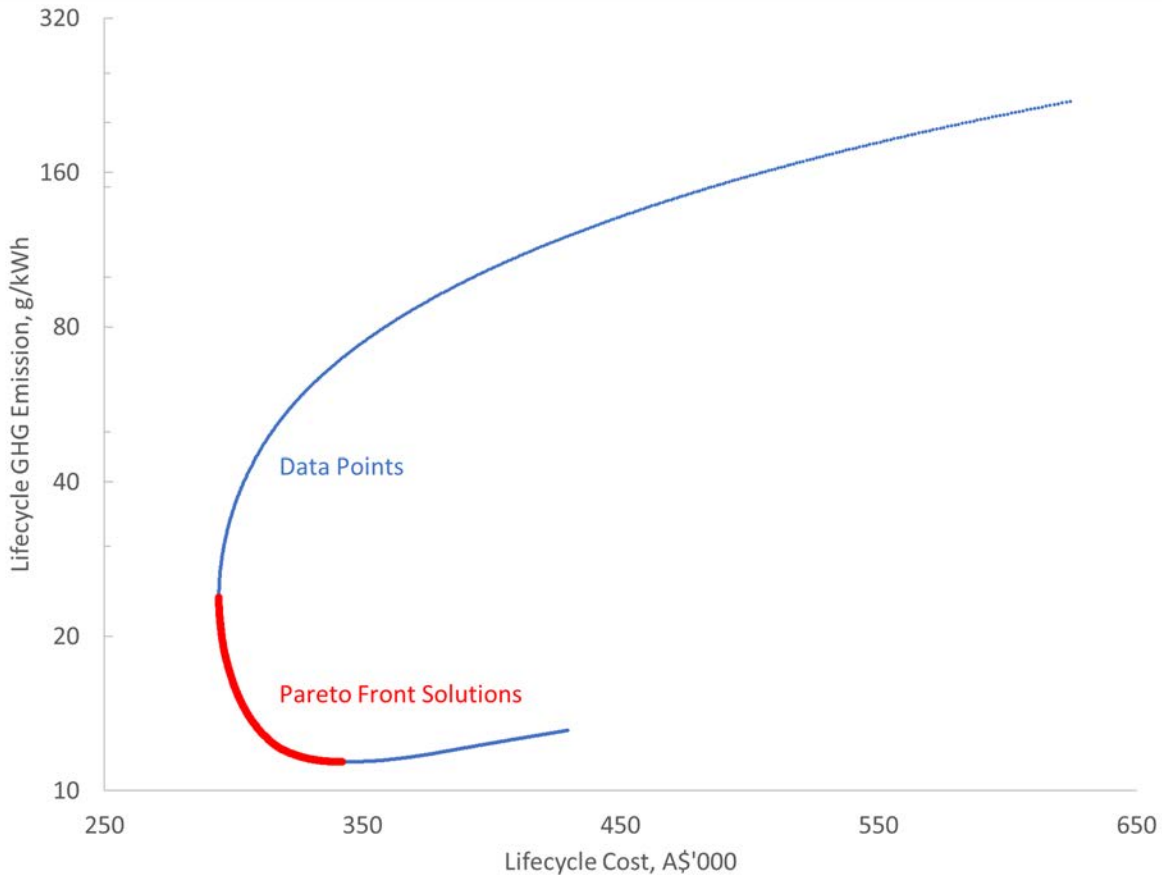


*Figure 4 Pareto Front Solutions of the Optimisation*

## • Conclusions

We investigated the optimisation of a hybrid geothermal-solar-gas system sized for a typical poultry shed located in Peats Ridge, New South Wales, Australia based on forty-year lifecycle GHG emissions and costs. The analysis started with building energy performance simulation model for the poultry shed. This model provided an hourly heating demand for the poultry shed. Based on this verified simulated hourly heating loads, the hybrid heating system with various sizes of components was analysed, through a simplified analysis using shave factors.

The results suggest that a hybrid geothermal-solar-gas system provides advantages in both lifecycle cost and life cycle GHG emissions over the gas only heating system. A significant amount of operational GHG emissions (up to 100%) and lifecycle GHG emissions (up to 95 %) can be reduced, should the current LPG gas system be replaced by a hybrid geothermal-solar-gas system. These energy and GHG emission savings were achieved because of the high energy efficiency of GSHPs and electricity offset by solar PV. Within the solar components of the hybrid system, Solar PVs are more beneficial than FPSCs as the former can fully offset the electricity bills and GHG emissions of the heating, while the later could only improve the performance of GSHPs by 5% to 10%.

With the lifecycle cost analysis from previous studies, a multi-objective optimisation was conducted and the Pareto front (between the shave factor 48% and 73%) for the system is identified. Further analysis requires a trade-off between lifecycle cost and lifecycle GHG emissions. A hybrid heating system is to be installed to supply the heating energy required to the shed and monitor its performance to validate the results of this investigation.

## • Acknowledgement

The authors would like to thank the farm owners for providing the detail information relevant to the chicken shed. The authors would also like to thank the Australian Research Council for the funding of Linkage Project LP160100070 and FT140100227 and industry partners Ground Source Systems Pty Ltd. and Golder Associates Pty Ltd.

## • References

Alavy, M, Nguyen, HV, Leong, WH & Dworkin, SB 2013, 'A methodology and computerized approach for optimizing hybrid ground source heat pump system design', Renewable Energy, vol. 57, pp. 404-12.

Allison Ball, Shamim Ahmad, Caitlin McCluskey, Pam Pham, Inja Ahn, Lauren Dawson, Thuong Nguyen &

Davin Nowakowski 2016, 'Australian energy update', Australian Government Bureau of Resources and Energy Economics, Canberra, October.

Allison Ball, Shamim Ahmad, Caitlin McCluskey, Pam Pham, Owen Pittman, Andrew Starr, Davin Nowakowski & Lambert, N 2017, Australian Energy Update 2017, Department of the Environment and Energy Canberra.

Australian Bureau of Statistics 2016, '7215.0 - Livestock Products, Australia, March 2016'.

Australian Government. Dept. of the Enviroment 2017, National Greenhouse Accounts Factors.

Department of the Environment and Energy 2017, Powering forward: A better energy future for Australia, Department of the Environment and Energy.

Eslami-Nejad, P & Bernier, M 2011, 'Coupling of geothermal heat pumps with thermal solar collectors using double U-tube boreholes with two independent circuits', Applied Thermal Engineering, vol. 31, no. 14, pp. 3066-77.

Hong, B & Howarth, RW 2016, 'Greenhouse gas emissions from domestic hot water: heat pumps compared to most commonly used systems', Energy Science & Engineering, vol. 4, no. 2, pp. 123-33.

Johnston, IW, Narsilio, GA & Colls, S 2011, 'Emerging geothermal energy technologies', KSCE Journal of Civil Engineering, vol. 15, no. 4, pp. 643-53.

Kharseh, M & Nordell, B 2011, 'Sustainable heating and cooling systems for agriculture', International Journal of Energy Research, vol. 35, no. 5, pp. 415-22.

Kjellsson, E, Hellström, G & Perers, B 2010, 'Optimization of systems with the combination of ground-source heat pump and solar collectors in dwellings', Energy, vol. 35, no. 6, pp. 2667-73.

Krauter, S & Rüther, R 2004, 'Considerations for the calculation of greenhouse gas reduction by photovoltaic solar energy', Renewable Energy, vol. 29, no. 3, pp. 345-55.

Leckner, M & Zmeureanu, R 2011, 'Life cycle cost and energy analysis of a Net Zero Energy House with solar combisystem', Applied Energy, vol. 88, no. 1, pp. 232-41.

Lund, JW & Boyd, TL 2016, 'Direct utilization of geothermal energy 2015 worldwide review', Geothermics, vol. 60, pp. 66-93.

Mikhaylova, O, R. Choudhary, K. Soga & Johnston, IW 2016, 'Benefits and optimisation of district hybrid ground source heat pump systems', Energy Geotechnics, pp. 535-41.

National Farmer's Federation 2016, 'NFF Annual Review 2014-15'.

Nawaz, I & Tiwari, G 2006, 'Embodied energy analysis of photovoltaic (PV) system based on macro-and micro-level', Energy Policy, vol. 34, no. 17, pp. 3144-52.

Natioanl Farmer’s Fact 2012, 'Farm Facts', The National Farmers' Federation (NFF), Canberra, Australia.

Qi Lu 2018, 'Shallow geothermal system: Feasibility and design practices in Melbourne, Australia (Unpublished PhD Thesis)', The University of Melbourne.

Sarbu, I & Sebarchievici, C 2014, 'General review of ground-source heat pump systems for heating and cooling of buildings', Energy and Buildings, vol. 70, pp. 441-54.

Zhou, Y, Asal Bidarmaghz, Guillermo Narsilio & Aye, L 2017, ‘Heating and cooling loads of a poultry house in Central Coast, NSW, Australia’, paper presented at World Sustainable Built Environment Conference 2017, Hong Kong, pp. 2127-32.

Zhou, Y, Olga Mikhaylova, Asal Bidarmaghz, Brad Donovan, Guillermo Narsilio & Aye, L 2018, 'Hybrid geothermal-gas and geothermal-solar-gas heating systems for poultry sheds', paper presented at Zero Energy Mass Custom Home (ZEMCH) 2018 conference, Melbourne, pp. 545-56.

## A.4 Conference paper 2 related to chapter 6

This appendix contains the author-accepted manuscript of conference paper of Proceedings of Zero Energy Mass Custom Home 2018 related to chapter 6. The published manuscript is:

Zhou Y, Mikhaylova O, Bidarmaghz A, Donovan B, Narsilio G, Aye L (2018), Hybrid geothermal-gas and geothermal-solar-gas heating systems for poultry sheds. Proceedings of Zero Energy Mass Custom Home 2018, ISBN: 978-0-7340-5486-9; pp. 545-554, 29 Jan – 01 Feb 2018, Melbourne, Australia

# HYBRID GEOTHERMAL-GAS AND GEOTHERMAL-SOLAR-GAS HEATING SYSTEMS FOR POULTRY SHEDS

Yu Zhou[1]*, Olga Mikhaylova[2], Asal Bidarmaghz[3], Brad Donovan[4], Guillermo Narsilio[5] & Lu Aye[6]

[1] Department of Infrastructure Engineering, Melbourne School of Engineering, The University of Melbourne, Vic 3010, Australia, *yu.zhou@unimelb.edu.au

[2] Department of Infrastructure Engineering, Melbourne School of Engineering, The University of Melbourne, Vic 3010, Australia, olga.mikhaylova@unimelb.edu.au

[3] Department of Infrastructure Engineering, Melbourne School of Engineering, The University of Melbourne, Vic 3010, Australia, bia@unimelb.edu.au

[4] Department of Infrastructure Engineering, Melbourne School of Engineering, The University of Melbourne, Vic 3010, Australia, narsilio@unimelb.edu.au

[5] Ground Source Systems Pty Ltd, Australia, brad@groundsourcesystems.com.au

[6] Renewable Energy and Energy Efficiency Group, Department of Infrastructure Engineering, Melbourne School of Engineering, The University of Melbourne, Vic 3010, Australia, lua@unimelb.edu.au

***Abstract:*** *Poultry sheds have unique indoor air temperature requirements to raise poultries (chickens: broilers & layers, turkeys, ducks), which determine their unique heating and cooling demand cycles. In this paper, heating options of a typical chicken shed for broilers in Peats Ridge, NSW are investigated. The farming operation of this shed involves six heating and cooling cycles in one year, each cycle lasting for seven weeks. The thermal load for the first three weeks of the cycle is heating dominated, while the load for the rest of the cycle is cooling dominated. The chicken shed typically utilises evaporative coolers and liquefied petroleum gas (LPG) heaters to maintain required indoor air temperature. To reduce the cost of heating the shed, hybrid geothermal-gas and geothermal-solar-gas heating systems are proposed. In these systems, the baseload heating capacity is supplied by ground source heat pumps (GSHPs) that use the ground as a heat source. It should be noted that a continuous operation of the heat pump may decrease the ground temperature over time and thus reduce the energy efficiency of the system; therefore, flat plate solar collectors are proposed to be coupled with the GSHPs to thermally recharge the ground and increase energy efficiency of the heating system. Moreover, gas boilers are proposed to be integrated with the GSHPs to reduce the overall installation costs of the heating system. This paper discusses the sizing of various components of these hybrid systems. Preliminary results revealed that, if hybrid systems are used for heating, significant savings of annual heating costs can be expected.*

***Keywords:*** *Geothermal energy, Rural industries, Hybrid systems, Energy efficiency, Heat pump.*

## 1 Introduction

In Australia, agriculture and related food processing industry contribute 12% to the national Gross Domestic Product (GDP) (NFF 2016; NFF 2012). Annually, about 600 million chickens are raised nationwide (Australian Bureau of Statistics 2016). Chicken sheds consume a significant amount of energy, which is mainly used for heating and cooling. An estimation by Zhou et al. (2017) suggested that about A$ 80 million is spent annually for this purpose. To reduce operational costs of chicken sheds, their energy bills could be reduced. Since existing cooling systems for chicken sheds can be very cost-effective to operate (for example, if evaporative cooling systems are used), the primary focus should be on the reduction of heating costs.

In Australia, the primary energy sources for heating are network piped natural gas and bottled liquefied petroleum gas (LPG) (Allison Ball et al. 2016). These fuels are not only expensive to utilise but also produce significant amount of greenhouse gas (GHG) emissions (Australian Government. Dept. of the Enviroment 2015). Through the partial replacement of current gas heating systems with high-performance equipment that uses renewable and more sustainable energy sources, both operational cost savings and GHG emission reductions could be potentially achieved.

A Ground Couple Heat Pump (GCHP) system extracts thermal energy from the ground during heating mode and rejects heat into the ground during cooling mode. By utilising the ground as a heat source and heat sink, GCHP systems provide low-carbon thermal energy for heating and cooling (Johnston, Narsilio & Colls 2011). If the systems are applied for heating only utilising ground as a source they are termed Ground Source Heat Hump (GSHP) systems. In the previous few decades, GSHP systems have been installed worldwide for different applications and such systems are especially popular in the United States, Canada, Sweden and China (Lund & Boyd 2016). GSHP systems have also been introduced for the heating of poultry sheds (Kharseh & Nordell 2011).

Despite the relatively high energy efficiency of the GSHP systems, they require considerable capital investments. It has been demonstrated that hybrid systems where GSHPs are coupled with other types of systems can be more economical for heating (Eslami-Nejad & Bernier 2011; Kjellsson, Hellström & Perers 2010). For example, gas boilers and gas burners have relatively low installation costs and can be integrated with GSHP systems to reduce installation costs of these systems. To boost heating efficiency of GSHP systems, renewable solar thermal systems can also be coupled to form solar assisted GSHP systems. By combining these three sources of thermal energy, lower operational heating costs as well as lower installation costs of heating systems can be potentially achieved.

This study investigates financial benefits of a geothermal-solar-gas hybrid heating system for poultry sheds in Australia. In particular, the paper discusses optimisation of a hybrid geothermal-solar-gas heating system for a typical chicken shed in Peats Ridge, NSW, Australia. A building energy simulation model of the shed was developed using EnergyPlus and verified against current energy consumptions. By using this verified energy model, an optimisation of the installed capacities of different components of the geothermal-gas-solar hybrid heating system was performed to minimise the operational cost of the hybrid as well as the 40-year lifetime cost of heating. The 40-year lifetime is considered in this study because the lifetime for ground heat exchangers is at least 40 years and the shed are also expected to be used for the next 40 years. Based on the optimisation study, the proposed design of the hybrid system for the shed is discussed.

## 2 Heating Cycles of Chicken Shed

In this case study, a chicken shed located in Peats Ridge, NSW, Australia was examined to exemplify the study for temperate climate regions. The main parameters of the shed are presented in Table 1. An EnergyPlus building energy simulation model was developed for the shed. The energy model simulates the heating and cooling loads for the shed using 'ideal air flow' option in EnergyPlus. The performance data of components (GSHP, FPSC, Solar PV) were based on the equipment currently available on the market in Australia.

**Table 9 Chicken Shed Parameters**

| | |
|---|---|
| Location | Peats Ridge, NSW, Australia (33°23'49"S, 150°24'09"E) |
| Dimensions | Width:18.3 m, Length:138.7 m, Height: 2.7 to 4.3 m |
| Wall/Roof Material | No windows; Insulation with thin layers of metal cladding. Insulation thickness: 0.075 m, thermal conductivity: 0.039 $Wm^{-1}K^{-1}$, density: 16 $kg\ m^{-3}$, specific heat: 340 $Jkg^{-1}K^{-1}$ |
| Climate Data | Typical Meteorological Year (TMY) data (Remund et al. 2016) |

Zhou et al. (2017) demostrated that the operational schedule significantly influences the heating energy consumption of chicken sheds. They estimated that up to 20% variation in the annual energy consumption can be expected for different starting dates of batches (growing cycles for young chicks grow up fully to the market which usually last seven to eight weeks in Australia). For this study, the first batch is assumed to start on 1st of January and that the shed is used for six batches per year. Each batch is assumed to last seven weeks with two weeks break time in between batches.

Similar to the normal operation of the case study shed, 50,000 chickens are assumed at the beginning of each batch. Three harvests are expected in one batch, happening in the mid-night of the end of the fifth, sixth and seventh weeks of the cycle. The first harvest is assumed to depopulate 15,000 chickens while the second one 10,000 chickens and the last harvest remaining 25,000 chickens. Mortality of chicken during growing cycles is not considered as no detailed reliable mortality data is available.

The chicken weight gain and metabolic heat generation data applied in each cycle are presented in Table 2. This data is in accordance with the chicken growing recommendations provided by the shed owner and operator.

**Table 2 Chicken growth and metabolic heat generation**

| Day of growing cycle | Mass per chicken (kg) | Heat generation per chicken (W) | Number of chicken (-) | Indoor setpoint temperature (°C) |
|---|---|---|---|---|
| 1 | 0.054 | 0.82 | 50,000 | 31.0 |
| 7 | 0.180 | 2.02 | 50,000 | 28.6 |
| 14 | 0.438 | 3.93 | 50,000 | 26.1 |
| 21 | 0.829 | 6.34 | 50,000 | 23.7 |
| 28 | 1.337 | 9.08 | 50,000 | 21.2 |
| 35 | 1.897 | 11.80 | 50,000 | 19.0 |
| 42 | 2.444 | 14.27 | 35,000 | 19.0 |
| 49 | 2.873 | 16.11 | 25,000 | 19.0 |

Currently, the case study shed has been heated by LPG burners. The energy consumption model developed was calibrated and verified with the two-year LPG bills provided by the farm owner. To match the actual LPG consumption, we adjusted the ventilation rate (air exchange rate with the outdoor environment). The calibrated ventilation rate of

$1.04\times10^{-4}\,m^3\,s^{-1}kg^{-1}$ (Vest & Tyson 1991) was applied to closely match the actual and calculated annual heating costs.

Fig. 1 shows the simulated heating power demand of the shed based on the verified energy consumption model developed. It was estimated that the annual heating energy of the shed is 143,811 $kWh_h$* with a peak heating power demand of 195 $kW_h$. During each heating cycle, the heating demand is at its maximum at the start of each cycle when the least metabolic heat is generated by chickens and, at the same time, the required indoor temperature is at maximum (Table 1). The heating demand decreases later in each cycle due to the increase in metabolic heat generated by chickens and lower indoor temperature requirement corresponding to the age of the batch (Table 1).

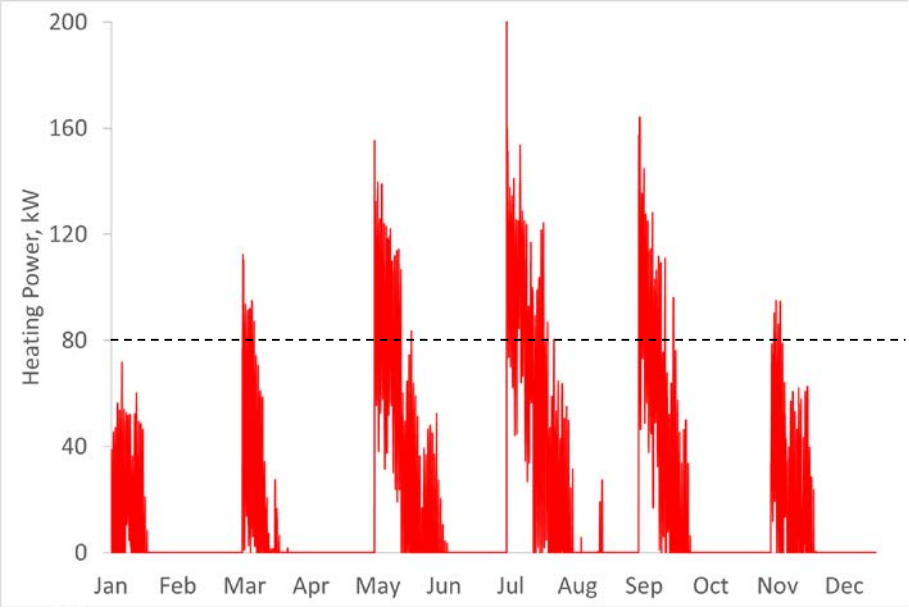


**Figure 16 Hourly heating demand of the chicken shed**

It should be noted that most of the time, the heating demand of the shed is lower than 80 $kW_h$ (Fig. 1). This means that if a hybrid heating system with an installed GSHP capacity of about 40% (~80 $kW_h$) of the peak heating power demand is used for heating, more than 86% of the annual heating energy can still be satisfied by the GSHP. This illustrates the advantage of a hybrid heating system as it could satisfy most heating requirement with cost-effective, renewable energy resources with a relatively lower initial capital cost. The next section of the paper discusses such potential operational cost savings of hybrid systems in detail.

## 3 Annual Heating Cost Analysis of Different Hybrid systems

This section discusses operational costs of different sizing combinations of the hybrid geothermal-gas and geothermal-solar-gas heating systems for the chicken shed presented in previous sections. To describe the capacity portion of the GSHP in the hybrid system, '*shave factor'* is used. It is defined as the ratio of the installed capacity of the GSHP system to the peak heating demand of the load to be satisfied (Eq. 1) by the hybrid system (Alavy et al. 2013; Mikhaylova et al. 2016).

*subscript *h* represents heating, while subscript *e* represents electricity.

$$S = \frac{\text{Installed capacity of GSHP}}{\text{Peak heating load}} \times 100\ \% \quad (1)$$

As an example, a shave factor of 40% in a geothermal-gas hybrid (195 $kW_h$ peak load) means that the installed capacity of a GSHP system within a hybrid system is $195\,\mathrm{kW_h} \times 40\% = 78\,\mathrm{kW_h}$ , and the installed capacity of a boiler will be 117 $kW_h$.

Table 2 presents the system component efficiencies and assumptions used in the analyses. The energy prices used in this study were obtained from the current gas and electricity contracts of the farm owner in NSW (note that gas and electricity prices can be differ for farm to farm depending on the contracts with the suppliers). System energy efficiency of each equipment was assumed based on the equipment currently available on the market in Australia. Annual operational costs of shed heating using a LPG boiler and a GSHP system as well as two types of hybrids with different shave factors were calculated using the annual heating demand presented in Fig. 1 and the assumptions shown in Table 2. It is important to note that for GSHP systems, the energy efficiency is usually expressed in Coefficient of Performance (COP), which is defined as the ratio of output heat power to the input electric power. To be consistent with the LPG system, the performance of GSHP systems are expressed in energy efficiency, where, 300% of energy efficiency means the COP of 3.0. The employments of flat plate solar collector (FPSC) and solar PV will reduce the electricity consumption by improving the efficiency as well as the electricity offset. The results of these calculations are discussed in the following section.

**Table 10 Energy Efficiency and Prices of Gas and Electricity for the Systems Investigated**

| | LPG Boiler | GSHP | Hybrid GSHP+FPSC | Hybrid GSHP+FPSC and Solar PV |
|---|---|---|---|---|
| System energy efficiency, % | 85 | 300 | 320 | 320 |
| Energy source price, c/kWh | 7 | 10 | 10 | 10 |
| Solar offset, % | Nil | Nil | Nil | 100 |

### *3.1 Hybrid Geothermal-Gas Heating System*

Fig. 2 shows the annual operational cost of the hybrid geothermal-gas heating system with different shave factors as well as the portions of the heating energy provided by the GSHP system in each sizing combination of the hybrid system. It is apparent from the figure that the maximum and the minimum annual heating costs are expected when the gas-only and the GSHP-only heating systems are used for the shed, respectively. In addition, as the shave factor increases, the annual heating cost decreases. These observations are explained by the higher energy efficiency of the GSHP compare to the LPG boiler (Table 1). At the same time, the increase in the shave factor to more than 50% does not seem to have any significant reduction of the annual operational cost (Fig. 2).

The maximum 60% reduction in operational cost in comparison with the original gas-only system can be achieved when the shave factor of the hybrid geothermal-gas system is 100%. However, with a shave factor of 40%, about 87% of the annual required heating energy can be delivered by the GSHP and the operational cost can be reduced by about 50% compared to the gas-only system. This observation implies that a significant reduction in operation costs may be still achieved with a GSHP system that is half the size of that corresponding to the maximum possible reduction, which in only marginally better.

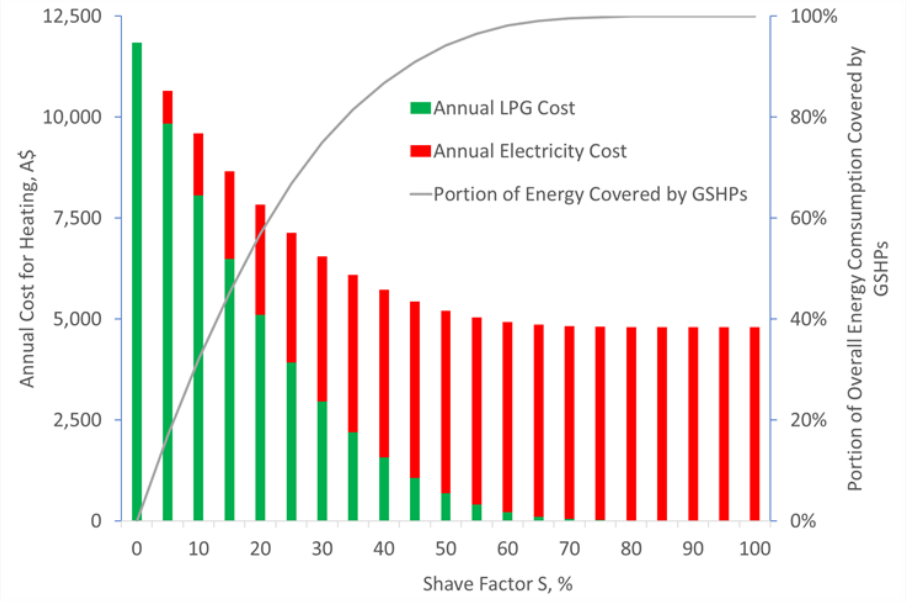


**Figure 17 Annual Heating Cost of a Hybrid Geothermal-Gas System**

### *3.2 Hybrid Geothermal-Solar-Gas Heating system*

"Solar" may refer to *solar thermal* or *solar photovoltaic* (PV) systems. FPSCs are cost-effective solar thermal collectors that utilise solar energy for heating. Previous studies (Eslami-Nejad & Bernier 2011; Kjellsson, Hellström & Perers 2010) confirmed that with the integration of FPSCs, the performance of the GSHPs can be increased. In this study, based on the work of Kjellsson, Hellström & Perers (2010) in Sweden, it was assumed that the system heating coefficient of performance (HCOP) of solar assisted GSHPs increases from 3.0 to 3.2, with the installation of 7.5 $m^2$ of FPSCs for 5 kW of heat pump nominal heating capacity.

Solar PV modules are the equipment that can convert solar radiation into electricity. In this study, solar PV modules are proposed to be installed to offset electricity consumption of the heating system for the shed. The PV array is sized to cover all the annual electricity used by the shed hybrid heating system. Hence, with the utilisation of the solar PV array, the cost of electricity for the shed heating system can be completely offset.

With the adoption of FPSCs and solar PV modules, a large amount of operational cost could be saved. Fig. 3 shows the annual operational costs of the different configurations of hybrid geothermal-solar-gas systems for the shed. With the FPSCs and solar PV modules, 50% operational cost reduction in comparison with the original gas-only system can be achieved for a shave factor of only 20%. In addition, with a shave factor of 75%, the annual heating cost can be effectively reduced to zero. It should be noted that as demonstrated in Fig. 3, the high operational cost savings can be achieved using hybrid geothermal-solar-gas heating system, however, this always comes at higher capital investment costs than the capital cost of the gas-only system. The next section discusses the lifecycle costs of hybrid systems to find a balance of capital cost and the operational cost savings.

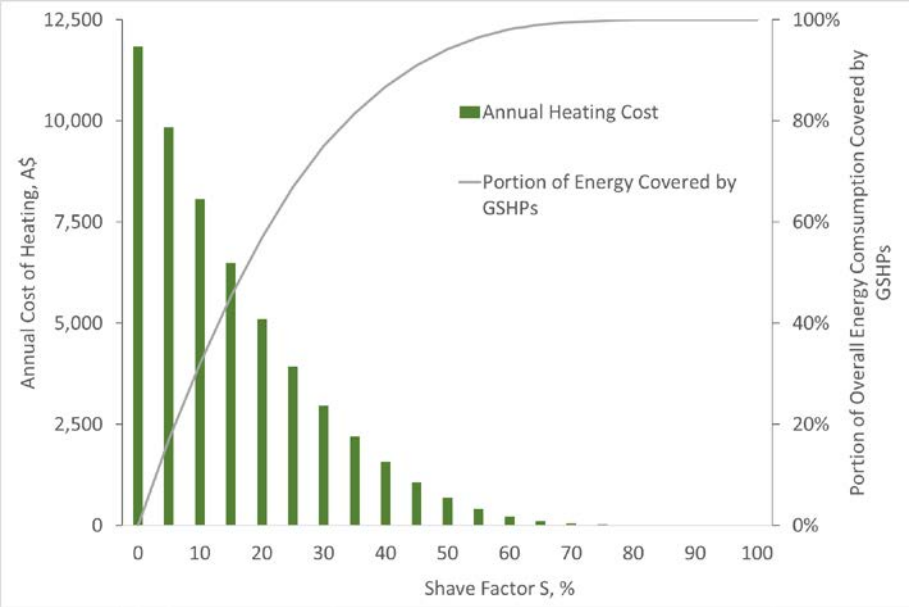


**Figure 18 Annual Heating Cost of a Hybrid Geothermal-Solar-Gas System**

## 4 Life Cycle Cost Analysis of Different Hybrid Systems

As discussed in the previous section, with the adoption of the hybrid geothermal-gas heating system, a significant amount of operational cost reduction can be expected (up to 60% as shown in Fig. 2). By employing FPSCs and with electricity offset from solar PV modules, the operational cost can be reduced even further down to zero (as shown in Fig. 3). However, high operational cost savings are often related to high capital investment costs of the systems.

For decision making in balancing initial investment and future return (operational cost savings), various methods have been applied, which include Simple Payback Period (SPP), Discounted Payback Period (DPP), Internal Rate of Return (IRR), External Rate of Return (ERR) and Lifecycle Cost Analysis (LCCA) (Lu et al. 2017). In this study, LCCA is used to guide the optimisation of size of different components of hybrid heating systems for the shed.

LCCA is a financial analysis that evaluates the financial feasibility of a project over a long period (Kirk & Dell'Isola 1995). This analysis considers the net present values of the capital investment cost, operational and maintenance costs and the final disposal cost. In this paper, the life cycle cost of the heating system is calculated using Eq. 2 (Markvart 1994):

$$LCC = C + \sum_{n=1}^{t} C_r \left( \frac{1}{1+d} \right)^n \qquad (2)$$

where, $C$ is the initial capital cost, $C_r$ is the recurring cost in a time period, $d$ is the real discount rate, and $t$ is the project life time in year.

The initial capital costs and life times of different components applied in the analysis are listed in Table 3. These figures are estimated based on average current market data for the various system components. The costs of LPG heaters, GSHPs and ground loops are

calculated per unit heating capacity. The cost of FPSCs is calculated per heating capacity of GSHPs. The cost of solar PV modules is calculated per installed peak electricity generation capacity of solar PV, while the overall installed capacity of solar PV panel is based on the annual electricity consumed by the system. The details regarding the sizing of these components are discussed in Section 5. The current energy prices and the energy efficiency of different components of heating systems were assumed to be the same values as provided in Table 2.

**Table 11 Initial Capital Costs and Life Times of Equipment**

| | LPG boiler | HP | Ground loops | FPSC | Solar PV Modules |
|---|---|---|---|---|---|
| Initial Cost, (A$/kW) | 100 | 750 | 750 | A$ 180 per $kW_h$ of GSHPs | A$ 1,250 per $kW_p$ of PV capacity |
| Life Time, (years) | 10 | 20 | 40 | 20 | 20 |

In this analysis, the price escalation rate for LPG was assumed to be the same as natural gas, which is 6.14% and the price escalation rate for electricity was assumed to be 6.20% (Lu et al. 2017). It should be noted that these rates were estimated based on the actual fuel prices in Australia from 2000 to 2015. As the project is assumed to be of relatively low risks, the real discount rate in this study is set to be 5.08%, which was derived from the typical current business loan rates of the major banks in Australia.

Fig. 4 shows the 40-year lifecycle costs of different configurations of a hybrid geothermal-gas heating system. As shown in the figure, the minimum lifecycle cost is found to be at the shave factor of 40%. This minimum lifecycle cost is 72% of the cost of the original gas-only system. When the shave factor is larger than 40%, the lifecycle costs of the system are higher than the minimum lifecycle cost because increase in capital investment and replacement costs outweigh reduction in operational costs.

With the adoption of FPSCs and solar PV modules, the minimum lifetime cost of the heating system (Fig. 5) is lower than the minimum lifetime cost of the system in geothermal-gas hybrid configurations (Fig. 4). From Fig. 5, the minimum lifecycle cost of the hybrid geothermal-solar-gas heating system is only 47% of the original gas-only system (A$294,843 vs A$624,277). This minimum cost corresponds to a shave factor of 50%. This considerable amount of saving is achieved due to the near to zero operational cost achieved by electricity offset provided by the solar PV modules (Fig. 3).

The results presented in Fig. 4 and 5 demonstrate that hybrid geothermal-gas and geothermal-solar-gas heating systems can be more beneficial than gas-only and geothermal-only systems. If geothermal-gas and geothermal-solar-gas systems are compared, the results show that geothermal-solar-gas hybrids with solar PV modules to offset the electricity used by heating system can have lower lifecycle cost (up to 53%) and be more financially attractive.

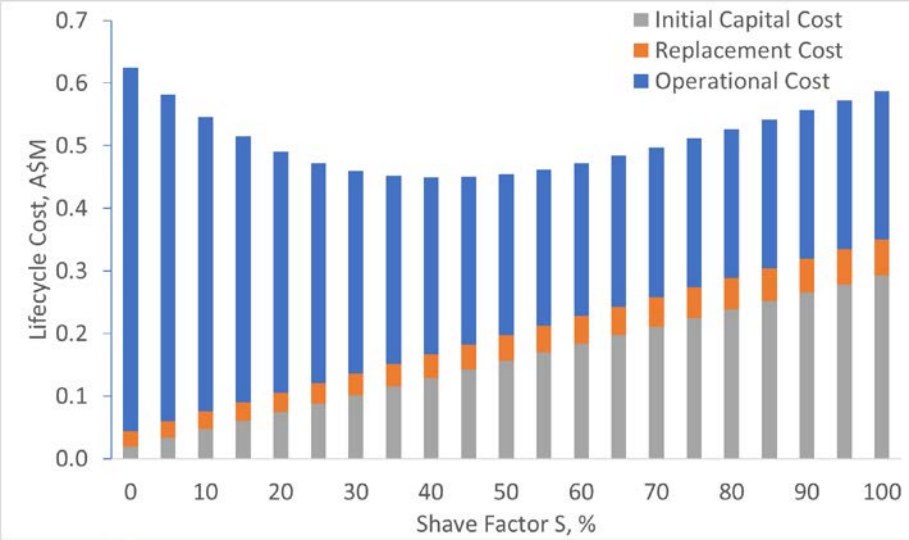


**Figure 4 Lifecycle Cost of Hybrid Geothermal-Gas Heating Systems**

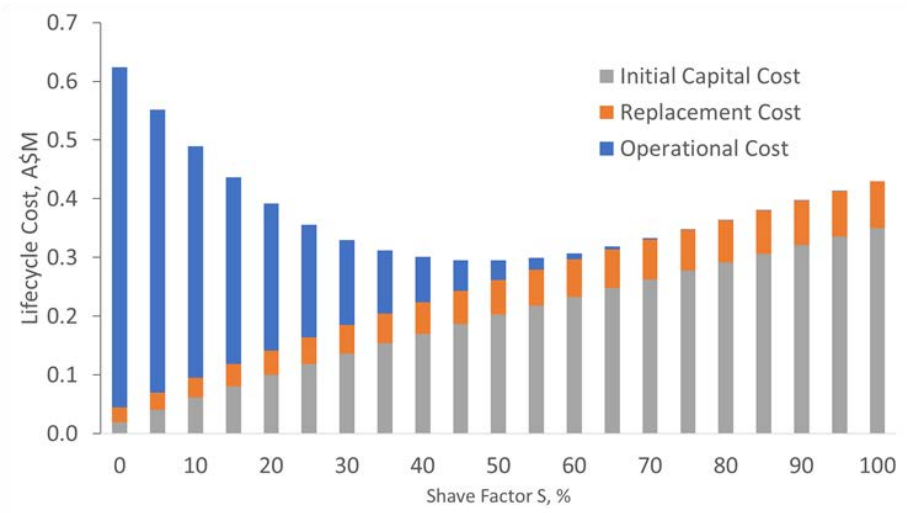


**Figure 5 Lifecycle Cost of Hybrid Geothermal-Solar-Gas Systems**

## 5 Future Investigation on Optimum Design for the Hybrid Geothermal-Solar-Gas System

Considering the results of the annual operational cost and lifecycle cost analyses (Fig. 2-5), a hybrid geothermal-solar-gas heating system has been proposed as a cost-effective and energy-efficient alternative to the current heating system of the chicken shed. The lifecycle cost analysis showed that a hybrid system with the shave factor of 50% is the most optimal configuration (Fig. 5) for the set of assumptions made. Such proposed hybrid system will be used for an experimental research of the performance of the system components and for validation of energy and ground heat exchanger models. However, due to budget constraint, an experimental hybrid system with a shave factor of 40% is being installed. Based on the LCCA results in Section 4, 52% reduction in the lifecycle cost can be achieved for a hybrid geothermal-solar-gas system with this shave factor of 40%. This is only 1% less than the maximum cost reduction when the hybrid is sized to the shave factor of 50%. The schematic drawing of the system proposed is shown in Fig. 6.

The heating is delivered by the four identical GSHPs connected in parallel to a main header. Each GSHP is coupled with a series of ground heat exchangers. The GSHPs are assisted by FPSCs connected to the ground heat changers, The FPSCs are designed to contribute to the heating energy extracted from the ground as well as to recharge the ground. The GSHPs are connected to a buffer tank to minimise heat pump on and off cycling. The existing gas burners installed in the shed will top up heating energy when needed.

## 6 Conclusions

This study evaluated the unique annual heating load pattern of a typical chicken shed in Peats Ridge, NSW, Australia. It proposed an energy-efficient and cost-effective heating system for the shed. Considering the annual heating demand of the shed, two alternative hybrid heating systems for the shed were considered: a hybrid geothermal-gas system and a hybrid geothermal-solar-gas system. For both systems, annual operational cost and lifecycle cost analyses were performed to optimise the sizes of the hybrids' components and determine the most cost-effective configuration of a hybrid. For the geothermal-solar-gas hybrid, solar PV modules are proposed to be installed to supply electricity to offset operational electricity costs of the heating system.

The results of the analyses suggest that both geothermal-gas (up to 28% lifecycle cost reduction) and geothermal-solar-gas (up to 53% lifecycle cost reduction) hybrids can be more economical than the original gas-only heating system of the shed considering the life cycle costs of the systems calculated for the 40-year lifetime of the shed. In addition, the geothermal-solar-gas hybrid heating system sized to 50% shave factor and supported by solar PV modules is the most cost-effective configuration (53% reduction in the life cycle cost) of the heating systems considered for the shed. Based on the analyses conducted, a preliminary schematic of the geothermal-solar-gas system proposed for the shed has been presented. After the installation, this system will be monitored and used as an experimental facility to investigate energy-efficiency of the system components and for validation of energy consumptions and ground heat exchanger models.

## Acknowledgements

The authors would like to thank the farm owners for kindly supporting the authors with the information regarding the chicken shed. The authors would also like to thank the Australian Research Council for the funding of Linkage Project LP160100070 and for FT140100227 supporting Dr Narsilio's salary.

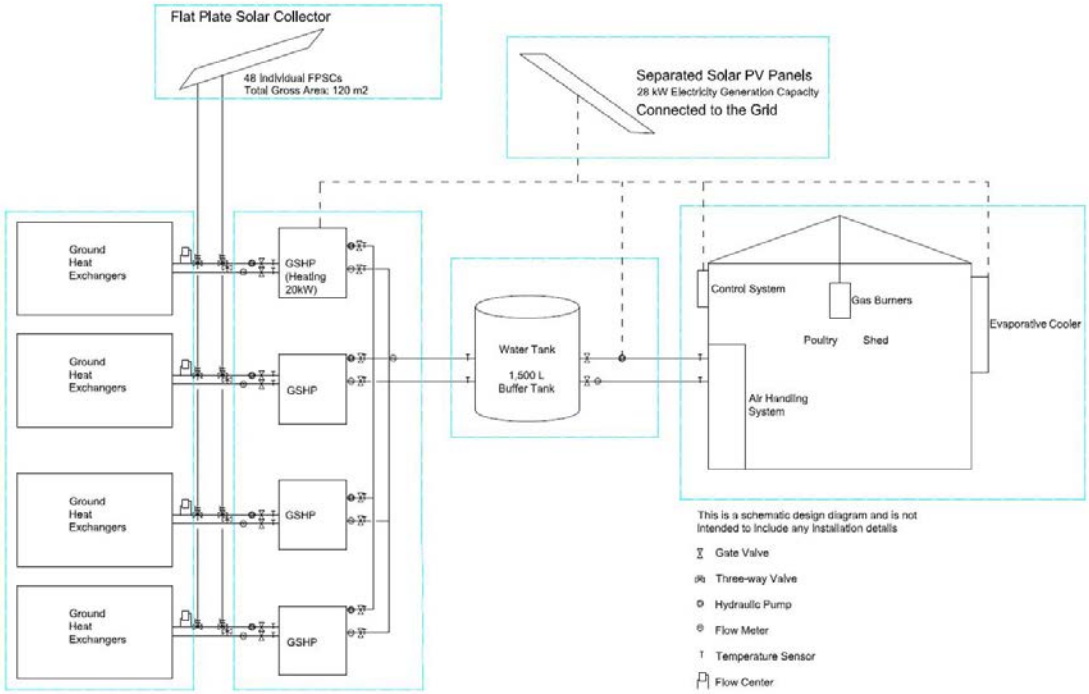


**Figure 6 Schematic of a Hybrid Geothermal-Solar-Gas Heating System for the Shed**

## References


Alavy, M, Nguyen, HV, Leong, WH & Dworkin, SB 2013, 'A methodology and computerized approach for optimizing hybrid ground source heat pump system design', *Renewable Energy*, vol. 57, pp. 404-12.

Allison Ball, Shamim Ahmad, Caitlin McCluskey, Pam Pham, Inja Ahn, Lauren Dawson, Thuong Nguyen & Davin Nowakowski 2016, 'Australian energy update', *Australian Government Bureau of Resources and Energy Economics, Canberra, October*.

Australian Bureau of Statistics 2016, '7215.0 - Livestock Products, Australia, March 2016'.

Australian Government. Dept. of the Enviroment 2016, *National Greenhouse Accounts Factors*, Published by the Department of the Environment and Energy, Commonwealth of Australia.

Eslami-Nejad, P & Bernier, M 2011, 'Coupling of geothermal heat pumps with thermal solar collectors using double U-tube boreholes with two independent circuits', *Applied Thermal Engineering*, vol. 31, no. 14, pp. 3066-77.

Johnston, IW, Narsilio, GA & Colls, S 2011, 'Emerging geothermal energy technologies', *KSCE Journal of Civil Engineering*, vol. 15, no. 4, pp. 643-53.

Kharseh, M & Nordell, B 2011, 'Sustainable heating and cooling systems for agriculture', *International Journal of Energy Research*, vol. 35, no. 5, pp. 415-22.

Kirk, SJ & Dell'Isola, AJ 1995, *Life cycle costing for design professionals*.

Kjellsson, E, Hellström, G & Perers, B 2010, 'Optimization of systems with the combination of ground-source heat pump and solar collectors in dwellings', *Energy*, vol. 35, no. 6, pp. 2667-73.

Lu, Q, Narsilio, GA, Aditya, GR & Johnston, IW 2017, 'Economic analysis of vertical ground source heat pump systems in Melbourne', *Energy*, vol. 125, pp. 107-17.

Lund, JW & Boyd, TL 2016, 'Direct utilization of geothermal energy 2015 worldwide review', *Geothermics*, vol. 60, pp. 66-93.

Markvart, T 1994, 'Solar Electricity, University of Southampton UK, John Wiley and Sons Ltd', *Baffin's lane, Chichester*.

Remund, J, Müller, S, Kunz, S, Huguenin-Landl, B, Studer, C & Cattin, R. 2016, 'Meteonorm Handbook', Meteotest, Switzerland.

Mikhaylova, O, R. Choudhary, K. Soga & Johnston, IW 2016, 'Benefits and optimisation of district hybrid ground source heat pump systems', *Energy Geotechnics*.

NFF (National Famers' Federation) 2016, 'NFF Annual Review 2014-15', National Famers' Federation, Barton ACT, Australia.

NFF (National Famers' Federation) 2012, 'NFF Farm Facts: 2012', National Famers' Federation, Barton ACT, Australia.

Vest, L & Tyson, B 1991, 'Key factors for poultry house ventilation', *Bulletin-Cooperative Extension Service, University of Georgia, College of Agriculture (USA)*.

Zhou, Y, Asal Bidarmaghz, Guillermo Narsilio & Aye, L 2017, *Heating and cooling loads of a poultry house in Central Coast, NSW, Australia*, the Conference Proceedings of World Sustainable Built Environment Conference 2017, Hong Kong, pp. 2127-32.

# Appendix B Golder Associate Pty Ltd Reports

This appendix contains the site investigation reports from our industry partner Golder Associate Pty Ltd which is related to Chapter 3

16 October 2017 Reference No. LP16010070-002-L-Rev0

Ms Olga Mikhaylova
The University of Melbourne
Melbourne School of Engineering
VICTORIA 3010

**LINKAGE PROJECT LP16010070, PEATS RIDGE, NSW – RESULTS OF LABORATORY TESTING**

Dear Olga

## Introduction

Golder Associates Pty Ltd (Golder) is collaborating with The University of Melbourne, University of California (Berkeley) and Ground Source Systems Pty Ltd on Australian Research Council linkage project LP16010070 'Direct geothermal energy: reducing the rural industries' carbon footprint'.

This letter presents the results of geotechnical classification tests performed on soil samples recovered from test pits excavated at the locations of proposed direct geothermal energy systems at the Brown's Farm, Slade's Farm #1, Slade's Farm #2 and Horticulture sites in Peats Ridge, NSW. Please refer to our transmittal dated 1 August 2017 (ref: LP16010070-001-T-Rev0) for preliminary Reports of Test Pits and test pit photographs.

## Laboratory testing

Laboratory test results are summarised in Table 1. Laboratory test reports are attached to this letter. Note that Atterberg limit tests were not performed on the samples with only 15% to 20% clay/silt materials.

**Table 1: Summary of classification test results**

| Site | Brown's Farm | | Slade's Farm (#1) | Slade's Farm (#2) | Horticulture |
|---|---|---|---|---|---|
| *Sample location and depth* | *TP01 2.3-2.5m* | *TP02 1.5-1.6m* | *TP05 1.0 – 1.1m* | *TP07 0.4-0.5m* | *TP09 1.6-1.7m* |
| % clay and silt | 15 | 20 | 15 | Not done | 58 |
| % sand | 79 | 79 | 68 | | 42 |
| % gravel or larger | 6 | 1 | 17 | | 0 |
| Moisture content | 9.7 | 10.0 | 13.0 | | 16.8 |
| MDD[1] (t/m$^3$) | 1.86 | 1.93 | 1.92 | 1.93 | 1.78 |
| OMC[1] (%) | 13.5 | 11.0 | 11.0 | 9.5 | 15.0 |
| Liquid limit (%) | Not done | | | | 33 |
| Plasticity index (%) | | | | | 16 |
| Linear shrinkage (%) | | | | | 6.5 |

[1]Maximum dry density (MDD) and optimum moisture content (OMC) for Standard compaction

The test results indicate that the samples typically comprise silty/clayey sand, with low plasticity fines and predominantly medium grained sand. The presence of ironstone cobbles at some test pit locations (refer to the preliminary Reports of Test Pits) should be noted as particle size distribution tests could not be performed on samples containing a high proportion of cobbles.


Golder, Golder Associates and the GA globe design are trademarks of Golder Associates Corporation.

With reference to the preliminary Reports of Test Pits, the sandy clay sample recovered from Test Pit TP09 (Horticulture site) is atypical of the predominantly sandy materials encountered in the test pits. The laboratory test results are generally consistent with the soil description based on visual and tactile assessments during test pit excavation.

Thermal conductivity tests on remoulded soil samples are underway. Results of these tests will be provided when they are available. The results of in-situ thermal conductivity measurements performed using a Decagon KD-2 Pro Thermal Properties Analyser are presented on the preliminary Reports of Test Pits and indicate a typical in-situ thermal conductivity of between about 1.8 W/mK and 2.4 W/mK, which is generally consistent with typical values for silty/clayey sand soils.

## Other comments

We understand that the ground heat exchangers (GHEs) for the proposed direct geothermal energy systems will be installed as either horizontal or vertical pipe loops in 1.5 m deep trenches. If requested, we would be pleased to provide geotechnical advice on trench construction once the layout (e.g. trench width and spacing) of the GHEs is confirmed. For preliminary purposes we provide the following comments for consideration in planning the construction works:

- The test pits were excavated using an IHI 55N 5 tonne mini excavator. Test Pits TP04 to TP06 (Slade's Farm #1) achieved excavation refusal and were terminated at a depth of about 1.2 m to 1.3 m. The other test pits achieved excavation refusal at depths ranging from about 2.0 m to 3.1 m. This information should be considered in selecting excavation plant for the proposed 1.5 m deep trenches.
- Vertical batter slopes excavated in predominantly sandy materials will not be stable in the long term. Temporary unsupported batter slopes to be adopted for construction purposes will depend on the proposed construction methodology including any requirements for personnel to enter trenches, trench spacing and the sequencing of trench excavation and backfilling.
- We understand the materials excavated from the trenches will be used as backfill once the pipe loops have been installed. Consideration should be given to excavating/stripping topsoil (e.g. materials with a high proportion of grass roots or other organic matter) and stockpiling them separately before commencing excavation into the underlying predominantly sandy natural soils. The topsoil could then be replaced as the uppermost backfill layer following backfilling of the trenches with the predominantly sandy soils. If it is practical to compact the backfill materials (excluding topsoil) we expect the thermal conductivity of the backfill to increase as the degree of compaction increases. Moisture conditioning of the backfill as it is placed will assist with achieving compaction.

We trust the information presented in this letter is satisfactory for your current requirements. Please do not hesitate to contact Stuart Colls on (03) 8862 3576 if you have any questions.

Yours sincerely,

**GOLDER ASSOCIATES PTY LTD**

Stuart Colls
Associate

SC/ASR/sc

CC: Guilermo Narsilio, Brad Donovan

Attachments: Laboratory test reports (9 pages)
Important information relating to this report (LEG04, RL2)

j:\2017\nc501 - melbourne uni, arc lp16010070\correspondence out\lp16010070-002-l\lp16010070-002-l-rev0.docx

## Soils testing - Particle size distribution & consistency limits test report

Standard method (by sieving)

**AS1289.3.6.1, 2.1.1, 3.1.2, 3.2.1, 3.3.1 & 3.4.1**


**Golder Associates Pty Ltd**

MELBOURNE GEOTECHNICAL LABORATORY
Building 7, Botanicca Corporate Park
570 - 588 Swan Street
Richmond, Victoria 3121


| | | | |
|---|---|---|---|
| **Test request #:** | TRM17-0390 | **Lab sample ID:** | LMEL2017082175 |
| **Client:** | The University of Melbourne | | |
| **Client address:** | | | |
| **Project ID:** | NC501 | **Lab report ref.:** | LMEL_17011733 |
| **Project name:** | ARC Linkage Project LP16010070, Peats Ridge | **Exploratory Hole:** | TP01 |
| **Location:** | The University of Melbourne | **Project reference:** | |

**Sample depth (m):** 2.30 - 2.50
**Client sample ref:** 2

| Specimen description: (Based on visual and tactile assessment) | Clayey/Silty SAND, low plasticity, pale yellow, trace of gravel | Sampling co-ordinates: Easting (m) | Northing (m) | Reduced Level |
|---|---|---|---|---|

**PARTICLE SIZE DISTRIBUTION** AS 1289.3.6.1

| Sieve Size | Passing | LB S | UB S |
|---|---|---|---|
| 125 mm | 100% | | |
| 75 mm | 100% | | |
| 63 mm | 100% | | |
| 53 mm | 100% | | |
| 37.5 mm | 100% | | |
| 26.5 mm | 100% | | |
| 19 mm | 100% | | |
| 13.2 mm | 97% | | |
| 9.5 mm | 97% | | |
| 6.7 mm | 96% | | |
| 4.75 mm | 96% | | |
| 2.36 mm | 95% | | |
| 1.18 mm | 93% | | |
| 600 µm | 88% | | |
| 425 µm | 79% | | |
| 300 µm | 54% | | |
| 150 µm | 21% | | |
| 75 µm | 15% | | |

| Method: | AS 1289.2.1.1 | AS 1289.3.1.2 | AS 1289.3.2.1 | AS 1289.3.3.1 | AS 1289.3.4.1 | |
|---|---|---|---|---|---|---|
| | Moisture content | 1 point Liquid limit | Plastic limit | Plasticity index | Linear shrinkage | Curling/ Crumbling/ Cracking |
| Result: | 9.7% As Rcvd. | | | | | |
| LB S: | | | | | | - |
| UB S: | | | | | | - |
| Att. preparation method: | | | | LSM length (mm): | | |

**Specimen history/notes:** Preparation of specimen and testing performed on sample supplied to the laboratory

**Definitions:**
LB S = Lower bound specification
LSM = Linear shrinkage mould
UB S = Upper bound specification
N/A = Not applicable
ND = Not determined; SIB = Slip in bowl
NO = Not obtainable; NP = Non plastic

**GRADING SUMMARY**

| Fines | Sand* | Gravel* | Cobbles* |
|---|---|---|---|
| (<75 µm) | (>75 µm - <2 mm) | (>2 mm - <60 mm) | (>60mm - <200 mm) |
| 15.2% | 79.2% | 5.6% | 0.0% |

**Proportions based on linear interpolation between sieve/particle of nearest size and smaller*

**PARTICLE SIZE DISTRIBUTION**

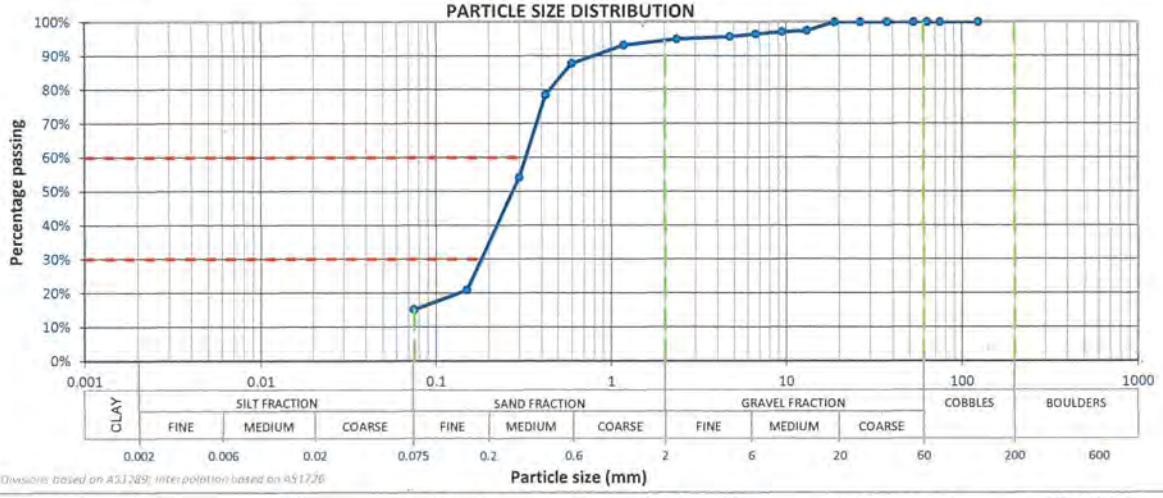


Divisions based on AS1289; interpolation based on AS1726

**Testing performed by:** MK **Results reviewed by:** StephenAbbey **Date reported:** 7/10/2017

**Cert. ref.:** NC501_TP01_TRM17-0390_PSD_17082175_Rep17011733

**Approved signatory:**

NATA accreditation number: 1961 - Site:1250 - Melbourne
Accredited for compliance with ISO/IEC 17025 - Testing


THIS DOCUMENT SHALL ONLY BE REPRODUCED IN FULL


**Stephen Abbey - Laboratory Manager**


Phone: +61 (03) 8862 3500 Fax: +61 (03) 8862 3501 E-mail: melbgeolab@golder.com.au Web: www.golder.com.au


These tests were carried out in accordance with the Australian standards identified in this certificate.

## Soils testing - Particle size distribution & consistency limits test report

Standard method (by sieving)

**AS1289.3.6.1, 2.1.1, 3.1.2, 3.2.1, 3.3.1 & 3.4.1**


Golder Associates

Golder Associates Pty Ltd

MELBOURNE GEOTECHNICAL LABORATORY

Building 7, Botanicca Corporate Park

570 - 588 Swan Street

Richmond, Victoria 3121


| | | | |
|---|---|---|---|
| **Test request #:** | TRM17-0390 | **Lab sample ID:** | LMEL2017082176 |
| **Client:** | The University of Melbourne | | |
| **Client address:** | | | |
| **Project ID:** | NC501 | **Lab report ref.:** | LMEL_17011734 |
| **Project name:** | ARC Linkage Project LP16010070, Peats Ridge | **Exploratory Hole** | TP02 |
| **Sample depth (m):** | 1.50 - 1.60 | **Client sample ref:** | 1 |
| **Location:** | The University of Melbourne | **Project reference:** | |

| Specimen description: (Based on visual and tactile assessment) | Clayey/Silty SAND, low plasticity, yellow brown | Sampling co-ordinates Easting (m) | Northing (m) | Reduced Level |
|---|---|---|---|---|
| PARTICLE SIZE DISTRIBUTION AS 1289.3.6.1 | | | | |

| Sieve Size | Passing | LB S | UB S |
|---|---|---|---|
| 125 mm | 100% | | |
| 75 mm | 100% | | |
| 63 mm | 100% | | |
| 53 mm | 100% | | |
| 37.5 mm | 100% | | |
| 26.5 mm | 100% | | |
| 19 mm | 100% | | |
| 13.2 mm | 100% | | |
| 9.5 mm | 100% | | |
| 6.7 mm | 100% | | |
| 4.75 mm | 100% | | |
| 2.36 mm | 100% | | |
| 1.18 mm | 98% | | |
| 600 µm | 93% | | |
| 425 µm | 83% | | |
| 300 µm | 60% | | |
| 150 µm | 28% | | |
| 75 µm | 20% | | |

| Method: | AS 1289.2.1.1 | AS 1289.3.1.2 | AS 1289.3.2.1 | AS 1289.3.3.1 | AS 1289.3.4.1 | |
|---|---|---|---|---|---|---|
| | Moisture content | 1 point Liquid limit | Plastic limit | Plasticity index | Linear shrinkage | Curling/ Crumbling/ Cracking |
| Result: | 10.0% As Rcvd. | | | | | |
| LB S: | | | | | | - |
| UB S: | | | | | | - |
| Att. preparation method: | | | | LSM length (mm): | | |

**Specimen history/notes:** Preparation of specimen and testing performed on sample supplied to the laboratory

**Definitions:** LB S = Lower bound specification; LSM = Linear shrinkage mould; UB S = Upper bound specification; N/A = Not applicable; ND = Not determined; SIB = Slip in bowl; NO = Not obtainable; NP = Non plastic

**GRADING SUMMARY**

| Fines (<75 µm) | Sand* (>75 µm - <2 mm) | Gravel* (>2 mm - <60 mm) | Cobbles* (>60mm - <200 mm) |
|---|---|---|---|
| 20.4% | 79.1% | 0.5% | 0.0% |

**Proportions based on linear interpolation between sieve/particle of nearest size and smaller*

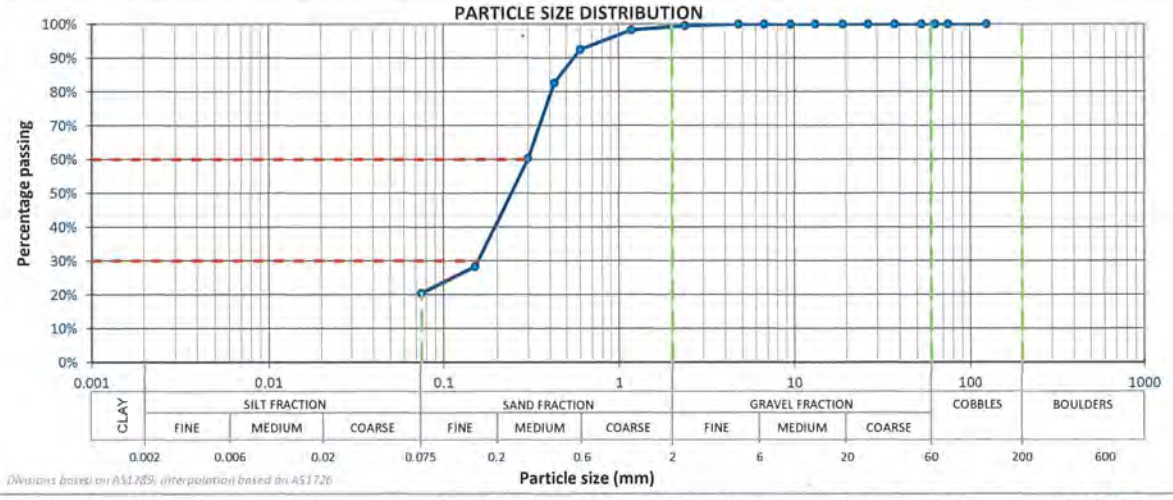


**Testing performed by:** MK **Results reviewed by:** StephenAbbey **Date reported:** 7/10/2017

| Cert. ref.: | NC501_TP02_TRM17-0390_PSD_17082176_Rep17011734 | Approved signatory: |
|---|---|---|
| NATA | NATA accreditation number: 1961 - Site:1250 - Melbourne<br>Accredited for compliance with ISO/IEC 17025 - Testing | |
| | THIS DOCUMENT SHALL ONLY BE REPRODUCED IN FULL | Stephen Abbey - Laboratory Manager |


Phone: +61 (03) 8862 3500 Fax: +61 (03) 8862 3501 E-mail: melbgeolab@golder.com.au Web: www.golder.com.au


These tests were carried out in accordance with the Australian standards identified in this certificate.

## Soils testing - Particle size distribution & consistency limits test report

Standard method (by sieving)

**AS1289.3.6.1, 2.1.1, 3.1.2, 3.2.1, 3.3.1 & 3.4.1**


**Golder Associates Pty Ltd**

MELBOURNE GEOTECHNICAL LABORATORY

Building 7, Botanicca Corporate Park

570 - 588 Swan Street

Richmond, Victoria 3121


| | | | |
|---|---|---|---|
| **Test request #:** | TRM17-0390 | **Lab sample ID:** | LMEL2017082177 |
| **Client:** | The University of Melbourne | | |
| **Client address:** | | | |
| **Project ID:** | NC501 | **Lab report ref.:** | LMEL_17011735 |
| **Project name:** | ARC Linkage Project LP16010070, Peats Ridge | **Exploratory Hole** | TP05 |
| **Location:** | The University of Melbourne | **Project reference:** | |

**Sample depth (m):** 1.00 - 1.10

**Client sample ref:** 1

**Specimen description:** (Based on visual and tactile assessment): Clayey/Silty SAND, low plasticity, pale orange,with gravel

| Sampling co-ordinates | | Reduced Level |
|---|---|---|
| Easting (m) | Northing (m) | |
| | | |

**PARTICLE SIZE DISTRIBUTION** AS 1289.3.6.1

| Sieve Size | Passing | LB S | UB S |
|---|---|---|---|
| 125 mm | 100% | | |
| 75 mm | 100% | | |
| 63 mm | 100% | | |
| 53 mm | 100% | | |
| 37.5 mm | 98% | | |
| 26.5 mm | 95% | | |
| 19 mm | 91% | | |
| 13.2 mm | 87% | | |
| 9.5 mm | 86% | | |
| 6.7 mm | 84% | | |
| 4.75 mm | 84% | | |
| 2.36 mm | 83% | | |
| 1.18 mm | 82% | | |
| 600 µm | 80% | | |
| 425 µm | 75% | | |
| 300 µm | 55% | | |
| 150 µm | 21% | | |
| 75 µm | 15% | | |

| Method: | AS 1289.2.1.1 | AS 1289.3.1.2 | AS 1289.3.2.1 | AS 1289.3.3.1 | AS 1289.3.4.1 | |
|---|---|---|---|---|---|---|
| | Moisture content | 1 point Liquid limit | Plastic limit | Plasticity index | Linear shrinkage | Curling/ Crumbling/ Cracking |
| Result: | 13.0% As Rcvd. | | | | | |
| LB S: | | | | | | - |
| UB S: | | | | | | - |

**Att. preparation method:** | **LSM length (mm):**

**Specimen history/notes:** Preparation of specimen and testing performed on sample supplied to the laboratory

**Definitions:** LB S = Lower bound specification; UB S = Upper bound specification; LSM = Linear shrinkage mould; N/A = Not applicable; ND = Not determined; SIB = Slip in bowl; NO = Not obtainable; NP = Non plastic

**GRADING SUMMARY**

| Fines | Sand* | Gravel* | Cobbles* |
|---|---|---|---|
| (<75 µm) | (>75 µm - <2 mm) | (>2 mm - <60 mm) | (>60mm - <200 mm) |
| 14.8% | 68.1% | 17.2% | 0.0% |

**Proportions based on linear interpolation between sieve/particle of nearest size and smaller*

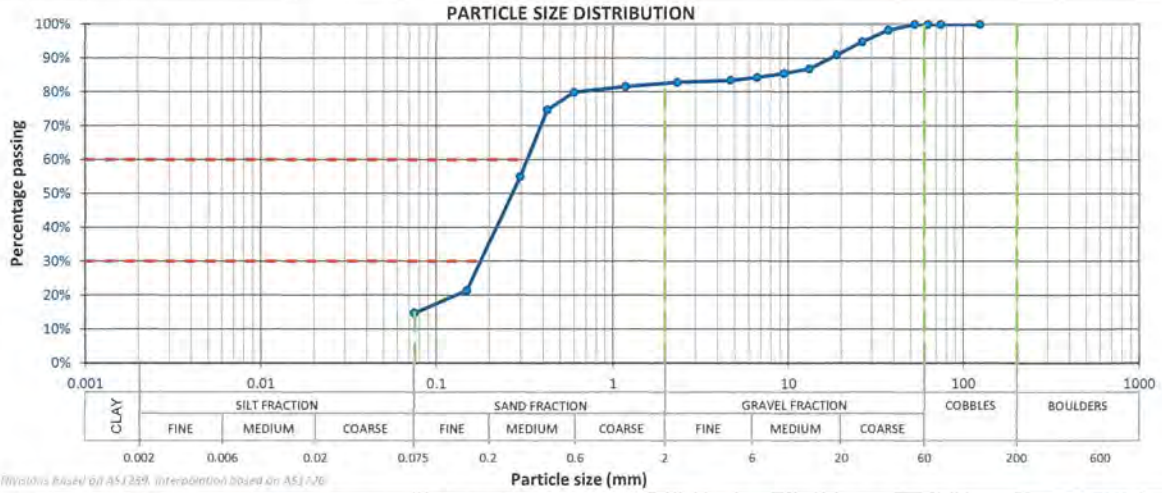


**Testing performed by:** MK **Results reviewed by:** StephenAbbey **Date reported:** 7/10/2017

**Cert. ref.:** NC501_TP05_TRM17-0390_PSD_17082177_Rep17011735

**Approved signatory:**

NATA accreditation number: 1961 - Site:1250 - Melbourne

Accredited for compliance with ISO/IEC 17025 - Testing


THIS DOCUMENT SHALL ONLY BE REPRODUCED IN FULL


**Stephen Abbey - Laboratory Manager**


Phone: +61 (03) 8862 3500 Fax: +61 (03) 8862 3501 E-mail: melbgeolab@golder.com.au Web: www.golder.com.au


These tests were carried out in accordance with the Australian standards identified in this certificate.

## Soils testing - Particle size distribution & consistency limits test report

Standard method (by sieving)

**AS1289.3.6.1, 2.1.1, 3.1.2, 3.2.1, 3.3.1, 3.4.1 & AS 1726:2017 Section 6.1**


**Golder Associates Pty Ltd**

MELBOURNE GEOTECHNICAL LABORATORY
Building 7, Botanicca Corporate Park
570 - 588 Swan Street
Richmond, Victoria 3121


| | | | |
|---|---|---|---|
| **Test request #:** | TRM17-0390 | **Lab sample ID:** | LMEL2017082179 |
| **Client:** | The University of Melbourne | | |
| **Client address:** | | | |
| **Project ID:** | NC501 | **Lab report ref.:** | LMEL_17011736 |
| **Project name:** | ARC Linkage Project LP16010070, Peats Ridge | **Exploratory Hole** | TP09 |
| **Sample depth (m):** | 1.60 - 1.70 | **Client sample ref:** | 2 |
| **Location:** | The University of Melbourne | **Project reference:** | |

| Specimen description: | | Sampling co-ordinates | | Reduced Level |
|---|---|---|---|---|
| (AS 1726:2017 Section 6.1) | CL, Sandy CLAY, low plasticity, white grey | Easting (m) | Northing (m) | |

**PARTICLE SIZE DISTRIBUTION** AS 1289.3.6.1

| Sieve Size | Passing | LB S | UB S |
|---|---|---|---|
| 125 mm | 100% | | |
| 75 mm | 100% | | |
| 63 mm | 100% | | |
| 53 mm | 100% | | |
| 37.5 mm | 100% | | |
| 26.5 mm | 100% | | |
| 19 mm | 100% | | |
| 13.2 mm | 100% | | |
| 9.5 mm | 100% | | |
| 6.7 mm | 100% | | |
| 4.75 mm | 100% | | |
| 2.36 mm | 100% | | |
| 1.18 mm | 100% | | |
| 600 µm | 99% | | |
| 425 µm | 98% | | |
| 300 µm | 94% | | |
| 150 µm | 80% | | |
| 75 µm | 58% | | |

| Method: | AS 1289.2.1.1 | AS 1289.3.1.2 | AS 1289.3.2.1 | AS 1289.3.3.1 | AS 1289.3.4.1 | |
|---|---|---|---|---|---|---|
| | Moisture content | 1 point Liquid limit | Plastic limit | Plasticity index | Linear shrinkage | Curling/ Crumbling/ Cracking |
| Result: | 16.8% As Rcvd. | 33% | 17% | 16% | 6.5% | None |
| LB S: | | | | | | - |
| UB S: | | | | | | - |
| Att. preparation method: | Dry sieved | | | LSM length (mm): | | 254 |

**Specimen history/notes:** Preparation of specimen and testing performed on sample supplied to the laboratory

**Definitions:** LB S = Lower bound specification; LSM = Linear shrinkage mould; UB S = Upper bound specification; N/A = Not applicable; ND = Not determined; SIB = Slip in bowl; NO = Not obtainable; NP = Non plastic

**GRADING SUMMARY**

| Fines | Sand* | Gravel* | Cobbles* |
|---|---|---|---|
| (<75 µm) | (>75 µm - <2.36 mm) | (>2.36 mm - <63 mm) | (>63mm - <200 mm) |
| 57.9% | 42.1% | 0.0% | 0.0% |

*Proportions based on guidance in AS1726-2017 Section 6.1.4.2*

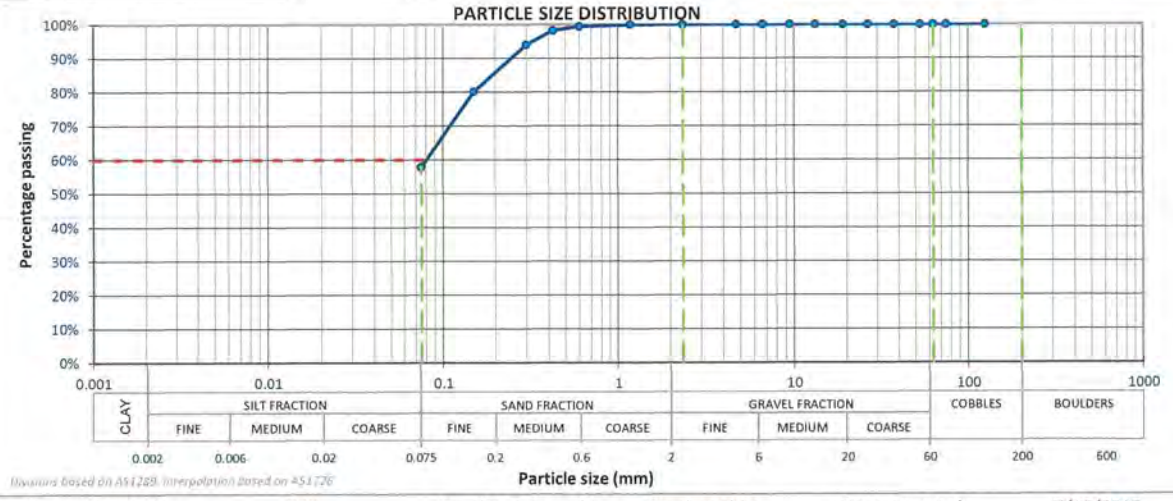


**Testing performed by:** MK **Results reviewed by:** StephenAbbey **Date reported:** 7/10/2017

| | | |
|---|---|---|
| **Cert. ref.:** | NC501_TP09_TRM17-0390_PSD_17082179_Rep17011736 | **Approved signatory:** |
| NATA | **NATA accreditation number: 1961 - Site:1250 - Melbourne**<br>Accredited for compliance with ISO/IEC 17025 - Testing | |
| | THIS DOCUMENT SHALL ONLY BE REPRODUCED IN FULL | **Stephen Abbey - Laboratory Manager** |


**Phone:** +61 (03) 8862 3500 **Fax:** +61 (03) 8862 3501 **E-mail:** melbgeolab@golder.com.au **Web:** www.golder.com.au


These tests were carried out in accordance with the Australian standards identified in this certificate.

## Soils testing - Determination of the dry density moisture relationship

Standard compaction method

**AS 1289.5.1.1-2003**


**Golder Associates Pty Ltd**

MELBOURNE GEOTECHNICAL LABORATORY

Building 7, Botanicca Corporate Park

570 - 588 Swan Street

Richmond, Victoria 3121


| | | | |
|---|---|---|---|
| **Test request ID:** | **TRM17-0390** | **Lab sample ID:** | LMEL2017082175 |
| **Client:** | The University of Melbourne | | |
| **Client address:** | | | |
| **Project ID:** | **NC501** | **Lab report ref.:** | LMEL_17011476 |
| **Project name:** | ARC Linkage Project LP16010070, Peats Ridge | **Exporatory Hole** | **TP01** |
| **Location:** | | **Project alias:** | - |
| **Specimen description:** (Based on visual and tactile assessment) | SAND, low plasticity, pale yellow | | |

**Sample depth (m):** 2.30 - 2.50

**Client sample ref:** 2

| **Sampling co-ordinates** | | **Reduced Level** |
|---|---|---|
| **Easting (m)** | **Northing (m)** | |
| | | |

| | | | | | |
|---|---|---|---|---|---|
| **Apparatus:** | **Mould - type:** A | **Compaction hammer** | **Balance** | **Drying oven** | |
| **Equipment ID:** | GAMGL09.01.03 | GAMGL10.01.06 | GAMGL01.21 | GAMGL02.11 | |
| **Calibration due:** | 10/01/18 | 19/06/18 | 27/09/17 | 12/07/18 | |

**Moisture content:** 11% Field — *AS 1289 2.1.1-2005*

**Portion test performed on:** -19 mm

### TEST REPORT - COMPACTION RESULTS

| | Point 1 | Point 2 | Point 3 | Point 4 | Point 5 | Point 6 |
|---|---|---|---|---|---|---|
| **Dry density (t/m³):** | | 1.79 | 1.81 | 1.85 | 1.81 | |
| **Moisture content:** | | 9.2% | 10.9% | 13.2% | 15.6% | |

**Oversize material** - (by wet mass)

No oversize correction required

**+19 mm:** 0%

**+37.5 mm:** 0%

*No oversize material present*

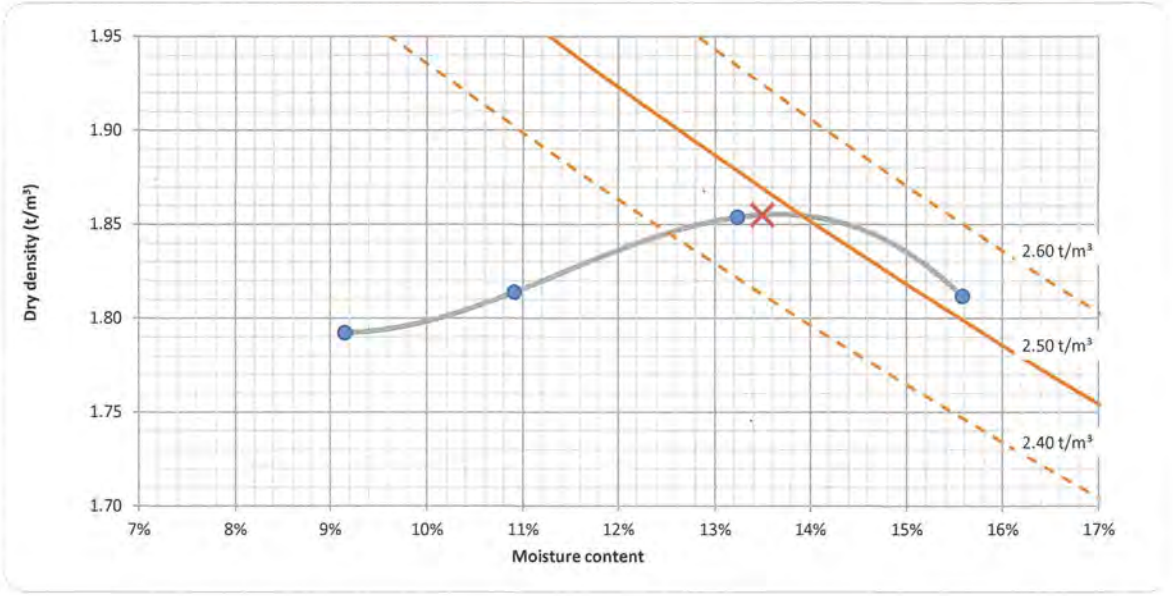


| | Result | Adjusted for oversize |
|---|---|---|
| **Standard maximum dry density (t/m³):** | 1.86 | |
| **Standard optimum moisture content:** | 13.5% | |

**Specimens prepared by:** **Tests performed by:** TK **Date tested:** 15/09/2017

**Definition:** ND = Not Determined **Results reviewed by:** NLobb **Date reported:** 19/09/2017

**Cert. ref.:** NC501_TP01_TRM17-0390_StndComp_s17082175_Rep17011476

**Approved signatory:**

NATA accreditation number: 1961 - Site:1250 - Melbourne

Accredited for compliance with ISO/IEC 17025 - Testing


THIS DOCUMENT SHALL ONLY BE REPRODUCED IN FULL


**Nick Lobb - Senior Technician**


Phone: +61 (03) 8862 3500 Fax: +61 (03) 8862 3501 E-mail: melbgeolab@golder.com.au Web: www.golder.com.au


This test was carried out in general accordance with AS 1289.5.1.1-2003.

## Soils testing - Determination of the dry density moisture relationship

Standard compaction method

**AS 1289.5.1.1-2003**


**Golder Associates Pty Ltd**

MELBOURNE GEOTECHNICAL LABORATORY

Building 7, Botanicca Corporate Park

570 - 588 Swan Street

Richmond, Victoria 3121


| | | | | | |
|---|---|---|---|---|---|
| **Test request ID:** | **TRM17-0390** | **Lab sample ID:** | LMEL2017082176 | | |
| **Client:** | The University of Melbourne | | | | |
| **Client address:** | | | | | |
| **Project ID:** | **NC501** | **Lab report ref.:** | LMEL_17011737 | | |
| **Project name:** | ARC Linkage Project LP16010070, Peats Ridge | | **Exporatory Hole** TP02 | **Sample depth (m):** | 1.50 - 1.60 |
| | | | | **Client sample ref:** | 1 |
| **Location:** | | | **Project alias:** | - | |
| **Specimen description:** (Based on visual and tactile assessment) | Clayey/Silty SAND, low plasticity, yellow brown | | | **Sampling co-ordinates** Easting (m) / Northing (m) | **Reduced Level** |

| | | | | | |
|---|---|---|---|---|---|
| **Apparatus:** | **Mould - type:** A | **Compaction hammer** | **Balance** | **Drying oven** | **Moisture content:** *AS 1289 2.1.1-2005* |
| **Equipment ID:** | GAMGL09.01.03 | GAMGL10.01.06 | GAMGL01.21 | GAMGL02.12 | |
| **Calibration due:** | 10/01/18 | 19/06/18 | 20/10/17 | 13/07/21 | **Portion test performed on:** -19 mm |

### TEST REPORT - COMPACTION RESULTS

| | Point 1 | Point 2 | Point 3 | Point 4 | Point 5 | Point 6 |
|---|---|---|---|---|---|---|
| **Dry density ($t/m^3$):** | 1.81 | 1.81 | 1.92 | 1.92 | 1.83 | |
| **Moisture content:** | 7.8% | 7.8% | 9.8% | 11.9% | 13.8% | |

**Oversize material** - (by wet mass)

No oversize correction required

**+19 mm:** 0%

**+37.5 mm:** 0%

*No oversize material present*

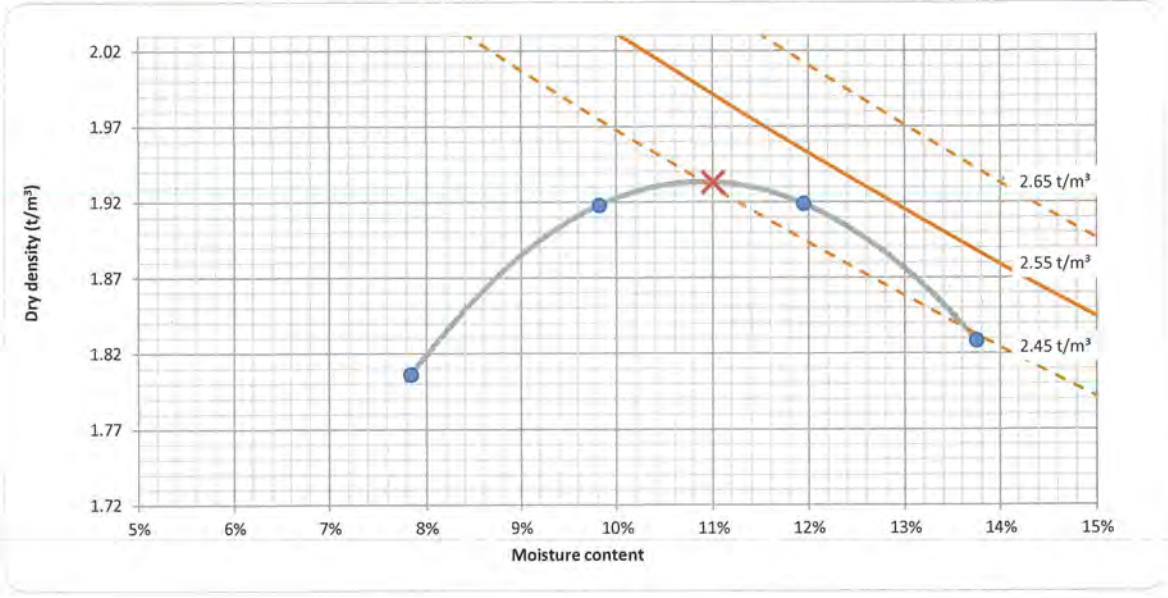


| | Result | Adjusted for oversize |
|---|---|---|
| **Standard maximum dry density ($t/m^3$):** | 1.93 | |
| **Standard optimum moisture content:** | 11.0% | |

**Specimens prepared by:** **Tests performed by:** TK **Date tested:** 15/09/2017

**Definition:** ND = Not Determined **Results reviewed by:** StephenAbbey **Date reported:** 07/10/2017

**Cert. ref.:** NC501_TP02_TRM17-0390_StndComp_s17082176_Rep17011737

**Approved signatory:**

NATA

**NATA accreditation number: 1961 - Site:1250 - Melbourne**

Accredited for compliance with ISO/IEC 17025 - Testing


THIS DOCUMENT SHALL ONLY BE REPRODUCED IN FULL


**Stephen Abbey - Laboratory Manager**


**Phone:** +61 (03) 8862 3500 **Fax:** +61 (03) 8862 3501 **E-mail:** melbgeolab@golder.com.au **Web:** www.golder.com.au


This test was carried out in general accordance with AS 1289.5.1.1-2003.

## Soils testing - Determination of the dry density moisture relationship

Standard compaction method

**AS 1289.5.1.1-2003**

Golder Associates


**Golder Associates Pty Ltd**

MELBOURNE GEOTECHNICAL LABORATORY

Building 7, Botanicca Corporate Park

570 - 588 Swan Street

Richmond, Victoria 3121


| | | | |
|---|---|---|---|
| **Test request ID:** | **TRM17-0390** | **Lab sample ID:** | LMEL2017082177 |
| **Client:** | The University of Melbourne | | |
| **Client address:** | | | |
| **Project ID:** | **NC501** | **Lab report ref.:** | LMEL_17011738 |
| **Project name:** | ARC Linkage Project LP16010070, Peats Ridge | **Exporatory Hole** | **TP05** |
| **Sample depth (m):** | 1.00 - 1.10 | | |
| **Client sample ref:** | 1 | | |
| **Location:** | | **Project alias:** | - |

**Specimen description:** (Based on visual and tactile assessment) Clayey/Silty SAND, low plasticity, pale orange,with gravel

**Sampling co-ordinates** — Easting (m) | Northing (m) | **Reduced Level**

| **Apparatus:** | **Mould - type: A** | **Compaction hammer** | **Balance** | **Drying oven** |
|---|---|---|---|---|
| **Equipment ID:** | GAMGL09.01.03 | GAMGL10.01.06 | GAMGL01.21 | GAMGL02.12 |
| **Calibration due:** | 10/01/18 | 19/06/18 | 20/10/17 | 13/07/21 |

**Moisture content:** 13% Field — *AS 1289 2.1.1-2005*

**Portion test performed on:** -19 mm

### TEST REPORT - COMPACTION RESULTS

| | Point 1 | Point 2 | Point 3 | Point 4 | Point 5 | Point 6 |
|---|---|---|---|---|---|---|
| **Dry density (t/m³):** | 1.85 | 1.88 | 1.88 | 1.81 | | |
| **Moisture content:** | 9.6% | 10.0% | 12.5% | 14.8% | | |

**Oversize material** - (by wet mass)

No oversize correction required

**+19 mm:** 0%

**+37.5 mm:** 0%

*No oversize material present*

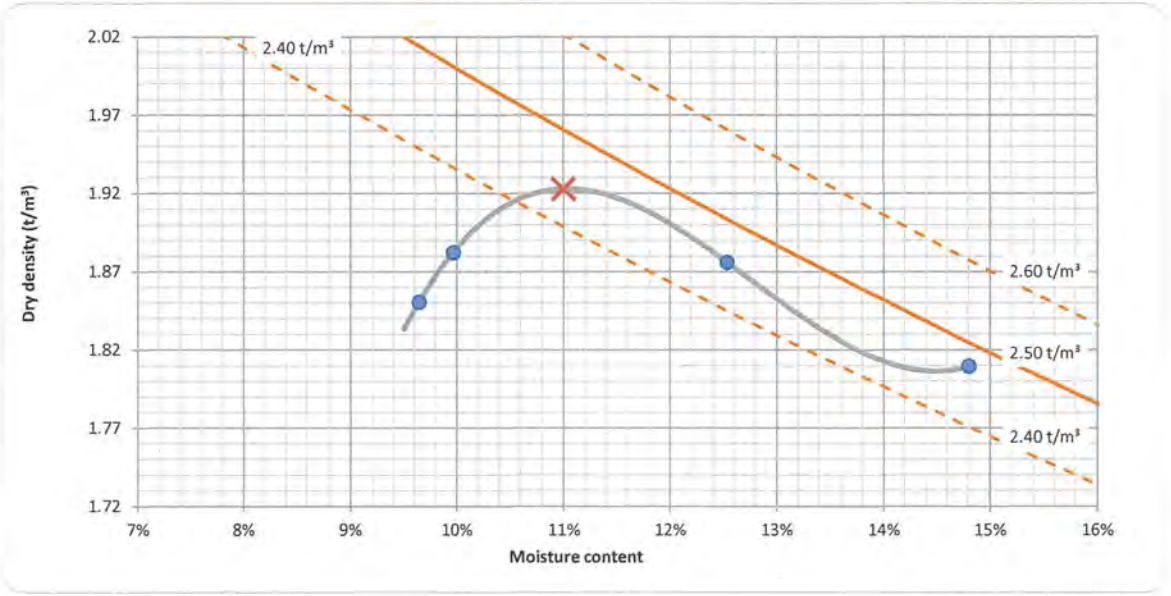


| | Result | Adjusted for oversize |
|---|---|---|
| **Standard maximum dry density (t/m³):** | 1.92 | |
| **Standard optimum moisture content:** | 11.0% | |

**Specimens prepared by:** **Tests performed by:** TK **Date tested:** 15/09/2017

**Definition:** ND = Not Determined **Results reviewed by:** StephenAbbey **Date reported:** 07/10/2017

**Cert. ref.:** NC501_TP05_TRM17-0390_StndComp_s17082177_Rep17011738

**Approved signatory:**

NATA accreditation number: 1961 - Site:1250 - Melbourne

Accredited for compliance with ISO/IEC 17025 - Testing


THIS DOCUMENT SHALL ONLY BE REPRODUCED IN FULL


**Stephen Abbey - Laboratory Manager**


**Phone:** +61 (03) 8862 3500 **Fax:** +61 (03) 8862 3501 **E-mail:** melbgeolab@golder.com.au **Web:** www.golder.com.au


This test was carried out in general accordance with AS 1289.5.1.1-2003.

## Soils testing - Determination of the dry density moisture relationship

Standard compaction method

**AS 1289.5.1.1-2003**


**Golder Associates Pty Ltd**

MELBOURNE GEOTECHNICAL LABORATORY

Building 7, Botanicca Corporate Park

570 - 588 Swan Street

Richmond, Victoria 3121


| | | | | | |
|---|---|---|---|---|---|
| **Test request ID:** | **TRM17-0390** | **Lab sample ID:** | LMEL2017082178 | | |
| **Client:** | The University of Melbourne | | | | |
| **Client address:** | | | | | |
| **Project ID:** | **NC501** | **Lab report ref.:** | LMEL_17011739 | | |
| **Project name:** | ARC Linkage Project LP16010070, Peats Ridge | | **Exporatory Hole** TP07 | **Sample depth (m):** | 0.40 - 0.50 |
| | | | | **Client sample ref:** | 1 |
| **Location:** | | | **Project alias:** | - | |
| **Specimen description:** (Based on visual and tactile assessment) | Clayey/Silty SAND, low plasticity, pale grey brown | | | **Sampling co-ordinates** Easting (m) / Northing (m) | **Reduced Level** |

| **Apparatus:** | **Mould - type: A** | **Compaction hammer** | **Balance** | **Drying oven** |
|---|---|---|---|---|
| **Equipment ID:** | GAMGL09.01.03 | GAMGL10.01.08 | GAMGL01.21 | GAMGL02.12 |
| **Calibration due:** | 10/01/18 | 22/06/18 | 20/10/17 | 13/07/21 |

**Moisture content:** *AS 1289 2.1.1-2005*

**Portion test performed on:** -19 mm

### TEST REPORT - COMPACTION RESULTS

| | Point 1 | Point 2 | Point 3 | Point 4 | Point 5 | Point 6 |
|---|---|---|---|---|---|---|
| **Dry density (t/m³):** | 1.93 | 1.92 | 1.89 | 1.82 | | |
| **Moisture content:** | 9.6% | 10.3% | 12.8% | 6.7% | | |

**Oversize material** - (by wet mass)

No oversize correction required

**+19 mm:** 0%

**+37.5 mm:** 0%

*No oversize material present*

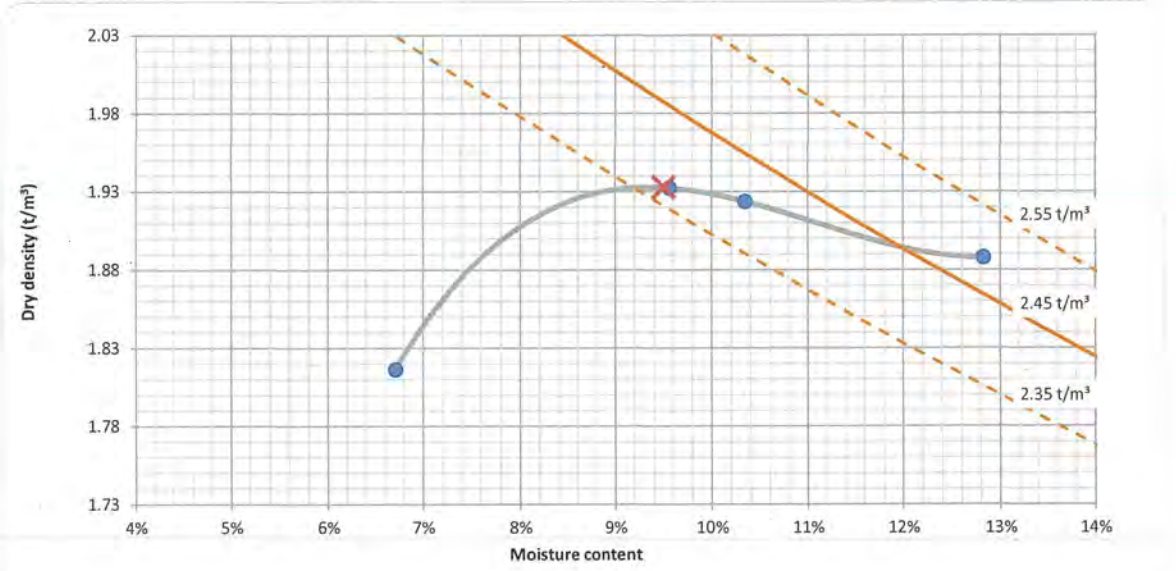


| | Result | Adjusted for oversize |
|---|---|---|
| **Standard maximum dry density (t/m³):** | 1.93 | |
| **Standard optimum moisture content:** | 9.5% | |

**Specimens prepared by:** **Tests performed by:** TK **Date tested:** 18/09/2017

**Definition:** ND = Not Determined **Results reviewed by:** StephenAbbey **Date reported:** 07/10/2017

**Cert. ref.:** NC501_TP07_TRM17-0390_StndComp_s17082178_Rep17011739

**Approved signatory:**

NATA

**NATA accreditation number: 1961 - Site:1250 - Melbourne**

Accredited for compliance with ISO/IEC 17025 - Testing


THIS DOCUMENT SHALL ONLY BE REPRODUCED IN FULL


**Stephen Abbey - Laboratory Manager**


**Phone:** +61 (03) 8862 3500 **Fax:** +61 (03) 8862 3501 **E-mail:** melbgeolab@golder.com.au **Web:** www.golder.com.au

## Soils testing - Determination of the dry density moisture relationship

Standard compaction method

**AS 1289.5.1.1-2003**


**Golder Associates Pty Ltd**

MELBOURNE GEOTECHNICAL LABORATORY

Building 7, Botanicca Corporate Park

570 - 588 Swan Street

Richmond, Victoria 3121


| | | | | | |
|---|---|---|---|---|---|
| **Test request ID:** | **TRM17-0390** | **Lab sample ID:** | LMEL2017082179 | | |
| **Client:** | The University of Melbourne | | | | |
| **Client address:** | | | | | |
| **Project ID:** | **NC501** | **Lab report ref.:** | LMEL_17011740 | | |
| **Project name:** | ARC Linkage Project LP16010070, Peats Ridge | | **Exporatory Hole** **TP09** | **Sample depth (m):** 1.60 - 1.70 **Client sample ref:** 2 | |
| **Location:** | | | | **Project alias:** | - |
| **Specimen description:** (Based on visual and tactile assessment) | CL, Sandy CLAY, low plasticity, white grey | | | **Sampling co-ordinates** Easting (m) / Northing (m) | **Reduced Level** |

| | | | | | |
|---|---|---|---|---|---|
| **Apparatus:** | **Mould - type:** A | **Compaction hammer** | **Balance** | **Drying oven** | **Moisture content:** *AS 1289 2.1.1-2005* |
| **Equipment ID:** | GAMGL09.01.03 | GAMGL10.01.06 | GAMGL01.21 | GAMGL02.13 | |
| **Calibration due:** | 10/01/18 | 19/06/18 | 20/10/17 | 16/01/19 | **Portion test performed on:** -19 mm |

### TEST REPORT - COMPACTION RESULTS

| | Point 1 | Point 2 | Point 3 | Point 4 | Point 5 | Point 6 |
|---|---|---|---|---|---|---|
| **Dry density ($t/m^3$):** | 1.72 | 1.78 | 1.76 | 1.71 | | |
| **Moisture content:** | 12.4% | 14.2% | 16.6% | 19.0% | | |

**Oversize material** - (by wet mass)

No oversize correction required

**+19 mm:** 0%

**+37.5 mm:** 0%

*No oversize material present*

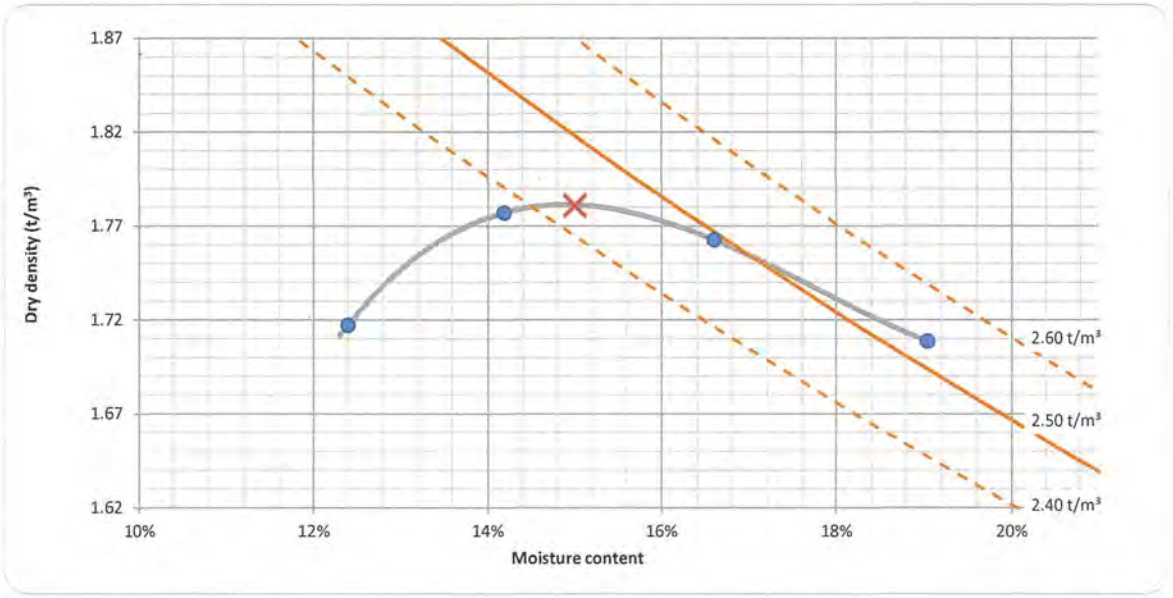


| | Result | Adjusted for oversize |
|---|---|---|
| **Standard maximum dry density ($t/m^3$):** | 1.78 | |
| **Standard optimum moisture content:** | 15.0% | |

**Specimens prepared by:** **Tests performed by:** TK **Date tested:** 18/09/2017

**Definition:** ND = Not Determined **Results reviewed by:** StephenAbbey **Date reported:** 07/10/2017

**Cert. ref.:** NC501_TP09_TRM17-0390_StndComp_s17082179_Rep17011740

**Approved signatory:**

NATA

**NATA accreditation number: 1961 - Site:1250 - Melbourne**

Accredited for compliance with ISO/IEC 17025 - Testing


THIS DOCUMENT SHALL ONLY BE REPRODUCED IN FULL


**Stephen Abbey - Laboratory Manager**


**Phone:** +61 (03) 8862 3500 **Fax:** +61 (03) 8862 3501 **E-mail:** melbgeolab@golder.com.au **Web:** www.golder.com.au


This test was carried out in general accordance with AS 1289.5.1.1-2003.

# IMPORTANT INFORMATION RELATING TO THIS REPORT

The document ("Report") to which this page is attached and which this page forms a part of, has been issued by Golder Associates Pty Ltd ("Golder") subject to the important limitations and other qualifications set out below.

This Report constitutes or is part of services ("Services") provided by Golder to its client ("Client") under and subject to a contract between Golder and its Client ("Contract"). The contents of this page are not intended to and do not alter Golder's obligations (including any limits on those obligations) to its Client under the Contract.

This Report is provided for use solely by Golder's Client and persons acting on the Client's behalf, such as its professional advisers. Golder is responsible only to its Client for this Report. Golder has no responsibility to any other person who relies or makes decisions based upon this Report or who makes any other use of this Report. Golder accepts no responsibility for any loss or damage suffered by any person other than its Client as a result of any reliance upon any part of this Report, decisions made based upon this Report or any other use of it.

This Report has been prepared in the context of the circumstances and purposes referred to in, or derived from, the Contract and Golder accepts no responsibility for use of the Report, in whole or in part, in any other context or circumstance or for any other purpose.

The scope of Golder's Services and the period of time they relate to are determined by the Contract and are subject to restrictions and limitations set out in the Contract. If a service or other work is not expressly referred to in this Report, do not assume that it has been provided or performed. If a matter is not addressed in this Report, do not assume that any determination has been made by Golder in regards to it.

At any location relevant to the Services conditions may exist which were not detected by Golder, in particular due to the specific scope of the investigation Golder has been engaged to undertake. Conditions can only be verified at the exact location of any tests undertaken. Variations in conditions may occur between tested locations and there may be conditions which have not been revealed by the investigation and which have not therefore been taken into account in this Report.

Golder accepts no responsibility for and makes no representation as to the accuracy or completeness of the information provided to it by or on behalf of the Client or sourced from any third party. Golder has assumed that such information is correct unless otherwise stated and no responsibility is accepted by Golder for incomplete or inaccurate data supplied by its Client or any other person for whom Golder is not responsible. Golder has not taken account of matters that may have existed when the Report was prepared but which were only later disclosed to Golder.

Having regard to the matters referred to in the previous paragraphs on this page in particular, carrying out the Services has allowed Golder to form no more than an opinion as to the actual conditions at any relevant location. That opinion is necessarily constrained by the extent of the information collected by Golder or otherwise made available to Golder. Further, the passage of time may affect the accuracy, applicability or usefulness of the opinions, assessments or other information in this Report. This Report is based upon the information and other circumstances that existed and were known to Golder when the Services were performed and this Report was prepared. Golder has not considered the effect of any possible future developments including physical changes to any relevant location or changes to any laws or regulations relevant to such location.

Where permitted by the Contract, Golder may have retained subconsultants affiliated with Golder to provide some or all of the Services. However, it is Golder which remains solely responsible for the Services and there is no legal recourse against any of Golder's affiliated companies or the employees, officers or directors of any of them.

By date, or revision, the Report supersedes any prior report or other document issued by Golder dealing with any matter that is addressed in the Report.

**Any uncertainty as to the extent to which this Report can be used or relied upon in any respect should be referred to Golder for clarification.**

17 November 2017 Reference No. LP16010070-004-L-Rev0

Dr Guillermo Narsilio
The University of Melbourne
Melbourne School of Engineering
VICTORIA 3010

**LINKAGE PROJECT LP16010070, PEATS RIDGE, NSW**
**RESULTS OF THERMAL CONDUCTIVITY TESTS ON REMOULDED SAMPLES**

Dear Guillermo

Golder Associates Pty Ltd (Golder) is collaborating with The University of Melbourne (UoM), University of California (Berkeley) and Ground Source Systems Pty Ltd on Australian Research Council linkage project LP16010070 'Direct geothermal energy: reducing the rural industries' carbon footprint'.

This letter presents the results of initial thermal conductivity tests performed on samples of remoulded soil recovered during geotechnical investigation works at the Brown's Farm site. Please refer to our transmittal dated 1 August 2017 (ref: LP16010070-001-T-Rev0) for preliminary Reports of Test Pits and test pit photographs.

Thermal conductivity tests were performed at Golder's Melbourne laboratory on samples remoulded to a target dry density ratio (DDR) of either 90% or 95% of the maximum dry density for Standard compaction (SMDD) at an initial moisture content equal to the optimum moisture content for Standard compaction (SOMC). Further thermal conductivity tests were performed as the remoulded samples were dried out from the initial moisture content.

Copies of the laboratory thermal conductivity test reports are attached to this letter, together with copies of the geotechnical classification test results for the sample tested (recovered from Test Pit TP01 over a depth interval of 2.3 m to 2.5 m).

The range in the target DDR was selected based on our understanding that excavated soil to be placed over pipe loops in the trenches of the proposed ground-source heat pump system will be only nominally compacted, i.e. track-rolled using an excavator. Figure 1 presents a comparison of the thermal conductivity/moisture content relationship for the remoulded samples. The following comments relate to the test results:

- The thermal conductivity of the sample remoulded to a DDR of 94% of the SMDD is, for the same moisture content, above the thermal conductivity of the sample remoulded to a DDR of 89% of the SMDD.
- At SOMC, the thermal conductivity of the more highly compacted sample (3.23 W/mK) is about 12% more than for the less well-compacted sample (2.88 W/mK). At a moisture content of 0%, the thermal conductivity is about 11% higher for the more highly compacted sample (0.97 W/mK compared to 0.87 W/mK).
- Typical in-situ thermal conductivity values of between about 1.8 W/mK and 2.4 W/mK were recorded during the site investigation. The results of the laboratory thermal conductivity tests are generally consistent with these in-situ values.


Golder, Golder Associates and the GA globe design are trademarks of Golder Associates Corporation

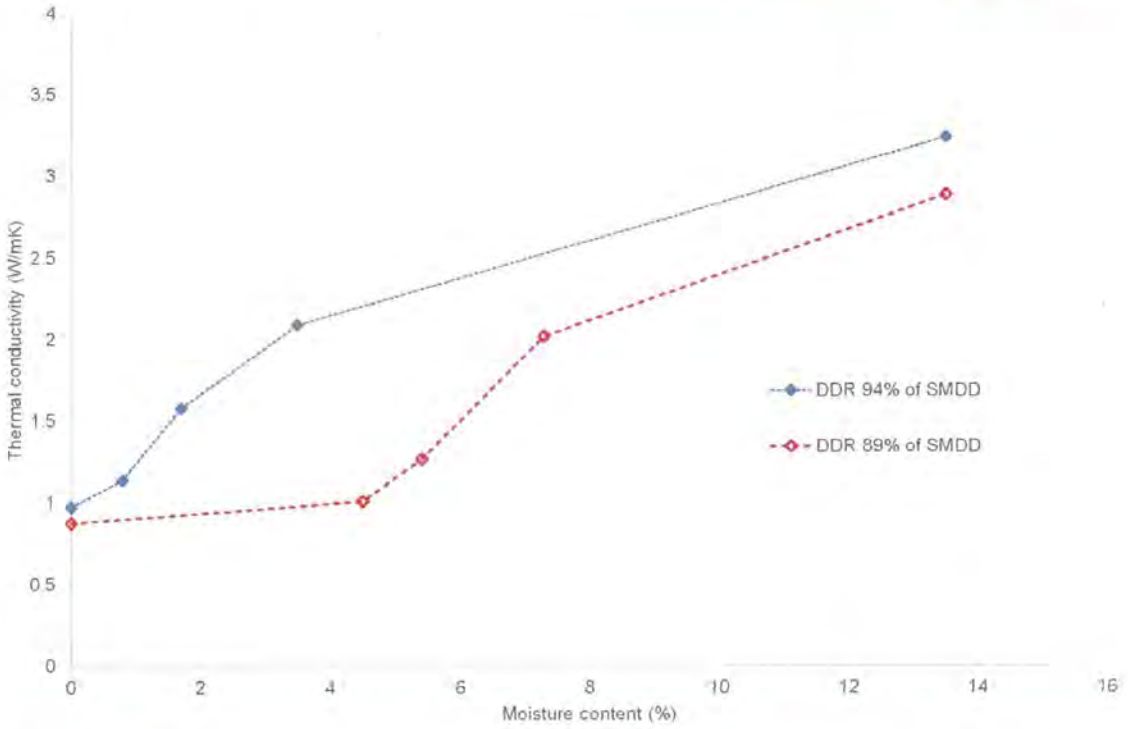


*Figure 1: Comparison of the thermal conductivity test results for samples from Test Pit TP01 (2.3 m to 2.5 m) remoulded to different dry density ratios*

We trust the information presented in this letter is satisfactory for your current requirements. Please do not hesitate to contact Stuart Colls on (03) 8862 3576 if you have any questions.

Yours sincerely,

**GOLDER ASSOCIATES PTY LTD**

Stuart Colls
Associate

SC/ASR/sc

CC: Olga Mikhaylova, Brad Donovan

Attachments: Laboratory test reports (4 pages)
Important information relating to this report (LEG04, RL2)

j:\2017\nc501 - melbourne uni, arc lp16010070\correspondence out\lp16010070-004-l\lp16010070-004-l-rev0.docx

## Soils testing - Particle size distribution & consistency limits test report

Standard method (by sieving)

**AS1289.3.6.1, 2.1.1, 3.1.2, 3.2.1, 3.3.1 & 3.4.1**


Golder Associates

Golder Associates Pty Ltd

MELBOURNE GEOTECHNICAL LABORATORY

Building 7, Botanicca Corporate Park

570 - 588 Swan Street

Richmond, Victoria 3121


| | | | |
|---|---|---|---|
| **Test request #:** | TRM17-0390 | **Lab sample ID:** | LMEL2017082175 |
| **Client:** | The University of Melbourne | | |
| **Client address:** | | | |
| **Project ID:** | NC501 | **Lab report ref.:** | LMEL_17011733 |
| **Project name:** | ARC Linkage Project LP16010070, Peats Ridge | **Exploratory Hole:** | TP01 |
| **Sample depth (m):** | 2.30 - 2.50 | **Client sample ref:** | 2 |
| **Location:** | The University of Melbourne | **Project reference:** | |

| Specimen description: (Based on visual and tactile assessment) | Clayey/Silty SAND, low plasticity, pale yellow, trace of gravel | Sampling co-ordinates: Easting (m) | Northing (m) | Reduced Level |
|---|---|---|---|---|
| PARTICLE SIZE DISTRIBUTION AS 1289.3.6.1 | | | | |

| Sieve Size | Passing | LB S | UB S |
|---|---|---|---|
| 125 mm | 100% | | |
| 75 mm | 100% | | |
| 63 mm | 100% | | |
| 53 mm | 100% | | |
| 37.5 mm | 100% | | |
| 26.5 mm | 100% | | |
| 19 mm | 100% | | |
| 13.2 mm | 97% | | |
| 9.5 mm | 97% | | |
| 6.7 mm | 96% | | |
| 4.75 mm | 96% | | |
| 2.36 mm | 95% | | |
| 1.18 mm | 93% | | |
| 600 µm | 88% | | |
| 425 µm | 79% | | |
| 300 µm | 54% | | |
| 150 µm | 21% | | |
| 75 µm | 15% | | |

| Method: | AS 1289.2.1.1 | AS 1289.3.1.2 | AS 1289.3.2.1 | AS 1289.3.3.1 | AS 1289.3.4.1 |
|---|---|---|---|---|---|
| | Moisture content | 1 point Liquid limit | Plastic limit | Plasticity index | Linear shrinkage | Curling/ Crumbling/ Cracking |
| Result: | 9.7% As Rcvd. | | | | | |
| LB S: | | | | | | - |
| UB S: | | | | | | - |
| Att. preparation method: | | | | LSM length (mm): | | |

**Specimen history/notes:** Preparation of specimen and testing performed on sample supplied to the laboratory

**Definitions:** LB S = Lower bound specification; LSM = Linear shrinkage mould; UB S = Upper bound specification; N/A = Not applicable; ND = Not determined; SIB = Slip in bowl; NO = Not obtainable; NP = Non plastic

**GRADING SUMMARY**

| Fines | Sand* | Gravel* | Cobbles* |
|---|---|---|---|
| (<75 µm) | (>75 µm - <2 mm) | (>2 mm - <60 mm) | (>60mm - <200 mm) |
| 15.2% | 79.2% | 5.6% | 0.0% |

*Proportions based on linear interpolation between sieve/particle of nearest size and smaller

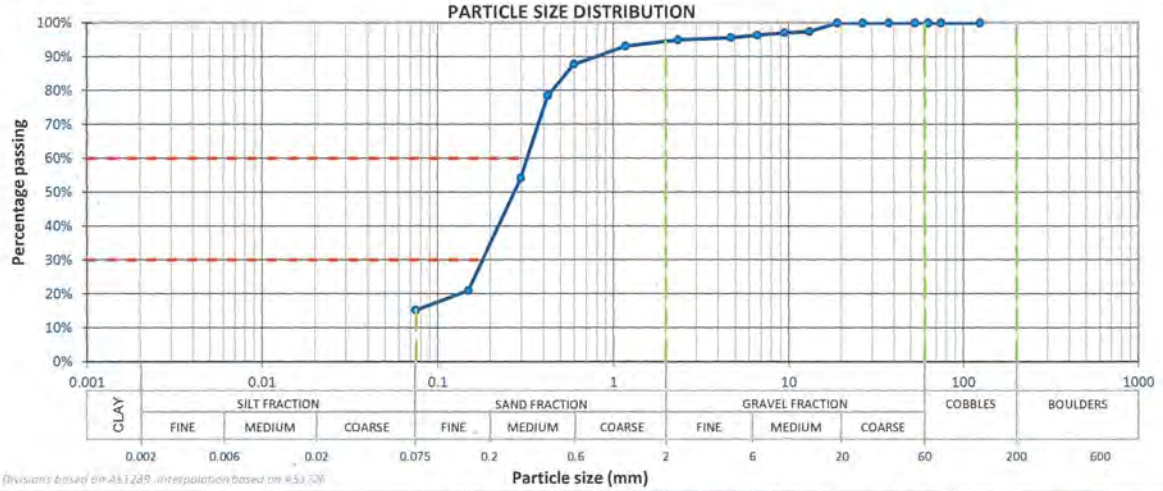


**Testing performed by:** MK **Results reviewed by:** StephenAbbey **Date reported:** 7/10/2017

| Cert. ref.: | NC501_TP01_TRM17-0390_PSD_17082175_Rep17011733 | Approved signatory: |
|---|---|---|
| NATA | NATA accreditation number: 1961 - Site:1250 - Melbourne<br>Accredited for compliance with ISO/IEC 17025 - Testing | |
| | THIS DOCUMENT SHALL ONLY BE REPRODUCED IN FULL | Stephen Abbey - Laboratory Manager |


Phone: +61 (03) 8862 3500 Fax: +61 (03) 8862 3501 E-mail: melbgeolab@golder.com.au Web: www.golder.com.au

## Soils testing - Determination of the dry density moisture relationship

Standard compaction method

**AS 1289.5.1.1-2003**


**Golder Associates Pty Ltd**

MELBOURNE GEOTECHNICAL LABORATORY

Building 7, Botanicca Corporate Park

570 - 588 Swan Street

Richmond, Victoria 3121


| | | | |
|---|---|---|---|
| **Test request ID:** | **TRM17-0390** | **Lab sample ID:** | LMEL2017082175 |
| **Client:** | The University of Melbourne | | |
| **Client address:** | | | |
| **Project ID:** | **NC501** | **Lab report ref.:** | LMEL_17011476 |
| **Project name:** | ARC Linkage Project LP16010070, Peats Ridge | **Exporatory Hole** | **TP01** |
| **Location:** | | **Project alias:** | - |
| **Specimen description:** (Based on visual and tactile assessment) | SAND, low plasticity, pale yellow | | |

**Sample depth (m):** 2.30 - 2.50

**Client sample ref:** 2

**Sampling co-ordinates** Easting (m) / Northing (m) / **Reduced Level**

| | | | | |
|---|---|---|---|---|
| **Apparatus:** | **Mould - type: A** | **Compaction hammer** | **Balance** | **Drying oven** |
| **Equipment ID:** | GAMGL09.01.03 | GAMGL10.01.06 | GAMGL01.21 | GAMGL02.11 |
| **Calibration due:** | 10/01/18 | 19/06/18 | 27/09/17 | 12/07/18 |

**Moisture content:** 11% Field — *AS 1289 2.1.1-2005*

**Portion test performed on:** -19 mm

### TEST REPORT - COMPACTION RESULTS

| | Point 1 | Point 2 | Point 3 | Point 4 | Point 5 | Point 6 |
|---|---|---|---|---|---|---|
| **Dry density ($t/m^3$):** | | 1.79 | 1.81 | 1.85 | 1.81 | |
| **Moisture content:** | | 9.2% | 10.9% | 13.2% | 15.6% | |

**Oversize material** - (by wet mass)

No oversize correction required

**+19 mm:** 0%

**+37.5 mm:** 0%

*No oversize material present*

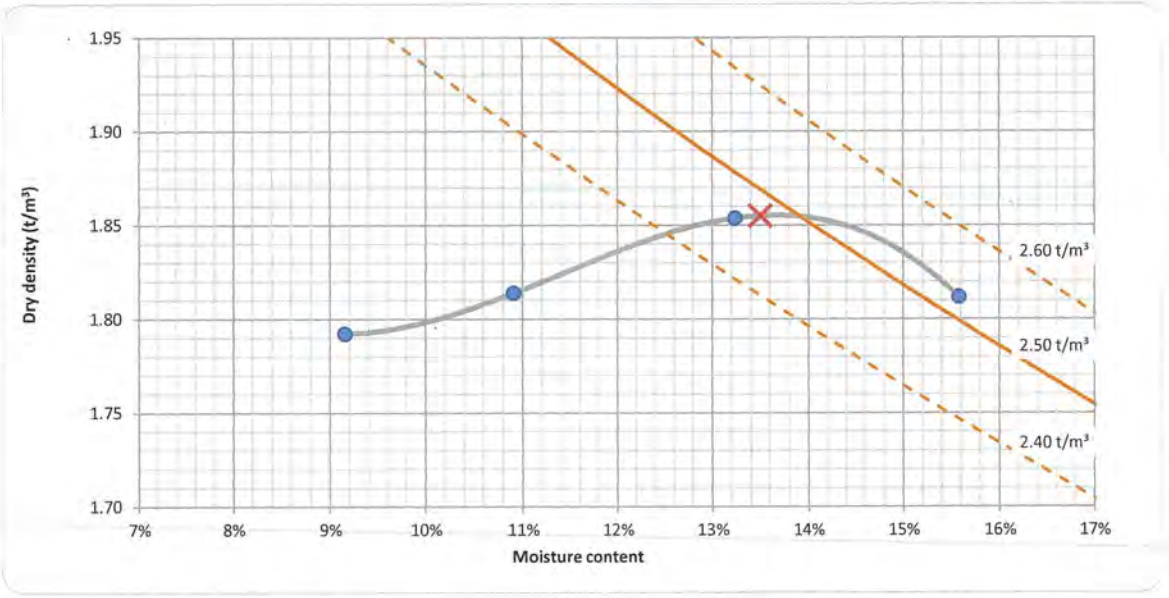


| | Result | Adjusted for oversize |
|---|---|---|
| **Standard maximum dry density ($t/m^3$):** | 1.86 | |
| **Standard optimum moisture content:** | 13.5% | |

**Specimens prepared by:**

**Tests performed by:** TK

**Date tested:** 15/09/2017

**Definition:** ND = Not Determined

**Results reviewed by:** NLobb

**Date reported:** 19/09/2017

**Cert. ref.:** NC501_TP01_TRM17-0390_StndComp_s17082175_Rep17011476

**Approved signatory:**

NATA accreditation number: 1961 - Site:1250 - Melbourne

Accredited for compliance with ISO/IEC 17025 - Testing


THIS DOCUMENT SHALL ONLY BE REPRODUCED IN FULL


**Nick Lobb - Senior Technician**


**Phone:** +61 (03) 8862 3500 **Fax:** +61 (03) 8862 3501 **E-mail:** melbgeolab@golder.com.au **Web:** www.golder.com.au


This test was carried out in general accordance with AS 1289.5.1.1-2003.

## Soils and soft rock testing - Determination of the Thermal Conductivity

By thermal needle probe procedure

**ASTM D5334-14**


**Golder Associates Pty Ltd**

MELBOURNE GEOTECHNICAL LABORATORY

Building 7, Botanicca Corporate Park
570 - 588 Swan Street
Richmond, Victoria 3121


| | | | |
|---|---|---|---|
| **Test request #:** | TRM17-0390 | **Lab sample ID:** | LMEL2017082175 |
| **Client:** | The University of Melbourne | | |
| **Client address:** | | | |
| **Project ID:** | NC501 | **Exporatory Hole** | |
| **Lab project name:** | ARC Linkage Project LP16010070, Peats Ridge | **TP01** | |
| **Sample depth (m):** | 2.30 - 2.50 | | |
| **Client sample ref.:** | 2 | | |
| **Location:** | - | **Project reference:** | - |
| **Specimen description:** (Based on visual and tactile assessment) | Clayey/Silty SAND, low plasticity, pale yellow, trace of gravel | **Sampled by:** | Client |
| | | **Sampled type:** | Remoulded |

### SPECIMEN PREPARATION - SUMMARY OF INITIAL DENSITY AND MOISTURE CONTENT TEST RESULTS

| | | |
|---|---|---|
| **Initial moisture content:** | 11.0% | As rcvd. |
| **Compaction method:** | AS1289.5.1.1-2003 Standard | |
| **Maximum dry density (t/m$^3$):** | 1.86 | |
| **Optimum moisture content:** | 13.5% | |
| **Oversize material (>19mm):** | 0.0% | |
| **Compaction density (t/m$^3$):** | 1.87 | |
| **Compaction moisture content:** | 13.5% | |
| **Density ratio at compaction:** | 89% | |
| **Moisture ratio at compaction:** | 100% | |

*Note:* Remoulded condition: Sample remoulded to target of 90% SMDD at 100% OMC.

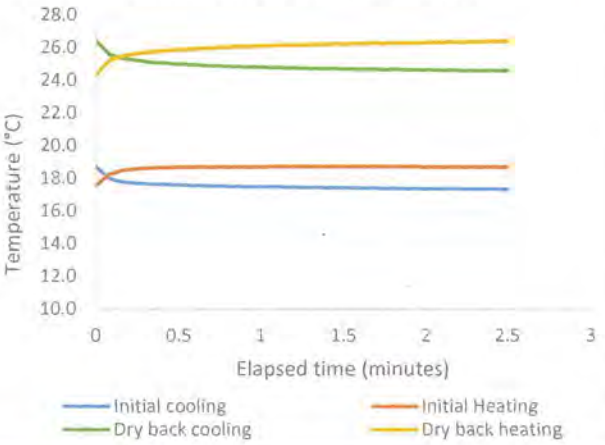


### SUMMARY OF THERMAL CONDUCTIVITY TESTING

| | | | | | | | | | | | | |
|---|---|---|---|---|---|---|---|---|---|---|---|---|
| **Moisture content when tested:** | 13.5% | 7.3% | 5.4% | 4.5% | | | | | | 0.0% | **OMC** | **Dry Back** |
| **Density when tested (t/m$^3$):** | 1.87 | ND | ND | ND | | | | | | ND | **1.87** | **ND** |
| **Thermal conductivity (W/(m.K)** | 2.883 | 2.017 | 1.266 | 1.006 | | | | | | 0.873 | **2.883** | **0.873** |
| **Thermal resistivity (m.K/W)** | 0.347 | 0.496 | 0.790 | 0.994 | | | | | | 1.145 | **0.347** | **1.145** |

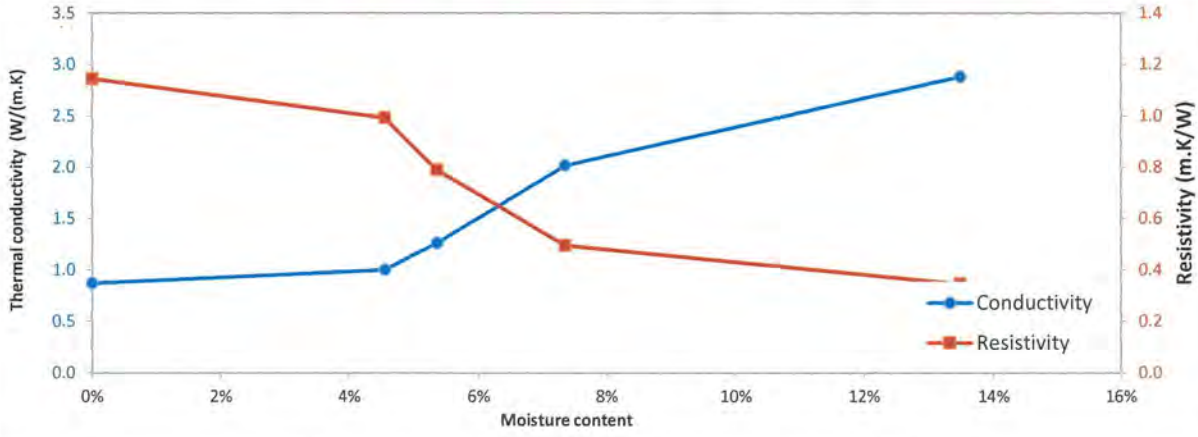


**Definitions:**
ND = Not determined

**Specimen prepared by:** MFA
**Results reviewed by:** GS

**Test performed by:** MFA
**Date reported:** 16-Nov-17

**Cert. ref.:** NC501_TP01_17082175_TRM17-0390_TR_R17012713

**Approved signatory:**


THIS DOCUMENT SHALL ONLY BE REPRODUCED IN FULL


GSamaradiwakara-Senior Laboratory Engineer


Phone: +61 (03) 8862 3500 Fax: +61 (03) 8862 3501 E-mail: melbgeolab@golder.com.au Web: www.golder.com.au


This test was carried out in general accordance with ASTM D5334-14.

## Soils and soft rock testing - Determination of the Thermal Conductivity

By thermal needle probe procedure

**ASTM D5334-14**


**Golder Associates Pty Ltd**

MELBOURNE GEOTECHNICAL LABORATORY

Building 7, Botanicca Corporate Park
570 - 588 Swan Street
Richmond, Victoria 3121


| | | | |
|---|---|---|---|
| **Test request #:** | TRM17-0390 | **Lab sample ID:** | LMEL2017082175 |
| **Client:** | The University of Melbourne | | |
| **Client address:** | - | | |
| **Project ID:** | NC501 | **Exporatory Hole** | TP01 |
| **Lab project name:** | ARC Linkage Project LP16010070, Peats Ridge | **Sample depth (m):** | 2.30 - 2.50 |
| | | **Client sample ref.:** | 2 |
| **Location:** | - | **Project reference:** | - |
| **Specimen description:** (Based on visual and tactile assessment) | Clayey/Silty SAND, low plasticity, pale yellow, trace of gravel | **Sampled by:** | Client |
| | | **Sampled type:** | Remoulded |

### SPECIMEN PREPARATION - SUMMARY OF INITIAL DENSITY AND MOISTURE CONTENT TEST RESULTS

| | | |
|---|---|---|
| **Initial moisture content:** | 11.0% | As rcvd. |
| **Compaction method:** | AS1289.5.1.1-2003 Standard | |
| **Maximum dry density (t/m$^3$):** | 1.86 | |
| **Optimum moisture content:** | 13.5% | |
| **Oversize material (>19mm):** | 0.0% | |
| **Compaction density (t/m$^3$):** | 1.99 | |
| **Compaction moisture content:** | 13.5% | |
| **Density ratio at compaction:** | 94% | |
| **Moisture ratio at compaction:** | 100% | |

*Note:* Remoulded condition: Sample remoulded to target of 95% SMDD at 100% OMC.

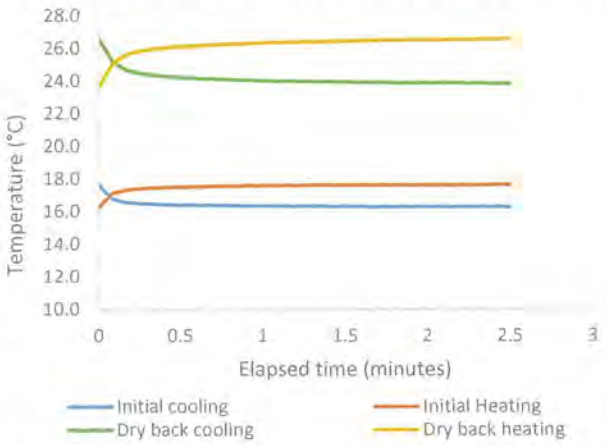


### SUMMARY OF THERMAL CONDUCTIVITY TESTING

| | | | | | | | | | | | | |
|---|---|---|---|---|---|---|---|---|---|---|---|---|
| **Moisture content when tested:** | 13.5% | 3.5% | 1.7% | 0.8% | | | | | | 0.0% | **OMC** | **Dry Back** |
| **Density when tested (t/m$^3$):** | 1.99 | ND | ND | ND | | | | | | ND | **1.99** | **ND** |
| **Thermal conductivity (W/(m.K)** | 3.234 | 2.088 | 1.577 | 1.138 | | | | | | 0.971 | **3.234** | **0.971** |
| **Thermal resistivity (m.K/W)** | 0.309 | 0.479 | 0.634 | 0.879 | | | | | | 1.030 | **0.309** | **1.030** |

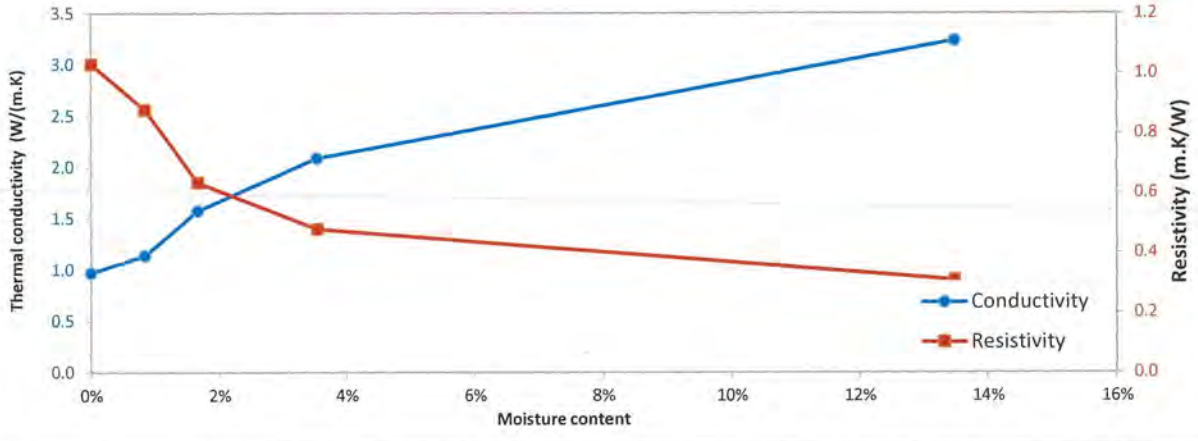


**Definitions:**

ND = Not determined

**Specimen prepared by:** MFA

**Results reviewed by:**

**Test performed by:** MFA

**Date reported:** 16-Nov-17

**Cert. ref.:** NC501_TP01_17082175_TRM17-0390_TR_R17012712

**Approved signatory:**

GSamaradiwakara-Senior Laboratory Engineer


THIS DOCUMENT SHALL ONLY BE REPRODUCED IN FULL



Phone: +61 (03) 8862 3500 Fax: +61 (03) 8862 3501 E-mail: melbgeolab@golder.com.au Web: www.golder.com.au


This test was carried out in general accordance with ASTM D5334-14.

# IMPORTANT INFORMATION RELATING TO THIS REPORT

The document ("Report") to which this page is attached and which this page forms a part of, has been issued by Golder Associates Pty Ltd ("Golder") subject to the important limitations and other qualifications set out below.

This Report constitutes or is part of services ("Services") provided by Golder to its client ("Client") under and subject to a contract between Golder and its Client ("Contract"). The contents of this page are not intended to and do not alter Golder's obligations (including any limits on those obligations) to its Client under the Contract.

This Report is provided for use solely by Golder's Client and persons acting on the Client's behalf, such as its professional advisers. Golder is responsible only to its Client for this Report. Golder has no responsibility to any other person who relies or makes decisions based upon this Report or who makes any other use of this Report. Golder accepts no responsibility for any loss or damage suffered by any person other than its Client as a result of any reliance upon any part of this Report, decisions made based upon this Report or any other use of it.

This Report has been prepared in the context of the circumstances and purposes referred to in, or derived from, the Contract and Golder accepts no responsibility for use of the Report, in whole or in part, in any other context or circumstance or for any other purpose.

The scope of Golder's Services and the period of time they relate to are determined by the Contract and are subject to restrictions and limitations set out in the Contract. If a service or other work is not expressly referred to in this Report, do not assume that it has been provided or performed. If a matter is not addressed in this Report, do not assume that any determination has been made by Golder in regards to it.

At any location relevant to the Services conditions may exist which were not detected by Golder, in particular due to the specific scope of the investigation Golder has been engaged to undertake. Conditions can only be verified at the exact location of any tests undertaken. Variations in conditions may occur between tested locations and there may be conditions which have not been revealed by the investigation and which have not therefore been taken into account in this Report.

Golder accepts no responsibility for and makes no representation as to the accuracy or completeness of the information provided to it by or on behalf of the Client or sourced from any third party. Golder has assumed that such information is correct unless otherwise stated and no responsibility is accepted by Golder for incomplete or inaccurate data supplied by its Client or any other person for whom Golder is not responsible. Golder has not taken account of matters that may have existed when the Report was prepared but which were only later disclosed to Golder.

Having regard to the matters referred to in the previous paragraphs on this page in particular, carrying out the Services has allowed Golder to form no more than an opinion as to the actual conditions at any relevant location. That opinion is necessarily constrained by the extent of the information collected by Golder or otherwise made available to Golder. Further, the passage of time may affect the accuracy, applicability or usefulness of the opinions, assessments or other information in this Report. This Report is based upon the information and other circumstances that existed and were known to Golder when the Services were performed and this Report was prepared. Golder has not considered the effect of any possible future developments including physical changes to any relevant location or changes to any laws or regulations relevant to such location.

Where permitted by the Contract, Golder may have retained subconsultants affiliated with Golder to provide some or all of the Services. However, it is Golder which remains solely responsible for the Services and there is no legal recourse against any of Golder's affiliated companies or the employees, officers or directors of any of them.

By date, or revision, the Report supersedes any prior report or other document issued by Golder dealing with any matter that is addressed in the Report.

**Any uncertainty as to the extent to which this Report can be used or relied upon in any respect should be referred to Golder for clarification.**

# TRANSMITTAL

30 August 2019

**Reference No.** LP16010070-005-T-Rev0

Yu (Jake) Zhou
University of Melbourne
Melbourne School of Engineering
VIC 3010
cc: Guillermo Narisilio

**FROM** Stuart Colls

**EMAIL** scolls@golder.com.au

**LINKAGE PROJECT LP16010070**
**REPORTS OF TEST PITS FROM INVESTIGATION AT PEATS RIDGE, NSW**

**Select one checkbox only**

| | |
|---|---|
| ☐ **Mail/Express Post** | ☐ **Enclosed** |
| ☐ **Same Day Courier** _____ | ☐ **Picked Up** |
| ☐ **Overnight Courier** _____ | ☐ **Hand Delivered** |
| ☐ **Air Freight** _____ | ☐ **Other** _____ |
| ☑ **Email** _____ | |

| Quantity | Item | Description |
|---|---|---|
| 9 | Reports of Test Pits | Reports of Test Pits TP01 to TP09 with test pit photographs. Test pits excavated July 2017. |
| 3 | Explanatory notes to be read in conjunction with Reports of Test Pits | Explanation of notes, abbreviations & terms used on borehole and test pit reports<br>Method of soil description used on borehole and test pit reports<br>Terms for rock material strength & weathering and abbreviations for defect descriptions |

Notes

Approximate test pit locations are as indicated on the Reports of Test Pits. The results of in-situ thermal conductivity measurements (performed using the Decagon KD-2 Pro Thermal Properties Analyser) are indicated on the Reports of Test Pits.

**Please advise us if enclosures are not as described.**

ACKNOWLEDGEMENT REQUIRED:
☐ YES (please email/fax to Golder) ☑ NO

LRL/SC/lrl

j:\2017\nc501 - melbourne uni, arc lp16010070\correspondence out\lp16010070-005-t\new format\lp16010070-005-t-rev0.docx

**Golder Associates Pty Ltd**
Building 7, Botanicca Corporate Park, 570 – 588 Swan Street, Richmond, Victoria 3121, Australia
A.B.N. 64 006 107 857

T: +61 3 8862 3500 F: +61 3 8862 3501

Golder and the G logo are trademarks of Golder Associates Corporation

# REPORT OF TEST PIT: TP01

| | | | |
|---|---|---|---|
| CLIENT: | Melbourne University | COORDS: 335966.7 m E 6307954.0 m N MGA94 56 | SHEET: 1 OF 1 |
| PROJECT: | Geothermal Chicken Farms | SURFACE RL: DATUM: AHD | MACHINE: IHI 55N |
| LOCATION: | Peats Ridge (Brown's) | PIT DEPTH: 2.60 m | CONTRACTOR: G.E.D. Civil |
| JOB NO: | NC501 | BUCKET TYPE: 450mm | LOGGED: PGS DATE: 25/7/17 |
| | | | CHECKED: SC DATE: 30/8/19 |

| Excavation | | | | | Sampling | | Field Material Description | | | | | |
|---|---|---|---|---|---|---|---|---|---|---|---|---|
| METHOD | EXCAVATION RESISTANCE | WATER | DEPTH (metres) | DEPTH RL | SAMPLE OR FIELD TEST | RECOVERED | GRAPHIC LOG | USCS SYMBOL | SOIL/ROCK MATERIAL DESCRIPTION | MOISTURE CONDITION | CONSISTENCY DENSITY | STRUCTURE AND ADDITIONAL OBSERVATIONS |
| EX | L | | 0.0 | 0.20 | | | | SP | TOPSOIL: SAND<br>fine to medium grained, sub-rounded, dark brown, trace silt, with some rootlets | | L | |
| | | | | | | | | | rootlets no longer observed | | | |
| | | | 0.5 | 0.50 | | | | SP | SAND<br>fine to medium grained, sub-rounded, orange brown | | | 0.70 m:<br>Temperature = 13.59 degrees C<br>Termal resistivity = 53.38 (degrees C.cm/W)<br>Error = 0.0040 |
| | | | 1.0 | 1.20 | | | | | with some ironstone cobbles | M | L - MD | |
| | | | 1.5 | | | | | | | | | |
| | | | 2.0 | 2.20 | | | | | | | | |
| | M | | | | TP01-02<br>BDS 2.30-2.50 m<br>Rec = 200/200 mm | | | | pale grey and orange brown with red, with boulders up to 450 mm in diameter | | MD | 2.20 m:<br>Temperature = 15.73 degrees C<br>Termal resistivity = 21.21 (degrees C.cm/W)<br>Error = 0.0364 |
| | | | 2.5 | 2.50 | | | | | | | | |
| | H<br>R | | | | | | | | SANDSTONE, medium grained, pale grey, very low strength, extremely to highly weathered | | | |
| | | | | | | | | | TEST PIT DISCONTINUED @ 2.60 m<br>REFUSAL ON SANDSTONE<br>GROUNDWATER NOT ENCOUNTERED<br>BACKFILLED AND TAMPED | | | |
| | | | 3.0 | | | | | | | | | |
| | | | 3.5 | | | | | | | | | |
| | | | 4.0 | | | | | | | | | |
| | | | 4.5 | | | | | | | | | |
| | | | 5.0 | | | | | | | | | |

This report of test pit must be read in conjunction with accompanying notes and abbreviations. It has been prepared for geotechnical purposes only, without attempt to assess possible contamination. Any references to potential contamination are for information only and do not necessarily indicate the presence or absence of soil or groundwater contamination.

GAP gINT FN. F01e
RL3

GAP 8_13.0 LIB.GLB Log GAP NON-CORED FULL PAGE NC501-GEOTHERMAL CHICKEN FARM.GPJ <<DrawingFile>> 30/08/2019 13:53 8.30.004 Datgel Tools

# REPORT OF TEST PIT PHOTOGRAPHS: TP01

| | | | |
|---|---|---|---|
| CLIENT: | Melbourne University | COORDS: 335966.7 m E 6307954.0 m N MGA94 56 | SHEET: 1 OF 1 |
| PROJECT: | Geothermal Chicken Farms | SURFACE RL: DATUM: AHD | MACHINE: IHI 55N |
| LOCATION: | Peats Ridge (Brown's) | PIT DEPTH: 2.60 m | CONTRACTOR: G.E.D. Civil |
| JOB NO: | NC501 | BUCKET TYPE: 450mm | LOGGED: PGS DATE: 25/7/17 |
| | | | CHECKED: SC DATE: 30/8/19 |

1. Excavation

2. Spoil

This report of test pit photographs must be read in conjunction with accompanying notes and abbreviations. It has been prepared for geotechnical purposes only, without attempt to assess possible contamination. Any references to potential contamination are for information only and do not necessarily indicate the presence or absence of soil or groundwater contamination.



GAP 8_13.0 LIB.GLB GrfcTbl GAP TEST PIT PHOTO 2 PER PAGE NC501-GEOTHERMAL CHICKEN FARM.GPJ <<DrawingFile>> 30/08/2019 14:09 8.30.004 Datgel Tools

# REPORT OF TEST PIT: TP02

| | | | |
|---|---|---|---|
| CLIENT: | Melbourne University | COORDS: 335985.5 m E 6308037.5 m N MGA94 56 | SHEET: 1 OF 1 |
| PROJECT: | Geothermal Chicken Farms | SURFACE RL: DATUM: AHD | MACHINE: IHI 55N |
| LOCATION: | Peats Ridge (Brown's) | PIT DEPTH: 2.60 m | CONTRACTOR: G.E.D. Civil |
| JOB NO: | NC501 | BUCKET TYPE: 450mm | LOGGED: PGS DATE: 25/7/17 |
| | | | CHECKED: SC DATE: 30/8/19 |

| Excavation | | | | | Sampling | | Field Material Description | | | | | |
|---|---|---|---|---|---|---|---|---|---|---|---|---|
| METHOD | EXCAVATION RESISTANCE | WATER | DEPTH (metres) | DEPTH RL | SAMPLE OR FIELD TEST | RECOVERED | GRAPHIC LOG | USCS SYMBOL | SOIL/ROCK MATERIAL DESCRIPTION | MOISTURE CONDITION | CONSISTENCY DENSITY | STRUCTURE AND ADDITIONAL OBSERVATIONS |
| EX | L | | 0.0 | 0.20 | | | | SP | TOPSOIL: SAND<br>fine to medium grained, sub-rounded, dark brown, trace silt, with some rootlets | | L | |
| | | | | | | | | | rootlets no longer observed | | | |
| | | | 0.5 | 0.50 | | | | SP | SAND<br>fine to medium grained, sub-rounded, orange brown | M | L - MD | |
| | | | 1.0 | | | | | | | | | |
| | | | 1.5 | 1.50 | TP02-01<br>BDS 1.50-1.60 m<br>Rec = /100 mm | | | | orange brown with pale grey and red brown, with some ironstone cobbles | | | 1.55 m:<br>Temperature = 15.01 degrees C<br>Termal resistivity = 40.96 (degrees C.cm/W)<br>Error = 0.0124 |
| | | | 2.0 | | | | | | | | | |
| | M | | | 2.30 | TP02-02<br>BDS 2.20-2.30 m<br>Rec = /100 mm | | | | with boulders up to 300 mm in diameter | | MD | |
| | H | | 2.5 | 2.50 | | | | | SANDSTONE, medium grained, pale grey and red brown, highly weathered, low to medium strength | | | |
| | R | | | | | | | | TEST PIT DISCONTINUED @ 2.60 m<br>REFUSAL ON SANDSTONE<br>GROUNDWATER NOT ENCOUNTERED<br>BACKFILLED AND TAMPED | | | |
| | | | 3.0 | | | | | | | | | |
| | | | 3.5 | | | | | | | | | |
| | | | 4.0 | | | | | | | | | |
| | | | 4.5 | | | | | | | | | |
| | | | 5.0 | | | | | | | | | |

This report of test pit must be read in conjunction with accompanying notes and abbreviations. It has been prepared for geotechnical purposes only, without attempt to assess possible contamination. Any references to potential contamination are for information only and do not necessarily indicate the presence or absence of soil or groundwater contamination.

GAP gINT FN. F01e RL3

GAP 8_13.0 LIB.GLB Log GAP NON-CORED FULL PAGE NC501-GEOTHERMAL CHICKEN FARM.GPJ <<DrawingFile>> 30/08/2019 13:53 8.30.004 Datgel Tools

# REPORT OF TEST PIT PHOTOGRAPHS: TP02

| | | | |
|---|---|---|---|
| CLIENT: | Melbourne University | COORDS: 335985.5 m E 6308037.5 m N MGA94 56 | SHEET: 1 OF 1 |
| PROJECT: | Geothermal Chicken Farms | SURFACE RL: DATUM: AHD | MACHINE: IHI 55N |
| LOCATION: | Peats Ridge (Brown's) | PIT DEPTH: 2.60 m | CONTRACTOR: G.E.D. Civil |
| JOB NO: | NC501 | BUCKET TYPE: 450mm | LOGGED: PGS DATE: 25/7/17 |
| | | | CHECKED: SC DATE: 30/8/19 |

1. Excavation

2. Spoil

This report of test pit photographs must be read in conjunction with accompanying notes and abbreviations. It has been prepared for geotechnical purposes only, without attempt to assess possible contamination. Any references to potential contamination are for information only and do not necessarily indicate the presence or absence of soil or groundwater contamination.



GAP 8_13.0 LIB.GLB GrfcTbl GAP TEST PIT PHOTO 2 PER PAGE NC501-GEOTHERMAL CHICKEN FARM.GPJ <<DrawingFile>> 30/08/2019 14:09 8.30.004 Datgel Tools

# REPORT OF TEST PIT: TP03

| | | | |
|---|---|---|---|
| CLIENT: | Melbourne University | COORDS: 336022.5 m E 6308049.3 m N MGA94 56 | SHEET: 1 OF 1 |
| PROJECT: | Geothermal Chicken Farms | SURFACE RL: DATUM: AHD | MACHINE: IHI 55N |
| LOCATION: | Peats Ridge (Brown's) | PIT DEPTH: 3.10 m | CONTRACTOR: G.E.D. Civil |
| JOB NO: | NC501 | BUCKET TYPE: 450mm | LOGGED: PGS DATE: 25/7/17 |
| | | | CHECKED: SC DATE: 30/8/19 |

| Excavation | | | | | Sampling | | Field Material Description | | | | | |
|---|---|---|---|---|---|---|---|---|---|---|---|---|
| METHOD | EXCAVATION RESISTANCE | WATER | DEPTH (metres) | *DEPTH* RL | SAMPLE OR FIELD TEST | RECOVERED | GRAPHIC LOG | USCS SYMBOL | SOIL/ROCK MATERIAL DESCRIPTION | MOISTURE CONDITION | CONSISTENCY DENSITY | STRUCTURE AND ADDITIONAL OBSERVATIONS |
| EX | L | | 0.0 | | | | | SP | TOPSOIL: SAND<br>fine to medium grained, sub-rounded, dark brown, trace silt, with some rootlets | | L | |
| | | | | *0.20* | | | | | rootlets no longer observed | | | |
| | | | | *0.40* | | | | SP | SAND<br>fine to medium grained, sub-rounded, orange brown | M | L - MD | |
| | | | 0.5 | | | | | | | | | |
| | | | 1.0 | | | | | | | | | |
| | | | 1.5 | | | | | | | | | |
| | | | 2.0 | | | | | | | | | |
| | | | 2.5 | *2.50* | TP03-01<br>BDS 2.50-2.70 m<br>Rec = 200/200 mm | | | | orange brown and pale grey | | | |
| | H | | | *2.90* | | | | | with some ironstone cobbles | | MD | |
| | R | | 3.0 | | | | | | TEST PIT DISCONTINUED @ 3.10 m<br>REFUSAL ON SANDSTONE<br>GROUNDWATER NOT ENCOUNTERED<br>BACKFILLED AND TAMPED | | | |
| | | | 3.5 | | | | | | | | | |
| | | | 4.0 | | | | | | | | | |
| | | | 4.5 | | | | | | | | | |
| | | | 5.0 | | | | | | | | | |

This report of test pit must be read in conjunction with accompanying notes and abbreviations. It has been prepared for geotechnical purposes only, without attempt to assess possible contamination. Any references to potential contamination are for information only and do not necessarily indicate the presence or absence of soil or groundwater contamination.



GAP 8_13.0 LIB.GLB Log GAP NON-CORED FULL PAGE NC501-GEOTHERMAL CHICKEN FARM.GPJ <<DrawingFile>> 30/08/2019 13:53 8.30.004 Datgel Tools

# REPORT OF TEST PIT PHOTOGRAPHS: TP03

| | | | |
|---|---|---|---|
| CLIENT: | Melbourne University | COORDS: 336022.5 m E 6308049.3 m N MGA94 56 | SHEET: 1 OF 1 |
| PROJECT: | Geothermal Chicken Farms | SURFACE RL: DATUM: AHD | MACHINE: IHI 55N |
| LOCATION: | Peats Ridge (Brown's) | PIT DEPTH: 3.10 m | CONTRACTOR: G.E.D. Civil |
| JOB NO: | NC501 | BUCKET TYPE: 450mm | LOGGED: PGS DATE: 25/7/17 |
| | | | CHECKED: SC DATE: 30/8/19 |

1. Excavation

2. Spoil

This report of test pit photographs must be read in conjunction with accompanying notes and abbreviations. It has been prepared for geotechnical purposes only, without attempt to assess possible contamination. Any references to potential contamination are for information only and do not necessarily indicate the presence or absence of soil or groundwater contamination.



GAP 8_13.0 LIB.GLB GrfcTbl GAP TEST PIT PHOTO 2 PER PAGE NC501-GEOTHERMAL CHICKEN FARM.GPJ <<DrawingFile>> 30/08/2019 14:09 8.30.004 Datgel Tools

# REPORT OF TEST PIT: TP04

CLIENT: Melbourne University
PROJECT: Geothermal Chicken Farms
LOCATION: Peats Ridge (Slade's 1)
JOB NO: NC501

COORDS: 335666.5 m E 6308366.7 m N MGA94 56
SURFACE RL: DATUM: AHD
PIT DEPTH: 1.30 m
BUCKET TYPE: 450mm

SHEET: 1 OF 1
MACHINE: IHI 55N
CONTRACTOR: G.E.D. Civil
LOGGED: PGS DATE: 25/7/17
CHECKED: SC DATE: 30/8/19

| Excavation | | | | | Sampling | | Field Material Description | | | | | |
|---|---|---|---|---|---|---|---|---|---|---|---|---|
| METHOD | EXCAVATION RESISTANCE | WATER | DEPTH (metres) | DEPTH RL | SAMPLE OR FIELD TEST | RECOVERED | GRAPHIC LOG | USCS SYMBOL | SOIL/ROCK MATERIAL DESCRIPTION | MOISTURE CONDITION | CONSISTENCY DENSITY | STRUCTURE AND ADDITIONAL OBSERVATIONS |
| EX | L | | 0.0 | 0.20 | | | | SP | TOPSOIL: SAND<br>fine to medium grained, sub-rounded, grey brown, trace silt, with some rootlets | D | L | |
| | | | 0.5 | 0.60 | TP04-01<br>BDS 0.50-0.60 m<br>Rec = 100/100 mm | | | SP | SAND<br>fine to medium grained, sub-rounded, orange brown and pale grey, trace ironstone gravel | | L - MD | |
| | M | | 1.0 | | | | | | with some ironstone cobbles and boulders up to 500 mm in diameter | M | MD | 0.60 m:<br>Temperature = 13.05 degrees C<br>Termal resistivity = 60.54 (degrees C.cm/W)<br>Error = 0.0019 |
| | R | | 1.5 | | | | | | TEST PIT DISCONTINUED @ 1.30 m<br>REFUSAL ON IRONSTONE BOULDERS<br>GROUNDWATER NOT OBSERVED<br>BACKFILLED AND TAMPED | | | |
| | | | 2.0 | | | | | | | | | |
| | | | 2.5 | | | | | | | | | |
| | | | 3.0 | | | | | | | | | |
| | | | 3.5 | | | | | | | | | |
| | | | 4.0 | | | | | | | | | |
| | | | 4.5 | | | | | | | | | |
| | | | 5.0 | | | | | | | | | |

This report of test pit must be read in conjunction with accompanying notes and abbreviations. It has been prepared for geotechnical purposes only, without attempt to assess possible contamination. Any references to potential contamination are for information only and do not necessarily indicate the presence or absence of soil or groundwater contamination.



GAP 8_13.0 LIB.GLB Log GAP NON-CORED FULL PAGE NC501-GEOTHERMAL CHICKEN FARM.GPJ <<DrawingFile>> 30/08/2019 13:53 8.30.004 Datgel Tools

# REPORT OF TEST PIT PHOTOGRAPHS: TP04

| | | | |
|---|---|---|---|
| CLIENT: | Melbourne University | COORDS: 335666.5 m E 6308366.7 m N MGA94 56 | SHEET: 1 OF 1 |
| PROJECT: | Geothermal Chicken Farms | SURFACE RL: DATUM: AHD | MACHINE: IHI 55N |
| LOCATION: | Peats Ridge (Slade's 1) | PIT DEPTH: 1.30 m | CONTRACTOR: G.E.D. Civil |
| JOB NO: | NC501 | BUCKET TYPE: 450mm | LOGGED: PGS DATE: 25/7/17 |
| | | | CHECKED: SC DATE: 30/8/19 |

1. Excavation

2. Spoil

This report of test pit photographs must be read in conjunction with accompanying notes and abbreviations. It has been prepared for geotechnical purposes only, without attempt to assess possible contamination. Any references to potential contamination are for information only and do not necessarily indicate the presence or absence of soil or groundwater contamination.



GAP 8_13.0 LIB.GLB GrfcTbl GAP TEST PIT PHOTO 2 PER PAGE NC501-GEOTHERMAL CHICKEN FARM.GPJ <<DrawingFile>> 30/08/2019 14:09 8.30.004 Datgel Tools

# REPORT OF TEST PIT: TP05

CLIENT: Melbourne University
PROJECT: Geothermal Chicken Farms
LOCATION: Peats Ridge (Slade's 1)
JOB NO: NC501

COORDS: 335648.2 m E 6308442.2 m N MGA94 56
SURFACE RL: DATUM: AHD
PIT DEPTH: 1.45 m
BUCKET TYPE: 450mm

SHEET: 1 OF 1
MACHINE: IHI 55N
CONTRACTOR: G.E.D. Civil
LOGGED: PGS DATE: 25/7/17
CHECKED: SC DATE: 30/8/19

| Excavation | | | | | Sampling | | Field Material Description | | | | | |
|---|---|---|---|---|---|---|---|---|---|---|---|---|
| METHOD | EXCAVATION RESISTANCE | WATER | DEPTH (metres) | DEPTH RL | SAMPLE OR FIELD TEST | RECOVERED | GRAPHIC LOG | USCS SYMBOL | SOIL/ROCK MATERIAL DESCRIPTION | MOISTURE CONDITION | CONSISTENCY DENSITY | STRUCTURE AND ADDITIONAL OBSERVATIONS |
| EX | L | ▽ | 0.0 | | | | | SP | TOPSOIL: SAND<br>fine to medium grained, sub-rounded, grey brown, trace silt, with some roots | D | L | |
| | | | | 0.20 | | | | SP | SAND<br>fine to medium grained, sub-rounded, orange brown | M | L - MD | |
| | | | 0.5 | 0.70 | | | | | with some iron stone cobbles | | | |
| | | | 1.0 | 1.00 | TP05-01<br>BDS 1.00-1.10 m<br>Rec = 100/100 mm | ■ | | | orange brown to pale grey | W | L | 0.85 m:<br>Temperature = 11.87 degrees C<br>Termal resistivity = 43.19 (degrees C.cm/W)<br>Error = 0.0066 |
| | R | | 1.5 | | | | | | TEST PIT DISCONTINUED @ 1.45 m<br>REFUSAL ON IRONSTONE BOULDERS<br>GROUNDWATER INFLOW @ 1.0 m DEPTH<br>BACKFILLED AND TAMPED | | | |
| | | | 2.0 | | | | | | | | | |
| | | | 2.5 | | | | | | | | | |
| | | | 3.0 | | | | | | | | | |
| | | | 3.5 | | | | | | | | | |
| | | | 4.0 | | | | | | | | | |
| | | | 4.5 | | | | | | | | | |
| | | | 5.0 | | | | | | | | | |

This report of test pit must be read in conjunction with accompanying notes and abbreviations. It has been prepared for geotechnical purposes only, without attempt to assess possible contamination. Any references to potential contamination are for information only and do not necessarily indicate the presence or absence of soil or groundwater contamination.



GAP 8_13.0 LIB.GLB Log GAP NON-CORED FULL PAGE NC501-GEOTHERMAL CHICKEN FARM.GPJ <<DrawingFile>> 30/08/2019 13:53 8.30.004 Datgel Tools

# REPORT OF TEST PIT PHOTOGRAPHS: TP05

| | | | |
|---|---|---|---|
| CLIENT: | Melbourne University | COORDS: 335648.2 m E 6308442.2 m N MGA94 56 | SHEET: 1 OF 1 |
| PROJECT: | Geothermal Chicken Farms | SURFACE RL: DATUM: AHD | MACHINE: IHI 55N |
| LOCATION: | Peats Ridge (Slade's 1) | PIT DEPTH: 1.45 m | CONTRACTOR: G.E.D. Civil |
| JOB NO: | NC501 | BUCKET TYPE: 450mm | LOGGED: PGS DATE: 25/7/17 |
| | | | CHECKED: SC DATE: 30/8/19 |

1. Excavation

2. Spoil

This report of test pit photographs must be read in conjunction with accompanying notes and abbreviations. It has been prepared for geotechnical purposes only, without attempt to assess possible contamination. Any references to potential contamination are for information only and do not necessarily indicate the presence or absence of soil or groundwater contamination.



GAP 8_13.0 LIB.GLB GrfcTbl GAP TEST PIT PHOTO 2 PER PAGE NC501-GEOTHERMAL CHICKEN FARM.GPJ <<DrawingFile>> 30/08/2019 14:09 8.30.004 Datgel Tools

# REPORT OF TEST PIT: TP06

CLIENT: Melbourne University
PROJECT: Geothermal Chicken Farms
LOCATION: Peats Ridge (Slade's 1)
JOB NO: NC501

COORDS: 335762.6 m E 6308465.6 m N MGA94 56
SURFACE RL: DATUM: AHD
PIT DEPTH: 1.20 m
BUCKET TYPE: 450mm

SHEET: 1 OF 1
MACHINE: IHI 55N
CONTRACTOR: G.E.D. Civil
LOGGED: PGS DATE: 25/7/17
CHECKED: SC DATE: 30/8/19

| Excavation | | | | | Sampling | | Field Material Description | | | | | |
|---|---|---|---|---|---|---|---|---|---|---|---|---|
| METHOD | EXCAVATION RESISTANCE | WATER | DEPTH (metres) | DEPTH RL | SAMPLE OR FIELD TEST | RECOVERED | GRAPHIC LOG | USCS SYMBOL | SOIL/ROCK MATERIAL DESCRIPTION | MOISTURE CONDITION | CONSISTENCY DENSITY | STRUCTURE AND ADDITIONAL OBSERVATIONS |
| EX | L | | 0.0 | | | | | SP | TOPSOIL: SAND<br>fine to medium grained, sub-rounded, brown grey, trace silt, trace rootlets | D | L | |
| | | | | 0.40 | | | | SP | SAND<br>fine to medium grained, sub-rounded, orange brown | M | L - MD | |
| | | | 0.5 | | TP06-01<br>BDS 0.60-0.70 m<br>Rec = 100/100 mm | | | | | | | 0.7 m:<br>Temperature = 12.81 degrees C<br>Termal resistivity = 57.13 (degrees C.cm/W)<br>Error = 0.0028 |
| | | | | 0.80 | | | | | orange brown and red brown, with some ironstone cobbles | | | |
| | M | | | | | | | | | | MD | |
| | | | 1.0 | 1.00 | | | | | with some ironstone boulders | | | |
| | H | | | | | | | | | | D | |
| | R | | | | | | | | TEST PIT DISCONTINUED @ 1.20 m<br>REFUSAL ON IRONSTONE<br>GROUNDWATER NOT OBSERVED<br>BACKFILLED AND TAMPED | | | |
| | | | 1.5 | | | | | | | | | |
| | | | 2.0 | | | | | | | | | |
| | | | 2.5 | | | | | | | | | |
| | | | 3.0 | | | | | | | | | |
| | | | 3.5 | | | | | | | | | |
| | | | 4.0 | | | | | | | | | |
| | | | 4.5 | | | | | | | | | |
| | | | 5.0 | | | | | | | | | |

This report of test pit must be read in conjunction with accompanying notes and abbreviations. It has been prepared for geotechnical purposes only, without attempt to assess possible contamination. Any references to potential contamination are for information only and do not necessarily indicate the presence or absence of soil or groundwater contamination.



GAP 8_13.0 LIB.GLB Log GAP NON-CORED FULL PAGE NC501-GEOTHERMAL CHICKEN FARM.GPJ <<DrawingFile>> 30/08/2019 13:53 8.30.004 Datgel Tools

# REPORT OF TEST PIT PHOTOGRAPHS: TP06

| | | | |
|---|---|---|---|
| CLIENT: | Melbourne University | COORDS: 335762.6 m E 6308465.6 m N MGA94 56 | SHEET: 1 OF 1 |
| PROJECT: | Geothermal Chicken Farms | SURFACE RL: DATUM: AHD | MACHINE: IHI 55N |
| LOCATION: | Peats Ridge (Slade's 1) | PIT DEPTH: 1.20 m | CONTRACTOR: G.E.D. Civil |
| JOB NO: | NC501 | BUCKET TYPE: 450mm | LOGGED: PGS DATE: 25/7/17 |
| | | | CHECKED: SC DATE: 30/8/19 |

1. Excavation

2. Spoil

This report of test pit photographs must be read in conjunction with accompanying notes and abbreviations. It has been prepared for geotechnical purposes only, without attempt to assess possible contamination. Any references to potential contamination are for information only and do not necessarily indicate the presence or absence of soil or groundwater contamination.



GAP 8_13.0 LIB.GLB GrfcTbl GAP TEST PIT PHOTO 2 PER PAGE NC501-GEOTHERMAL CHICKEN FARM.GPJ <<DrawingFile>> 30/08/2019 14:09 8.30.004 Datgel Tools

# REPORT OF TEST PIT: TP07

| | | | |
|---|---|---|---|
| CLIENT: | Melbourne University | COORDS: 335040.7 m E 6307851.4 m N MGA94 56 | SHEET: 1 OF 1 |
| PROJECT: | Geothermal Chicken Farms | SURFACE RL: DATUM: AHD | MACHINE: IHI 55N |
| LOCATION: | Peats Ridge (Slade's 2) | PIT DEPTH: 2.60 m | CONTRACTOR: G.E.D. Civil |
| JOB NO: | NC501 | BUCKET TYPE: 450mm | LOGGED: PGS DATE: 25/7/17 |
| | | | CHECKED: SC DATE: 30/8/19 |

| Excavation | | | | | Sampling | | Field Material Description | | | | | |
|---|---|---|---|---|---|---|---|---|---|---|---|---|
| METHOD | EXCAVATION RESISTANCE | WATER | DEPTH (metres) | DEPTH RL | SAMPLE OR FIELD TEST | RECOVERED | GRAPHIC LOG | USCS SYMBOL | SOIL/ROCK MATERIAL DESCRIPTION | MOISTURE CONDITION | CONSISTENCY DENSITY | STRUCTURE AND ADDITIONAL OBSERVATIONS |
| EX | L | ▽ | 0.0 | | | | | SP | TOPSOIL: SAND<br>fine to medium grained, sub-rounded, dark brown, trace silt, trace rootlets | D | L | |
| | | | | 0.20 | | | | SP | SAND<br>fine to medium grained, sub-rounded, orange brown, trace clay | | | |
| | | | 0.5 | 0.60 | TP07-01<br>BDS 0.40-0.50 m<br>Rec = 100/100 mm | ■ | | SC | Clayey SAND<br>fine to medium grained, sub-rounded, pale grey with red brown, high plasticity clay | M | L - MD | 0.85 m:<br>Temperature = 13.48 degrees C<br>Termal resistivity = 42.46 (degrees C.cm/W)<br>Error = 0.0021 |
| | | | 1.0 | | | | | | | | | |
| | | | 1.5 | | | | | | | W | L | |
| | | | 2.0 | | | | | | | | | |
| | | | 2.5 | | | | | | TEST PIT DISCONTINUED @ 2.60 m<br>GROUNDWATER ENCOUNTERED AT 1.5 M<br>BACKFILLED AND TAMPED | | | |
| | | | 3.0 | | | | | | | | | |
| | | | 3.5 | | | | | | | | | |
| | | | 4.0 | | | | | | | | | |
| | | | 4.5 | | | | | | | | | |
| | | | 5.0 | | | | | | | | | |

This report of test pit must be read in conjunction with accompanying notes and abbreviations. It has been prepared for geotechnical purposes only, without attempt to assess possible contamination. Any references to potential contamination are for information only and do not necessarily indicate the presence or absence of soil or groundwater contamination.



GAP 8_13.0 LIB.GLB Log GAP NON-CORED FULL PAGE NC501-GEOTHERMAL CHICKEN FARM.GPJ <<DrawingFile>> 30/08/2019 13:53 8.30.004 Datgel Tools

# REPORT OF TEST PIT PHOTOGRAPHS: TP07

| | | | |
|---|---|---|---|
| CLIENT: | Melbourne University | COORDS: 335040.7 m E 6307851.4 m N MGA94 56 | SHEET: 1 OF 1 |
| PROJECT: | Geothermal Chicken Farms | SURFACE RL: DATUM: AHD | MACHINE: IHI 55N |
| LOCATION: | Peats Ridge (Slade's 2) | | CONTRACTOR: G.E.D. Civil |
| JOB NO: | NC501 | PIT DEPTH: 2.60 m | LOGGED: PGS DATE: 25/7/17 |
| | | BUCKET TYPE: 450mm | CHECKED: SC DATE: 30/8/19 |

1. Excavation

2. Spoil

This report of test pit photographs must be read in conjunction with accompanying notes and abbreviations. It has been prepared for geotechnical purposes only, without attempt to assess possible contamination. Any references to potential contamination are for information only and do not necessarily indicate the presence or absence of soil or groundwater contamination.



GAP 8_13.0 LIB.GLB GrfcTbl GAP TEST PIT PHOTO 2 PER PAGE NC501-GEOTHERMAL CHICKEN FARM.GPJ <<DrawingFile>> 30/08/2019 14:09 8.30.004 Datgel Tools

# REPORT OF TEST PIT: TP08

CLIENT: Melbourne University
PROJECT: Geothermal Chicken Farms
LOCATION: Peats Ridge (Slade's 2)
JOB NO: NC501

COORDS: 335016.0 m E 6307752.9 m N MGA94 56
SURFACE RL: DATUM: AHD
PIT DEPTH: 2.40 m
BUCKET TYPE: 450mm

SHEET: 1 OF 1
MACHINE: IHI 55N
CONTRACTOR: G.E.D. Civil
LOGGED: PGS DATE: 25/7/17
CHECKED: SC DATE: 30/8/19

| Excavation | | | | | Sampling | | Field Material Description | | | | | |
|---|---|---|---|---|---|---|---|---|---|---|---|---|
| METHOD | EXCAVATION RESISTANCE | WATER | DEPTH (metres) | DEPTH RL | SAMPLE OR FIELD TEST | RECOVERED | GRAPHIC LOG | USCS SYMBOL | SOIL/ROCK MATERIAL DESCRIPTION | MOISTURE CONDITION | CONSISTENCY DENSITY | STRUCTURE AND ADDITIONAL OBSERVATIONS |
| EX | L | | 0.0 | | | | | SP | TOPSOIL: SAND<br>fine to medium grained, sub-rounded, dark brown, trace silt | D | L | |
| | | | | 0.30 | | | | SP | SAND<br>fine to medium grained, sub-rounded, orange brown, trace clay | M | L - MD | |
| | | | 0.5 | | | | | | | | | |
| | | | | 0.90 | | | | SC | Clayey SAND<br>fine to medium grained, sub-rounded, orange brown | | | |
| | | | 1.0 | | | | | | | | | |
| | | | | 1.50 | | | | | with some medium to coarse grained, sub-rounded gravel | | | |
| | | | 1.5 | | | | | | | | | |
| | | | | 1.80 | | | | | | | | |
| | M | | | | TP08-01<br>BDS 1.80-1.90 m<br>Rec = 100/100 mm | | | GC | Clayey Sandy GRAVEL<br>medium to coarse grained, sub-rounded to sub-angular, orange brown, fine to medium grained sand | | MD - D | |
| | | | 2.0 | | | | | | | | | |
| | R | | 2.5 | | | | | | TEST PIT DISCONTINUED @ 2.40 m<br>REFUSAL ON IRONSTONE<br>GROUNDWATER NOT OBSERVED<br>BACKFILLED AND TAMPED | | | |
| | | | 3.0 | | | | | | | | | |
| | | | 3.5 | | | | | | | | | |
| | | | 4.0 | | | | | | | | | |
| | | | 4.5 | | | | | | | | | |
| | | | 5.0 | | | | | | | | | |

This report of test pit must be read in conjunction with accompanying notes and abbreviations. It has been prepared for geotechnical purposes only, without attempt to assess possible contamination. Any references to potential contamination are for information only and do not necessarily indicate the presence or absence of soil or groundwater contamination.



GAP 8_13.0 LIB.GLB Log GAP NON-CORED FULL PAGE NC501-GEOTHERMAL CHICKEN FARM.GPJ <<DrawingFile>> 30/08/2019 13:53 8.30.004 Datgel Tools

# REPORT OF TEST PIT PHOTOGRAPHS: TP08

| | | | |
|---|---|---|---|
| CLIENT: | Melbourne University | COORDS: 335016.0 m E 6307752.9 m N MGA94 56 | SHEET: 1 OF 1 |
| PROJECT: | Geothermal Chicken Farms | SURFACE RL: DATUM: AHD | MACHINE: IHI 55N |
| LOCATION: | Peats Ridge (Slade's 2) | PIT DEPTH: 2.40 m | CONTRACTOR: G.E.D. Civil |
| JOB NO: | NC501 | BUCKET TYPE: 450mm | LOGGED: PGS DATE: 25/7/17 |
| | | | CHECKED: SC DATE: 30/8/19 |

1. Excavation

2. Spoil

This report of test pit photographs must be read in conjunction with accompanying notes and abbreviations. It has been prepared for geotechnical purposes only, without attempt to assess possible contamination. Any references to potential contamination are for information only and do not necessarily indicate the presence or absence of soil or groundwater contamination.

GAP gINT FN. F27 RL1

GAP 8_13.0 LIB.GLB GrfcTbl GAP TEST PIT PHOTO 2 PER PAGE NC501-GEOTHERMAL CHICKEN FARM.GPJ <<DrawingFile>> 30/08/2019 14:09 8.30.004 Datgel Tools

# REPORT OF TEST PIT: TP09

| | | | |
|---|---|---|---|
| CLIENT: | Melbourne University | COORDS: 334814.8 m E 6306268.8 m N MGA94 56 | SHEET: 1 OF 1 |
| PROJECT: | Geothermal Chicken Farms | SURFACE RL: DATUM: AHD | MACHINE: IHI 55N |
| LOCATION: | Peats Ridge (Horticulture) | PIT DEPTH: 2.00 m | CONTRACTOR: G.E.D. Civil |
| JOB NO: | NC501 | BUCKET TYPE: 450mm | LOGGED: PGS DATE: 25/7/17 |
| | | | CHECKED: SC DATE: 30/8/19 |

| Excavation | | | | | Sampling | | Field Material Description | | | | | |
|---|---|---|---|---|---|---|---|---|---|---|---|---|
| METHOD | EXCAVATION RESISTANCE | WATER | DEPTH (metres) | DEPTH RL | SAMPLE OR FIELD TEST | RECOVERED | GRAPHIC LOG | USCS SYMBOL | SOIL/ROCK MATERIAL DESCRIPTION | MOISTURE CONDITION | CONSISTENCY DENSITY | STRUCTURE AND ADDITIONAL OBSERVATIONS |
| EX | L | | 0.0 | | | | | SP | TOPSOIL: SAND<br>fine to medium grained, sub-rounded, dark brown, trace silt, with some rootlets | | L | |
| | | | | 0.35 | | | | SP | SAND<br>fine to medium grained, sub-rounded, brown | M | L - MD | |
| | | | 0.5 | | | | | | | | | |
| | | | 1.0 | | | | | | | | | |
| | | | | 1.20 | TP09-01<br>BDS 1.20-1.30 m<br>Rec = 100/100 mm | | | SC | Clayey SAND<br>fine to medium grained, sub-rounded, pale grey with orange brown and red brown, high plasticity clay | | | |
| | | | 1.5 | 1.50 | | | | CL | Sandy CLAY<br>low plasticity, pale grey with red brown and orange brown, fine grained sand | w > PL | VSt - H | 1.6 m: Thermal resistivity test undertaken on excavated lump of clay<br>Temperature = 14.58 degrees C<br>Termal resistivity = 42.02 (degrees C.cm/W)<br>Error = 0.0057 |
| | M | | | 1.70 | TP09-02<br>BDS 1.60-1.70 m<br>Rec = 100/100 mm | | | | | | | |
| | M-H | | | | | | | | SANDSTONE, fine grained, pale grey, extremely weathered, extremely low strength | | | |
| | R | | 2.0 | | | | | | TEST PIT DISCONTINUED @ 2.00 m<br>REFUSAL ON SANDSTONE<br>GROUNDWATER NOT OBSERVED<br>BACKFILLED AND TAMPED | | | |
| | | | 2.5 | | | | | | | | | |
| | | | 3.0 | | | | | | | | | |
| | | | 3.5 | | | | | | | | | |
| | | | 4.0 | | | | | | | | | |
| | | | 4.5 | | | | | | | | | |
| | | | 5.0 | | | | | | | | | |

This report of test pit must be read in conjunction with accompanying notes and abbreviations. It has been prepared for geotechnical purposes only, without attempt to assess possible contamination. Any references to potential contamination are for information only and do not necessarily indicate the presence or absence of soil or groundwater contamination.

GAP gINT FN. F01e RL3

GAP 8_13.0 LIB.GLB Log GAP NON-CORED FULL PAGE NC501-GEOTHERMAL CHICKEN FARM.GPJ <<DrawingFile>> 30/08/2019 13:53 8.30.004 Datgel Tools

# REPORT OF TEST PIT PHOTOGRAPHS: TP09

| | | | |
|---|---|---|---|
| CLIENT: | Melbourne University | COORDS: 334814.8 m E 6306268.8 m N MGA94 56 | SHEET: 1 OF 1 |
| PROJECT: | Geothermal Chicken Farms | SURFACE RL: DATUM: AHD | MACHINE: IHI 55N |
| LOCATION: | Peats Ridge (Horticulture) | PIT DEPTH: 2.00 m | CONTRACTOR: G.E.D. Civil |
| JOB NO: | NC501 | BUCKET TYPE: 450mm | LOGGED: PGS DATE: 25/7/17 |
| | | | CHECKED: SC DATE: 30/8/19 |

1. Excavation

2. Spoil

This report of test pit photographs must be read in conjunction with accompanying notes and abbreviations. It has been prepared for geotechnical purposes only, without attempt to assess possible contamination. Any references to potential contamination are for information only and do not necessarily indicate the presence or absence of soil or groundwater contamination.



GAP 8_13.0 LIB.GLB GrfcTbl GAP TEST PIT PHOTO 2 PER PAGE NC501-GEOTHERMAL CHICKEN FARM.GPJ <<DrawingFile>> 30/08/2019 14:09 8.30.004 Datgel Tools

# EXPLANATION OF NOTES, ABBREVIATIONS & TERMS USED ON BOREHOLE AND TEST PIT REPORTS

**DRILLING/EXCAVATION METHOD**

| | | | | | |
|---|---|---|---|---|---|
| AS* | Auger Screwing | RD | Rotary blade or drag bit | NQ | Diamond Core - 47 mm |
| AD* | Auger Drilling | RT | Rotary Tricone bit | NMLC | Diamond Core - 52 mm |
| *V | V-Bit | RAB | Rotary Air Blast | HQ | Diamond Core - 63 mm |
| *T | TC-Bit, e.g. ADT | RC | Reverse Circulation | HMLC | Diamond Core – 63mm |
| HA | Hand Auger | PT | Push Tube | BH | Tractor Mounted Backhoe |
| ADH | Hollow Auger | CT | Cable Tool Rig | EX | Tracked Hydraulic Excavator |
| DTC | Diatube Coring | JET | Jetting | EE | Existing Excavation |
| WB | Washbore or Bailer | NDD | Non-destructive digging | HAND | Excavated by Hand Methods |

**PENETRATION/EXCAVATION RESISTANCE**

**L** **Low resistance.** Rapid penetration possible with little effort from the equipment used.

**M** **Medium resistance.** Excavation/possible at an acceptable rate with moderate effort from the equipment used.

**H** **High resistance** to penetration/excavation. Further penetration is possible at a slow rate and requires significant effort from the equipment.

**R** **Refusal or Practical Refusal.** No further progress possible without the risk of damage or unacceptable wear to the digging implement or machine.

These assessments are subjective and are dependent on many factors including the equipment power, weight, condition of excavation or drilling tools, and the experience of the operator.

**WATER**

| | | | |
|---|---|---|---|
| ▽ | Water level at date shown | ◁ | Partial water loss |
| ▷ | Water inflow | ◀ | Complete water loss |

| | |
|---|---|
| GROUNDWATER NOT OBSERVED | The observation of groundwater, whether present or not, was not possible due to drilling water, surface seepage or cave in of the borehole/test pit. |
| GROUNDWATER NOT ENCOUNTERED | The borehole/test pit was dry soon after excavation. However, groundwater could be present in less permeable strata. Inflow may have been observed had the borehole/test pit been left open for a longer period. |

**SAMPLING AND TESTING**

| | |
|---|---|
| SPT | Standard Penetration Test to AS1289.6.3.1-2004 |
| 4,7,11 N=18 | 4,7,11 = Blows per 150mm. N = Blows per 300mm penetration following 150mm seating |
| 30/80mm | Where practical refusal occurs, the blows and penetration for that interval are reported |
| RW | Penetration occurred under the rod weight only |
| HW | Penetration occurred under the hammer and rod weight only |
| HB | Hammer double bouncing on anvil |
| DS | Disturbed sample |
| BDS | Bulk disturbed sample |
| G | Gas Sample |
| W | Water Sample |
| FP | Field permeability test over section noted |
| FV | Field vane shear test expressed as uncorrected shear strength ($s_v$ = peak value, $s_r$ = residual value) |
| PID | Photoionisation Detector reading in ppm |
| PM | Pressuremeter test over section noted |
| PP | Pocket penetrometer test expressed as instrument reading in kPa |
| U63 | Thin walled tube sample - number indicates nominal sample diameter in millimetres |
| WPT | Water pressure tests |
| DCP | Dynamic cone penetration test |
| CPT | Static cone penetration test |
| CPTu | Static cone penetration test with pore pressure (u) measurement |

**Ranking of Visually Observable Contamination and Odour** (for specific soil contamination assessment projects)

| | | | |
|---|---|---|---|
| R = 0 | No visible evidence of contamination | R = A | No non-natural odours identified |
| R = 1 | Slight evidence of visible contamination | R = B | Slight non-natural odours identified |
| R = 2 | Visible contamination | R = C | Moderate non-natural odours identified |
| R = 3 | Significant visible contamination | R = D | Strong non-natural odours identified |

**ROCK CORE RECOVERY**

TCR = Total Core Recovery (%)

$$= \frac{\text{Length of core recovered}}{\text{Length of core run}} \times 100$$

SCR = Solid Core Recovery (%)

$$= \frac{\sum \text{Length of cylindrical core recovered}}{\text{Length of core run}} \times 100$$

RQD = Rock Quality Designation (%)

$$= \frac{\sum \text{Axial lengths of core} > 100 \text{ mm}}{\text{Length of core run}} \times 100$$

# METHOD OF SOIL DESCRIPTION USED ON BOREHOLE AND TEST PIT REPORTS

FILL

GRAVEL (GP or GW)

SAND (SP or SW)

SILT (ML or MH)

CLAY (CL, CI or CH)

ORGANIC SOILS (OL or OH or Pt)

COBBLES or BOULDERS

Combinations of these basic symbols may be used to indicate mixed materials such as sandy clay.

## CLASSIFICATION AND INFERRED STRATIGRAPHY

Soil and Rock is classified and described in Reports of Boreholes and Test Pits using the preferred method given in AS1726 – 1993, (Amdt1 – 1994 and Amdt2 – 1994), Appendix A. The material properties are assessed in the field by visual/tactile methods.

### Particle Size

| Major Division | Sub Division | Particle Size |
|---|---|---|
| BOULDERS | | > 200 mm |
| COBBLES | | 63 to 200 mm |
| GRAVEL | Coarse | 20 to 63 mm |
| | Medium | 6.0 to 20 mm |
| | Fine | 2.0 to 6.0 mm |
| SAND | Coarse | 0.6 to 2.0 mm |
| | Medium | 0.2 to 0.6 mm |
| | Fine | 0.075 to 0.2 mm |
| SILT | | 0.002 to 0.075 mm |
| CLAY | | < 0.002 mm |

### Plasticity Properties

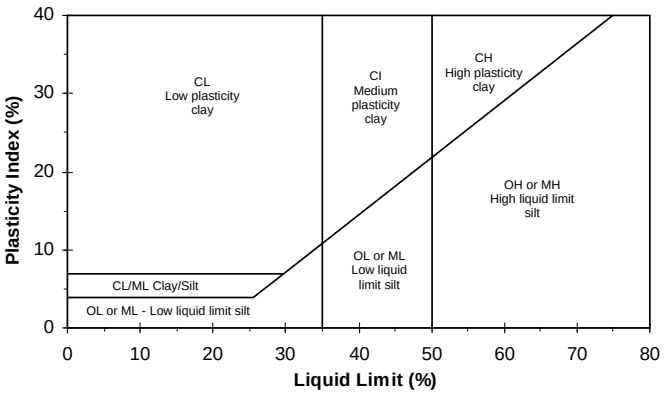


## MOISTURE CONDITION

AS1726 - 1993

| Symbol | Term | Description |
|---|---|---|
| D | Dry | Sands and gravels are free flowing. Clays & Silts may be brittle or friable and powdery. |
| M | Moist | Soils are darker than in the dry condition & may feel cool. Sands and gravels tend to cohere. |
| W | Wet | Soils exude free water. Sands and gravels tend to cohere. |

## CONSISTENCY AND DENSITY

AS1726 - 1993

| Symbol | Term | Undrained Shear Strength |
|---|---|---|
| VS | Very Soft | 0 to 12 kPa |
| S | Soft | 12 to 25 kPa |
| F | Firm | 25 to 50 kPa |
| St | Stiff | 50 to 100 kPa |
| VSt | Very Stiff | 100 to 200 kPa |
| H | Hard | Above 200 kPa |

| Symbol | Term | Density Index % | SPT "N" # |
|---|---|---|---|
| VL | Very Loose | Less than 15 | 0 to 4 |
| L | Loose | 15 to 35 | 4 to 10 |
| MD | Medium Dense | 35 to 65 | 10 to 30 |
| D | Dense | 65 to 85 | 30 to 50 |
| VD | Very Dense | Above 85 | Above 50 |
| | | | |

In the absence of test results, consistency and density may be assessed from correlations with the observed behaviour of the material.

# SPT correlations are not stated in AS1726 – 1993, and may be subject to corrections for overburden pressure and equipment type.

# TERMS FOR ROCK MATERIAL STRENGTH & WEATHERING AND ABBREVIATIONS FOR DEFECT DESCRIPTIONS

**STRENGTH**

| Symbol | Term | Point Load Index, $Is_{(50)}$ (MPa) | Field Guide |
|---|---|---|---|
| EL | Extremely Low | < 0.03 | Easily remoulded by hand to a material with soil properties. |
| VL | Very Low | 0.03 to 0.1 | Material crumbles under firm blows with sharp end of pick; can be peeled with knife; too hard to cut a triaxial sample by hand. Pieces up to 30 mm can be broken by finger pressure. |
| L | Low | 0.1 to 0.3 | Easily scored with a knife; indentations 1 mm to 3 mm show in the specimen with firm blows of pick point; has dull sound under hammer. A piece of core 150 mm long by 50 mm diameter may be broken by hand. Sharp edges of core may be friable and break during handling. |
| M | Medium | 0.3 to 1 | Readily scored with a knife; a piece of core 150 mm long by 50 mm diameter can be broken by hand with difficulty. |
| H | High | 1 to 3 | A piece of core 150 mm long by 50 mm diameter cannot be broken by hand but can be broken with pick with a single firm blow; rock rings under hammer. |
| VH | Very High | 3 to 10 | Hand specimen breaks with pick after more than one blow; rock rings under hammer. |
| EH | Extremely High | >10 | Specimen requires many blows with geological pick to break through intact material; rock rings under hammer. |

**ROCK STRENGTH TEST RESULTS**

▼ Point Load Strength Index, $I_s(50)$, Axial test (MPa)

◀ Point Load Strength Index, $I_s(50)$, Diametral test (MPa)

Relationship between $I_s(50)$ and UCS (unconfined compressive strength) will vary with rock type and strength, and should be determined on a site-specific basis. UCS is typically 10 to 30 x $I_s(50)$, but can be as low as 5.

**ROCK MATERIAL WEATHERING**

| Symbol | | Term | Field Guide |
|---|---|---|---|
| RS | | Residual Soil | Soil developed on extremely weathered rock; the mass structure and substance fabric are no longer evident; there is a large change in volume but the soil has not been significantly transported. |
| EW | | Extremely Weathered | Rock is weathered to such an extent that it has soil properties - i.e. it either disintegrates or can be remoulded, in water. |
| DW | HW | Distinctly Weathered | Rock strength usually changed by weathering. The rock may be highly discoloured, usually by iron staining. Porosity may be increased by leaching, or may be decreased due to deposition of weathering products in pores. In some environments it is convenient to subdivide into Highly Weathered and Moderately Weathered, with the degree of alteration typically less for MW. |
| | MW | | |
| SW | | Slightly Weathered | Rock is slightly discoloured but shows little or no change of strength relative to fresh rock. |
| FR | | Fresh | Rock shows no sign of decomposition or staining. |

**ABBREVIATIONS FOR DEFECT TYPES AND DESCRIPTIONS**

**Defect Type**

| | |
|---|---|
| B | Bedding parting |
| X | Foliation |
| C | Contact |
| L | Cleavage |
| J | Joint |
| SS/SZ | Sheared seam/zone (Fault) |
| CS/CZ | Crushed seam/zone (Fault) |
| DS/DZ | Decomposed seam/zone |
| IS/IZ | Infilled seam/zone |
| S | Schistocity |
| V | Vein |

**Coating or Infilling**

| | |
|---|---|
| Cn | Clean |
| Sn | Stain |
| Vr | Veneer |
| Ct | Coating or Infill |

**Planarity**

| | |
|---|---|
| Pl | Planar |
| Un | Undulating |
| St | Stepped |

**Roughness**

| | |
|---|---|
| Sl | Slickensided |
| Sm | Smooth |
| Ro | Rough |

**Vertical Boreholes –** The dip (inclination from horizontal) of the defect is given.

**Inclined Boreholes –** The inclination is measured as the acute angle to the core axis.

# Appendix C System design and instrumentation drawings

This appendix contains the system design and instrumentation drawings (as-built status) prepared by the author which is related mainly to Chapter 3.

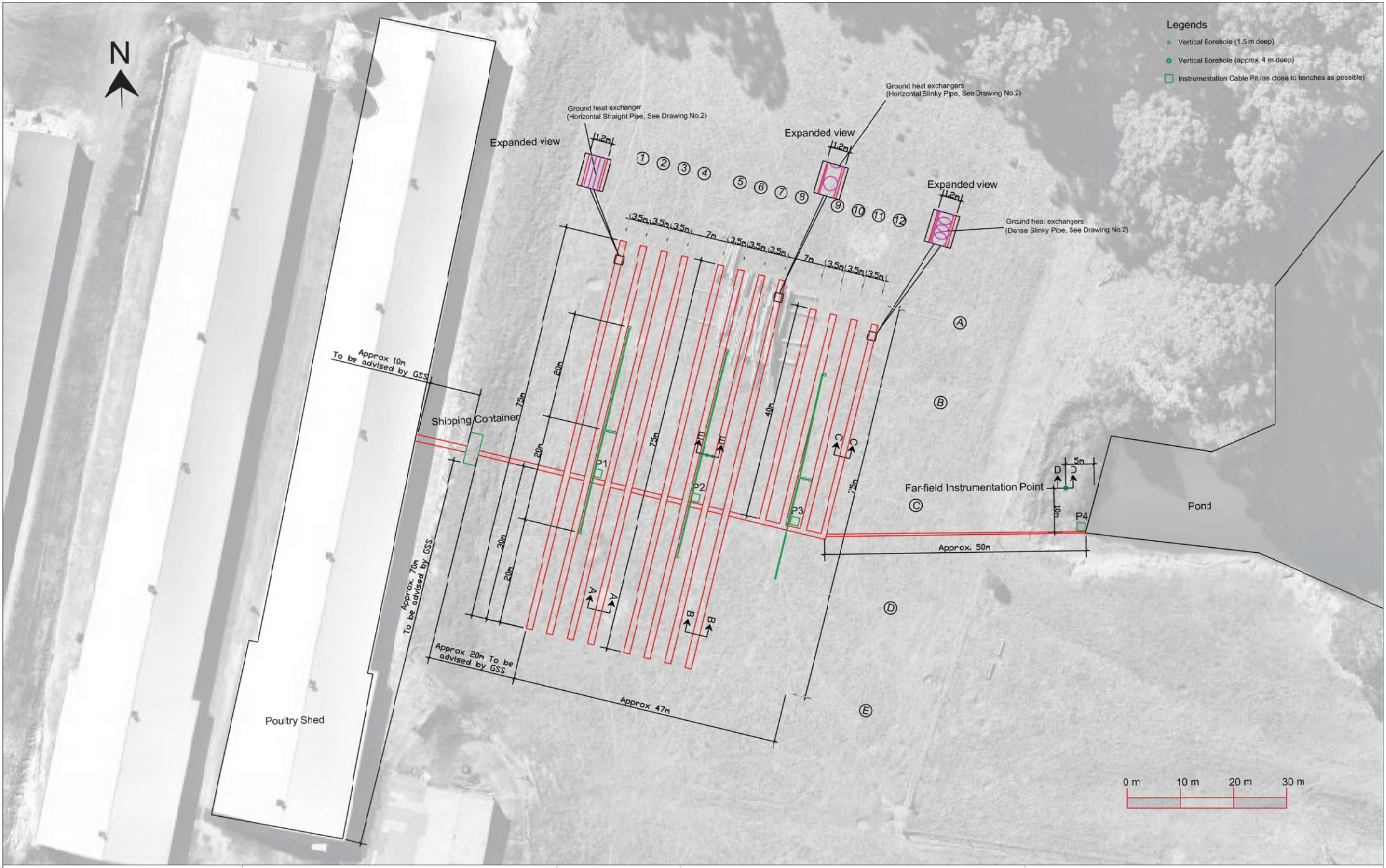


REVISIONS:

| No. | DATE | DESCRIPTION | APP'D. |
|---|---|---|---|
| | | | |
| | | | |
| | | | |
| | | | |
| | | | |
| | | | |

PROJECT

Browm Farm Project
University of Melbourne Research Project

TITLE

Trench Layouts

DESIGNED : YZ,OM,LA,GN,RA DATE : 17/May/2018

DRAWN: YZ SCALE :

APPROVED : CHECKED :

PROJECT NO : DRWG. NO : 01 REV 16

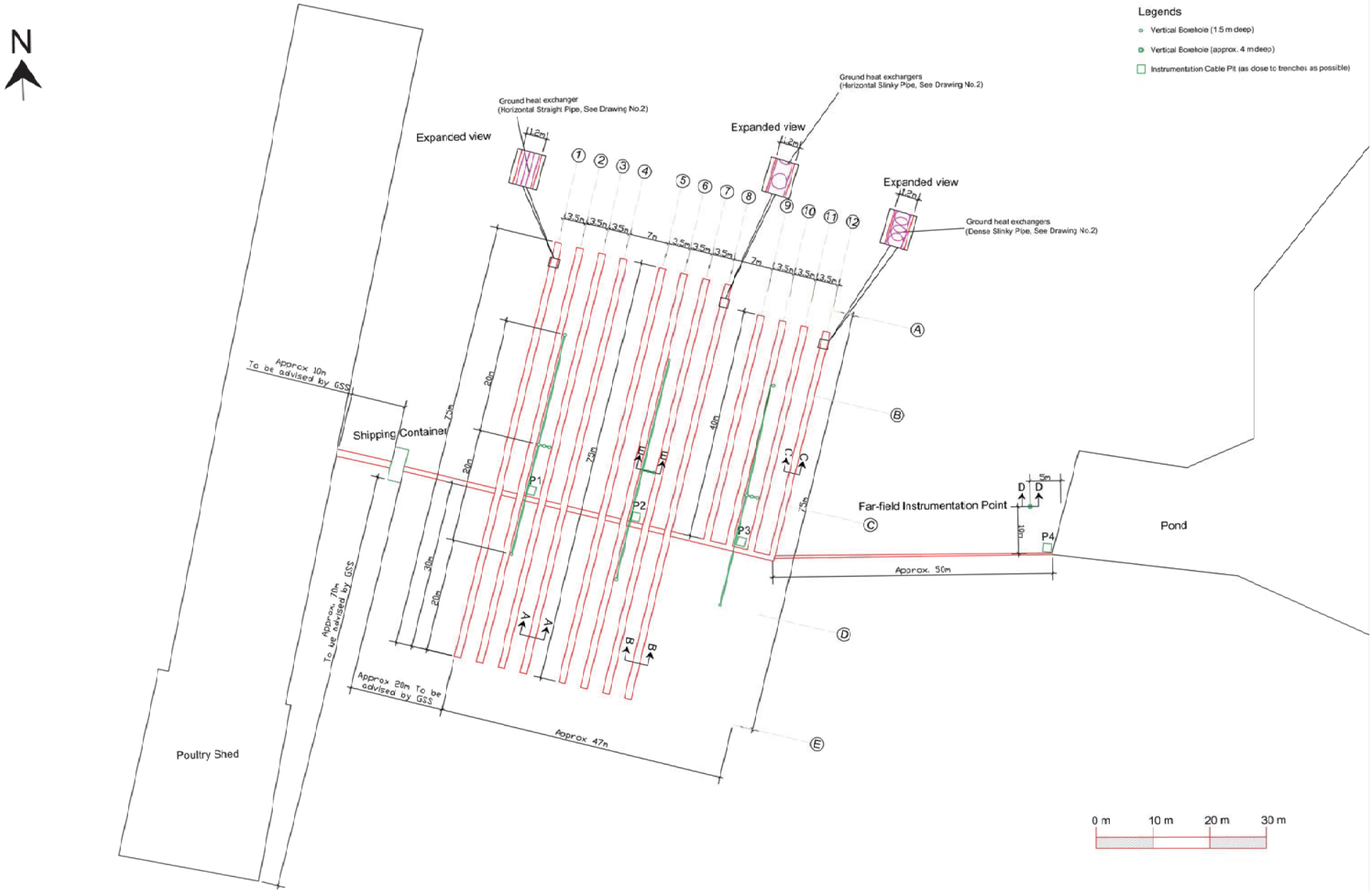


REVISIONS:

| No. | DATE | DESCRIPTION | APP'D |
|---|---|---|---|
| | | | |

PROJECT

Brown Farm Project
University of Melbourne Research Project

TITLE

Trench Layouts

DESIGNED : YZ,OM,LA,GN,RA DATE : 17/May/2018

DRAWN: YZ SCALE :

APPROVED : CHECKED :

PROJECT NO : DRWG. NO : 02 REV. 16

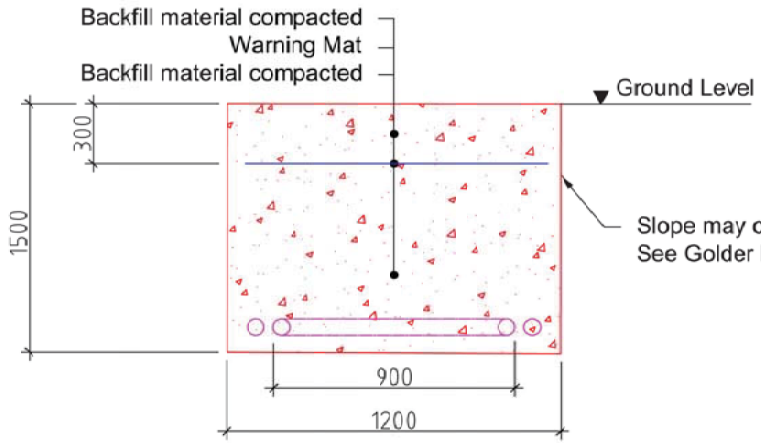


SECTION A-A 1
Horizontal Slinky
Loop Trench

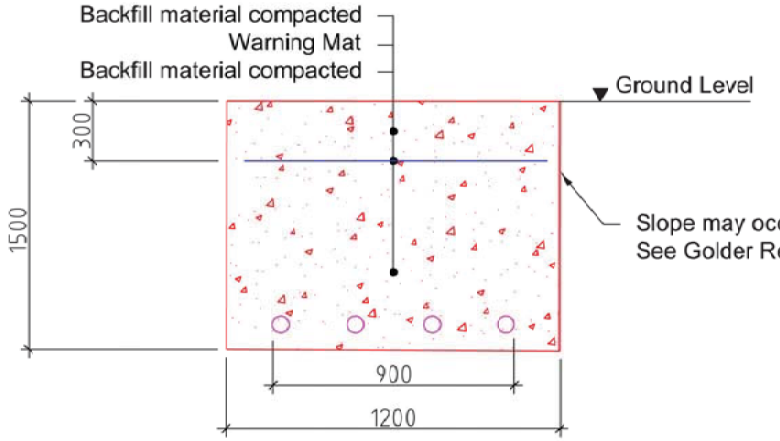


SECTION B-B 1
Horizontal Ground
Loop Trench

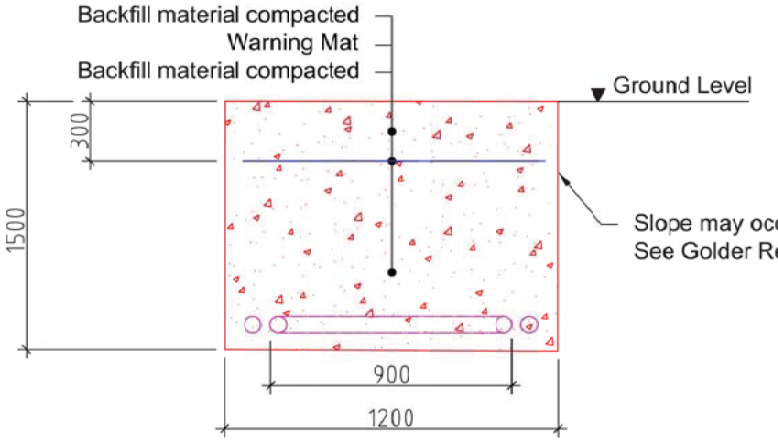


SECTION C-C 1
Horizontal Dense Slinky
Loop Trench

NOT to Scale

REVISIONS:

| No. | DATE | DESCRIPTION | APP'D. |
|---|---|---|---|
| | | | |

PROJECT
Brown Farm Project
University of Melbourne Research Project

TITLE
Trench Cross-section Views

DESIGNED :YZ,OM,LA,GN,RA DATE : 17/May/2018
DRAWN: YZ SCALE :
APPROVED : CHECKED :
PROJECT NO : DRWG. NO : 03 REV. 16

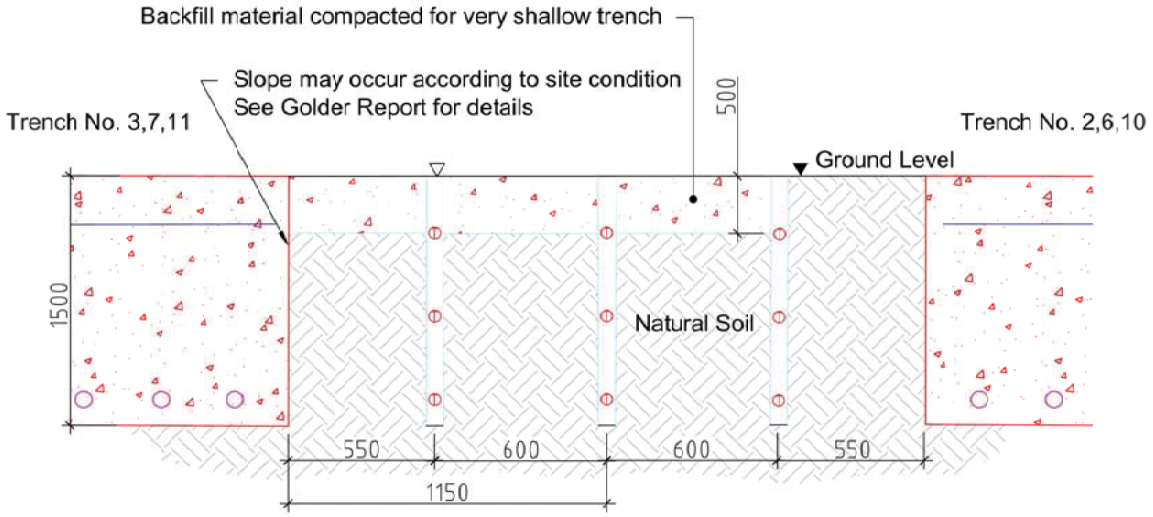


SECTION E-E 1

Instrumentation Boreholes in between Trench No.6&7

**(Same for Trench No. 2&3, Same for Trench No. 10&11)**

| REVISIONS: | | | |
|---|---|---|---|
| No. | DATE | DESCRIPTION | APP'D |
| | | | |

PROJECT

Brown Farm Project

University of Melbourne Research Project

TITLE

Instrumentation Cross-section Views

DESIGNED :YZ,OM,LA,GN,RA DATE : 17/May/2018

DRAWN: YZ SCALE :

APPROVED : CHECKED :

PROJECT NO : DRWG. NO : 04 REV. 16

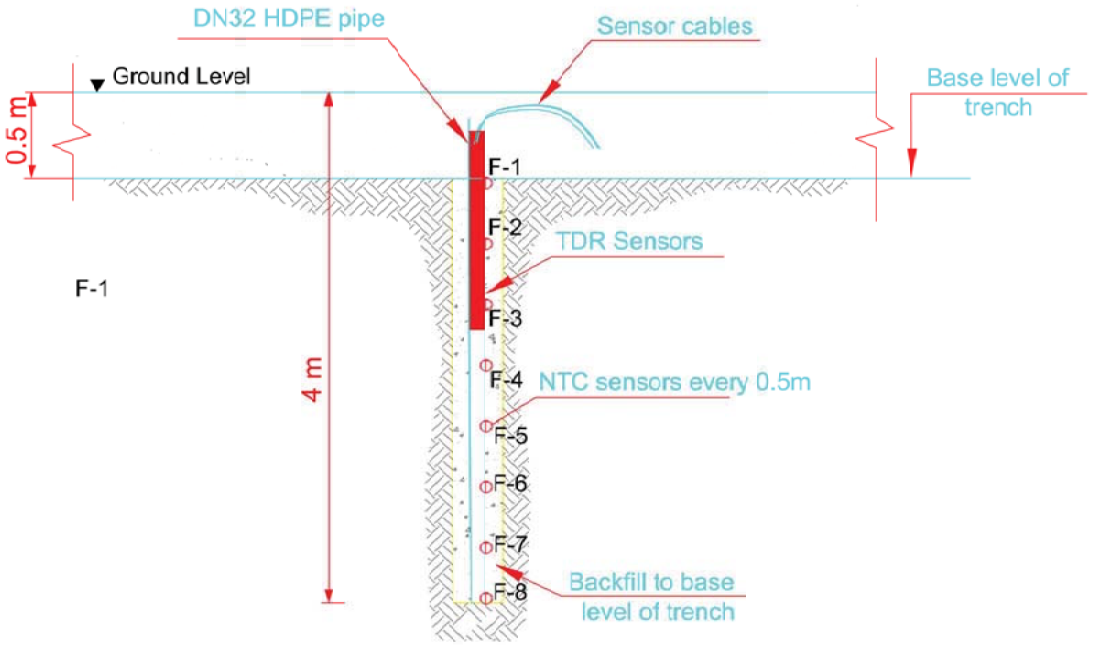


SECTION D–D 1

Farfield temperature & moisture monitoring borehole

NOT to Scale

| REVISIONS: | | | |
|---|---|---|---|
| No. | DATE | DESCRIPTION | APP'D |
| | | | |

PROJECT
Brown Farm Project
University of Melbourne Research Project

TITLE
Farfield Borehole Cross-section Views

DESIGNED :YZ,OM,LA,GN,RA DATE : 17/May/2018
DRAWN: YZ SCALE :
APPROVED : CHECKED :
PROJECT NO : DRWG. NO : 05 REV. 16

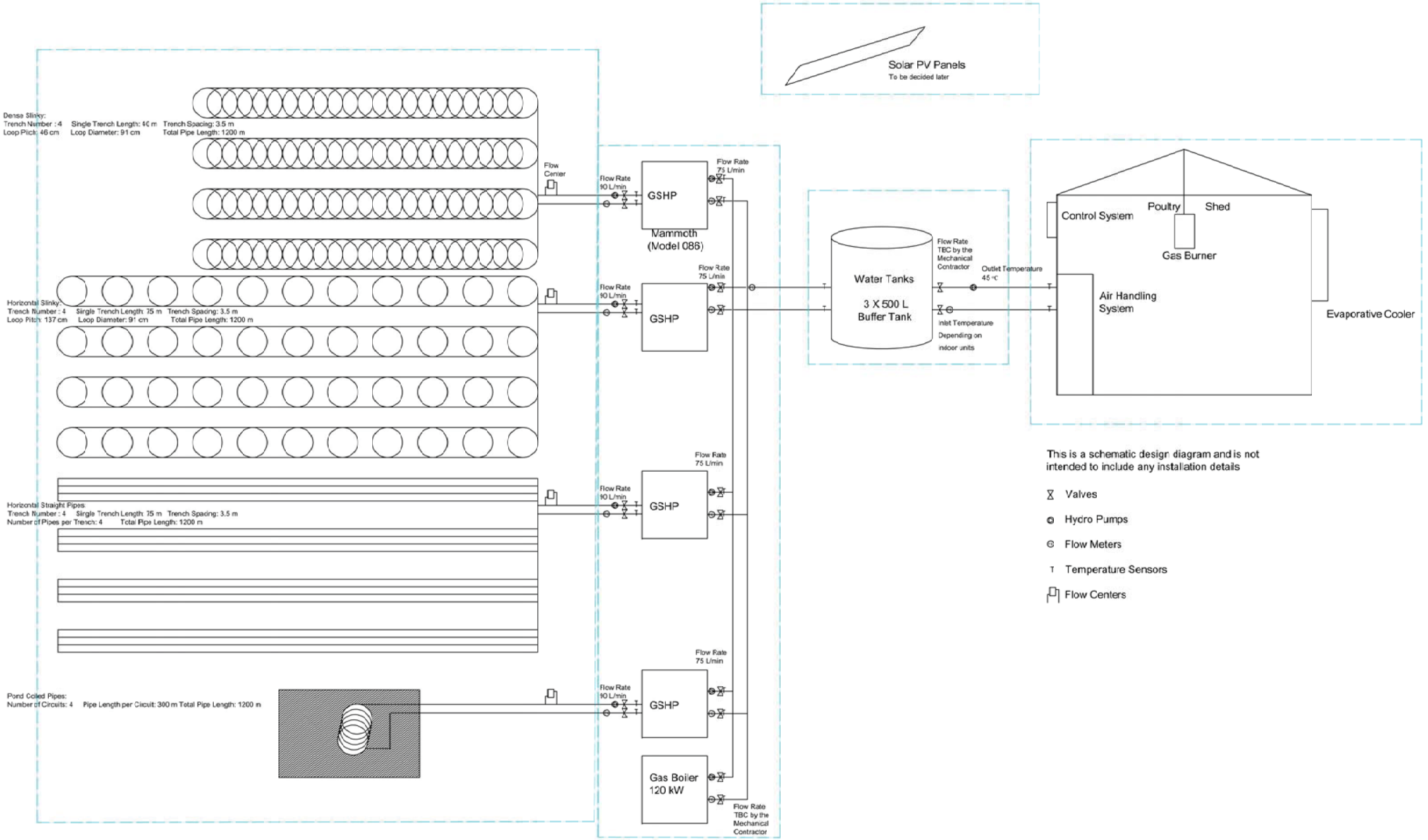


REVISIONS:

| No. | DATE | DESCRIPTION | APP'D |
|---|---|---|---|
| 00 | 30/05/2017 | For discussion | |
| 01 | 06/07/2017 | For discussion | |
| 02 | 28/09/2017 | For discussion | |

PROJECT

Brown Farm Project

University of Melbourne Research Project

TITLE

Hybrid Solar-Geothermal-Gas System Schematic Design

DESIGNED : YZ,OM,LA,GN,RA DATE : 17/May/2018

DRAWN: YZ SCALE :

APPROVED : CHECKED :

PROJECT NO : DRWG. NO : 06 REV. 16

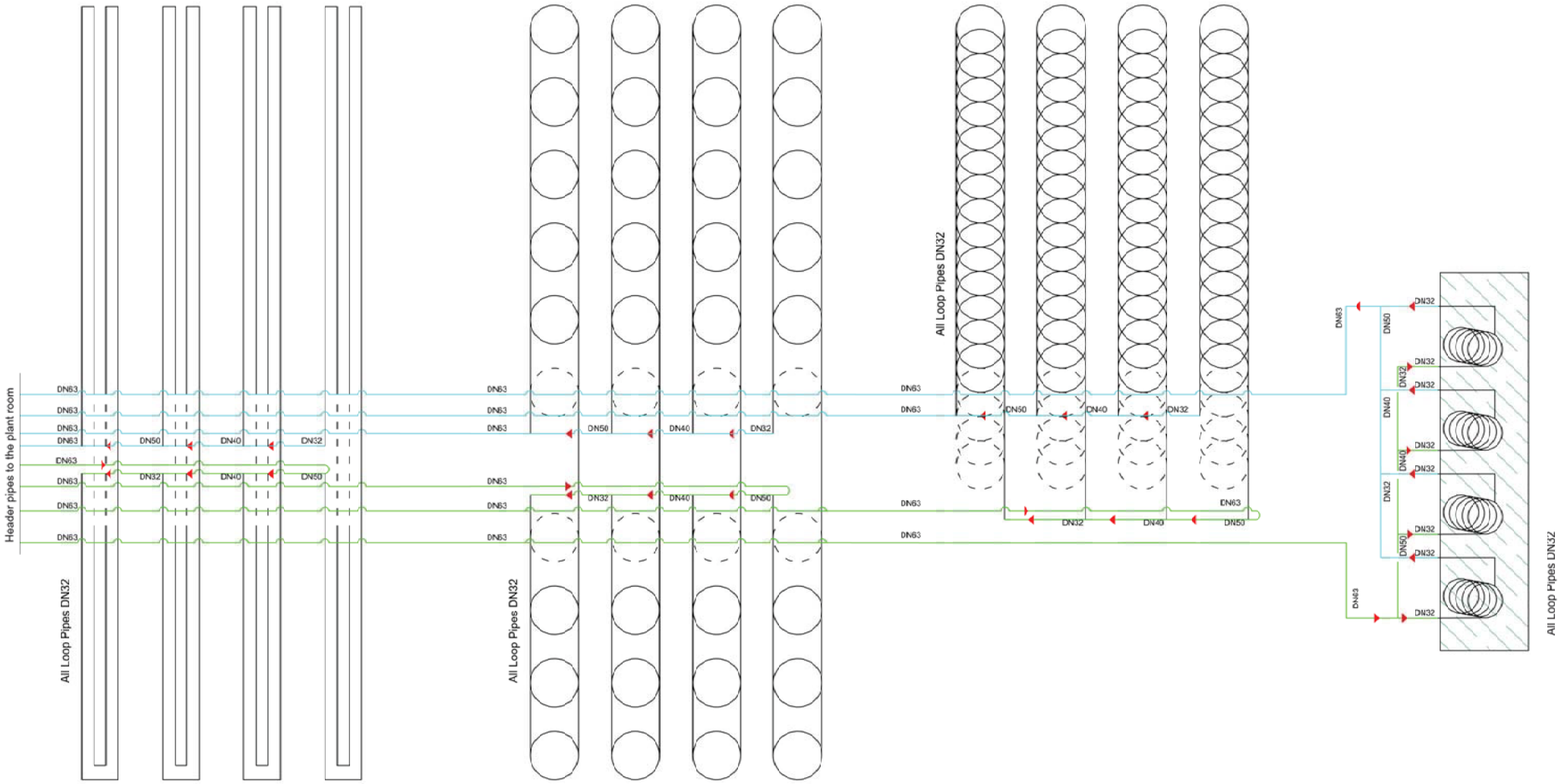


NOT TO SCALE

Note all pipe diameters are outside diameter

REVISIONS:

| No. | DATE | DESCRIPTION | APP'D |
|---|---|---|---|
| | | | |

PROJECT

Brown Farm Project

University of Melbourne Research Project

TITLE

Ground Loop Layout (Reverse Return)

DESIGNED :YZ,OM,LA,GN,RA DATE : 17/May/2018

DRAWN: YZ SCALE :

APPROVED : CHECKED :

PROJECT NO : DRWG. NO : 07 REV. 16

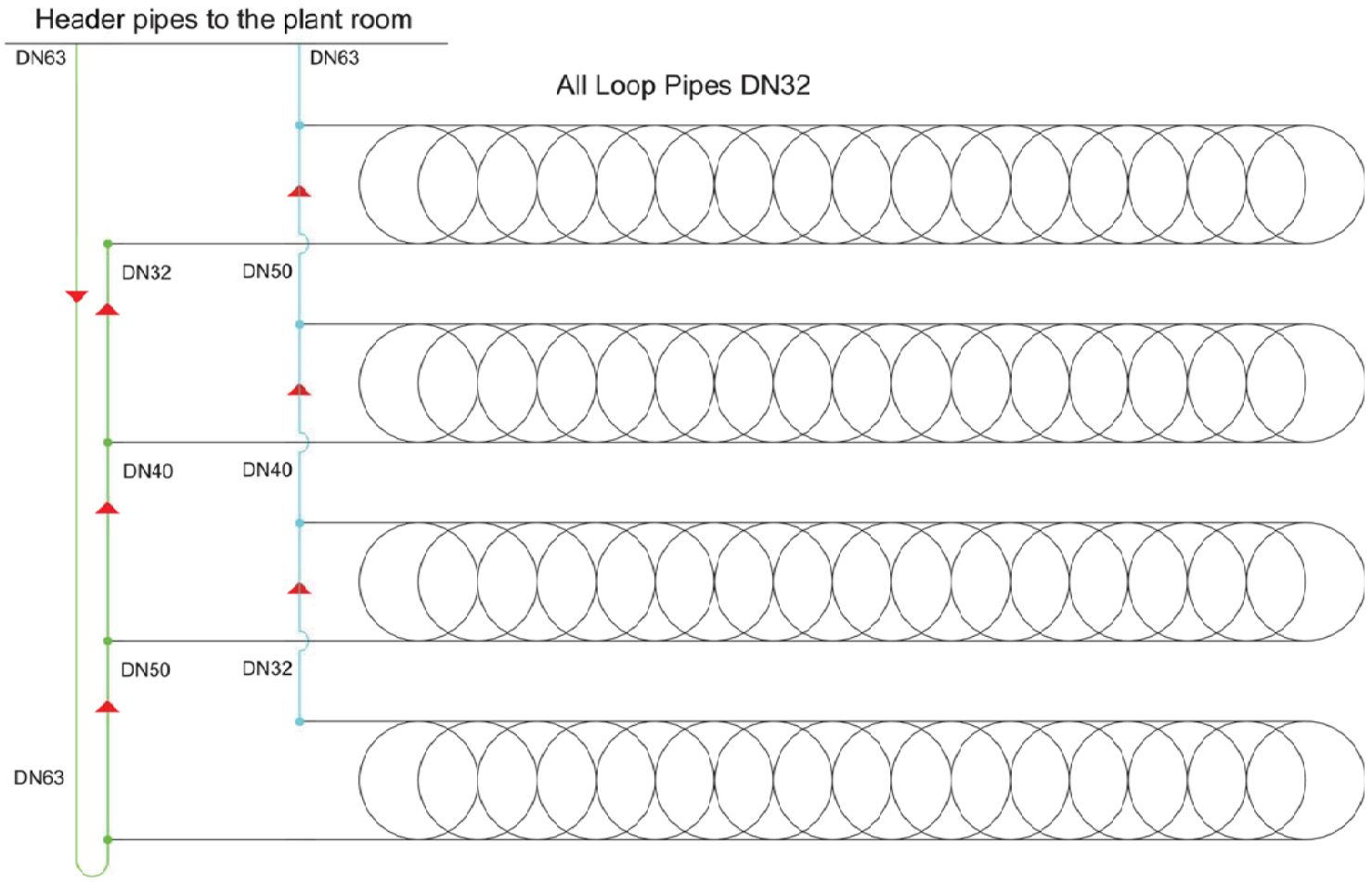


NOT TO SCALE

Note all pipe diameters are outside diameter

| REVISIONS: | | | |
|---|---|---|---|
| No. | DATE | DESCRIPTION | APP'D |
| | | | |

PROJECT

Brown Farm Project

University of Melbourne Research Project

TITLE

Dense Slinky Loop Layout (Reverse Return)

DESIGNED :YZ,OM,LA,GN,RA DATE : 17/May/2018

DRAWN: YZ SCALE :

APPROVED : CHECKED :

PROJECT NO : DRWG. NO : 08 REV. 16

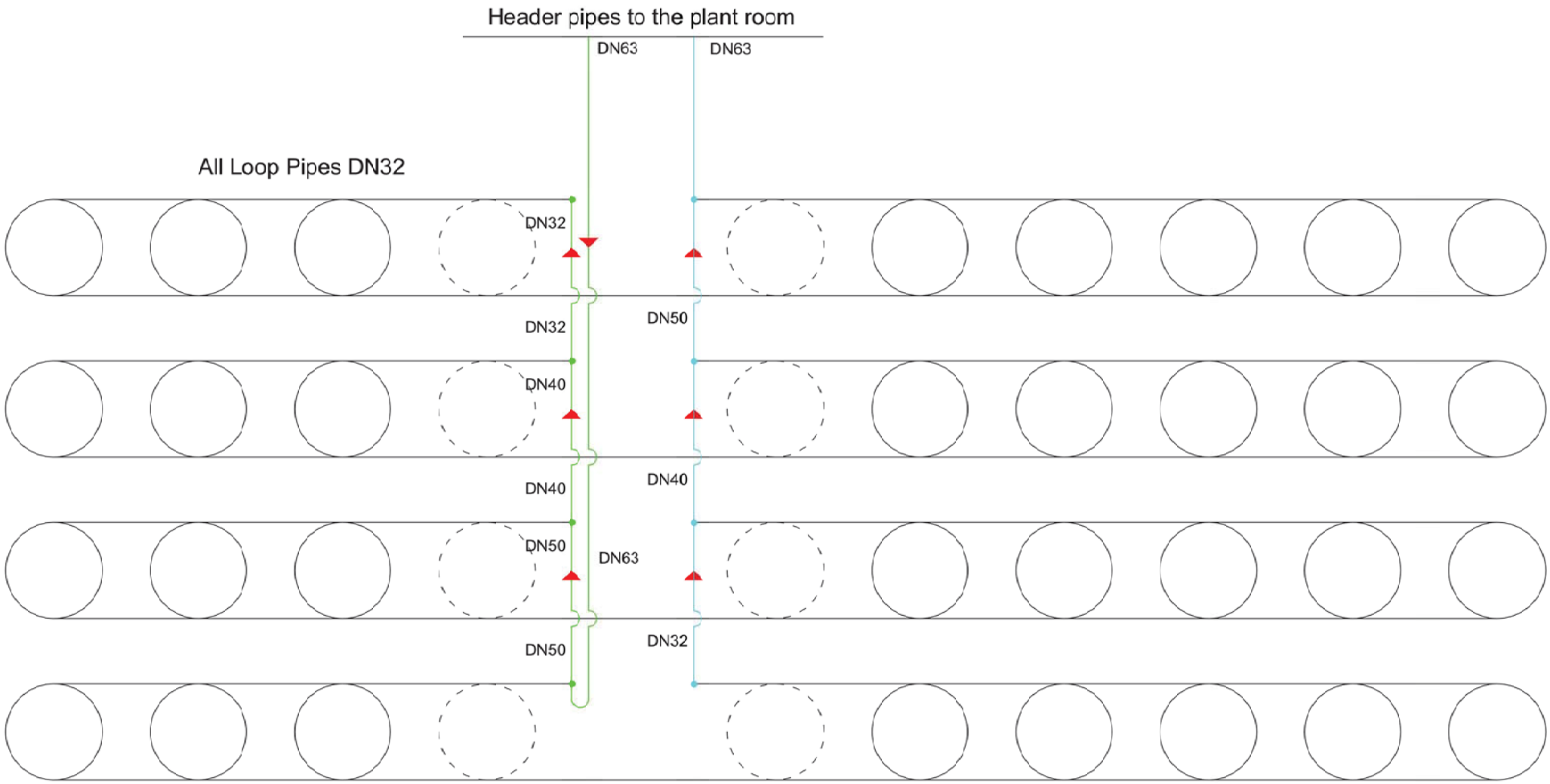


NOT TO SCALE

Note all pipe diameters are outside diameter

REVISIONS:

| No. | DATE | DESCRIPTION | APP'D |
|---|---|---|---|
| | | | |

PROJECT

Brown Farm Project

University of Melbourne Research Project

TITLE

Slinky Loop Layout (Reverse Return)

DESIGNED : YZ,OM,LA,GN,RA DATE : 17/May/2018

DRAWN: YZ SCALE :

APPROVED : CHECKED :

PROJECT NO : DRWG. NO : 09 REV. 16

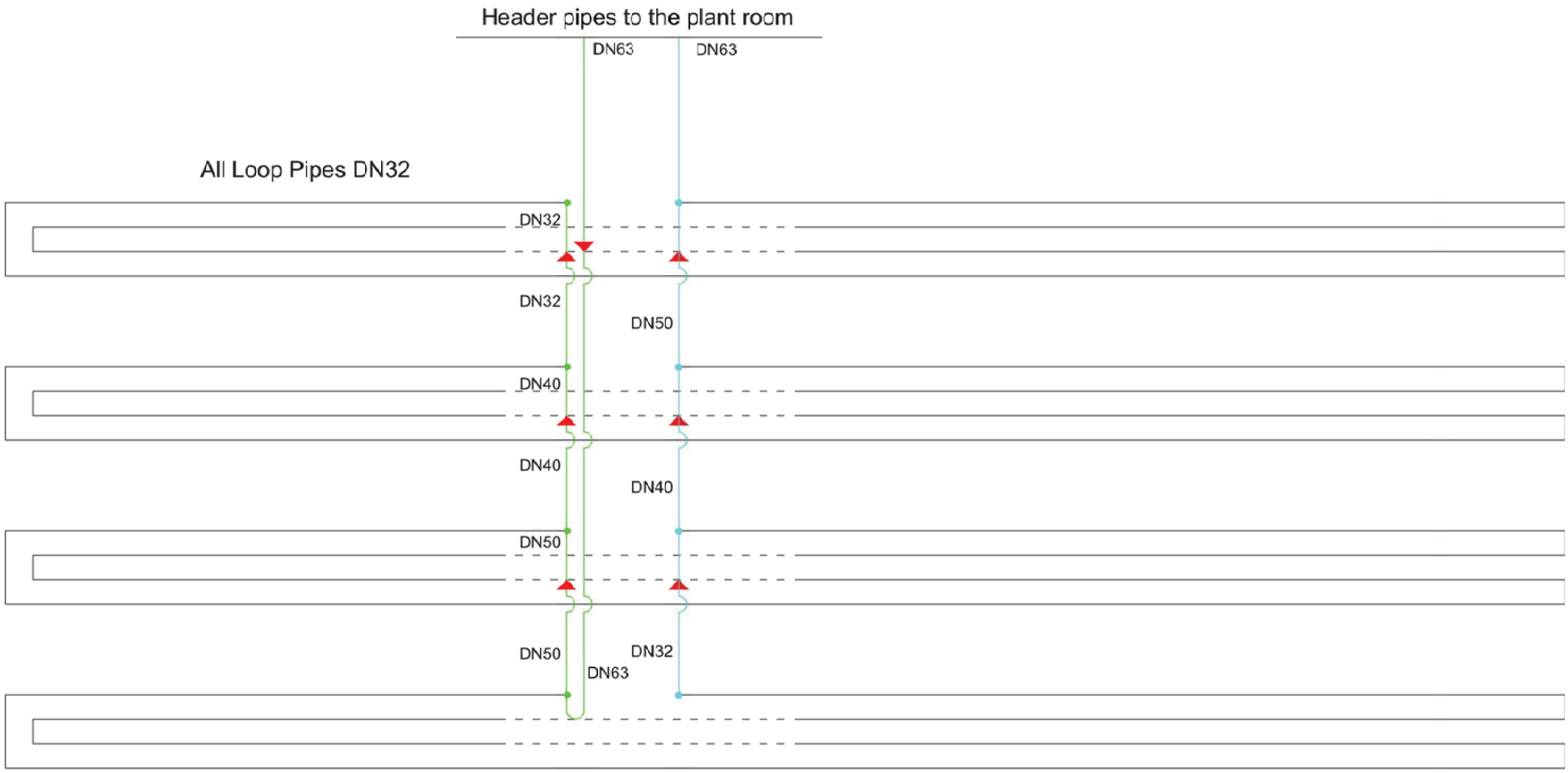


NOT TO SCALE

Note all pipe diameters are outside diameter

REVISIONS:

| No. | DATE | DESCRIPTION | APP'D |
|---|---|---|---|
| | | | |

PROJECT

Brown Farm Project

University of Melbourne Research Project

TITLE

Straight Loop Layout (Reverse Return)

DESIGNED :YZ,OM,LA,GN,RA DATE : 17/May/2018

DRAWN: YZ SCALE :

APPROVED : CHECKED :

PROJECT NO : DRWG. N0 : 10 REV. 16

Purging Flow Rates

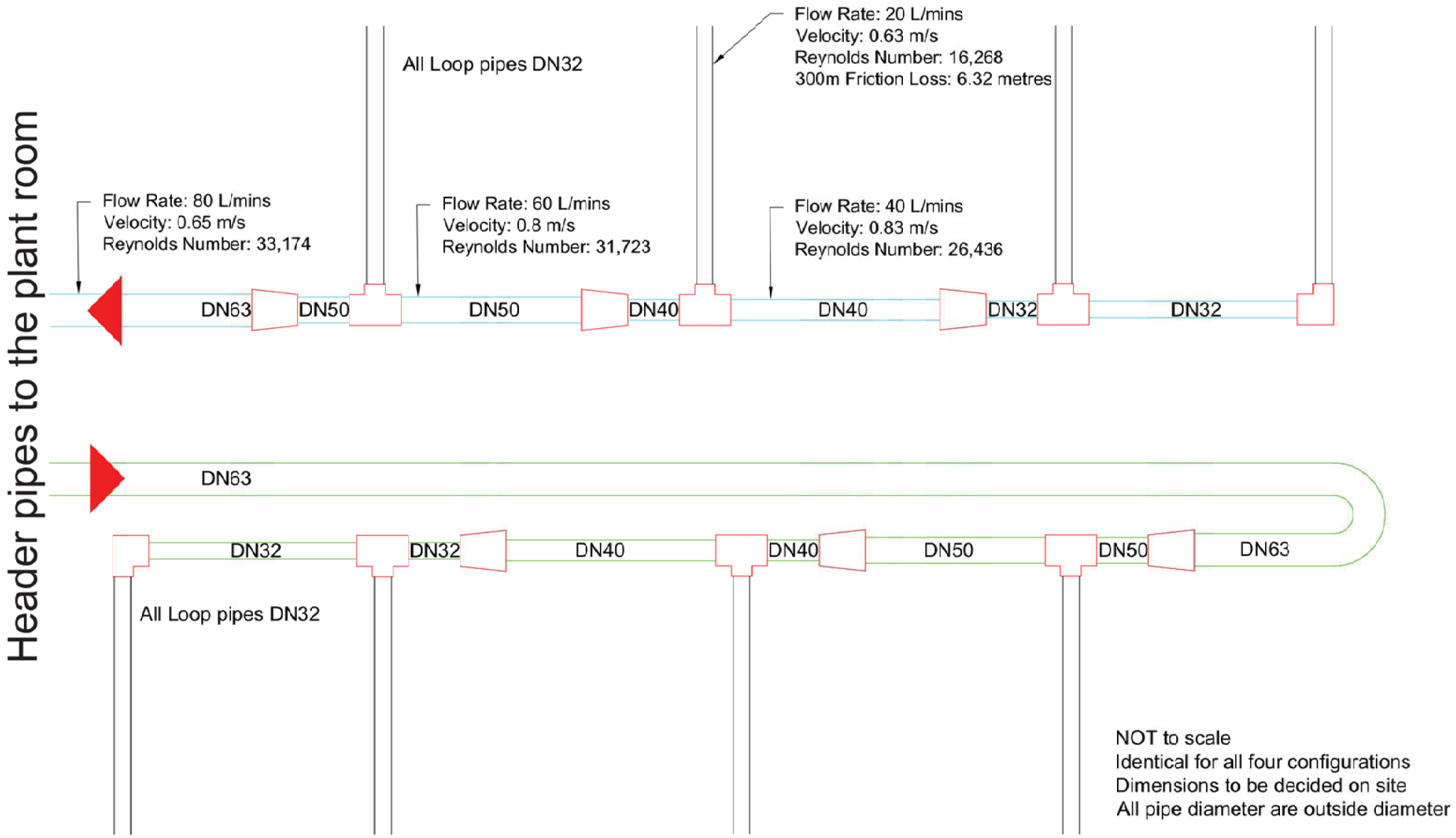


REVISIONS:

| No. | DATE | DESCRIPTION | APP'D |
|---|---|---|---|
| | | | |

PROJECT
Brown Farm Project
University of Melbourne Research Project

TITLE
Header Pipe Schematic Drawing

DESIGNED :YZ,OM,LA,GN,RA DATE : 17/May/2018
DRAWN: YZ SCALE :
APPROVED : CHECKED :
PROJECT NO : DRWG. NO : 11 REV. 16

Operational Flow Rates

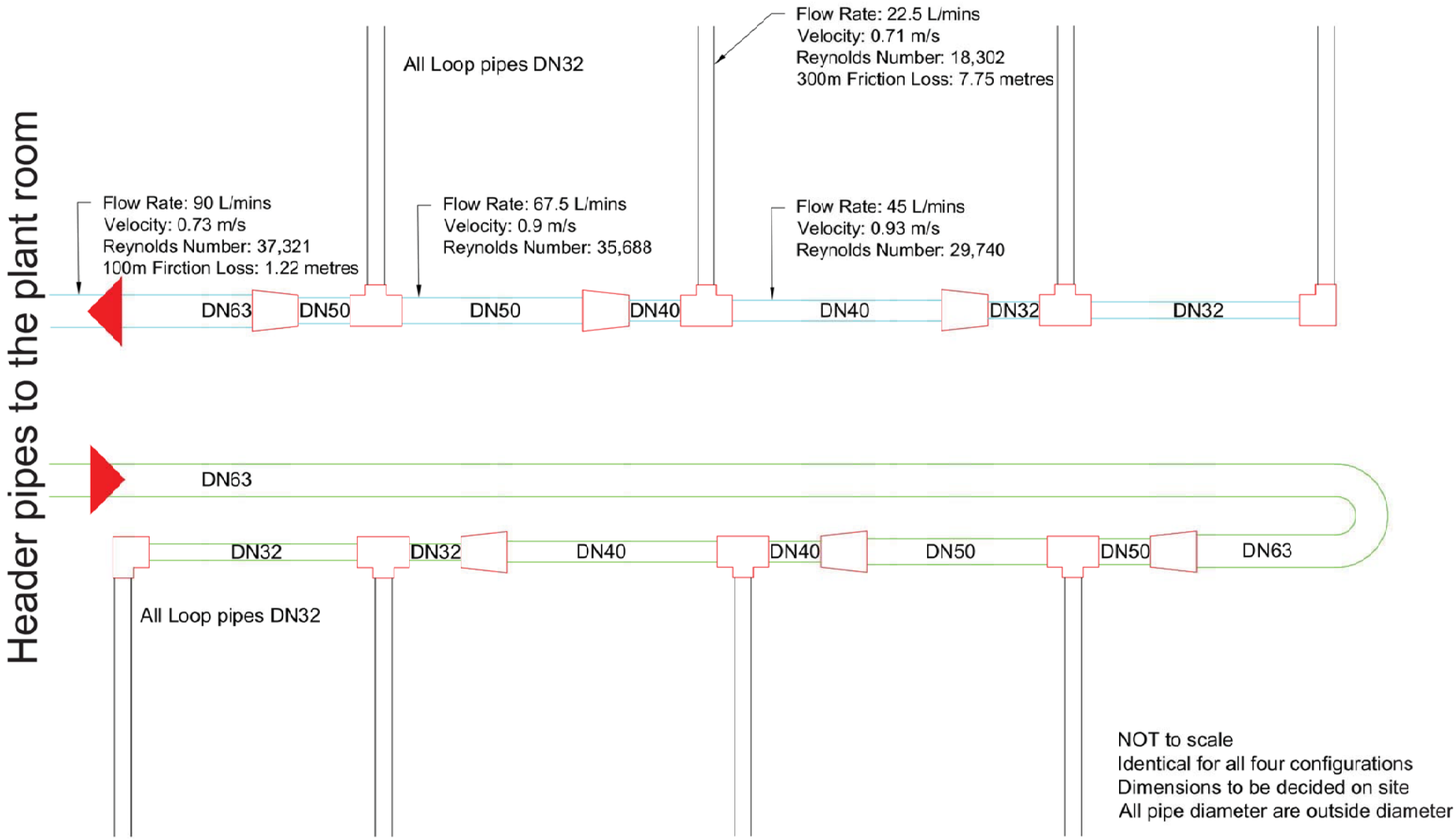


REVISIONS:

| No. | DATE | DESCRIPTION | APP'D |
|---|---|---|---|
| | | | |

PROJECT
Brown Farm Project
University of Melbourne Research Project

TITLE
Header Pipe Schematic Drawing

DESIGNED :YZ,OM,LA,GN,RA DATE : 17/May/2018
DRAWN: YZ SCALE :
APPROVED : CHECKED :
PROJECT NO : DRWG. NO : 12 REV. 16

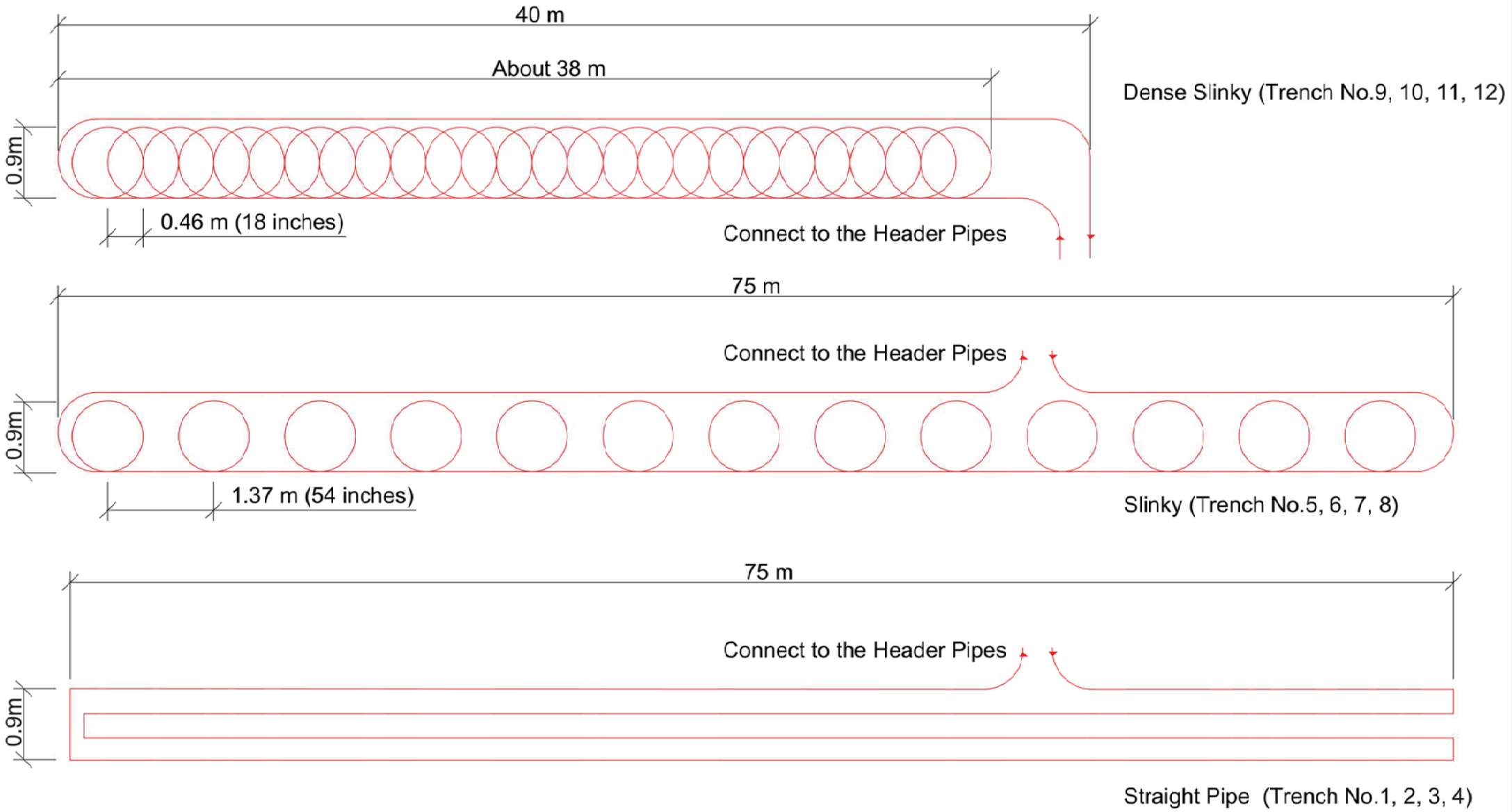


NOT to Scale

| REVISIONS: | | | |
|---|---|---|---|
| No. | DATE | DESCRIPTION | APP'D |
| | | | |

PROJECT
Brown Farm Project
University of Melbourne Research Project

TITLE
Ground Loop Schematic Drawing

DESIGNED :YZ,OM,LA,GN,RA DATE : 17/May/2018
DRAWN: YZ SCALE :
APPROVED : CHECKED :
PROJECT NO : DRWG. NO : 13 REV. 16

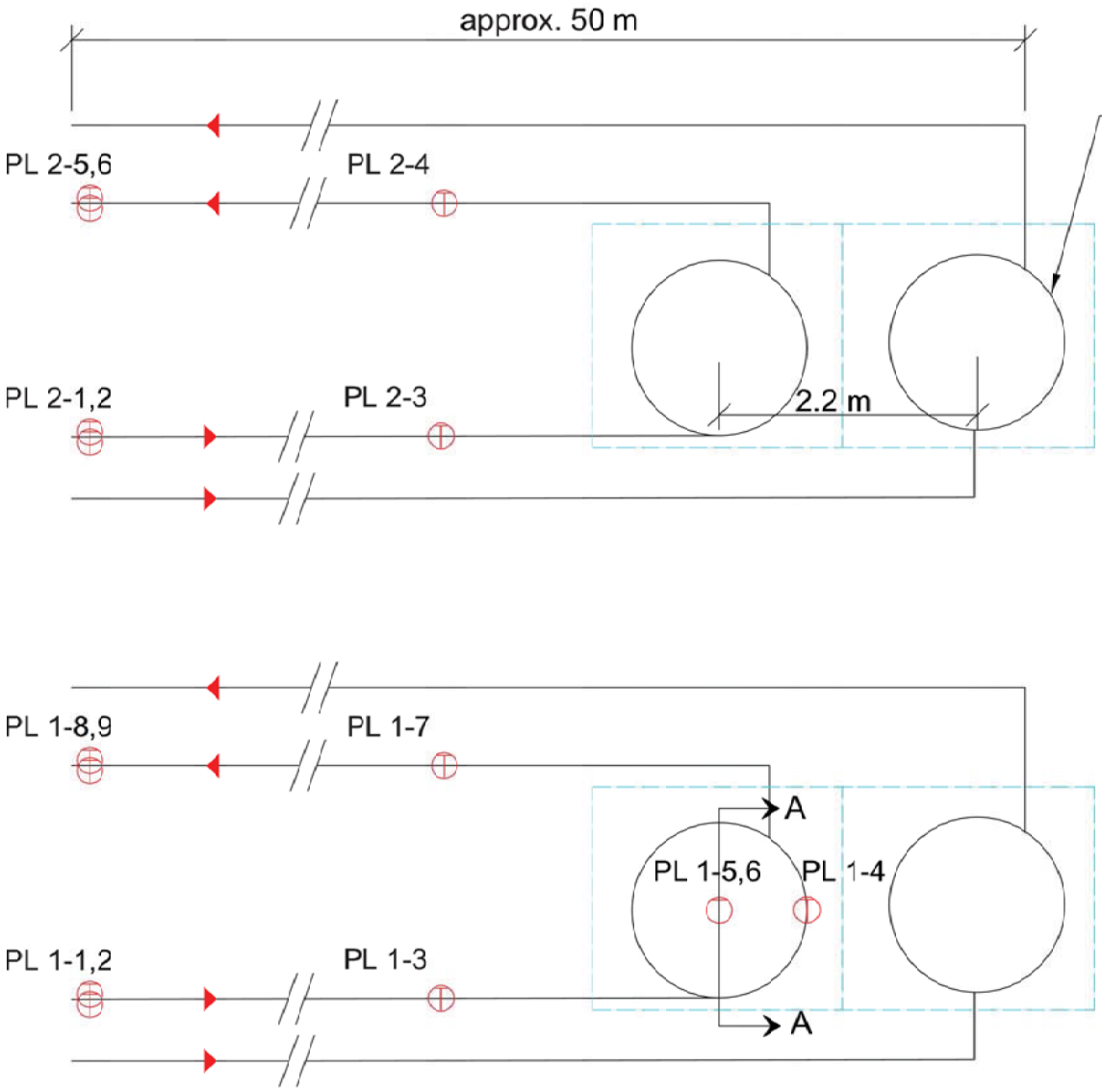


Loop Diameter approx. 1.2 m
Total Pipe length 200m per loop

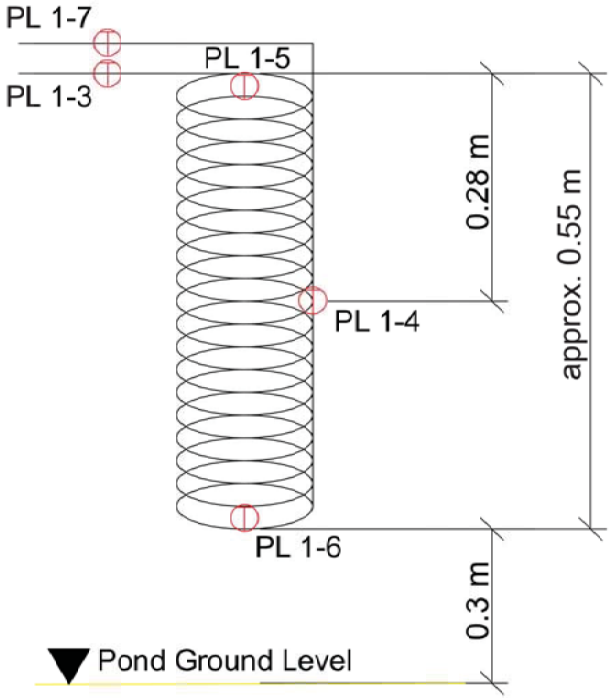


SECTION A–A
Cross-section view of the pond loop

NOT TO SCALE

REVISIONS:

| No. | DATE | DESCRIPTION | APP'D |
|---|---|---|---|
| | | | |

PROJECT
Brown Farm Project
University of Melbourne Research Project

TITLE
Pond Loop Schematic Drawing

DESIGNED : YZ,OM,LA,GN,RA DATE : 17/May/2018
DRAWN: YZ SCALE :
APPROVED : CHECKED :
PROJECT NO : DRWG. NO : 14 REV. 16

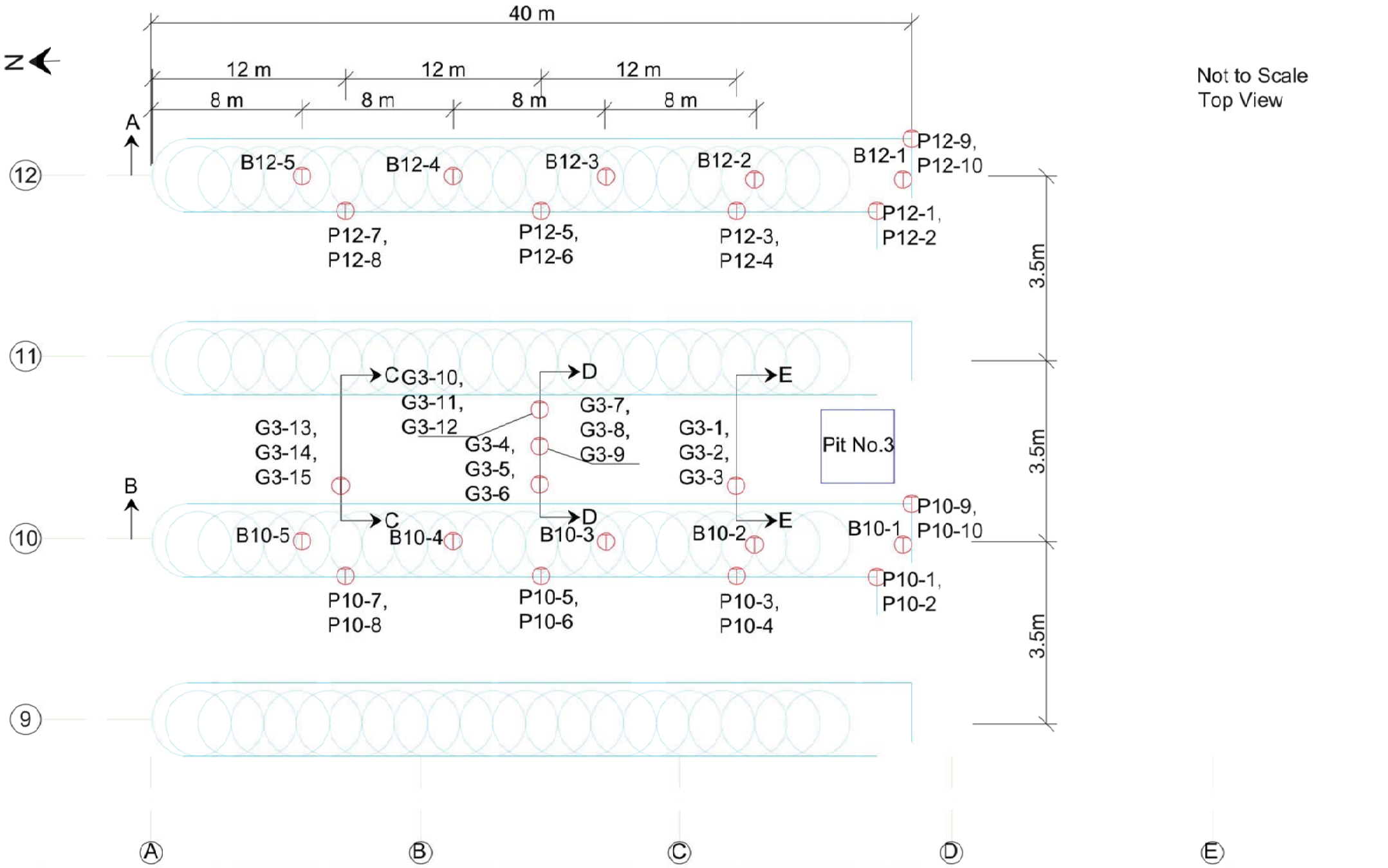


REVISIONS:

| No. | DATE | DESCRIPTION | APP'D. |
|---|---|---|---|
| | | | |

PROJECT
Brown Farm Project
University of Melbourne Research Project

TITLE
Dense Slinky Instrumentation Drawing

DESIGNED :YZ,OM,LA,GN,RA DATE : 17/May/2018
DRAWN: YZ SCALE :
APPROVED : CHECKED :
PROJECT NO : DRWG. NO : 15 REV. 16

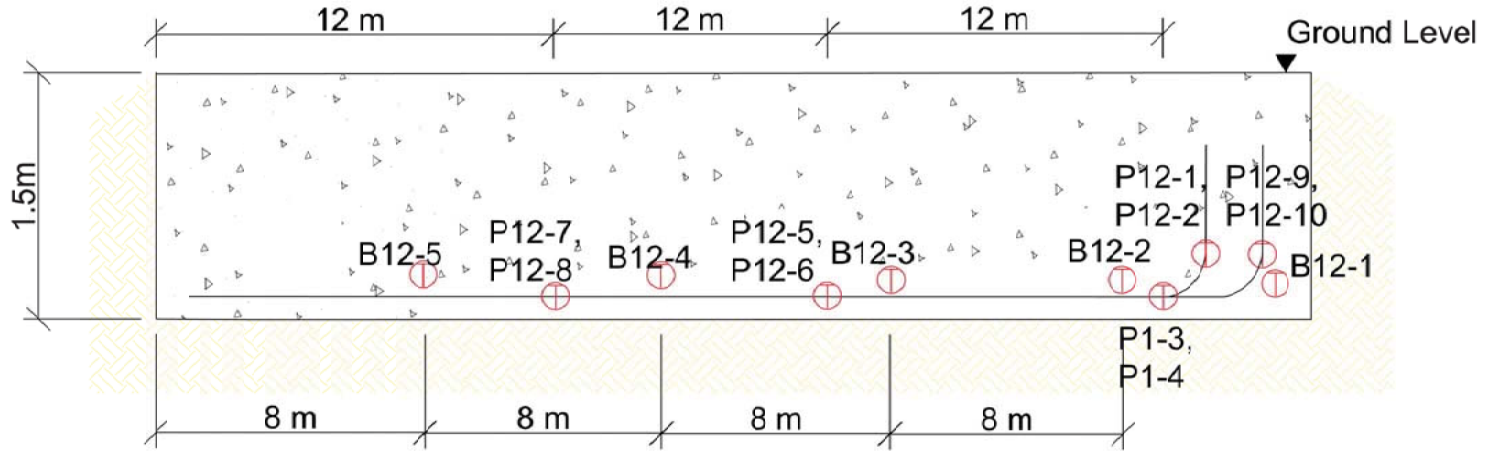


SECTION A–A
15
Sensors in the trench No.12
(Dense Slinky)

N

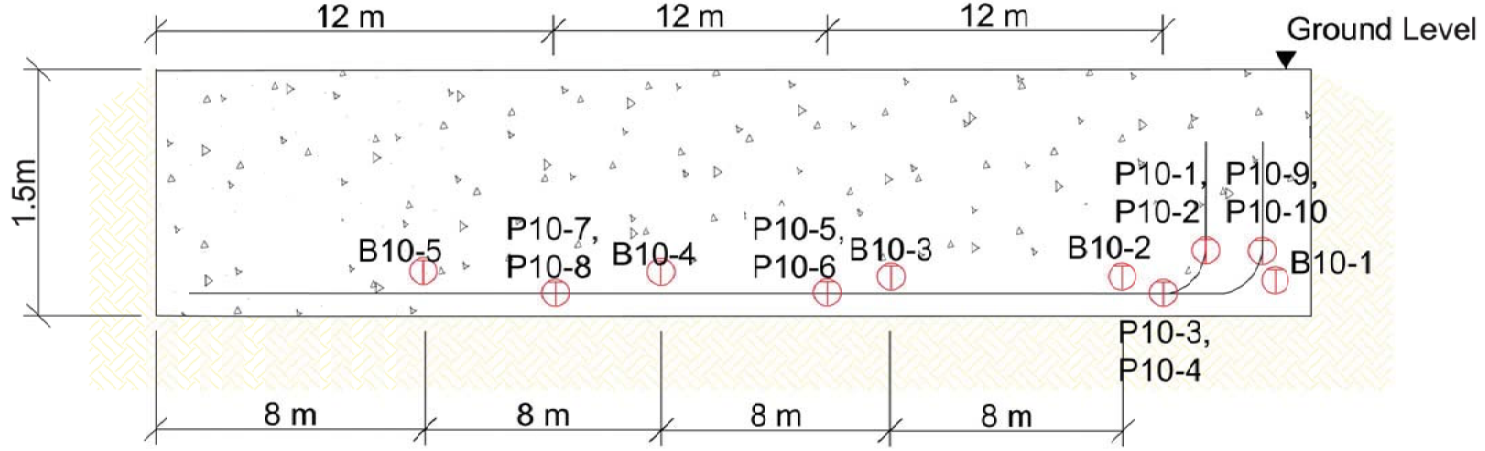


SECTION B–B
15
Sensors in the trench No.10
(Dense Slinky)

Not to Scale
Side View

REVISIONS:

| No. | DATE | DESCRIPTION | APP'D |
|---|---|---|---|
| | | | |

PROJECT
Brown Farm Project
University of Melbourne Research Project

TITLE
Dense Slinky Instrumentation Trench Cross-section
(Trench No.12 & No.10)

DESIGNED : YZ,OM,LA,GN,RA DATE : 17/May/2018
DRAWN: YZ SCALE :
APPROVED : CHECKED :
PROJECT NO : DRWG. NO : 15 REV. 16

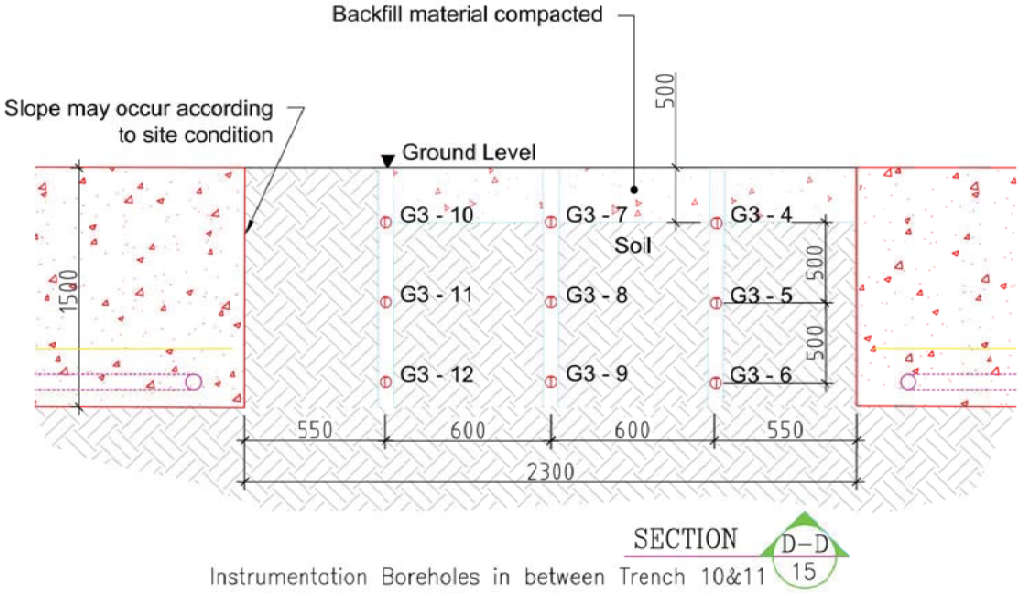


SECTION D–D

Instrumentation Boreholes in between Trench 10&11 15

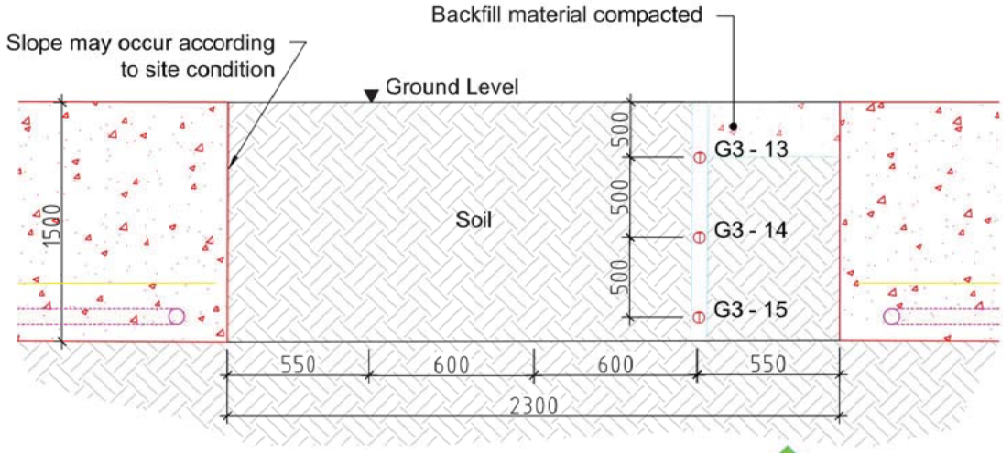


SECTION C–C

Instrumentation Boreholes in between Trench 10&11 15

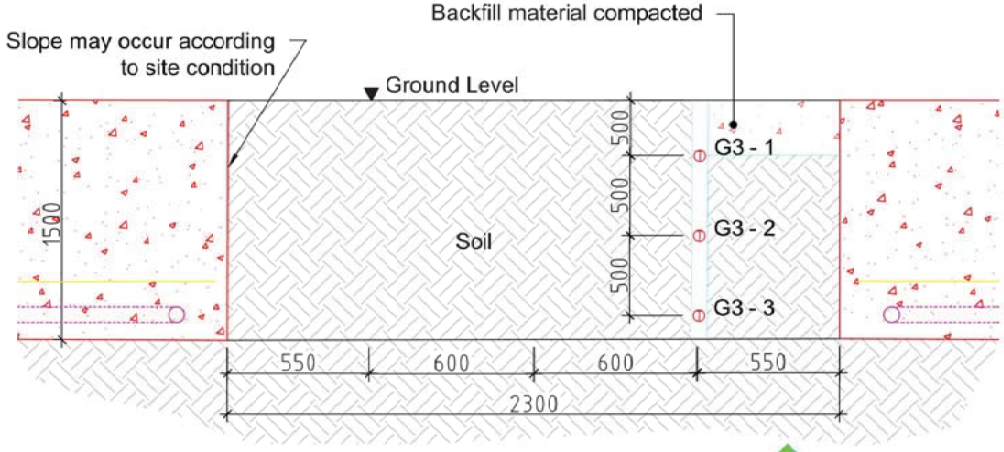


SECTION E–E

Instrumentation Boreholes in between Trench 10&11 15

REVISIONS:

| No. | DATE | DESCRIPTION | APP'D. |
|---|---|---|---|
| | | | |

PROJECT

Brown Farm Project

University of Melbourne Research Project

TITLE

Dense Slinky Between-Trench Cross-Section

DESIGNED : YZ,OM,LA,GN,RA DATE : 17/May/2018

DRAWN: YZ SCALE :

APPROVED : CHECKED :

PROJECT NO : DRWG. NO : 17 REV. 16

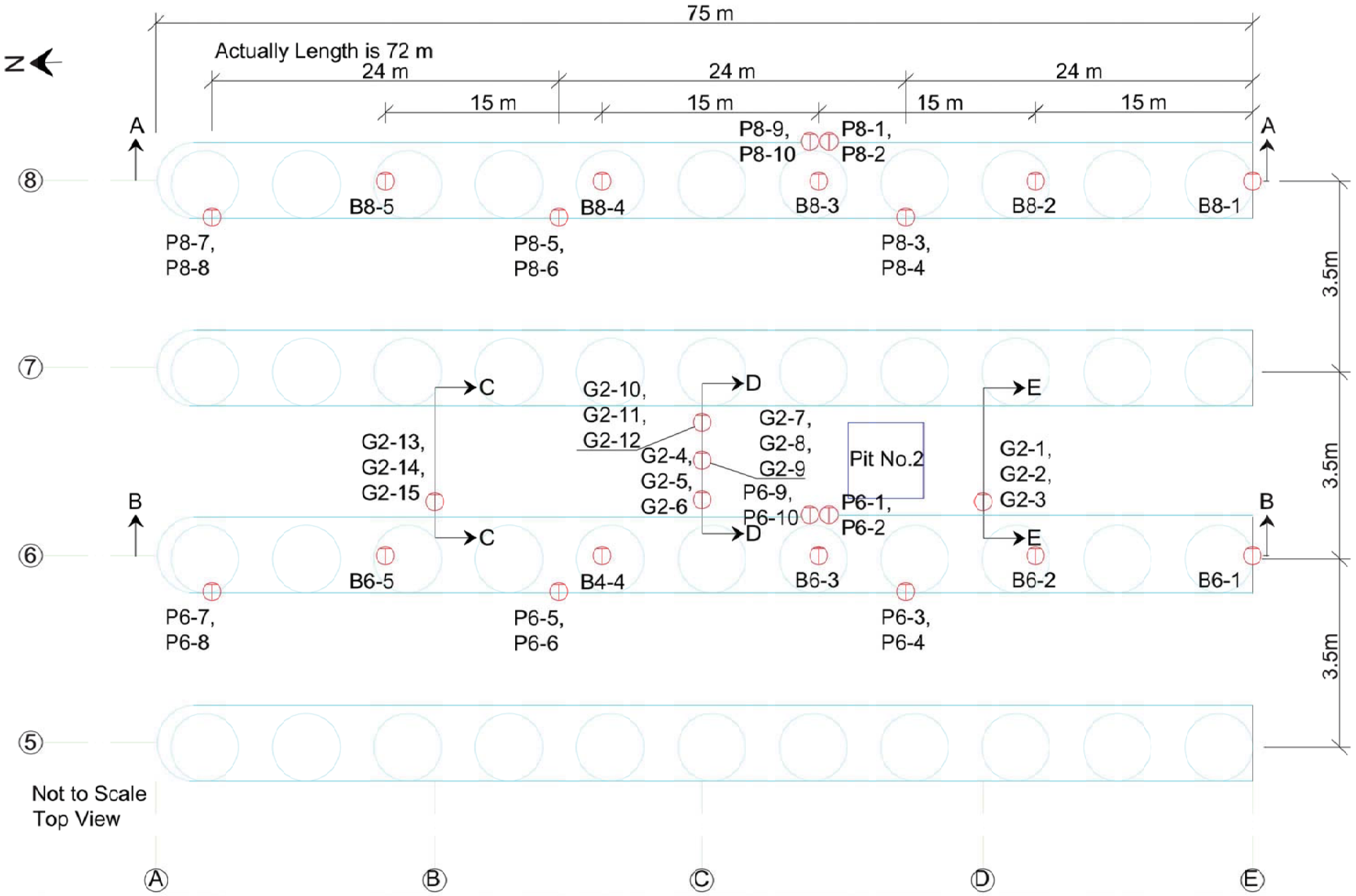


REVISIONS:

| No. | DATE | DESCRIPTION | APP'D |
|---|---|---|---|
| | | | |

PROJECT
Brown Farm Project
University of Melbourne Research Project

TITLE
Horizontal Slinky Instrumentation Drawing

DESIGNED : YZ,OM,LA,GN,RA DATE : 17/May/2018
DRAWN: YZ SCALE :
APPROVED : CHECKED :
PROJECT NO : DRWG. NO : 18 REV. 16

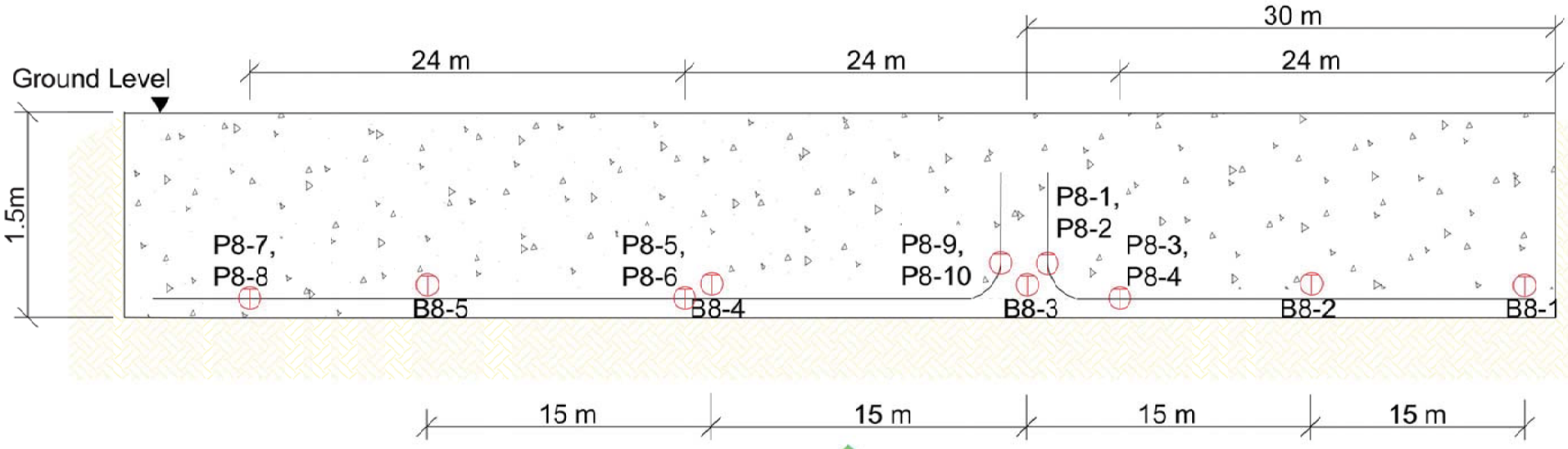


SECTION A–A 18

Sensors in the trench No.8
(Horizontal Slinky)

N

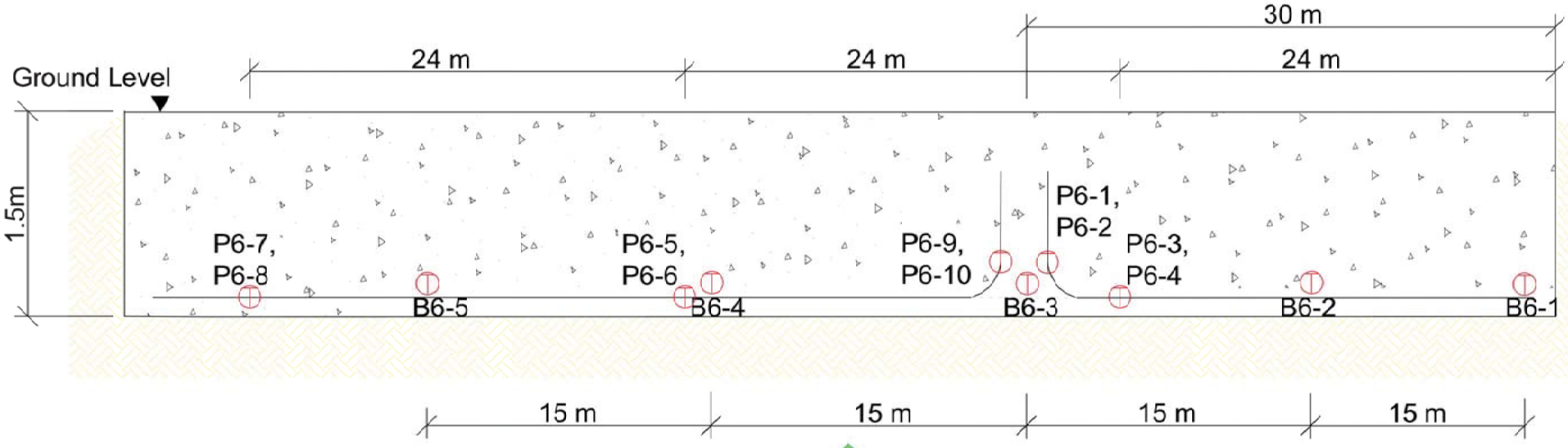


SECTION B–B 18

Sensors in the trench No.6
(Horizontal Slinky)

Not to Scale
Side View

| REVISIONS: | | | |
|---|---|---|---|
| No. | DATE | DESCRIPTION | APP'D. |
| | | | |

PROJECT
Brown Farm Project
University of Melbourne Research Project

TITLE
Horizontal Slinky Instrumentation Trench Cross-section
(Trench No.6 & No.8)

| | | | |
|---|---|---|---|
| DESIGNED : YZ,OM,LA,GN,RA | | DATE : | 17/May/2018 |
| DRAWN: | YZ | SCALE : | |
| APPROVED : | | CHECKED : | |
| PROJECT NO : | | DRWG. NO : | 19 REV. 16 |

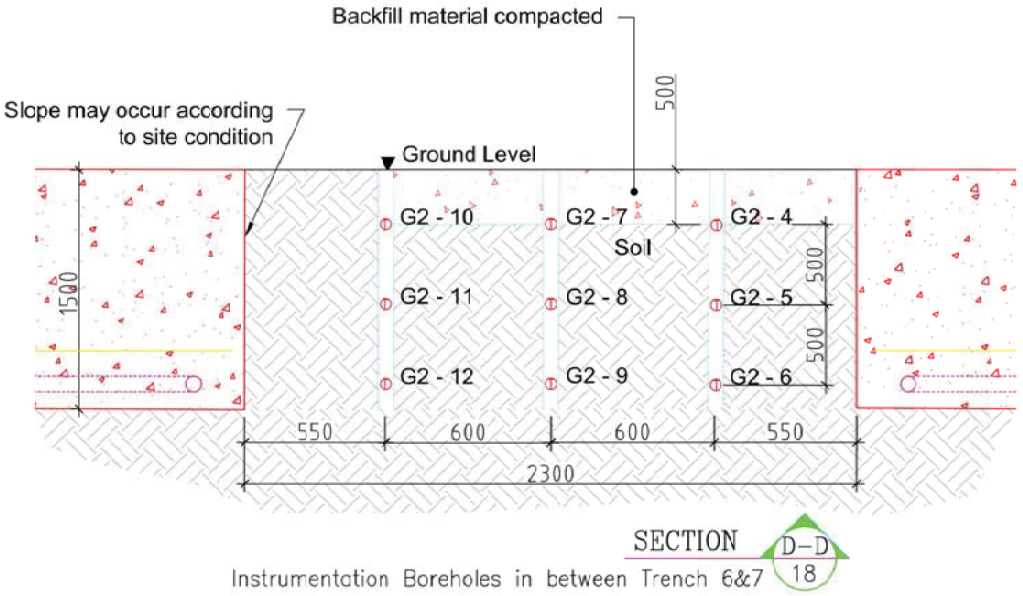


SECTION D–D

Instrumentation Boreholes in between Trench 6&7 18

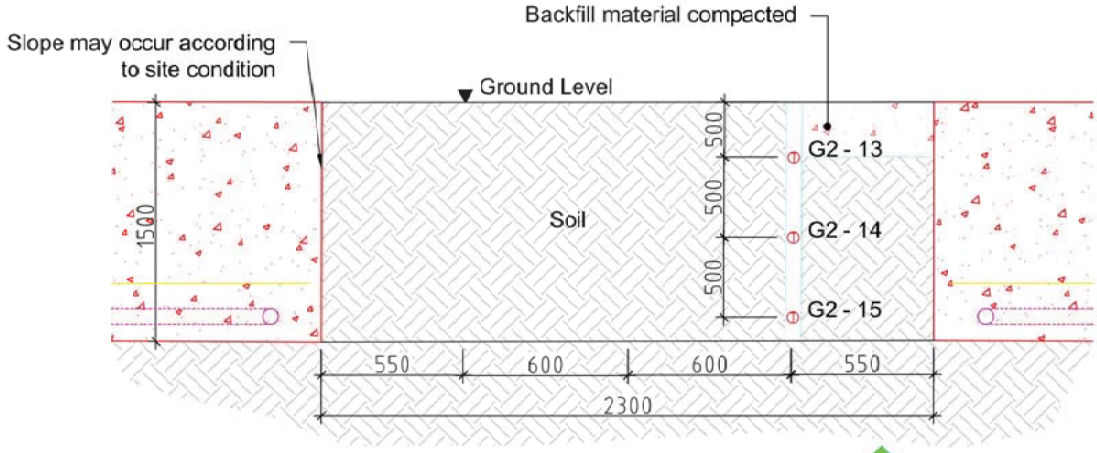


SECTION C–C

Instrumentation Boreholes in between Trench 6&7 18

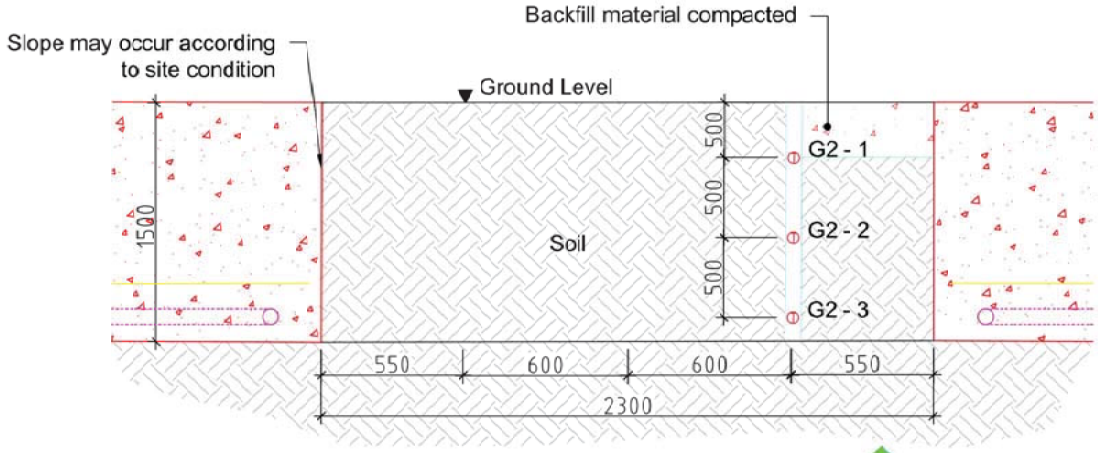


SECTION E–E

Instrumentation Boreholes in between Trench 6&7 18

REVISIONS:

| No. | DATE | DESCRIPTION | APP'D. |
|---|---|---|---|
| | | | |

PROJECT

Brown Farm Project

University of Melbourne Research Project

TITLE

Horizontal Slinky Between-Trench Cross-Section

DESIGNED : YZ,OM,LA,GN,RA DATE : 17/May/2018

DRAWN: YZ SCALE :

APPROVED : CHECKED :

PROJECT NO : DRWG. NO : 20 REV. 16

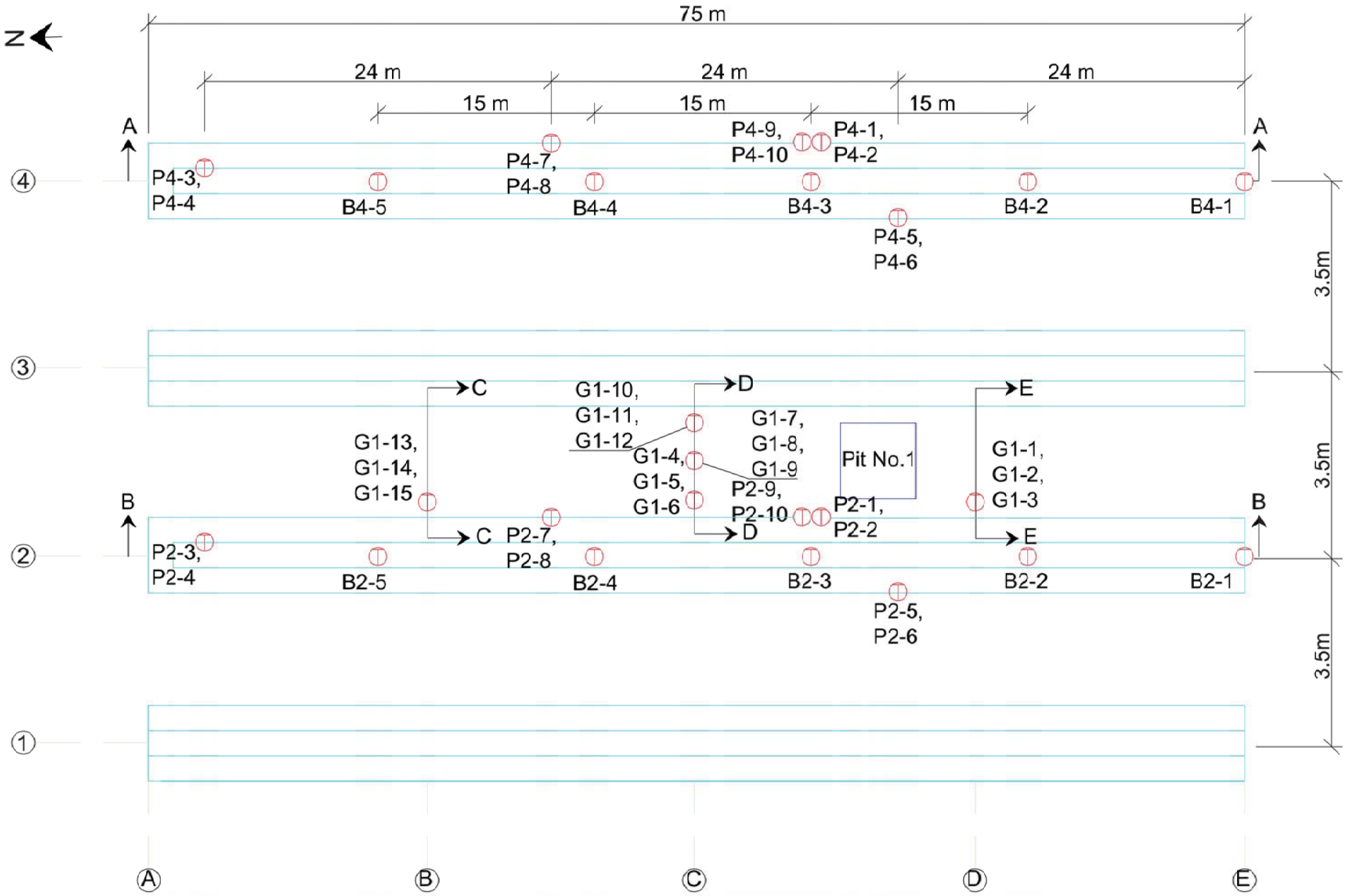


REVISIONS:

| No. | DATE | DESCRIPTION | APP'D. |
|---|---|---|---|
| | | | |

PROJECT

Brown Farm Project

University of Melbourne Research Project

TITLE

Horizontal Straight Pipe Instrumentation Drawing

DESIGNED :YZ,OM,LA,GN,RA DATE : 17/May/2018

DRAWN: YZ SCALE :

APPROVED : CHECKED :

PROJECT NO : DRWG. NO : 21 REV. 16

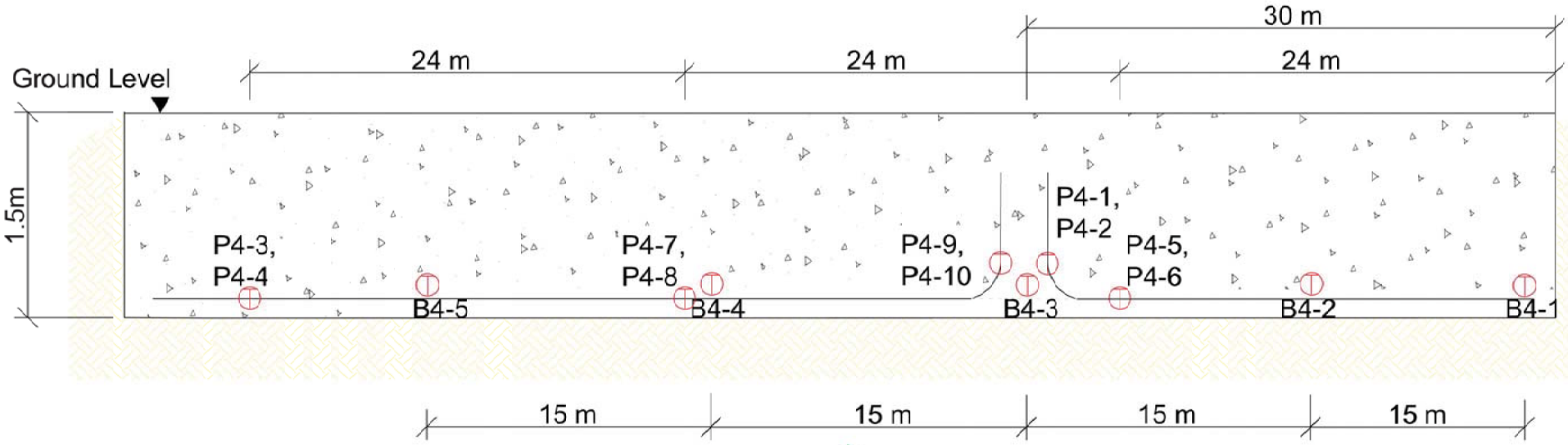


SECTION A–A 21

Sensors in the trench No.4
(Horizontal Straight Pipe)

N

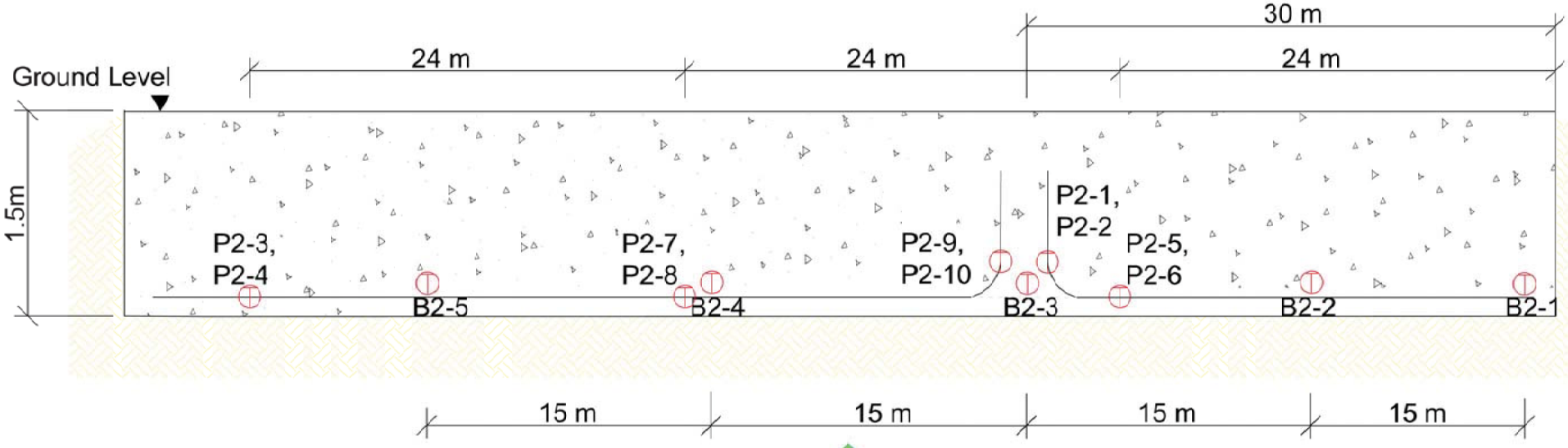


SECTION B–B 21

Sensors in the trench No.2
(Horizontal Straight Pipe)

Not to Scale
Side View

| REVISIONS: | | | |
|---|---|---|---|
| No. | DATE | DESCRIPTION | APP'D. |
| | | | |

PROJECT
Brown Farm Project
University of Melbourne Research Project

TITLE
Horizontal Straight Pipe Instrumentation Trench Cross-section
(Trench No.4 & No.2)

DESIGNED : YZ,OM,LA,GN,RA DATE : 17/May/2018
DRAWN: YZ SCALE :
APPROVED : CHECKED :
PROJECT NO : DRWG. NO : 22 REV. 16

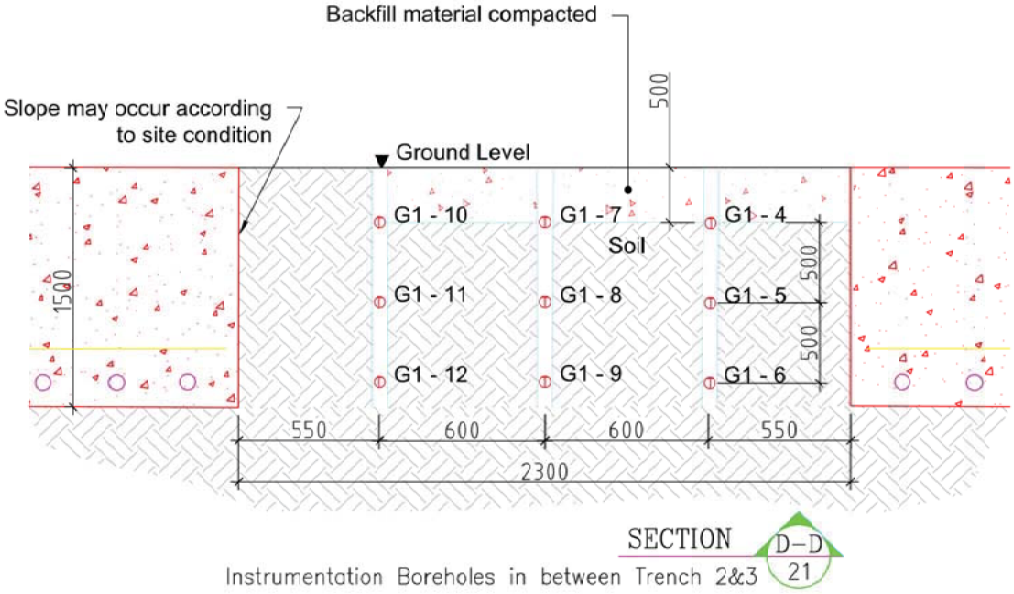


SECTION D–D

Instrumentation Boreholes in between Trench 2&3 21

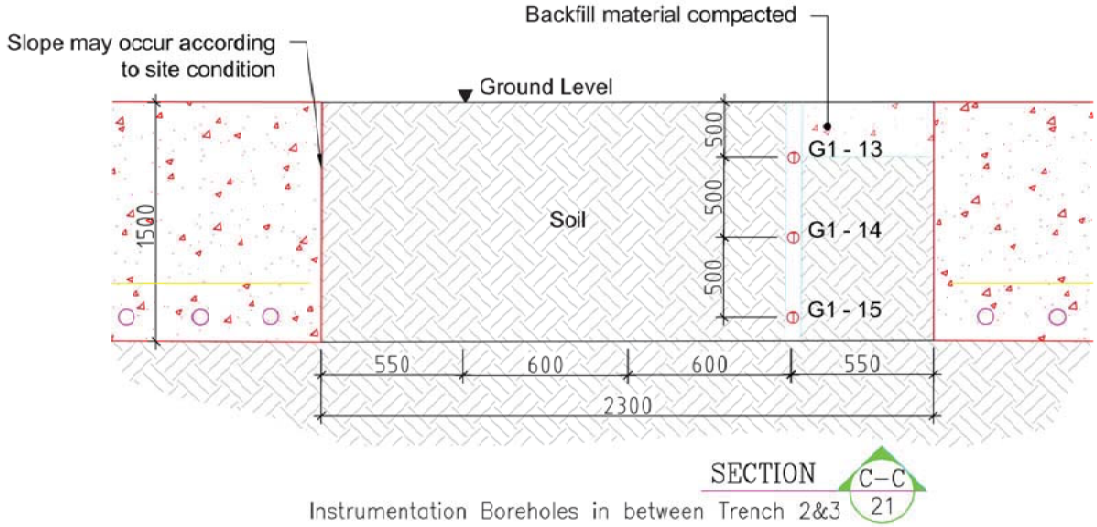


SECTION C–C

Instrumentation Boreholes in between Trench 2&3 21

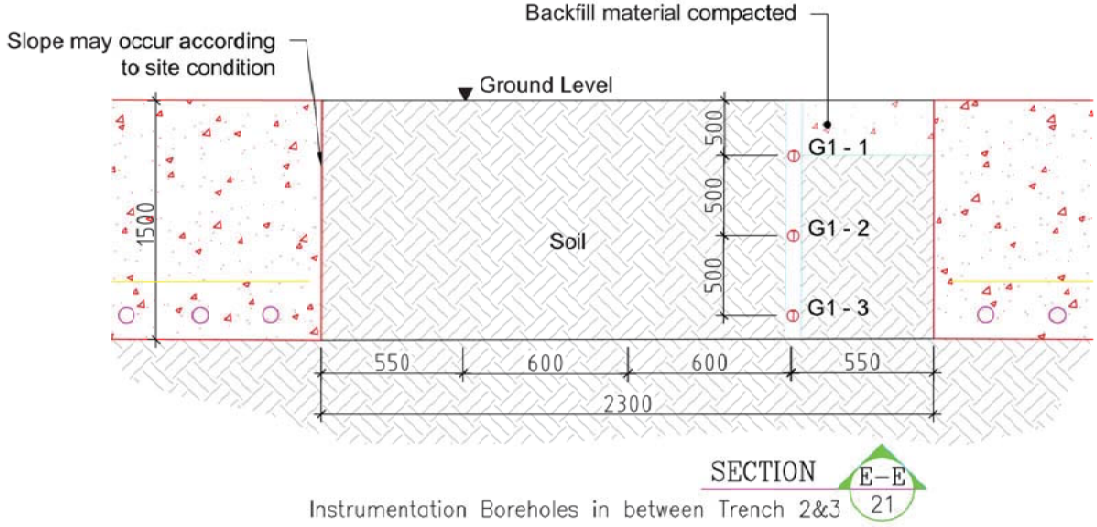


SECTION E–E

Instrumentation Boreholes in between Trench 2&3 21

REVISIONS:

| No. | DATE | DESCRIPTION | APP'D. |
|---|---|---|---|
| | | | |

PROJECT

Brown Farm Project

University of Melbourne Research Project

TITLE

Horizontal Straight Pipe Between-Trench Cross-Section

DESIGNED : YZ,OM,LA,GN,RA DATE : 17/May/2018

DRAWN: YZ SCALE :

APPROVED : CHECKED :

PROJECT NO : DRWG. NO : 23 REV. 16

**80-kW Shallow Geothermal System for Brown Farm**
**Specifications for Ground Loops and Headers**

## General

1. All HDPE pipes placed in horizontal trenches are referred to as **horizontal ground loops**.
2. All HDPE pipes placed in horizontal trenches connecting the horizontal ground loops to the heat pumps are referred to as **header pipes**.
3. The University of Melbourne is referred to as the university.
4. The Ground Source Systems is referred to as GSS.

## Materials and equipment

5. All horizontal ground loops and header pipes are to be HDPE, PE100, PN16 and shall be manufactured in accordance with AS/NZS 4130:2003.
6. All horizontal ground loops and header pipes with a nominal diameter of 90 mm and smaller shall have dimension ratio (SDR) of 11.
7. All horizontal ground loops and header pipes should be handled, stored and installed in accordance with Australian Standard AS2033 "Installation of Polyethylene Pipe Systems".
8. All fittings shall be of the electro-fusion type. Butt fusion acceptable as well.
9. All horizontal ground loop and header pipe locations are shown on Drawings 01 and 02, and pipe sizes are shown on Drawing 14.
10. All equipment for controlling the flow through the geothermal system, including the heat pumps, and all instruments (with suitable lengths of cable) and logging equipment shall be remotely accessible by the university and GSS.
11. The sub-contractor shall provide as-built drawings, an operation and maintenance manual, a commissioning report and participate in training of building management's staff.

## Manufacture of horizontal ground loops

12. Instrumentation in the form of thermistors to be attached to the outside of selected horizontal ground loops shall be secured by cable ties and gaffer tape at the appropriate position on completion of the manufacture of the loops. The cables shall be secured against the ground loops by gaffer tape. The position of the thermistors on the ground loops will be determined by the university.
13. Prior to backfilling, each horizontal ground loop shall be flushed, and pressure tested to 820 kPa for 1 hour as specified below.
14. Prior to backfilling, each thermistor shall be tested for output compliance.

## Installation of horizontal ground loops and headers

15. All horizontal ground loops and header pipes under the geothermal loop field shall be installed prior to the installation of all other services.
16. The depths of trenches for the installation of horizontal ground loops shall be 1.5 m. The minimum depths of trenches for the installation of headers shall be 0.5 m. The bottom level of all trenches shall be the same.
17. Inspect trenches to ensure that all rocks or sharp angular gravel are removed.
18. Horizontal ground loops shall prefabricated, using thermal fusion if needed (either electro-fusion joints or butt fusion joints).
19. Once the horizontal ground loops are in position in the trenches, they shall be pressure tested. The nominated test pressure is 820 kPa. This pressure will be held for 1 hour.
20. Following pressure testing, loops shall be kept filled with water and capped on both flow and return for backfilling.
21. Once the horizontal ground loops are in position in the trenches, for the ground loops which have thermistors attached, the thermistors shall be tested for output compliance.
22. The trenches shall be backfilled with the excavated soil.
23. The pressure in the horizontal ground loops can be released after the backfilling. The open ends of the loops shall be capped.
24. The pipes forming the ground loops should be trimmed and connected to the header pipes using appropriate electro-fusion fittings or well executed butt fusion.
25. If and where hydraulic pipes cross the header pipes, a distance of no less than 150mm is to be allowed between a header pipe and a hydraulic pipe and 20mm plywood (over width of trench to at least 500mm either side of hydraulic pipes) shall be used to cover header pipes.

## Flushing, purging and pressure testing

26. A minimum flow rate of 0.6 m/s (2 feet per second) throughout the piping system is required to completely remove any trapped air.
27. Each circuit of the horizontal ground loops shall be flushed and purged separately while the other circuits and the heat pumps are isolated. There are 12 circuits of horizontal ground loops in total and four pond loops grouped by every four circuits. If a large enough circulation pump was available, 4 loops grouped for a single GSHP can be flushed and purged at once, but ensuring no air is trapped in the system. Heat pump and other systems (tank, etc) shall be flushed and purged while the ground loops are isolated.
28. The minimum flushing velocity shall be 2.0 feet/second (i.e. flow rate shall be 5.7 US gallons/minutes for a DN32 pipe loop). For the first 30 minutes of flushing or until the water runs clear, the water emerging from each circuit shall be discarded. Once the water is clear, it shall be circulated into the water tank of the flushing cart for 2 hours. Care shall be taken that there is adequate capacity in the tank and water available so that the circuits remain full at all times. A filter shall be employed to remove the debris and pipe shavings during this process.
29. After flushing the horizontal ground loops sequentially, the heat pumps, water tank and the remaining header pipes shall be flushed in a similar manner.
30. After assembling each circuit of the horizontal ground loops, it shall be pressurized to 820 kPa and it locked to this pressure for at least 1 hour. Examine or inspect visually the pressurized pipes.
31. After installing headers, the whole system should be pressurized to 820 kPa and it should be locked to this pressure for at least 8 hours. This should be done before backfilling the headers so that the pipes can be visually inspected or examined.
32. The heat pumps, water tank and hydraulic pumps shall be installed in a dry enclosure under a canopy.

## Installation of above ground geothermal equipment

33. All above ground equipment shall be installed by the Nominated Sub-Contractor who shall jointly agree with The University of Melbourne on placements prior to installation.

## Pre-commissioning

34. The University of Melbourne and Nominated Sub-Contractor will perform the pre-commissioning of geothermal equipment which includes flushing and purging whole geothermal system.

## Insulation

35. The above ground pipework must be thermally insulated with Armaflex or equivalent material.
36. The Nominated Sub-Contractor shall ensure that all insulation are zero ozone depleting in both composition and manufacture (Armaflex or equivalent).

## Refrigerant

37. The Nominated Sub-Contractor shall ensure that all refrigerants (including those used in heat pumps) are zero ozone depleting in both composition and manufacture.

## Heat Pump details

38. Four Mammoth heat pump (Model: MSR-J086WLES) shall be installed in an enclosure as specified.

| REVISIONS: | | | |
|---|---|---|---|
| No. | DATE | DESCRIPTION | APP'D |
| | | | |

PROJECT
Brown Farm Project
University of Melbourne Research Project
TITLE
Specifications for Ground Loops and Headers

DESIGNED : YZ,OM,LA,GN,RA DATE : 17/May/2018
DRAWN: YZ SCALE :
APPROVED : CHECKED :
PROJECT NO : DRWG. N0 : 24 REV. 16

**80-kW Shallow Geothermal System for Brown Farm**
**Specifications for instrumentation and monitoring control**

## General

1. The instruments shall comprise thermistors (x200), flow meters (x11), valves, power meters (x5), gas meters (x3), TDR (soil moisture and temperature) sensors (2x4) and a weather station (x1).
2. All equipment for controlling the flow through the geothermal system, including the heat pumps, and all instruments (with suitable lengths of cable) and logging equipment shall be provided by the university via the Nominated sub-contractor (Donovan Electrical).
3. All cables and their connections shall be made waterproof by using appropriate "heat-shrink" protection.
4. Considerable care must be exercised with the cables from the instrumentation so that they are not damaged during installation.
5. Labelling of cables is also extremely important and methods should be used so that the cables can always be identified.
6. Thermistors shall be placed on selected horizontal ground loops, in separate monitoring boreholes adjacent to some ground loops (locations to be jointly agreed between the university and partner GSS), at the flow and return header pipes in the manifold in the plan room, at the flow and return pipes for both source and demand sides of each heat pump and at the flow and return pipes of the buffer tank on the building side.
7. [item to be confirm once the plant room designed is finalised, see Drawing 15] Flow meters shall be placed at either the flow or return header pipes, at the return pipes for both source and demand sides of each heat pump and at the return of the buffer tank on the building side.
8. Power meters shall be placed on all power lines to the heat pump and the circulation pump.
9. Photos and videos may be taken and published during the construction and monitoring period for research purpose.

## Instrumentation in the ground loops

10. Thermistors shall be placed on selected ground loops as shall be determined by the university and partner GSS (see Drawings 5, 6, 8, 9, 11, and 12).
11. The thermistors shall be secured against the outside of the ground loops by cable ties during the manufacture of the ground loops prior to installation - the university will assist with this task. The cables from the thermistors shall also be secured against the ground loops by gaffer tape.
12. Following ground loops installation and excavation of the header trenches, the cables shall be laid out in the base of the trenches and bundled together with gaffer tape and led to the inspection pit area
13. At the inspection pits, each cable shall be connected to a backbone cable which takes the instrument signals to the main data collection point via the main header trenches.
14. All entry and exit points in the inspection pits shall be waterproofed.

## Instrumentation in the separate monitoring boreholes

15. Thermistors and soil moisture content (humidity) sensors (TDRs) shall be placed in separate small diameter monitoring boreholes adjacent to some ground loops as shall be determined by the university.
16. The monitoring boreholes must be maintained open until the instruments are inserted.
17. The monitoring boreholes shall be drilled to depths of 1.5 m on the ground loops area and to a minimum of 4 m on a far-field as indicated in Drawings 3, 4, 7, 10, and 13.
18. Following backfilling of each monitoring borehole, and following excavation of the connecting trench, the cables shall be laid out in the base of the trenches to the inspection pit and then bundled together with gaffer tape.
19. At the inspection pits, each cable shall be connected to a backbone cable which takes the instrument signals to the main data collection point via the main header trenches.
20. A separate far-field monitoring borehole of a 4 m minimum depth shall be installed at a suitable location near the building with a string of thermistors grouted into this borehole. A shallow trench shall be required for the cables to be taken to the data collection (See Drawing 04).

## Instrumentation in the header pipes

21. As described in points 6, 7 and 8 and as shown in Drawing 15.

## Instrumentation at the circulation pumps

22. As described in points 6, 7 and 8 (see Drawing 15)
23. A single speed circulation pump shall be provided with a power meter.

## Instrumentation at the heat pump

24. As described in points 6, 7 and 8. Thermistors shall be secured by cable ties to metallic pipes. Where these pipes are non-metallic, suitably sealed P/T ports shall be provided so that the water temperature can be measured directly. All instruments insulated with UV resistant jacket.
25. Flow meters shall be placed at the return pipes for both source and demand sides of each heat pump.
26. Each heat pump shall be provided with a power meter.

## Building performance monitoring

27. Access to data of measured temperature and humidity must be provided.

## Climate monitoring

28. A digital weather station or equivalent shall be mounted on the roof of the building to provide data on the weather as per architectural specification. This shall include both dry and wet bulb temperatures, solar energy, rainfall and wind speed and direction.

## Data logger

29. The data logger cabinet shall be located inside the store room or the staff store room or the plant room and the data cables will be connected to it through penetrations of an appropriate size. The cabinet for data logger will be wall mounted as appropriated.

## Installation of Instruments

30. All instrumentation in ground loops, separate monitoring boreholes, header pipes, circulation pumps and heat pumps to be assisted by the university.
All instrumentation within the plant/store room to be undertaken by the Nominated sub-contractor, with guidance from the university and GSS.

REVISIONS:

| No. | DATE | DESCRIPTION | APP'D |
|---|---|---|---|
| | | | |
| | | | |
| | | | |
| | | | |
| | | | |
| | | | |

PROJECT
Brown Farm Project
University of Melbourne Research Project
TITLE
Specifications for instrumentation and monitoring control

DESIGNED :YZ,OM,LA,GN,RA DATE : 17/May/2018
DRAWN: YZ SCALE :
APPROVED : CHECKED :
PROJECT NO : DRWG. N0 : 25 REV. 16

# Appendix D Parameters for FEM model

## 1. Finite Element Model

To conduct this research, a state of art transient 3D finite element model was developed at The University of Melbourne, using COMSOL Multiphysics, a widely-used finite element simulation software. This model was developed by coupling both the governing equations of the heat transfer in soil and the fluid flow in horizontal ground heat exchangers [37]. Heat transfer around and in the GHEs occurs primarily by conduction and convection. Heat conduction takes place in the ground (soil or rock) and pipe wall, and partially in the carrier fluid; while heat convection dominates in the carrier fluid circulating in the pipes (i.e., water or water-antifreeze solution). It is assumed that there is no groundwater flow in the ground, although this condition can be included with an additional coupled Darcy's model. The fluid flow in the pipes is described by the Navier-Stokes (NS) equations in the laminar regime. In the transitional and turbulent regimes, obtaining detailed information about the fluid fluctuations is computationally expensive. To this end, the Reynolds-averaged-Navier-Stokes (RANS) equations, which are the governing equations used in so-called k-ε turbulent models, will be employed instead of NS.

On the other hand, as the existence of moving fluid within the pipes requires heat to be modelled by conduction and convection, the heat equation should also include a convective term. For incompressible fluids, a generalised energy conservation law is used. The velocity field u, found by solving the governing NS or RAMS Equations for fluid flow, is used in the convective term of the generalised energy conservation equation when modelling the heat transfer by conduction and convection within the pipes. In the ground and the pipe wall, the velocity field is null in the absence of groundwater flow. In fact, heat transfer occurs in ground primarily by conduction under the expected site conditions. The heat capacity and thermal conductivity are the key fundamental thermal properties, which will be known for the site and fluid, including their variations with temperature. These equations must be solved with appropriate initial and boundary conditions, importantly the ground far-field temperature (ground and surface air) and fluid temperature at the inlet of the ground circuit. Taken together, these equations can be used to calculate total heat exchanged between the ground and the sheds. This model is capable of accurately predicting the GHE performance in both laminar and turbulent regimes, homogeneous and heterogeneous ground profiles, and is adequately flexible to explore a number of different pipe placement configurations, ranging from well-known U-pipe configurations to slinky and others. Given the non-symmetries encountered for a number of such configurations, the expensive 3D simulations are supported by using more powerful workstations and the 'Argali' supercomputer of the High-Performance Computing facilities at The University of Melbourne.

In this study, three different pipe configurations with same pipe length (300 metres) are considered. Theses configurations are horizontal straight pipe, slinky and dense slinky. These configurations have same length of pipe in one trench, while the first two have the same trench length as well. This study will then evaluate the effect of variable trench separation of horizontal ground heat exchangers. Trench separations of 3.5 metre was selected and analysed considering three different horizontal pipe configurations. Different effective thermal conductivities of the ground have also been evaluated as different scenarios. The detailed simulation parameters are discussed next.

## 2. Simulation Parameters

The modelling mimics typical weather and ground conditions in Peats Ridge, NSW, Australia, with the material properties used presented in table. The geometry and dimensions used for the modelled GHE are of typical practice in the region as well and are depicted in Figure 3-11 a and b. It should be noted that while typical GSHP systems include a field with multiple GHEs, in this model each simulation focuses on one single GHE to isolate the effects of pipe separation within the GHE from the thermal interference that may arise from adjacent GHEs. This is indeed the case for the relative short-term testing data collected (see Figure 3-23).

**Material Properties.**

| Parameter | Value(s) | Unit | Description |
|---|---|---|---|
| $\lambda_{ground}$ | 1.0, 1.5, 2.5 | W/(mK) | Effective thermal conductivity of ground |
| $\rho_{ground}$ | 2000 | kg/m$^3$ | Density of ground |
| $C_{p\ ground}$ | 1480 | J/(kgK) | Specific heat capacity of ground |
| $T_{undisturbed}$ | 16.1 | °C | Undisturbed ground temperature |
| $\lambda_{fluid}$ | 0.582 | W/(mK) | Thermal conductivity of carrier fluid |
| $\rho_{fluid}$ | 1000 | kg/m$^3$ | Density of carrier fluid |
| $C_{p\ fluid}$ | 4190 | J/(kgK) | Specific heat capacity of carrier fluid |
| $Q_{fluid}$ | 0.42 | L/s | Flow rate of carrier fluid |

To find the reasonable dimension of the soil field, different dimensions of the soil has been modelled in a steady state simulation. It was found that with the increase of the dimension, the inlet and outlet temperature of the fluid become more stable and reach a plateau. The acceptable length and depth of the field were determined as 120 m (90 m for dense slinky loops, which is 30 m shorter) and 60 m. A temporal and special mesh sensitivity analyses was also undertaken, resulting in different mesh sizes, with high refinement near the pipe loops and time step needs to be set to about 1 hour.

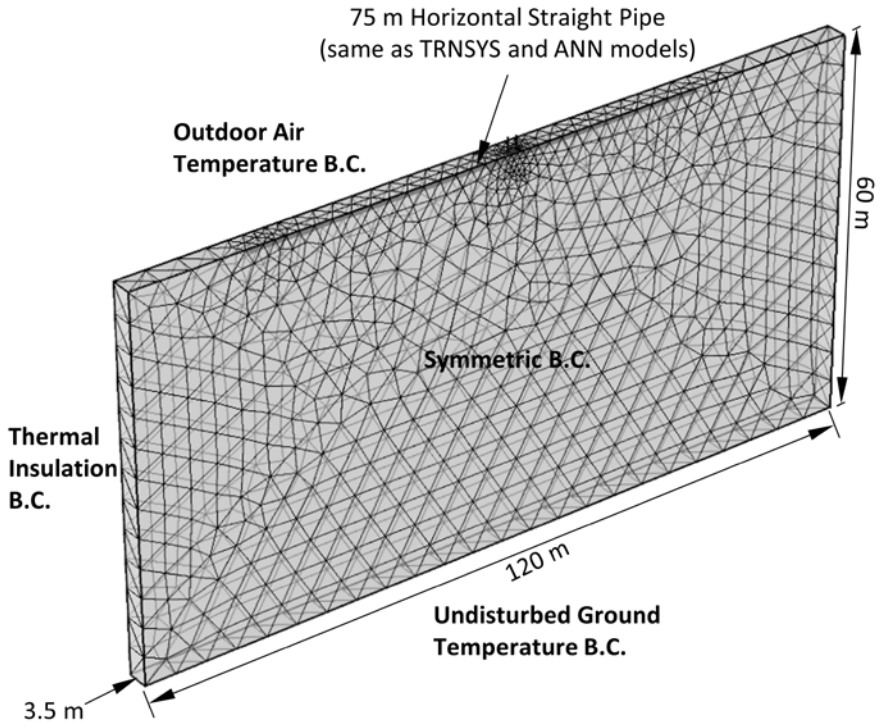


**Boundary conditions of the FEM model.**

In terms for boundary conditions, thermal insulation was prescribed on both short side of the field and symmetric condition on both long side of the field. The top boundary was set to be the outdoor temperature and the bottom to be undisturbed ground temperature (16.1 deg C in the experimental field). Based on the fluid flow rate and heating loads shown in Fig 5-5, the GHE inlet temperature is generated as input parameter for the GHE and the experimental field. With these input and boundary conditions, and by numerically solving the governing equations, the GHE outlet temperatures are computed over time. This is an accurate and rigorous treatment, but it is computationally expensive, and in many cases prohibit use for large scale optimisation studies.

With the boundary and initial conditions shown above, a comparison between the FEM simulation and experimental data recorded (shown in Fig. 3-22) was made to validate this model. In the validation, the geometry of the pipe was redesigned to slinky loop to mimic the experimental condition. The following figure shows the comparison results, from 12:00 pm to 10:00 pm, Oct. 8, 2019. It can be seen that the simulation data is in reasonably good agreement with the experimental data recorded. The RMSE calculated for this case is only 0.169 °C.

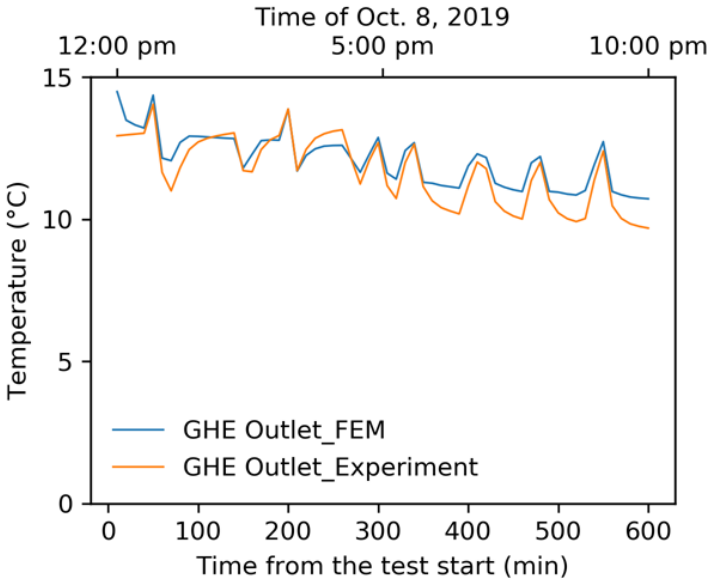


**Comparison of the FEM simulation with experimental data recorded.**